



Performance of Large-Scale Gezira Irrigation Scheme and its Implications for Downstream River Nile Flow

Der Fakultät für Physik und Geowissenschaften
der Universität Leipzig
eingereichte

DISSERTATION

zur Erlangung des akademischen Grades

Doktor rerum naturalium
(*Dr. rer. nat.*)

Vorgelegt von

MSc.

Islam Sabry Al Zayed

geboren am 25.09.1984
in Kairo (Ägypten)

Gutachter: Prof. Dr. Jürgen Heinrich
Prof. Dr. Karl Schneider

Tag der Verleihung: 22 June 2015



AN INITIATIVE OF THE



Federal Ministry
of Education
and Research

This research was funded by International Postgraduate Studies in Water Technologies (IPSWaT) scholarship programme (2010-2013), an initiative of the German Federal Ministry of Education and Research (BMBF)

Dedication

I dedicate this research to my family who I owe everything to them

To:

My mother: Faten,

My Father: Sabry,

My Wife: Nourhan,

My daughter: Elsa,

Father in law: Mahmoud,

Mother in law: Hala,

Lastly my brothers and sister: Mohamed, Amr, Seif and Merna

Islam Al Zayed

Acknowledgements

First of all, I thankfully prostrate myself before ALLAH for His uncountable bounties that He bestowed on me; among them is the completion of this thesis.

I would like to express my sincere thanks to my supervisors Professors Lars Ribbe and Jürgen Hienrich for their keen advice, support, cooperation and skillful guidance toward making completion of this thesis possible. I am very grateful to them as they gave their best to support me in this work, leading my promotion with simplicity and conviviality. In spite of their tight schedule, they always found time for progress meetings. Special gratitude goes to Dr. Nadir Elagib, my co-supervisor, who has fully supported me throughout the research period and during the field visits in Sudan. I would like to thank him for his ever-friendly and social support during my residence in Cologne.

I would like to extend my gratitude to all staff members (Professors, Mitarbeiter, Secretariat, IT staff and PhD candidates) at my host institute in Germany, the Institute for Technology and Resources Management in the Tropics and Subtropics (ITT), Cologne University of Applied Science. Big thanks go to my officemates (Wifag, Tekalegn and Mahsa); I wish you the best ever and thank you for the wonderful time and working environment. Special thanks go to Joern, Mohamed, Vanesa, Mario, Almut and Juan, who always helped me when needed – my sincere gratitude.

Sincere thanks and appreciation go to the German government through the International Postgraduate Studies in Water Technologies (IPSWaT) for their awarding me a scholarship for my studies at Leipzig University and Cologne University of Applied Science, Germany. I would like also to express my sincere thanks and gratitude to Frau Parisus, Frau Sabzian, Dr Sattler and Ricarda for coordinating the scholarship that enabled the completion of this work.

I wish to express my deep gratitude to the Egyptian Government through the Water Resources Research Institute (WRRI) for granting me a leave for this study, and to the Nile Water Sector (NWS) for all the support I received during my stay in Sudan. In particular, I am very grateful to Prof. Mohamed Abdel-Motaleb, Prof. Sameh Sakr, Prof. Karima Attia, Dr. Sherif Elmohamady, Eng. Amr Fawzy, Eng. Amal Gasser, Dr. Mansour Yackoub and Dr.

Ihab. I would also like to extend my gratitude to Prof. Abdeen Saleh and Dr. Gamal Abdo of the Faculty of Engineering, Khartoum University for their keen support during my field visits to Sudan.

I am deeply grateful to my German family represented by Andreas and his lovely parents – thanks a lot.

During the whole period of my research in Germany, I received attention in several ways from so many people that I might not be able to list them by name. I am deeply grateful to all of them. Last, but not least, I would like to thank my relatives and friends who made this achievement possible by their prayers and blessings. Finally, my affectionate thanks go to my family, my father, mother and tender wife Nourhan, who supported me and endured my long stay away from them.

Abstract

Policy makers adopt irrigated agriculture for food security, since irrigation doubles crop production. Therefore, the development of large irrigation systems has a long history in many places worldwide. Although large-scale irrigation schemes play an important role in improving food security, many schemes, especially in Africa, do not yield the expected outcomes. This is related to poor water management, which is generally due to a lack of effective evaluation and monitoring. The objective of this study, therefore, is to propose a new methodology to assess, evaluate and monitor large-scale irrigation systems.

Information on irrigation indicators is needed to enable the evaluation of irrigation performance. The evaluation is the first and the most significant step in providing information about how it is performing. After reviewing extensive literature, a list of indicators related to the performance of irrigation, rainwater supply and productivity is suggested. The irrigation efficiency indicators Relative Irrigation Supply (RIS) and Relative Water Supply (RWS) are selected. Potential rainwater supply to crops can be tested based on the Moisture Availability Index (MAI) and the Ratio of Moisture Availability (RMA). Water productivity can be assessed by Crop Yield (Y) and Water Use Efficiency (WUE). However, the central problem facing large-scale irrigation schemes is always the lack of data, which calls for the development of a new method of data acquisition that allows evaluation and monitoring. Remote Sensing (RS) technology makes it possible to retrieve data across large areas. Two different approaches via RS, the Normalized Difference Vegetation Index (NDVI) and Actual Evapotranspiration (ET_a), can be utilized for monitoring. The well-known Vegetation Condition Index (VCI), derived from the NDVI, is modified (MVCI) to allow a qualitative spatio-temporal assessment of irrigation efficiency. MVCI takes into account crop response to water availability, while ET_a indicates whether water is used as intended. Furthermore, the assessment of the possible hydrological impact of the irrigation system should be considered in the evaluation and monitoring process. The Sudanese Gezira Scheme of 8,000 square kilometers in the Nile Basin, where performance evaluation and monitoring are absent or poorly conducted, is no exception. This research takes the large-scale irrigation of the Gezira Scheme as a case study, as it is the largest scheme, not only in the Nile Basin but also in the world, under single management.

The first long-term historical evaluation of the scheme is conducted for the period 1961–2012 rather than only on a short-time scale as is the common practice. An increase in RIS and RWS values from 1.40 and 1.70 to 2.23 and 2.60, respectively, since the 1993/94 season shows decreasing irrigation efficiency. MAI and RMA for summer crops indicate a promising rainfall contribution to irrigation in July and August. The Gezira Scheme achieves low yield and WUE in comparison to many irrigation schemes of the globe. Low productivity is mainly due to poor distribution and irrigation mismanagement. This is indicated by the 15-year MVCI spatio-temporal analysis, which shows that the northern part of the scheme experiences characteristic drought during the summer crop season. Although MVCI can be considered a monitoring tool, the index does not deduct the soil water content, and water could be wasted and available in other ways (e.g. water depressions).

Spatio-temporal information for ET_a is required to better quantify water depletion and establish links between land use and water allocation. However, several RS models have been developed for estimating ET_a . Thus, improving the understanding of performance of such models in arid climates, as well as large-scale irrigation schemes, is taken into account in this study. Four different models based on the energy balance method, the Surface Energy Balance Algorithm for Land (SEBAL), Mapping Evapotranspiration at High Resolution with Internalized Calibration (METRICTM), Simplified Surface Energy Balance (SSEB) and MOD16ET are applied in order to determine the optimal approach for obtaining ET_a . Outputs from these models are compared to actual water balance (WB) estimates during the 2004/05 season at field scale. Several statistical measures are evaluated, and a score is given for each model in order to select the best-performing model. Based on ranking criteria, SSEB gives the best performance and is seen as a suitable operational ET_a model for the scheme. SSEB subsequently is applied for summer and winter crop seasons for the period 2000–2014.

Unfortunately, one of the limitations faced in the current research is the absence of validation data on a regional scale. Therefore, the assessment focuses on spatial distribution and trends rather than absolute values. As with the MSCI distribution, the seasonal ET_a for the Gezira Scheme is higher in the southern and central parts than in the northern part. This confirms the robustness of the developed MSCI. To avoid using absolute values of ET_a , the ratio of ET_a from agricultural areas (ET_{agr}) to the total evapotranspiration (ET) from the scheme (ET_{sum}) is calculated. The ET_{agr}/ET_{sum} ratio shows a descending trend over recent years, indicating that the water is available but not being utilized for agricultural production.

This study shows that SSEB is also useful for identifying the location of water losses on a daily basis. Around 80 channels are identified as having leakage problems for the 2013/14 crop season. Such information is very useful for reducing losses at the scheme. In addition, Rainwater Harvesting (WH) is addressed and found to be applicable as an alternative solution for accounting for rainfall in irrigation. It is seen that these management scenarios could save water and increase the overall efficiency of the scheme. It is possible to save 68 million cubic meters of water per year when the overall irrigation efficiency of the scheme is improved by only 1%. A level of efficiency of 75% is predicted from the proposed management scenarios, which could save about 2.6 billion cubic meters of water per year.

In conclusion, the present study has developed an innovative method of identifying the problems of large-scale schemes as well as proposing management scenarios to enhance irrigation water management practice. Improved agricultural water management in terms of crop, water and land management can increase food production, thereby alleviating poverty and hunger in an environmentally sustainable manner.

Keywords: Irrigation performance; Irrigation water management; Remote sensing; Actual evapotranspiration (ET_a); SEBAL; METRIC; SSEB; NDVI; MSCI; MSCI; Water harvesting; Monitoring; Implications on downstream.

Table of Content

Abstract	i
Table of Content	iii
List of Figuers	v
List of Tables	x
List of Abbreviations	xii
CHAPTER ONE	1
INTRODUCTION	1
1.1 Water for food security.....	1
1.2 Irrigation water management	2
1.2.1 Overview	2
1.2.2 Irrigation performance assessment.....	3
1.2.3 The Remote Sensing (RS) approach to agricultural water management ...	3
1.2.4 The impact of irrigated agriculture on basin hydrology.....	4
1.3 Large-scale irrigation schemes in the Nile Basin.....	5
1.4 Problem definition	7
1.5 Research questions	8
1.6 Research objectives	9
1.7 Structure of the thesis	9
CHAPTER TWO	11
1. DESCRIPTION OF THE GEZIRA IRRIGATION SCHEME	11
2.1 Geographical description.....	11
2.2 Climate conditions.....	12
2.3 Management authority.....	15
2.3.1 Administrative structure.....	15
2.3.2 Institutional management	16
2.4 Water resources	17
2.4.1 Irrigation water system.....	17
2.4.2 Groundwater.....	21
2.5 Crops and water demand	22
2.5.1 Cropping pattern and yields	22
2.5.2 Crop water requirements	23

CHAPTER THREE	25
ASSESSING THE IRRIGATION PERFORMANCE OF GEZIRA SCHEME	25
3.1 Introduction	25
3.2 Material and methods	26
3.2.1 Source of data.....	26
3.2.2 Crop and actual evapotranspiration.....	26
3.2.3 Irrigation supply indices.....	28
3.2.4 Rainwater supply assessment.....	29
3.2.5 Productivity of land and water	30
3.2.6 Monitoring of spatial efficiency.....	30
3.3 Results and discussion.....	31
3.3.1 Crop stress.....	31
3.3.2 Irrigation supply indices.....	33
3.3.3 Rainwater supply.....	38
3.3.4 Water productivity.....	41
3.3.5 Monitoring of spatial efficiency.....	44
3.4 Conclusions	50
CHAPTER FOUR.....	52
DETERMINING THE OPTIMAL REMOTELY SENSED APPROACH TO OBTAINING ACTUAL EVAPOTRANSPIRATION FOR THE GEZIRA SCHEME.....	52
4.1 Introduction	52
4.2 Materials and methods.....	53
4.2.1 Model selection	53
4.2.2 Source of data.....	54
4.2.3 Energy balance method	56
4.2.4 SSEB	58
4.2.5 MOD16 evapotranspiration.....	58
4.2.6 Seasonal ET _a extrapolation	59
4.2.7 Validation of ET estimates from the models.....	59
4.3 Results and discussion.....	60
4.3.1 Evapotranspiration models validation.....	60
4.3.2 Spatial variability of actual evapotranspiration.....	63
4.3.3 Models performance evaluation.....	67

4.3.4	Best-performing model	70
4.4	Conclusions	71
CHAPTER FIVE.....		73
MONITORING WATER ABSTRACTION FROM LARGE-SCALE IRRIGATION SCHEMES.....		73
5.1	Introduction	73
5.2	Material and methods	74
5.2.1	Agricultural water policies for the Gezira Scheme	74
5.2.2	Historical RS-based ET estimates at the Gezira Scheme.....	76
5.2.3	SSEB model	77
5.2.4	Source of data.....	79
5.2.5	SSEB model performance evaluation	82
5.3	Results and discussion.....	83
5.3.1	Model performance evaluation.....	83
5.3.2	The scheme level.....	85
5.3.3	The administrative levels	96
5.3.4	Evaluation of the applied water policies	105
5.4	Conclusions	107
CHAPTER SIX		108
POSSIBLE IRRIGATION MANAGEMENT SCENARIOS AND THEIR IMPLICATIONS FOR DOWNSTREAM FLOW		108
6.1	Introduction	108
6.2	Material and methods	110
6.2.1	A drought monitoring tool for the Gezira Scheme.....	110
6.2.2	Water harvesting for the Gezira Scheme.....	112
6.2.3	Implications of improving irrigation performance on downstream Blue Nile flow.....	115
6.3	Results and discussion.....	117
6.3.1	The Monitoring assessment.....	117
6.3.2	Water harvesting potential	121
6.3.3	Implications of improving irrigation performance on downstream Blue Nile flow.....	123
6.4	Conclusions	124

CHAPTER SEVEN	126
CONCLUSIONS AND RECOMMENDATIONS	126
7.1 Conclusions	126
7.2 Recommendations	129
REFERENCES	131
APPENDICES	149

List of Tables

Table 2-1. Group names and areas of Gezira Scheme; after Adam et al. (2002)	16
Table 2-2. Actual crop yields (1997–2007) in the Gezira Scheme	22
Table 3-1. Values adopted for the parameters in Equation 3-1 to estimate the seasonal ET_a	28
Table 3-2. Monthly dependable rainfall (DP) and monthly derived k_c values for the Gezira Irrigation Scheme	31
Table 4-1 . Landsat ETM+ images used for season 2004/05 in the Gezira Scheme	55
Table 4-2. Location of the meteorological stations	56
Table 4-3. ET_a (mm/day) obtained from the four Remote Sensing (RS) models compared with the Water Balance (WB) measurement	61
Table 4-4. The parameters of best-fit linear equations for the four models at the field and scheme levels	61
Table 4-5. Sum of scores for the four models according to each performance criterion	71
Table 5-1. The day of year of the used Landsat and Moderate Resolution Imaging Spectroradiometer (MODIS) satellite images for the summer crop season	80

Table 5-2. The day of year of the used Landsat and Moderate Resolution Imaging Spectroradiometer (MODIS) satellite images for the winter crop season	81
Table 5-3. The group names with the area in order from upstream to downstream with their corresponding channels.....	97
Table 6-1. The date of the used Landsat 8 satellite images for the monitoring tool	112
Table 6-2. Reported leakage channels for the irrigation season 2013/14.....	120
Table 6-3. Probability and return period for the different rainfall values	122
Table 6-4. Adopted parameter and calculated catchment to cultivated areas ratio (CA:CU)	123

List of Abbreviations

Abbreviate	Meaning
AMSL	Above Mean Sea Level
AMSR-E	Advanced microwave scanning radiometer-Eos
BCM	Billion cubic meter
CA	Catchment area
CU	Cultivated area
CWR	Crop water requirements
DEM	Digital elevation model
DP	Dependable precipitation
DR	Design rainfall
DSS	Decision support system
DW	Change in water storage
EF	Evaporative fraction
ET	Evapotranspiration
ETa	Actual evapotranspiration
ETa-SEBAL	ETa from SEBAL
ETc	Crop evapotranspiration
ETM+	Landsat enhanced thematic mapper plus
ETo	Grass reference evapotranspiration
ETp	Potential evapotranspiration
ETr	Alfalfa reference ET
ETrF	Reference et fraction for metric
ETr-inst	Instantaneous ETr
FAO	Food and agriculture organization of the united nations
G	Soil heat flux
GIS	Geographic information system
Gr	Groundwater recharge
Hs	Solar radiation
H	Sensible heat flux
Ho	Extraterrestrial radiation
HQ	Head quarters
IMT	Irrigation management transfer
iNDVI	Integrated normalized difference vegetation index
kc	Crop coefficients
ks	Crop stress factor

Abbreviate	Meaning
LAI	Leaf Area Index
LST	Land Surface Temperature
MAI	Moisture Availability Index
MD	Moisture Deficit
METRIC	Mapping EvapoTranspiration at high Resolution with Internalized Calibration
MODIS	MODerate resolution Imaging Spectroradiometer
MOI	Ministry of Irrigation
MoIWR	Ministry of Irrigation and Water Resources
MVCI	modified Vegetation Condition Index
MWRE	Ministry of Water Resources and Electricity
NASA	National Aeronautics and Space Administration
NBI	Nile Basin Initiativ
NDVI	Normalized Difference Vegetation Index
P	Total precipitation
Pe	Effective rainfall
R ²	Correlation coefficient
R _{in}	Irrigation discharge
RIS	Relative Irrigation Supply
RMA	Ratio of Moisture Availability
RMSE	Root mean square errors
RMSE	Root Mean Square Error
R _n	Instantaneous net radiation
R _{out}	Outflows
RS	Remote Sensing
RSD	Regime Shift Detector
RWB	Regional Water Balance
RWS	Relative Water Supply
SAVI	Soil Adjusted Vegetation index
SEBAL	Surface Energy Balance Algorithm for Land
SGB	Sudan Gezira Board
SLC	Scan line corrector
SMADA	Stormwater Management and Design Aid

Abbreviate	Meaning
SRTM	Shuttle Radar Topography Mission
S-SEBI	Simplified-Surface Energy Balance Index
TM	Thematic Mapper
T _{mean}	Mean daily air temperature
T _s	Surface temperature
UNEP	United Nations Environment Programme
USGS	U.S. Geological Survey
UTM	Universal Transverse Mercator
VCI	Vegetation Condition Index
WB	Water Balance
WUAs	Water User Associations
WUE	Water Use Efficiency
Y	Crop yield
Z _{om}	Empirical surface roughness
λ	Latent heat of the vaporization
λE	Instantaneous latent heat flux
τ_{sw}	Atmospheric transmissivity

CHAPTER ONE

INTRODUCTION

1.1 Water for food security

Population dynamics influence development at both country and regional levels. In the past 50 years, the world has experienced unprecedented population growth, and the total has now surpassed 9.1 billion. By 2050, the world's population is projected to increase by a further 34% (Alexandridis et al., 2009). Population growth certainly increases the pressure on and problems associated with food security (Viala, 2008; FAO, 2003; Godfray et al., 2010) as greater food production is required to satisfy demand. Water development is critical for food security in many regions of the world (Rosegrant et al., 2003). Erratic rainfall, especially in arid and semi-arid zones, requires farmers to adopt irrigated agriculture to secure food production. Also, the crop yield from irrigated agriculture is double that of rain-fed agriculture (FAO, 2002). Thus, irrigated agriculture is the main water user in many regions of the world and consumes around 70% of global fresh water. Future demand for the sector is projected to increase by 20% by 2025 (Rosegrant et al., 2003); it accounts more than 40% of total global food production and uses only about 17% of the land area (Feres and Connor, 2004). Even non-food crops such as cotton occupy 9% of the total global irrigated area, and their demand is expected to double by 2050 (Fraiture and Wichelns, 2010). Irrigation in developing countries is expected to increase by an aggregated 14% by 2030 (FAO, 2003), and the rising water demand, in terms of increasing food security and population need, puts great pressure on the limited supply.

Irrigated agriculture is an important source of food production. As a result, the development of large irrigation systems has a long history in many places worldwide. In Asia, the Chinese Dujiangyan irrigation system was built 2000 years ago and is still functioning with a current irrigated area of 670,000 hectares (Chen, 2005). In Africa, the British Emperor focused on increasing agricultural productivity a century ago. Therefore, dams and large-scale irrigation schemes were designed and constructed in the British Empire territories (i.e. the Nile Delta in Egypt and the Gezira Scheme in Sudan) at the end of the nineteenth century (Bastiaanssen and Perry, 2009). Although large-scale irrigation schemes play an important role in improving food security at both national and global levels (Alexandridis et al., 2009), many of these schemes, especially in Africa, do not yield the expected outcomes (Borgia et al., 2012). The poor performance of large-scale irrigation systems is generally related to poor water management (FAO, 2011), which has adversely affected productivity and hence reduced actual benefits

(Hamid et al., 2011). Irrigation water is lost and never fully utilized to produce food (Gleick, 2000). As a result, large irrigation systems have been seen by development institutions as financially and economically unattractive, not only for rehabilitation and maintenance, but also for future new developments (Hamid et al., 2011). In the future, water withdrawals for irrigation will increase by almost 11% by 2050 (Alexandridis et al., 2009). Furthermore, Gleick (2000) stresses the importance of higher water productivity in irrigated systems in order to meet the food demands of this century. Therefore, the irrigation sector should be managed to utilize water resources more efficiently and productively (Van Dam and Malik, 2003).

1.2 Irrigation water management

1.2.1 Overview

Management of irrigation water is the process of determining and controlling the volume, frequency and application rate of irrigation water in an efficient manner. The goal of such management is to obtain maximum sustainable production levels from the available resources (Alexandridis et al., 2009). However, better irrigation management is required to achieve greater efficiency in the use of water (Bastiaanssen et al., 1998b). As mentioned earlier, large-scale irrigation schemes are very important to national food security and agricultural growth if they are well managed (FAO, 2011).

The planning and management of water resources have become very important issues worldwide. Information on agricultural water supply and usage can thus support operational decisions. A major reason for the inefficiency of irrigation projects is a lack of effective monitoring and evaluation of these irrigation projects (Biswas, 1984; Leenhardt et al., 2004). Knowledge of the performance indicators within and among irrigation schemes can help policy makers and managers wisely allocate funds for intervention and rehabilitation (Bastiaanssen et al., 1998b). The problem of data acquisition for a large area is always difficult (Leenhardt et al., 2004), but Remote Sensing (RS) technology makes it possible for the retrieval of data across large areas (Wu et al., 2013).

Despite the fact that irrigated agriculture is important to food production, it has extremely negative environmental effects (FAO, 1997). In particular, diversion of water through large-scale irrigation projects from rivers has the potential to change the hydrology of river basins (Rosenberg et al., 2000) and reduce the quantity and quality of the water supply for downstream users (FAO, 1997). Therefore, it is essential that irrigation projects be planned and assessed in the context of the river basin as a whole. The following section will describe briefly the major actions of managing a large-scale irrigation scheme.

1.2.2 Irrigation performance assessment

Increasing food production with limited water resources is a challenge to the irrigated agricultural sector. Consequently, improvement of irrigation efficiency is meaningful. Monitoring and evaluation of an irrigation scheme is the first and the most significant step in providing information about how it is performing (Savva and Frenken, 2002). Monitoring achieves efficient and effective project performance (Biswas, 1984). Information on irrigation indicators is thus needed to enable the evaluation of irrigation performance and improve irrigation water management (Kloezen and Garcés, 1998). The assessment of current performance will identify efficiency shortfalls and enable them to be corrected. This will also help to improve irrigation system performance, which leads to enhanced food productivity and greater water availability (Bos and Clemmens, 1990). Irrigation performance is characterized by the system's ability to deliver sufficient water to satisfy crop demand (Clemmens and Bos, 1990) and the outcome in terms of crop productivity (Bandara, 2003). Since the 1970s, scholars have developed several indicators to measure irrigation performance, such as efficiency of conveyance, distribution, the fields and the system (Bos and Nugteren, 1990; Clemmens and Bos, 1990; Molden and Gates, 1990). Kloezen and Garcés (1998) suggested a list of indicators related to the performance of the hydrological, agronomic, economic, financial and environmental performance of irrigation systems. These indicators are used to describe hydrological behavior in complex irrigation schemes through few and understandable numbers (Bastiaanssen et al., 2001). Adequate monitoring and evaluation of performance of the irrigation scheme are needed to improve water management practices in order to achieve high performance.

1.2.3 The Remote Sensing (RS) approach to agricultural water management

Agricultural water management is meaningful to the efficient use of water resources. Monitoring and quantifying consumption over irrigated agricultural areas, rather than quantifying the delivered irrigation water (Folhes et al., 2009), can help to conserve water by improving efficiency and water productivity (Allen et al., 2011; Martin et al., 2013). Accurate estimation of agricultural water demand is a key need for water management (Leenhardt et al., 2004). Generally, the actual evapotranspiration (ET_a) of a crop represents the actual water consumption (Allen et al., 1998). ET_a is important to evaluating irrigation water management practices (Feres and Soriano, 2007), as well as improving crop productivity through enhancing soil moisture management (Fraiture and Wichelns, 2010). Scholars have developed many methods to estimate ET_a , such as the pan evaporation method, lysimeters, flux profile measurements, the Food and Agricultural Organization (FAO) Penman–Monteith method, the

Bowen ratio, and eddy-correlation measurements (Prueger et al., 1997; Allen et al., 1998; Immerzeel et al., 2006). These methods are point methods based on meteorological information for a specific station and do not provide spatial patterns of ET_a (Immerzeel et al., 2006; Folhes et al., 2009). Particularly, agricultural water use is difficult to estimate in large irrigation systems, due to the absence of water meters (Alexandridis et al., 2009). In addition, the classical approaches to estimating water consumption are not sufficient, as the field data can become outdated (Bastiaanssen et al., 1998a). Spatio-temporal information on ET_a , specifically for large-scale irrigation schemes, assists decision-makers to better quantify water depletion and establishes links between land use and water allocation (Bastiaanssen et al., 2005). RS is an efficient way of gathering large amounts of information from vast areas without the need to be physically present at the observed surface. The potential of RS techniques in ET_a estimation has been widely acknowledged for enhancing the management of irrigation systems (Bastiaanssen et al., 1998b). There are several different models of ET_a based on RS data: the Surface Energy Balance Algorithm for Land (SEBAL) (Bastiaanssen et al., 1998a, 1998b), the Simplified Surface Energy Balance Index (S-SEBI) (Roerink et al., 2000), Mapping EvapoTranspiration at High Resolution with Internalized Calibration (METRIC™) (Allen et al., 2007a), ETLook (Pelgrum et al., 2010) and the Operational Simplified Surface Energy Balance Model (SSEB_{op}) (Senay et al., 2013). Biswas (1984) reported that the monitoring tool should be cost-effective, have maximum coverage (especially for large-scale irrigated projects) and obtain accurate real-time information. However, selecting the most appropriate model as a monitoring tool is still a challenge, as many requirements should be considered.

1.2.4 The impact of irrigated agriculture on basin hydrology

Irrigated agriculture plays a vital role in increasing food productivity, which has led to it becoming a major consumer of water. Large-scale irrigation projects are, then, implemented in many regions all over the world because of their paramount importance. These projects are normally located at the upstream end of river basins, and have proliferated in semi-arid regions (Chen, 2005). Many researchers (e.g. Stanzel et al., 2002; Van Oel et al., 2008; Petes et al., 2012) have highlighted the impact of irrigation systems on water availability (quantity and quality) in the downstream areas of river basins. Upstream water abstraction has a decreasing effect on the inflow volume downstream (Van Oel et al., 2008). In terms of water quality, water withdrawals from the upstream watershed lead to decreased freshwater input, which poses threats to downstream ecosystems (Petes et al., 2012). Also, the quality of water is affected by the return flow from irrigation schemes, due to higher concentrations of fertilizer and pesticides (Stanzel et al., 2002). The implications of large-scale irrigation schemes, especially in Africa,

have had inadequate attention (FAO, 1997). Water shortages and low quality often lead to conflicts between upstream and downstream users (Petes et al., 2012); therefore, the assessment of possible impacts caused by irrigation systems is a relevant subject.

1.3 Large-scale irrigation schemes in the Nile Basin

In the Nile Basin, agriculture is a major livelihood strategy, sustaining tens of millions of people. Agricultural workers account for greater than 75% of the basin's labor force, and the agricultural sector contributes one-third of the Gross Domestic Product (GDP) (Karimi et al., 2013). The total irrigated area in the Nile Basin, including large- and small-scale traditional types, is about 7.5 million hectares (FAO, 2011). Despite the basin's abundant natural resources, its people face environmental degradation, food insecurity and poverty, which is probably linked to poor water resources management (FAO, 2011). While irrigation can enhance food production through higher yield, the yield of the main crops in most of the Nile Basin's irrigated farming systems, except the Egyptian Nile Delta, are still very low (Karimi et al., 2013).

Sudan is a part of the basin whose economy relies on agriculture (Abdelhadi et al., 2000). The country is facing a situation of fast-growing demand versus limited water resources, just as the other Nile Basin countries are. Therefore, Sudan must produce more, using less water. Although the country has around 80 million hectares of arable land, the current cropped area does not exceed 17 million hectares, and only 2 million hectares are served by irrigation networks (Ian, 2012). Sudan hosts the second-largest area of national irrigated land in the Nile Basin countries (Bastiaanssen and Perry, 2009), as shown in Figure 1-1. The Sudanese large-scale irrigation systems (Gezira at 900,000 ha, New Halfa at 190,000 ha, Rahad at 126,000 ha and El Suki at 38,000 ha) show poor performance resulting from a lack of performance evaluation and monitoring (Hamid et al., 2011). Improved agricultural water management in terms of crop, water and land management can increase food production, thereby alleviating poverty and hunger in an environmentally sustainable manner (Karimi et al., 2013). However, increasing food production with limited water resources is still a challenge to the irrigated-agriculture sector.

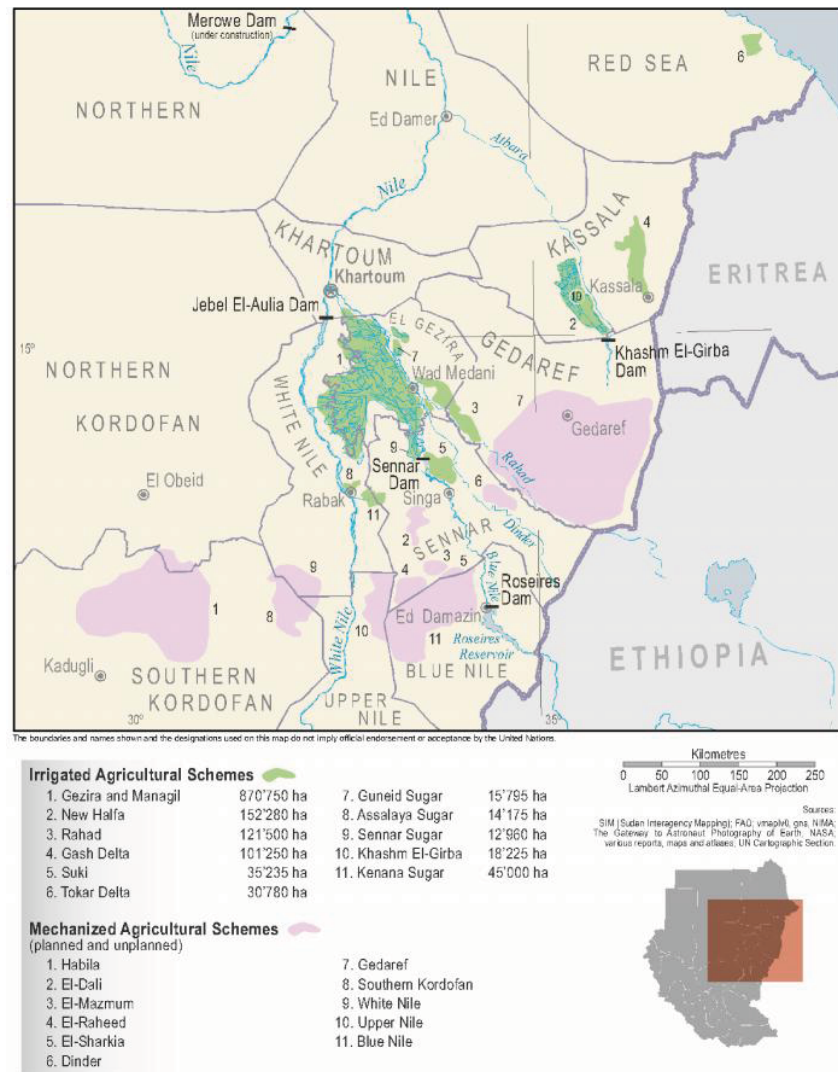


Figure 1-1. Location of the large-scale irrigated schemes in Sudan

Source: UNEP (2007)

As mentioned earlier, the absence of a physical assessment of an irrigation system leads to poor management and operation of that irrigation system, and the Sudanese Gezira Scheme, where performance evaluation and monitoring are absent, is no exception. This research focuses on the Gezira Scheme as a case study, as it is the largest scheme, not only in the Nile Basin but also in the world, under one management. The primary water source for the scheme, as for all large schemes in Nile countries, is surface water. The scheme withdraws between 6 and 7 billion cubic meters (BCM) annually, which is equivalent to one-third of Sudan's share of the Nile waters, as determined under the Nile Waters Agreement with Egypt in 1959 (Ibrahim et al., 2002). The Gezira Scheme has experienced severe irrigation water wastage problems in the last two decades, and inefficient productivity (Ibrahim et al., 2002; Adeeb, 2006).

Developing suitable tools and a strategy for identifying the reasons and managing the agriculture water use at the scheme could save water and increase water productivity. The Gezira case study may serve as a model to evaluate other large agricultural projects, especially in Sudan, with similar criteria. Thus, it may lead to an increase in overall irrigation and productivity efficiency, and is highly relevant to overall basin planning.

1.4 Problem definition

Despite the large annual volume of irrigation water released to the scheme, Ahmed (2009) points out that crop water demand is not met. Accurate information is lacking, and the reasons for and locations of the water shortages in the area, unclear (Woldegebriel, 2011). Poor distribution and management of irrigation water are major factors contributing to this situation and create conflict between upstream and downstream farmers (World Bank, 2000; Woldegebriel, 2011; Karimi et al., 2013). As a result, reduced and untimely irrigation, and volume of water per crop became the practice, which led to declining crop yields and declining tenant and scheme income (Eldaw, 2004). The poor water distribution is caused by the huge amounts of sediment entering the scheme (Ibrahim et al., 2002; Ahmed, 2009). In addition, the drainage network does not work properly, as it is limited to major and collector drains with an absence of field drains (Plusquellec, 1990). The drained water is ponded in large local depressions unsuitable for agriculture, and lost to evaporation (Ahmed, 2009). Hence, no return flow from the excess irrigation water is reused. These factors led to low water productivity and wastage (FAO, 2011). Despite the frustrating problems facing the Gezira Irrigation Scheme, the causes and consequences of the problems are not yet known precisely. In particular, it is not clear how sediment concentration has affected the water distribution pattern in the Gezira Scheme. This calls for a spatio-temporal distribution investigation utilizing RS and Geographic Information System (GIS) techniques.

The Sudanese government has conducted several reforms and actions in the scheme, changing the agricultural crops and increasing water diversion from the Blue Nile. No long-term quantitative assessment of the irrigation performance of the Gezira Scheme has been carried out. Most previous studies have evaluated the performance of the scheme for a specific year (e.g. Thiruvarduchelvan (2010), Mohamed et al., (2011)). Other research has focused on crop productivity and crop yield for evaluating the conducted water policies (e.g. Guvele (2001), Adeeb (2006), and Elamin et al., (2011)). However, the irrigation efficiency and rainwater supply have not yet been assessed.

There are several challenges related to irrigation water management in the Nile Basin, and one of the main ones is weak water monitoring (NBI, 2012). Evaluating the performance of the Gezira Scheme based on point (one value) measurement is not an accurate assessment, especially as it covers thousands of square kilometers. This vast area limits large-scale data collection for the scheme. Therefore, RS techniques are useful for monitoring water consumption (ET_a). Yet estimating ET_a using such methods has been carried out to determine crop coefficients for specific farms and years (Ahmed et al., 2010; Bashir et al., 2007, 2008). It is still a challenge to obtain accurate and up-to-date information on the spatial and temporal distribution of crop water requirement (CWR). As the Gezira Scheme covers a vast area, even utilizing a remotely sensed water consumption monitoring system still demands real-time and historical analysis.

The volume of water available to Sudan is about 37 BCM per year, of which 90% is consumed by the agricultural sector (Ahmed et al., 2007). Any further expansion in agricultural activity will result in more demand for irrigation water. Sudan has plans to unilaterally develop the water resources of the Blue Nile for irrigation, which will increase large-scale irrigation scheme withdrawals from 8.5 to 13.8 BCM (McCartney et al., 2012). According to the Sudanese 2025 water strategy, the currently available water resources are far below the projected demand. Increasing large-scale irrigation efficiency is seen as a water conservation measure, and management need to face the increasing future water demand (Bastiaanssen and Perry, 2009).

1.5 Research questions

- Can irrigation, rainfall and productivity give a clear indication of opportunities to improve the efficiency and productivity situation?
- Can satellite data and its acquisition help to provide reasonable estimates of water abstraction values on a regional scale?
- What is the accuracy of using satellite images combined with meteorological data to determine the large-scale distribution of evapotranspiration?
- What is a suitable algorithm for calculating remotely sensed ET_a for the Gezira Scheme?
- Can satellite images be used to identify water surplus and deficit areas?
- What are the possible water management scenarios for the scheme?
- How much water can be saved when increasing irrigation efficiency?

1.6 Research objectives

Given the above stated problem, the following research objectives have been formulated:

General objective:

The aim of this research is to use remotely sensed techniques complemented by actual measurements to improve the management decisions of large-scale irrigation systems through feedback information made available by a performance evaluation process.

Specific objectives:

- Evaluate the irrigation performance of the large-scale irrigation schemes in terms of irrigation water supply, rainwater supply and crop productivity.
- Assess the optimal approach of obtaining ET_a for large-scale irrigation schemes, using different RS-based techniques.
- Develop an RS monitoring tool to determine water abstraction from large irrigated schemes.
- Investigate possible irrigation management scenarios and their implications for the downstream river flow.

1.7 Structure of the thesis

Evaluation of the irrigation performance of the Gezira Scheme and the study of its implications for the downstream Nile flow requires a combination of hydrological, geographical and climatic sciences methods. This involves a strong focus on remotely sensed satellite image analysis. The overall methodology chart is shown in Figure 1-2.

The thesis is designed to have four chapters (Chapters Three, Four, Five and Six) to achieve the stated objectives. The literature review of the selected methodologies (irrigation performance indicators and RS monitoring of water consumption) and the results will be discussed in detail in those chapters. Understanding the characteristics of the study area is meaningful; therefore, the research area is illustrated in Chapter Two in terms of geographical location, climate, availability of water supply and demand.

As the historical monitoring and evaluation of irrigation schemes is considered the first and most important step, Chapter Three describes the methods and the obtained results for the spatio-temporal performance of the large-scale Gezira Irrigation Scheme.

Chapter Four shows the comparison of four different remote-sensing-based ET models applied at the Gezira Scheme.

The lack of an actual monitoring system of water consumption for the Gezira Scheme presents an opportunity to develop a tool to monitor agricultural water use, and its application is illustrated in Chapter Five. The chapter further discusses the monitoring of water abstraction by utilizing two different sources of satellite images for the last 14 years. Both summer and winter crop seasons have been investigated. In addition, the total water volume diverted from the river to the Scheme can be obtained from the remotely sensed data.

Chapter Six investigates possible management scenarios to save water, and the expected volume of saved water is quantified.

Finally, Chapter Seven presents the conclusions and recommendations of the current research, and possible paths toward enhancing the achieved results.

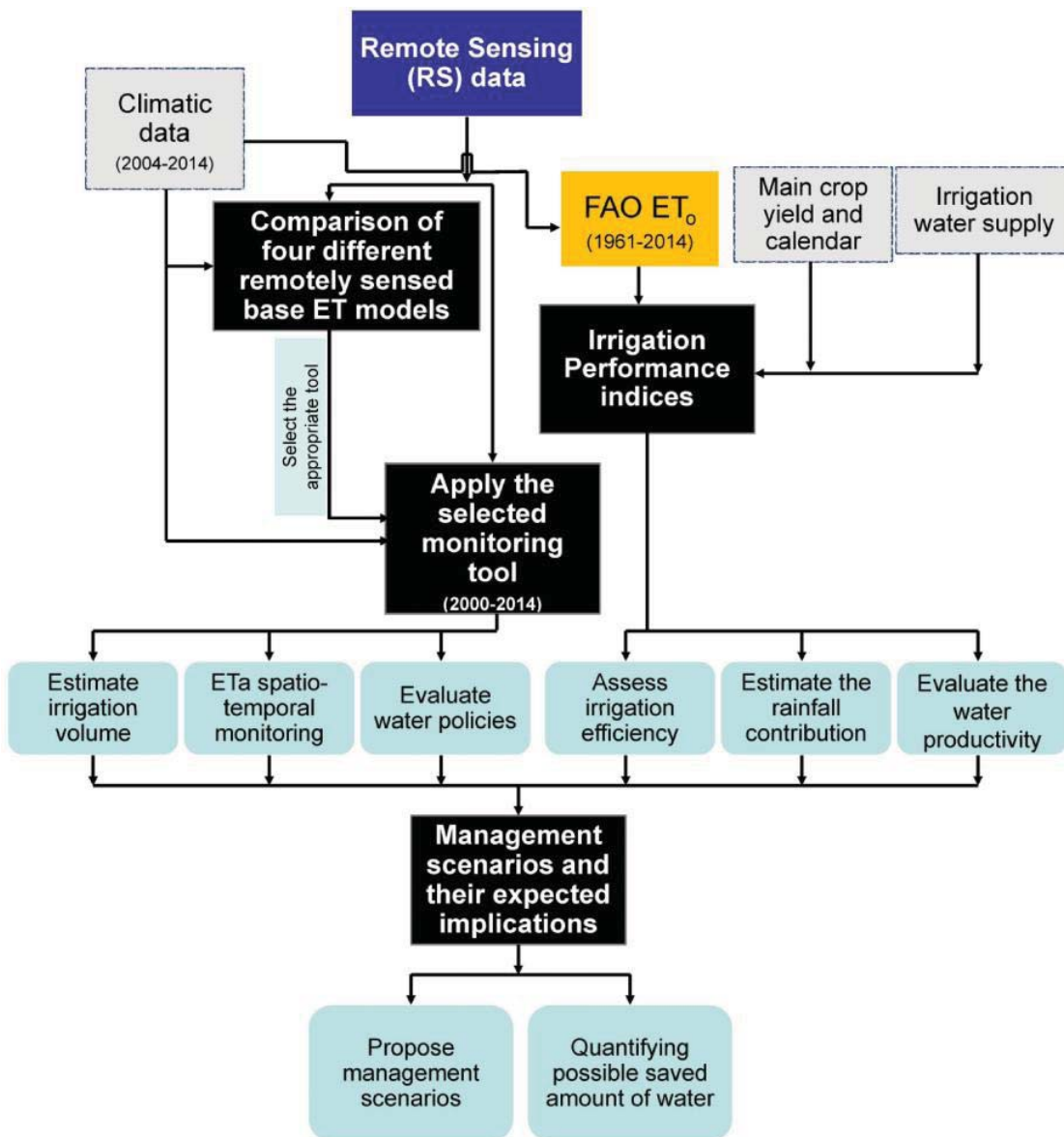


Figure 1-2. Methodological outline of the research

CHAPTER TWO

DESCRIPTION OF THE GEZIRA IRRIGATION SCHEME

2.1 Geographical description

The Gezira Scheme is located in the heart of Sudan, which has a long irrigation history. The scheme started in 1911, in the early years of Anglo-Egyptian rule of the Sudan, as a pilot project for growing cotton as a cash crop and was officially inaugurated in 1925 (Worldbank, 2010). The irrigated area lies in the flat, central plains between the Blue and White Nile rivers south of Khartoum, as shown in Figure 2-1, and covers an area of about 1 million hectares (FAO, 2011). The scheme is split into two main areas, Gezira (0.5 million ha) and Managel (0.4 million ha). It lies between latitudes 13°30' N and 15°30' N, and longitudes 32°15' E and 33°45' E. Elevations vary between 385 m and 415 m above mean sea level (AMSL), with an average elevation of 405 m. The width of the scheme from east to west is about 75 km, and its maximum length from north to south is approximately 245 km. The whole area is flat with a very gentle slope of 15 cm/km from south to north and east to west, thus providing an ideal situation for gravity flow (Plusquellec, 1990). The soil is also uniform and characterized as high clay content (50%–60%), vertisols soil.

Despite the Gezira Scheme being part of the White Nile Basin from a hydrological point of view, the irrigation water is diverted from the Blue Nile. The Blue Nile has an average annual flow of 50 BCM and contributes about 70% of the yield of the Nile (NBI, 2012). The seasonal variation of its discharge ranges from over 10,000 m³/s at the peak of a high flood, to 60 m³/s in a very low year. The flow of the Blue Nile is regulated by the Sennar Dam, built in 1925, and the Roseires dam, completed in 1966. The total live storage capacity of the two reservoirs represents only 5% of the average annual flow of the river.

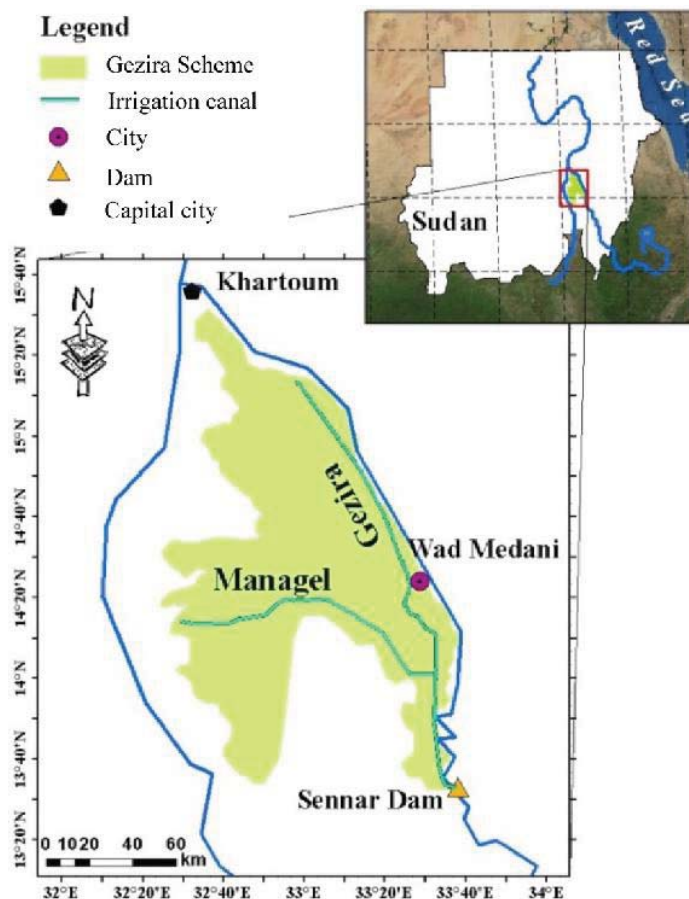


Figure 2-1. Location of Gezira Irrigation Scheme in Sudan

2.2 Climate conditions

The Gezira Scheme is located in an arid, hot climate (Elagib and Mansell, 2000; Elagib, 2010). There are three distinct seasons: autumn (June–September), winter (November–February) and summer (April and May) (Ahmed et al., 2007; Bashier et al., 2008; FAO, 2011). The area experiences low annual rainfall of 350 mm in the southern part close to Sennar, and 150 mm in the northern part near Khartoum, as shown in Figure 2-2. The rainfall records in Figure 2-3 show that peak rainfall is in July and August. The climatic data of the Wad Medani station (14°24'0.00"N, 33°28'48.00"E), shown in Figure 2-1, represents the climate of the scheme quite well. Many researchers (e.g. Adeen, 2006; Ahmed et al., 2007; Bashir et al., 2007, 2008) have utilized the climatic data from this station to calculate grass reference evapotranspiration (ET_o) using the FAO Penman–Monteith ET_o equation (Allen et al., 1998), and the measured rainfall at the scheme.

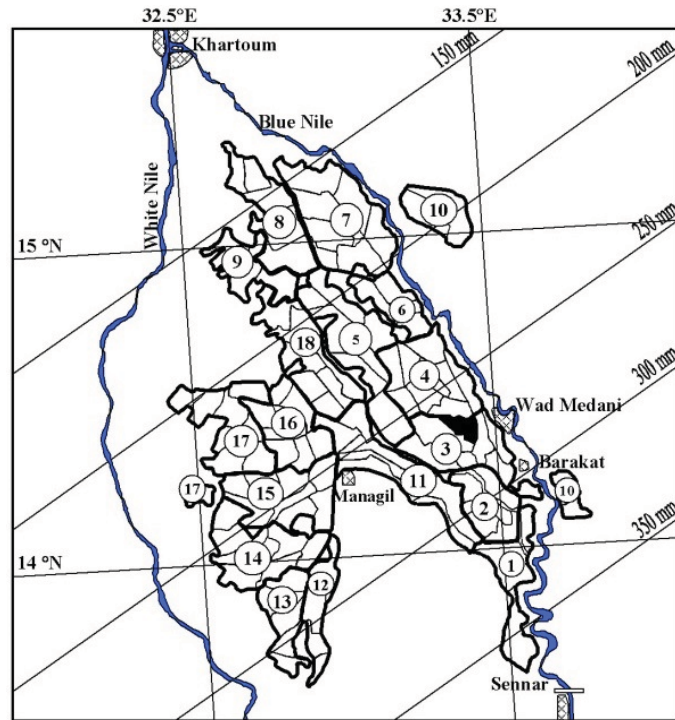


Figure 2-2. Isohyetal rainfall map (1971–2000) and Gezira groups. (The group name is defined in Table 2-1 by the ID number)

Source: Adam et al. (2002)

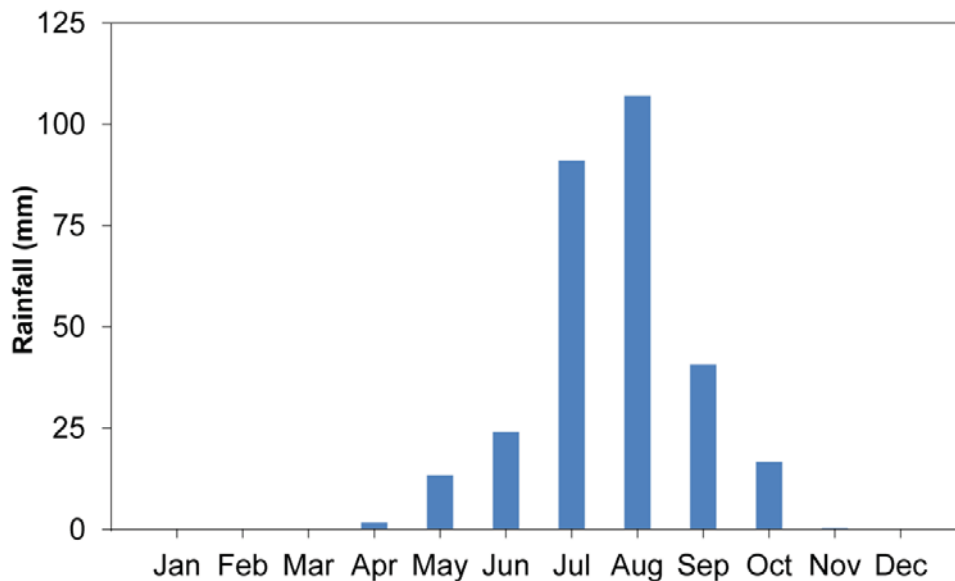


Figure 2-3. Average monthly rainfall for the Wad Medani station (1961–2012)

The mean daily temperatures at the Wad Medani meteorological station are 31°C in summer, 29°C in autumn and 25°C in winter. Figure 2-4 shows the mean monthly maximum and minimum temperatures for the scheme. Both parameters have their minimum values during the period November–January (winter season). The highest values were recorded during April and June, then a drop in temperature occurs during the autumn due to the rainy season. The mean daily relative humidity (Figure 2-5) is relatively low (18%) in summer, high (55%) in autumn, and moderate (28%) in winter. The variation of the annual ET_0 and Rainfall is presented in Figure 2-6.

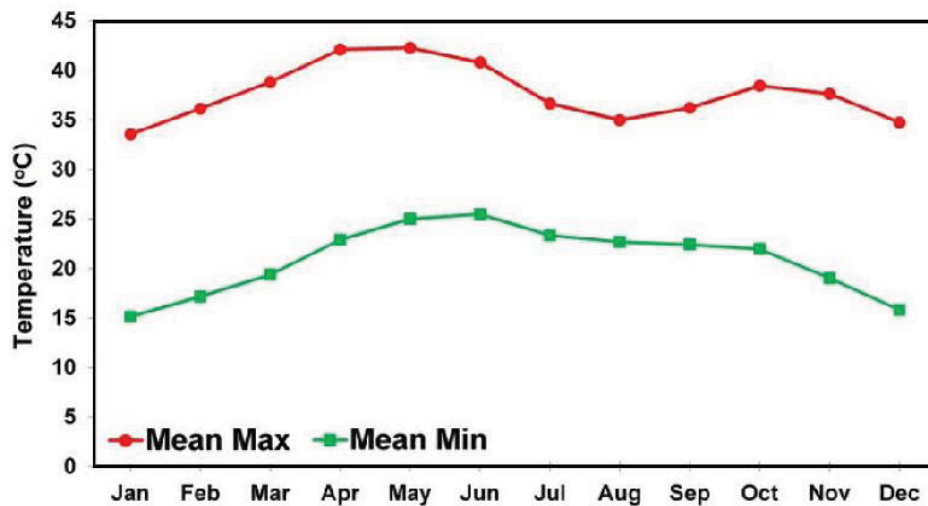


Figure 2-4. Monthly average maximum and minimum temperatures for the Gezira Scheme (1961–2012)

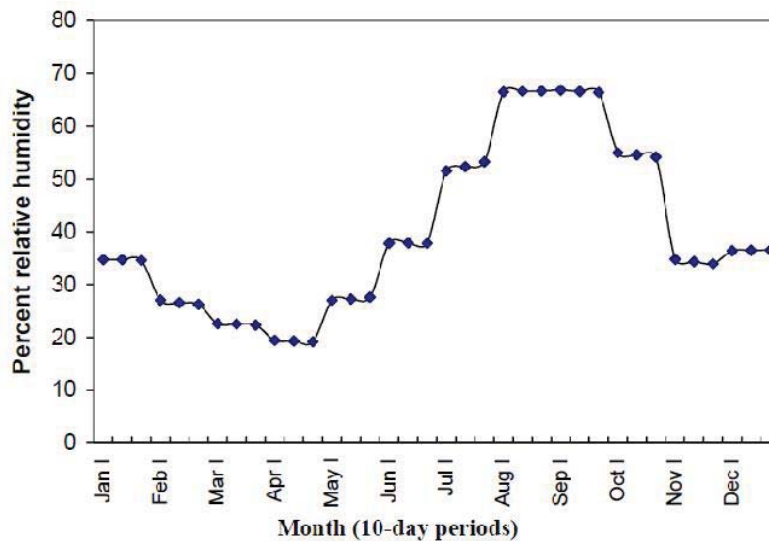


Figure 2-5. Mean percentage relative humidity for the Gezira Scheme

Source: Ahmed et al. (2007)

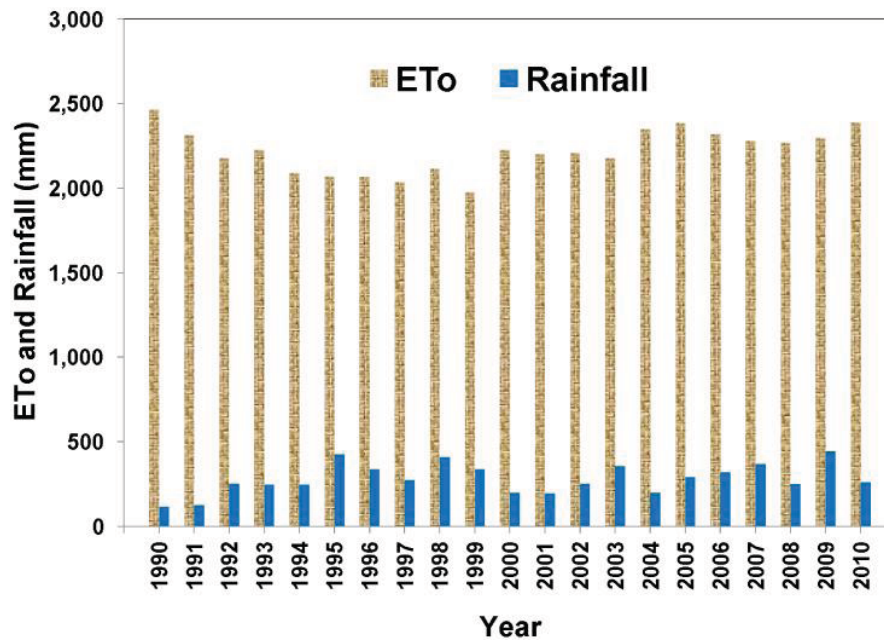


Figure 2-6. Annual variation of reference evapotranspiration (ET_o) in comparison with rainfall in the Gezira Scheme

This climate allows the Gezira Scheme to have two farming seasons: a summer crop season (the wet season, June–November) when the monsoon brings average rains of 300 mm per year to the area, and a winter crop season (the dry season, November–March). This makes the irrigation crop season June–March. Normally, the remaining months (April and May) are allocated for irrigation network maintenance (Adeeb, 2006).

2.3 Management authority

2.3.1 Administrative structure

The scheme is divided into 18 administrative groups, as listed in Table 2-1, each of which is divided into 4–8 blocks, making a total of 113 blocks, as shown in Figure 2-2. The Gezira area has around 120,000 farmers (FAO, 2011), each of whom is assigned an area of 6–8 hectares (Adam et al., 2002). The whole scheme is under the management of the Sudan Gezira Board (SGB), as shown in Figure 2-7, which has assistants in the Head Quarters (HQ) and is helped by 18 Group Managers and 113 Block Inspectors (BI) in the field (Plusquellec, 1990).

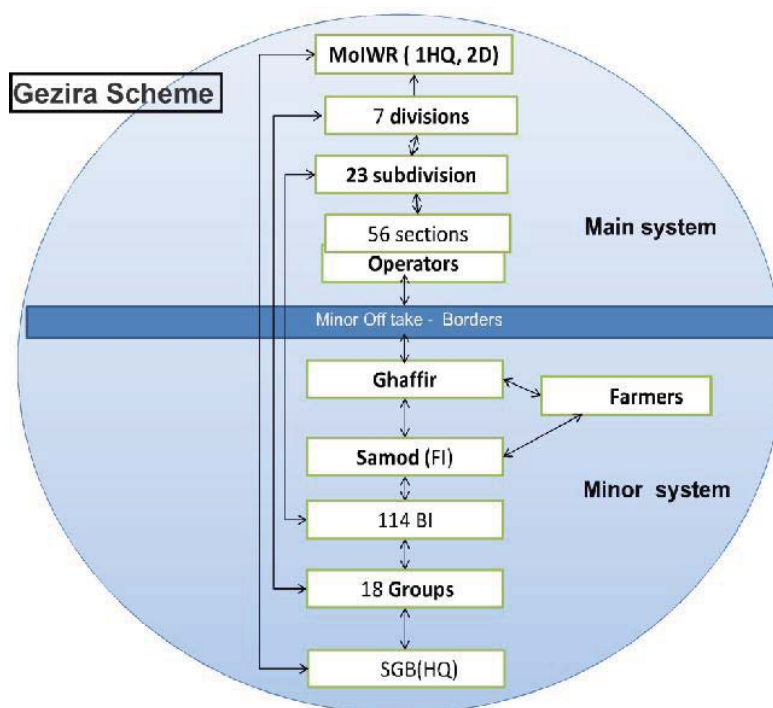


Figure 2-7. Operation system and management interaction in the Gezira Scheme
Source: Woldegebriel (2011)

Table 2-1. Group names and areas of Gezira Scheme; after Adam et al. (2002)

ID	Block	Area (km ²)	ID	Block	Area (km ²)
1	South	698.2	10	Eastern*	—
2	Hosh	449.6	11	Mikashfi	811.6
3	Center	712.6	12	Shawal	345.9
4	Massallamia	758.7	13	Gamusi	409.7
5	Wadi Sha'eer	877.2	14	Matori	809.0
6	Wad Habouba	315.2	15	Ma'toug	750.3
7	North	1011.7	16	Mansi	571.4
8	North West	683.7	17	Shawal	345.9
9	Abu Gouta	412.8	18	Huda	812.3

*The block is not irrigated from the irrigation network; thus it is ignored in this study.

2.3.2 Institutional management

The operation of the scheme is centrally controlled. Management is distributed between the Ministry of Irrigation and Water Resources (MOIWR), which is responsible for the irrigation network, and the Sudan Gezira Board (SGB), whose role is agricultural operation

(Plusquellec, 1990). However, many water policies have been changed, which will be discussed in Chapter Five. Previously, the orders of agricultural water demand used to pass on to the MOIWR engineers and were then summed up throughout the system to the head works at the Sennar Dam. Then, the MOIWR used to deliver the required discharge at the head of the main channels, while SGB used to be responsible for the operation of the minor channels and, finally, the delivery of water to the farmers. This created conflict between the SGB and the MOIWR over management methods (Adam et al., 2002).

In 1999, responsibility for the minor channels (maintenance and distribution of irrigation water) was transferred to the SGB, leaving the main and major channels to the MOIWR. Since that time, the system has experienced serious deterioration by mismanagement of maintenance of the irrigation channels (Ahmed, 2009). Therefore, irrigation management was handed over again to the MOIWR in 2006 by the new Gezira Law. The law created Water User Associations (WUAs) for better distribution management. Ahmed (2009) did not expect the new law to be successful for managing the scheme, which underwent a complete change in management in 2009/10 through the implementation of the 2005 Gezira Act. This effectively privatized the scheme and transferred responsibility for irrigation to landowners, WUAs devolving control and, by association, planting decision-making to the farmers, thereby allowing planting flexibility within the water delivery regimes (Ian, 2012).

Since 2011, the MOIWR and the Ministry of Water Resources and Electricity (MWRE) have merged, and irrigation handed over to the Ministry of Agriculture, Livestock and Irrigation (formerly the Ministry of Agriculture) (MWRE, 2014; KRT, 2014).

2.4 Water resources

2.4.1 Irrigation water system

Water storage. The Blue Nile supplies the water for the Gezira Scheme. Irrigation water is supplied from two reservoirs, at Roseires and Sennar. The Blue Nile has an average annual flow of 50 BCM at Roseires, with large seasonal and annual variations. The flow of the Blue Nile rises steeply between the end of June and the end of August, and carries large quantities of sediment as a result of land degradation caused by the heavy seasonal rainfall on the Ethiopian Plateau.

Conveyance and water distribution system. The Gezira is the only gravity-fed large irrigation scheme in Sudan. Only about 70,000 feddans of the total command area of 2.1 million feddans (3.3%) are not under gravity irrigation (World Bank, 2000). Most of the non-gravity-fed areas lie on the eastern bank of the Blue Nile (Eastern Blocks), in addition to a small area

in Hag Abdallah Block (Southern Gezira), which, for topographical reasons, is irrigated by pumps (Eldaw, 2004). Irrigation water is supplied through an extensive system of low-percolation, unlined earth channels consisting of two main channels, the Gezira (14.5 million m³/day) and the Managel (16.0 million m³/day). The discharge of these channels is calculated through an updated equation using the measured water level as a function. The water level is measured three times per day by MOIWR engineers, as shown in Figure 2-8.

The scheme has unlined channels because of the physical properties of the impermeable clay soils of the area, and the conveyance and distribution efficiency of the network of unlined channels in the scheme was estimated by Plusquellec (1990) to be 93%.



Figure 2-8. Measuring the water level to estimate the daily discharge of the Gezira channel during the field visit (26/12/2011)

A schematic map of the twin channels is presented in Figure 2-9. They run north to the first group of channel regulators, 57 km from the dam. From there, four branch channels convey water to the Managel extension, while the main Gezira channel runs north for another 137 km. Major channels take water from the main and branch channels, supplying water to minor channels. These channels flow continuously throughout the growing season. The network consists of 2,300 km of branch and major channels, and over 8,000 km of minor channels. The latter supply water via gated outlet pipes to field channels (Abu XX), which irrigate 38 hectares. Each is divided into 18 fields of five feddans (called hawasha). However, the irrigation infrastructure is in serious disrepair, and the distribution of water is inefficient and wasteful, with low cost recovery (World Bank, 2000).

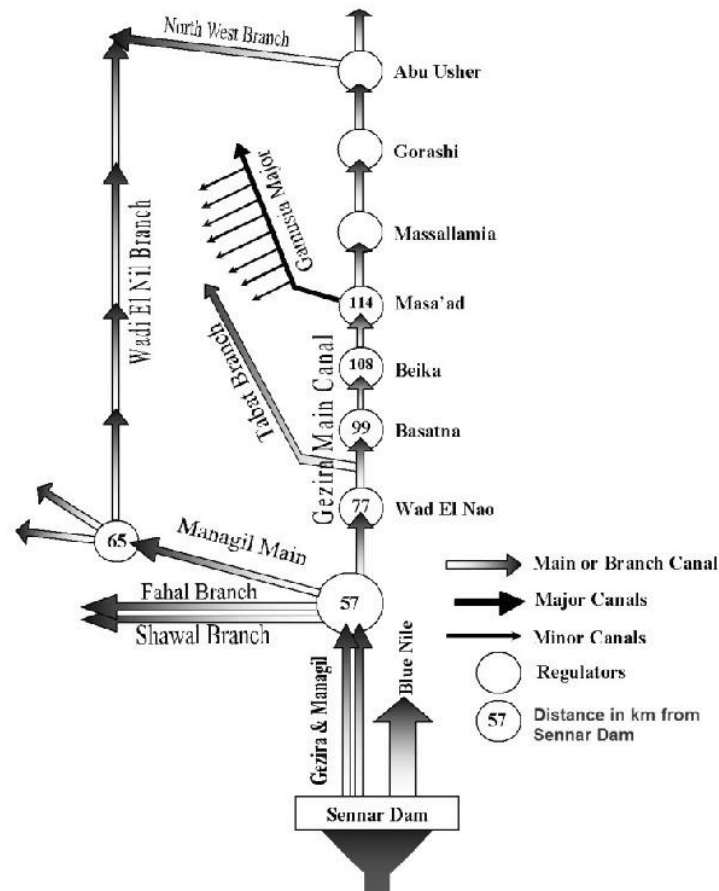


Figure 2-9. Schematic diagram showing the irrigation water system in the Gezira Scheme
Source: Adam et al. (2002)

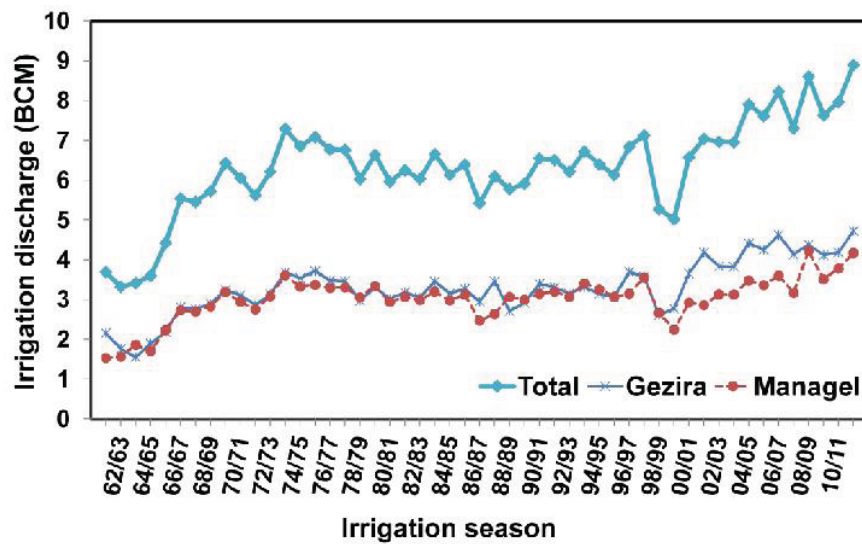


Figure 2-10. Total annual irrigation water diversion to the Gezira Scheme through the two main channels (Gezira and Managel) for 1961–2012

A group of regulators and hydraulic structures was built to convey irrigation water. However, due to a lack of maintenance and management, the efficiency of these regulators and structures has widely deteriorated. As a result, water delivery became difficult at various times and in certain regions within the irrigated area (Eldaw, 2004).



Figure 2-11. The Basatna regulator hydraulic structure 99 km from the Sennar Dam

All channels in the system are infested with two main problems: siltation and weeds (Plusquellec, 1990; Ahmed and Ismail, 2008). The siltation problem caused a reduction of the Sennar Dam storage capacity, which negatively impacted the regulations governing the release of water (Eldaw, 2004). In addition, more silt is carried into the system, causing increasing silt deposits in the irrigation channels. Ahmed (2009) mentioned that the huge amounts of sediment entering the scheme and the mismanagement of the irrigation system caused inequity in water distribution and, as a result, a reduction in crop production. The accumulation of silt over the years has also created conducive conditions for channel infestation by abundant weed growth (Eldaw, 2004). The weeds (defined as a plant that is not desired at its place of occurrence) are classified in the Gezira Scheme into three categories: floating, submerged and emerged (Ahmed et al., 1989 as cited in World Bank, 2000). The weed phenomenon is considered a vital problem for the minor channels (Ahmed, 2009). It limits water flow to the extent that water cannot reach the end of minor channels (World Bank, 2000). During the field visit, it was noted that one of the reasons proffered by farmers for water shortage at the tail end of the system was the prevalence of these weeds. Therefore, some farmers were using pumps to abstract water from the channels into their fields, as shown in Figure 2-12.

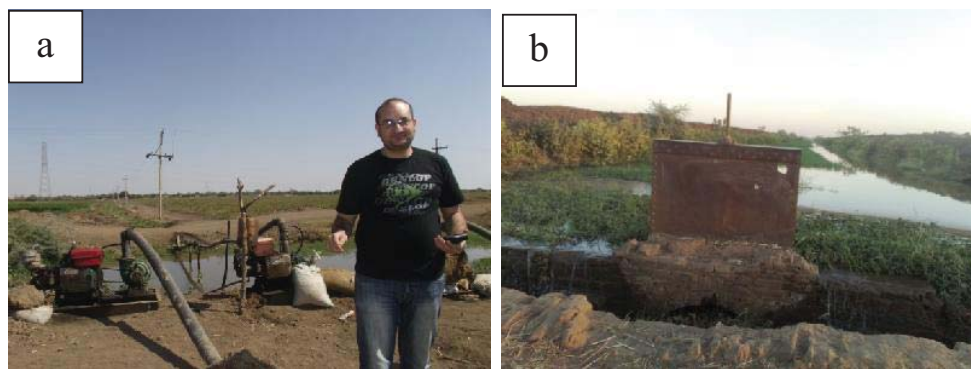


Figure 2-12. Farmers' water pumps are used to convey water to their fields (a) and weeds in a minor channel (b); Center block, 20/12/2011.

Siltation and weed infestation have become serious problems in the Gezira Scheme. Both reduce the transit capacity of channels, which, in turn, decreases the discharge (World Bank, 2000) as a result of the failure to provide adequate funds for operation and maintenance (World Bank, 2010).

Drainage system. The soil of the Gezira Scheme is characterized by high clay content (50%–60%) (Bashir et al., 2008). Therefore, the original design of the drainage network is limited to major and collector drains without field drainage (Plusquellec, 1990). The main purpose of the drainage network is to remove surface runoff due to rain or excess irrigation, not drained water from the farm, because of the nature of the soil and absence of a high groundwater table (World Bank, 2000). Plusquellec (1990) mentioned that the existing minor drains are completely silted up. The drained water is ponded in large local depressions unsuitable for agriculture, and thus lost to evaporation (Plusquellec, 1990; Ahmed, 2009). As part of the present study, several field visits were conducted during 2011–13, including interviews with irrigation engineers, which confirmed that the situation still exists. Generally, there is no reuse of drainage water in the Sudanese irrigation system (Achamyeleh, 1993). The scheme faces a lack of appropriate operation and maintenance of the irrigation and drainage network (FAO, 2011). Hence, no return flow from the excess irrigation water is reused.

2.4.2 Groundwater

The Gezira area has a groundwater aquifer whose storage capacity is estimated at 60 BCM, with an annual recharge of 0.6 BCM and annual abstraction of 0.15 BCM (Abdo and Salih, 2012). Groundwater abstraction for irrigation purposes is estimated to be 1.4 BCM, which represents 87% of the total annual groundwater abstraction, and takes place mainly in the Northern River Nile, Khartoum, Gezira, Sennar and Kassala states, and also some wadis in the western states (Mukhtar, 1997).

2.5 Crops and water demand

2.5.1 Cropping pattern and yields

Typically, there is a two-season cropping pattern in the Gezira Scheme. Summer crops include cotton, groundnut and sorghum, while winter crops are dominated by wheat. The summer crops are normally planted between the start of June and mid-July, depending on the crop type. The planting date of sorghum, for example, varies between the end of June and the beginning of July (Farbrother, 1996; Ahmed et al., 2007). The present cropping pattern is the result of a rigidly set, five-year crop rotation sequence. The scheme was designed with the main objective of producing cotton. After adoption of the liberalization policy in 1981, farmers started to grow other crops such as sorghum, wheat and groundnut (Karimi et al., 2013). The current crop rotation sequence in the Gezira has been used since the 1991/92 crop year and is as follows: cotton–wheat–sorghum–groundnut–vegetable/fallow (World Bank, 2000). Recently, sorghum, as an important staple food in Sudan, has become the main crop in terms of cropped area in the Gezira Scheme, covering an average of 35% of the total planted area, followed by wheat (25%–30%), then cotton (less than 24%) and groundnut (about 20%). Wheat is not a traditional crop in the Gezira, but the recent rapid rise in demand has led to an expansion of production promoted by the government in the mid-1980s. In the early 1990s, wheat became a mandatory part of the four-crop, one-fallow rotation.

In general and based on field trials, the crop yields in the Gezira Scheme are below potential yield (World Bank, 2000). The yields for sorghum and groundnut have been low (half of the potential yield) principally due to a termite problem (World Bank, 2000; FAO, 2011). Table 2-2 demonstrates that yearly yields vary. Factors held to be responsible include water shortages, inadequate application of fertilizers, and lack of information and technical guidance for farmers (FAO, 2011). Additionally, Plusquellec (1990) mentioned that waterlogging due to impermeable clay soils badly depresses yields. The cropping pattern and their average yields for the main crops (1990–2007) are shown in Figure 2-13.

Table 2-2. Actual crop yields (1997–2007) in the Gezira Scheme

Crop	Unit	1997/98	1998/99	1999/00	2000/01	2001/02	2002/03	2003/04	2004/05	2005/06	2006/07	Average
Groundnut	t/fed	1.04	0.50	0.65	0.66	0.73	0.80	0.81	0.92	0.82	0.90	0.78
Cotton	k/fed	4.48	4.42	2.57	4.47	5.25	5.05	3.51	4.30	4.09	3.20	4.13
Sorghum	t/fed	1.04	0.79	0.67	0.95	0.98	0.98	0.83	1.06	0.90	1.02	0.92
Wheat	t/fed	0.70	0.31	0.50	0.80	0.80	0.85	0.83	0.73	0.65	0.99	0.72

Source: FAO (2011)

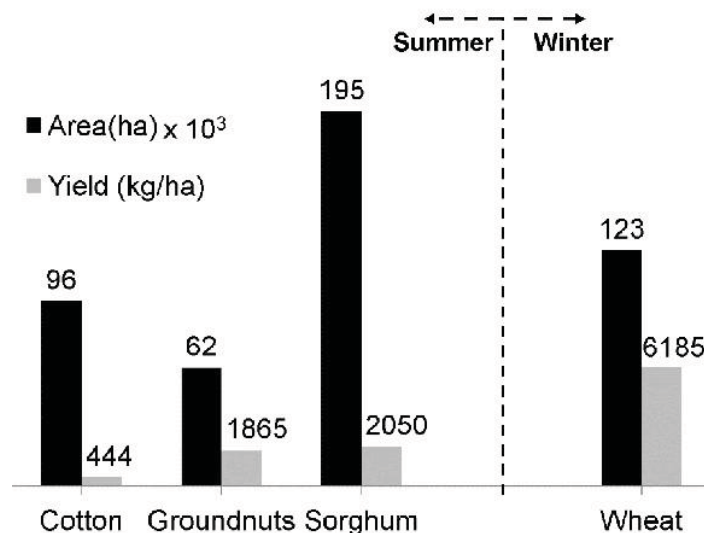


Figure 2-13. Average cropping pattern areas and yield for the main crops in the Gezira Scheme (1990–2006)

2.5.2 Crop water requirements (CWR)

CWR depends on climatic and crop factors. In the Gezira Scheme, the crops are grown on flat clay soil, so the deep percolation and runoff losses are negligible (Farbrother, 1996; Ahmed et al., 2007; Adam, 2008). Therefore, CWR in the Gezira Scheme is just the water needed to cover water losses through crop evapotranspiration (ET_c).

Farbrother (1996) conducted a series of experiments under Gezira research farm conditions to estimate the crop factors, which are still in use for the scheme (Abdelhadi et al., 2000). Farbrother used the Penman (1948) formula to estimate ET_o and developed k_c values. However, the FAO Penman–Monteith (Allen et al., 1998) equation is globally recommended for CWR. Later, Ahmed et al. (2007) and Adam (2008) reported updated k_c values from Farbrother (1996) for irrigated crops in the Gezira Scheme to be compatible with the FAO Penman–Monteith formula. Ahmed et al. (2007) found that the highest summer seasonal volume required was by cotton (1268 mm), followed by groundnut (815 mm). Of the winter crops, wheat requires (657 mm). For sorghum, the seasonal ET_c takes a range of 642–704 mm (Bashir et al., 2007a, 2007b, 2008). Figure 2-14 shows the 10-day CWR average for groundnut, sorghum and cotton for the Gezira Scheme. As shown, the contribution of rainfall cannot be neglected, especially for groundnut and sorghum (Ahmed and Ribbe, 2011). However, farmers are often required to take water into their fields, even when the fields are already flooded by heavy rain (Plusquellec, 1990). The author attributed this need to the limited capacity for the escape of surplus water of the scheme, which is designed to allow spillage resulting from the sudden decrease in irrigation demand following rain.

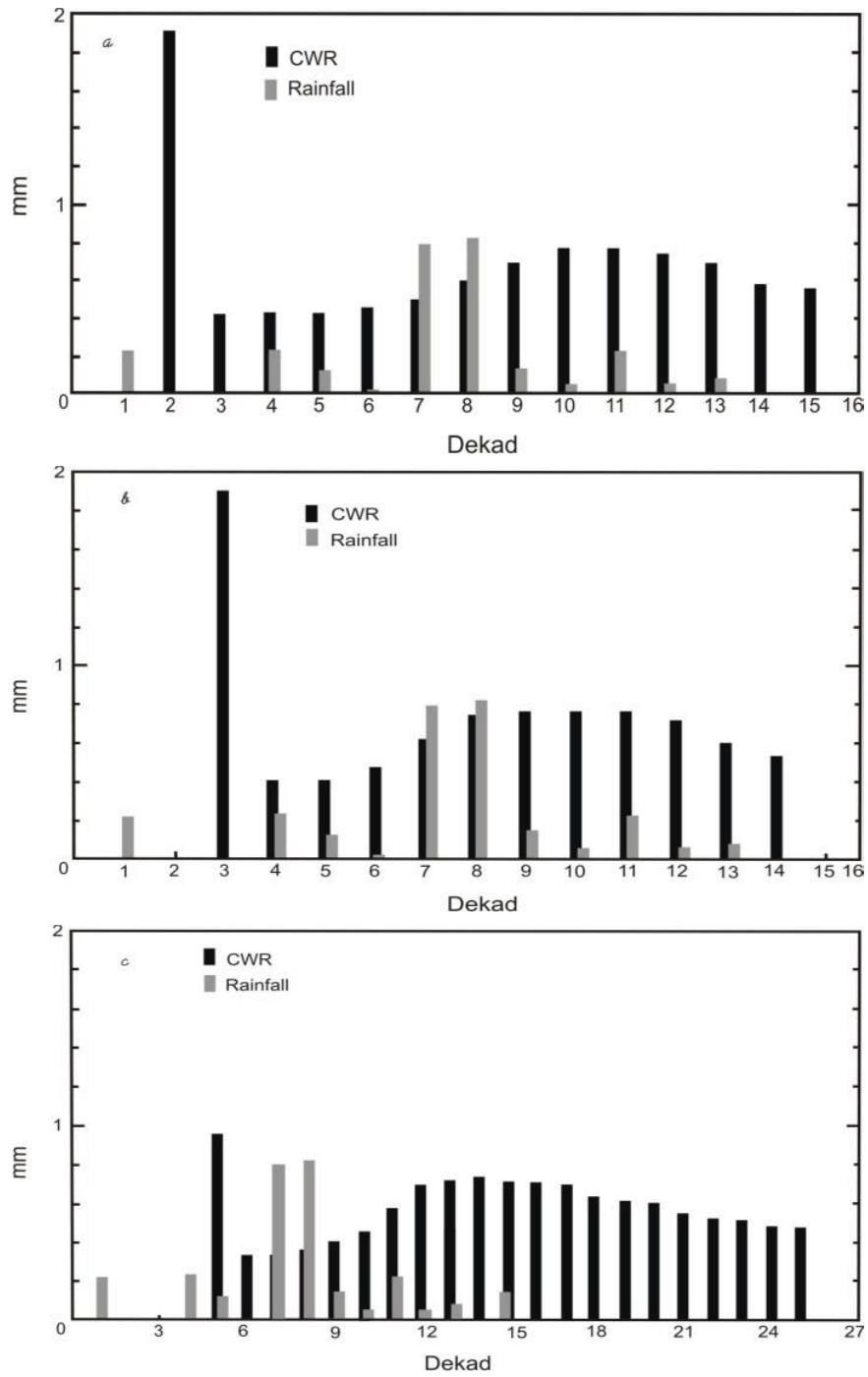


Figure 2-14. Crop water requirements (CWR m^3/ha) of (a) groundnut, (b) sorghum and (c) cotton and rainwater (mm)

Source: Ahmed and Ribbe (2011)

CHAPTER THREE

ASSESSING THE IRRIGATION PERFORMANCE OF GEZIRA SCHEME*

3.1 Introduction

Information on irrigation indicators is needed to enable the evaluation of irrigation performance and to improve irrigation water management (Kloezen and Garcés-Restrepo, 1998). Irrigation performance is characterized by the system's ability to deliver a water supply which satisfies that demanded by crops (Clemmens and Bos, 1990), and the outcome in terms of crop productivity (Bandara, 2003). Evaluation of irrigated-agriculture performance has two major components: on-farm and off-farm systems. The on-farm system, as operated by farmers, is based on the management skills of farmers, the irrigation technique and the system design (FAO, 1996). On the other hand, the off-farm system includes supply and distribution to test the system's capability to deliver water to farms with adequacy, efficiency, dependability and equity (Molden and Gates, 1990). Since the 1970s, scholars have developed several indicators to measure performance, such as efficiencies for conveyance, distribution, fields and systems (Bos and Nugteren, 1990; Clemmens and Bos, 1990; Molden and Gates, 1990). After reviewing extensive literature, Kloezen and Garcés-Restrepo (1998) suggested a list of indicators related to the performance of hydrological, agronomic, economic, financial, and environmental performance of irrigation systems. These indicators are used to describe hydrological behavior in complex irrigation schemes through few and understandable numbers (Bastiaanssen et al., 2001).

The Gezira Scheme has experienced severe problems related to irrigation water wastage in the last two decades (Ibrahim et al., 2002; Adeeb, 2006). Poor distribution and management of irrigation water are major factors contributing to this situation (Karimi et al., 2013). Adequate monitoring and evaluation of performance are needed to improve water management practices in order to achieve high overall irrigation efficiency. Therefore, the overall objective of this chapter is to assess the irrigation performance of the off-farm Gezira Scheme of Sudan.

* Part of this chapter is published in Agricultural System journal: Al Zayed, I.S., Elagib, N.A., Ribbe, L., Heinrich, J. (2015). Spatio-temporal performance of large-scale Gezira Irrigation Scheme, Sudan. *Agricultural Systems* 133, 131-142.

3.2 Material and methods

3.2.1 Source of data

Historical mean monthly climatic elements (maximum and minimum temperatures, wind speed, sunshine hours and rainfall) for 1961–2010 are available for the Wad Medani meteorological station (Latitude: 14°24'0"N, Longitude: 33°28'48"E) from the Sudan Meteorological Authority in Khartoum. Actual water supply data are obtained as irrigation discharge for the main channels (Gezira and Managel) from the former MOIWR office in Wad Medani. In addition, crop yield data for cultivated areas with crop calendars for cotton, groundnut, wheat, sorghum and vegetables for 1970–2010 are acquired from the former Ministry of Agriculture in Khartoum. All the data were acquired from official sources in Sudan during the field visits in 2011 and 2012 (Appendix One). The same data were checked for quality, and have been used and published previously by many researchers (e.g. Plusquellec, 1990; Elagib and Mansell, 2000a; Elagib, 2010; FAO 2011).

A time series of Moderate Resolution Imaging Spectroradiometer (MODIS), 16-day composite Normalized Difference Vegetation Index (NDVI), 250 m resolution, (MOD13Q1 data product) satellite images is obtained for January 2000–March 2014. The MOD13Q1 data set is freely available from the Oak Ridge National Laboratory Distributed Active Archive Center (ORNL DAAC, 2011) in GeoTIFF format. Subsequently, the Gezira area is extracted using the Extract-by-Mask tool in the ArcGIS 10 software (ESRI, 2013). The non-agriculture pixels are masked using yearly MODIS Land Cover layers (MCD12Q1 data product) obtained from the National Aeronautics and Space Administration (NASA) RS data distribution center (NASA, 2013) in Hierarchical Data Format (HDF). Finally, the extracted images are projected into a Projected Coordinate System with Universal Transverse Mercator (UTM) WGS84 datum so that all pixels in the study area have equal size, thereby making pixel-level analysis easier.

3.2.2 Crop and actual evapotranspiration

The crop water demand and corresponding cultivated land area are the two essential factors affecting water requirement. The recommended FAO Penman–Monteith (Allen et al., 1998) equation is used to calculate reference evapotranspiration (ET_o) with updated parameters such as day length (S_o) and extraterrestrial radiation (H_o) from Elagib et al. (1999). Also, solar radiation (H) is obtained with modified Ångström coefficients developed by Elagib (2009). Then, the crop coefficients (k_c) of the main crops are utilized to estimate crop evapotranspiration (ET_c) (i.e. CWR), where ET_c (mm/day) = $k_c \times ET_o$. The k_c values are adopted from Farbrother (1996), who conducted a series of experiments under Gezira research

farm conditions to estimate the crop factors, which are still in use for the scheme (Abdelhadi et al., 2000). Farbrother used the Penman (1948) formula to estimate ET_o and develop kc values. The Penman–Monteith equation is superior to the Farbrother method for predicting ET_c (Abdelhadi et al., 2000). Later, Ahmed et al. (2007) and Adam (2008) reported updated kc values from Farbrother (1996) for irrigated crops in the Gezira Scheme which are compatible with the FAO Penman–Monteith formula. Ahmed et al. (2007) recommend adjustment factors of 1.1 and 1.2 for the summer season and the rest of the year, respectively, while Adam (2008) recommended an average adjustment value of 1.1 for the whole year. Therefore, kc values in this study are adopted from those offered by Ahmed et al. (2007), which are more accurate for estimating ET_c . The kc values were given for a 10-day time scale, but these are converted to monthly averages in the present study in order to conduct monthly irrigation performance assessment, as shown in Table 3-2. ET_c is defined as the potential water needed for plant growth under conditions of optimum water supply. However, the actual condition presented by ET_a always falls below the optimum value when the stomata close up, due to environmental circumstances.

Due to the lack of ET_a measurements for the Gezira Scheme, such data are estimated using the concept suggested by the FAO 33 paper (Doorenbos and Kassam, 1979), which is seen as the only method available for this purpose and is given by the following equation:

$$\left[1 - \frac{Y_a}{Y_m}\right] = K_y \times \left[1 - \frac{ET_a}{ET_c}\right] \quad (\text{Equation 3-1})$$

where K_y is the yield response factor, Y_a is the actual crop yield, Y_m is the maximum crop yield, and ET_a and ET_c are the actual and potential CWR, respectively. The ratio ET_a/ET_c is referred to as the crop stress factor. The parameters are taken from previous on-farm research (Ibrahim et al., 2002; Ahmed et al., 2010; FAO, 2011) for the Gezira Scheme, as presented in Table 3-1. This method has been exploited in several practical applications and recommended for estimating water productivity at both scheme and regional levels (Wahaj et al., 2007; Smith and Steduto, 2012).

Table 3-1. Values adopted for the parameters in Equation 3-1 to estimate the seasonal ET_a

Parameter	Sorghum	Groundnut	Wheat
Y_a (kg/m ²)		Time series 1970–2007*	
Y_m (kg/m ²)	0.475 [†]	0.35 [‡]	0.37 [†]
K_y (no units)	6.250 [‡]	2.60 [‡]	1.50 [§]
ET_c (m/season)		Time series 1970–2007**	

Source: *Ministry of Agriculture in Khartoum; [†]FAO (2011); [‡]Ibrahim et al. (2002); [§]calculated from Ahmed et al. (2010); **Author's calculations. No data were available for cotton.

3.2.3 Irrigation supply indices

The performance of an irrigation system is concerned with the assessment of water flow. The irrigation efficiency indicators Relative Water Supply (RWS) and Relative Irrigation Supply (RIS) are chosen to assess the scheme irrigation service delivery performance (Kloezen and Garcés-Restrepo, 1998; Malano and Burton, 2001). Both indicators were applied in irrigation performance assessment in Sri Lanka (Bandara, 2003) and Spain (Salvador et al., 2011; Moreno-Pérez and Roldán-Cañas, 2013). RWS is defined as the ratio of total water supply to total water demand. In the Gezira Scheme, the total water supply is the irrigation water supply from the Sennar Dam through the main channels (Gezira and Managel) plus the total rainfall in cubic meters (though it is not taken into account in the irrigation scheduling), and the ET_c is the total crop water demand (m³), which is taken to be the maximum water demand for the whole area. The land-use factor is used in this study to represent the cropped area. Then, the total water demand is converted to water volume by multiplying the ET_c by the corresponding cultivated area. Hence, the RWS is expressed as:

$$RWS = \frac{\text{precepitation+irrigation supply}}{ET_c} \quad (\text{Equation 3-2})$$

The climate of the area is hot and arid (Elagib and Mansell, 2000b; Elagib, 2010). Thus, precipitation is likely negligible compared to the irrigation supply. Therefore, RIS is calculated to estimate the performance of the irrigation water supply. The index represents the ratio of irrigation water supply to irrigation water demand as follows:

$$RIS = \frac{\text{irrigation water supply}}{ET_c - P_e}, \quad (\text{Equation 3-3})$$

where irrigation water supply and ET_c are as mentioned above, and P_e is the effective rainfall. The latter is assumed to be 75% of the total rainfall (Mohammed, 2008).

Neither RWS nor RIS reflects whether or not the crop receives the required volume of water in time. They just highlight the overall status of supply and demand. However, the

indicators do not reveal that the supply is consumed by the crop. An RWS or RIS value of 1.00 implies that the irrigation water supply equals the crop water demand. This situation represents 100% irrigation efficiency, which is not possible under field conditions (Salvador et al., 2011). In surface irrigation projects, an irrigation efficiency of 75% ($RIS \cong 1.4$) is considered the highest level, excluding a system with a high degree of reuse of drainage flow (Plusquellec, 1990). In addition, RWS values between 0.9 and 1.2 (using ET_a) imply adequate irrigation efficiency (Moreno-Pérez and Roldán-Cañas, 2013). At this hypothetical efficiency, an RWS or RIS value below 1.4 implies under-irrigation, whereas above 1.4 implies over-irrigation for surface irrigation systems (Plusquellec, 1990; Salvador et al., 2011).

3.2.4 Rainwater supply assessment

The area experiences average summer crop season rainfall of 300 mm. On irrigated land, salinity is generally considered a critical problem which causes loss of production and harm to the environment (FAO, 1997). It was believed that the Gezira rainfall had a direct benefit for the soil leaching process; however, there is no leaching water requirement, as there is no salt problem in the Gezira (Plusquellec, 1990; Adam, 2008). This is because the Blue Nile water is almost distilled with very little salt content (130 ppm) (Ministry of Irrigation and HEE, 1975). In addition, the water table in the Gezira area is very deep (more than 15 m), which saves the Gezira from salt accumulation (Plusquellec, 1990; Adam, 2008). Therefore, it is worth assessing the adequacy of this rainfall. Hargreaves (1975) proposed many indices, such as Moisture Availability Index (MAI), Moisture Deficit (MD) and Ratio of Moisture Availability (RMA), for evaluating crop rainwater supply availability for irrigation scheduling. MAI is the ratio of the DP to ET_c , where DP is the precipitation at a 75% probability level of occurrence. MD is the difference between ET_c and DP. Although the original formula for RMA is the ratio of actual rainfall to ET_c , the effective rainfall is used in the current assessment to represent the actual situation in the Gezira Scheme.

MD is calculated to show the deficit or excess of the desired rainfall moisture content. MAI and MD are considered to assess the designed system for utilizing such rainfall, while RMA evaluates the actual moisture available from the atmosphere. DP is determined using the DISTRIB application in the Stormwater Management and Design Aid (SMADA) software (Eaglin et al., 1996) to analyze the monthly rainfall data for 1961–2010. A three-parameter, log-normal statistical model was found to give the best fit for the distribution.

3.2.5 Productivity of land and water

Crop yield (Y), which expresses the physical mass of production (kg) per unit of cultivated area (m²), is a good indicator for monitoring land productivity from year to year (Bandara, 2003; Sadras et al., 2010). In addition, water productivity is important in water-scarce regions. Water Use Efficiency (WUE) is considered a suitable indicator for water productivity assessment and is important from the point of view of gaining maximum return from a limited water resource (Shih, 1987; Stroosnijder et al., 2012). It has been applied in many case studies to quantify the crop gained from every drop (Kiziloglu et al., 2009; Zhang et al., 2011), and is calculated for each crop as the ratio of actual crop yield (Y_a) to the seasonal ET_a (m) for the crop season. Since ET_a in this research is estimated from yield data, the relationship between ET_a and yield is already assumed. Therefore, WUE (kg/m³) is defined by assuming ET_a = ET_c as follows:

$$WUE = \frac{Y_a}{\text{Seasonal ET}_c} \quad (\text{Equation 3-4})$$

3.2.6 Monitoring of spatial efficiency

RS is a powerful management tool which provides system-wide and spatially distributed information. Spatial information and identification of the drought areas can help to conserve water by improving efficiency and water productivity. NDVI is commonly used to assess the impacts of drought in agricultural areas and to understand the crop response to water availability (Kogan, 1995; Kogan, 1997; Wan et al., 2004). Kogan (1995) developed the Vegetation Condition Index (VCI) to assess agricultural drought areas by using multi-season maximum NDVI and multi-season minimum NDVI for each grid-raster pixel. Nevertheless, the temporal VCI assessment of irrigated agricultural areas may not reflect water availability in drought areas, as every crop type and grid pixel has a distinct seasonal spectral and NDVI behavior (Wardlow and Egbert, 2008; Foerster et al., 2012). The NDVI values for each grid-raster pixel may show seasonal fluctuations due to crop-pattern rotation, as in the case in the Gezira Scheme. In order to correct this anomalous behavior and isolate the effect of crop rotation, given the objective of the current assessment to evaluate water distribution efficiency, in this study the modified VCI (MVCI) is calculated individually for each season using the following formula:

$$MVCI = 100 \times \frac{(NDVI_i - NDVI_{\min})}{(NDVI_{\max} - NDVI_{\min})} \quad (\text{Equation 3-5})$$

where $NDVI_i$ is the NDVI value of the current grid image pixel, and $NDVI_{max}$ and $NDVI_{min}$ are the maximum and the minimum NDVIs of the given image for the whole scheme, respectively, rather than the extremes of the time series as suggested by Kogan (1995). MSCI takes values between zero and 100, where the lower limit represents the driest condition, and the upper value, the wettest condition.

The crop stress factor (ks) is considered another method to identify drought areas and irrigation deficit (Fereres and Soriano, 2007). Therefore, monitoring using ks on both spatial and temporal scales is critical for improving irrigation water management (Bastiaanssen et al., 2005). In this study, the actual and potential (ET_a and ET_p) MOD16A2 ET products are used, which are operationally produced from the MODIS sensor (Mu et al., 2011). Besides, the MOD16A2 product has been validated with ET measurements all over the world (Mu et al., 2011; Kim et al., 2012; Velpuri et al., 2013; Ruhoff et al., 2013; Chen et al., 2014).

The bimonthly composite MODIS NVDI and the 8-day MOD16A2-ET images for each season are stacked individually using the Cell-Statistics tool in ArcGIS 10 to represent the summer crop season, June–October, and the winter crop season, November–March. Later, the MSCI assessment is conducted for 28 images constituting the summer crop and the winter crop seasons (14 images for each season) for 2000–2014. On the other hand, the ks assessment is conducted for 2000–2009 (9 images per season) due to data availability.

3.3 Results and discussion

3.3.1 Crop stress

ET_o results for 1961–2010 have minimum monthly values of 153–177 mm during the winter climate season (November–January). The maximum monthly values were recorded during April and May as 253 and 255 mm, respectively. Table 3-2 presents the developed monthly kc values for the main crops.

Table 3-2. Monthly dependable rainfall (DP) and monthly derived kc values for the Gezira Irrigation Scheme

Month	Jan.	Feb.	Mar.	Apr.	May	Jun.	Jul.	Aug.	Sep.	Oct.	Nov.	Dec
DP (mm)	0.0	0.0	0.0	0.2	1.9	10.6	47.3	65.5	24.6	3.7	0.0	0.0
kc cotton	1.04	0.82	–	–	–	–	0.55	0.59	0.91	1.36	1.42	1.30
kc sorghum	–	–	–	–	–	0.55	0.80	1.22	1.11	0.78	–	–
kc wheat	1.30	0.74	–	–	–	–	–	–	–	–	0.70	1.24
kc groundnut	–	–	–	–	–	–	0.75	1.10	1.17	0.95	0.72	–

The highest seasonal crop water demand is calculated as 1430 mm for cotton, while the lowest demand is for wheat (670 mm). Elagib and Mansell (2000) reported that the area experienced increasing evapotranspiration rates (Figure 3-1) for the dry period of 1960/61–1989/90, after which recovery from drought is noticeable for 1990/91–2003/04 (Elagib, 2009). This led to decreased ET_c for all summer crops, indicating lower atmospheric demand. The ET_a trends of sorghum, groundnut and wheat series follow various patterns. In the case of sorghum and groundnut, ET_a values do not show trends over time (giving averages of 743 and 770 mm/season, respectively), while wheat ET_a rises steadily after the 1999/2000 crop season (the average varies from 345 to 432 mm/season).

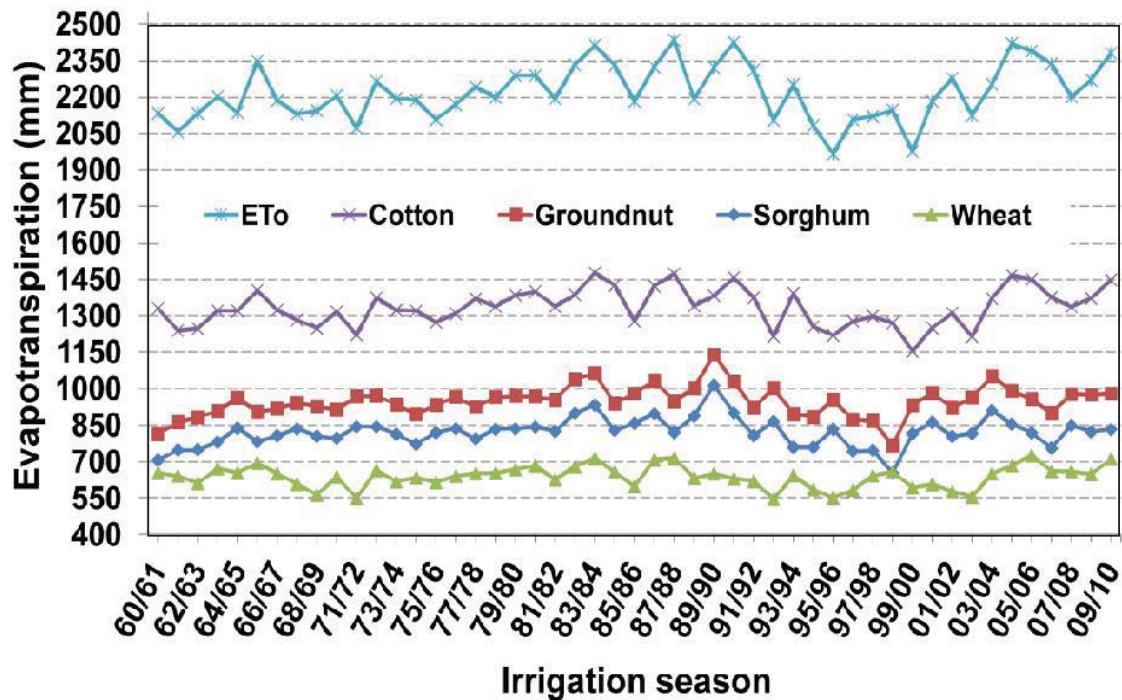
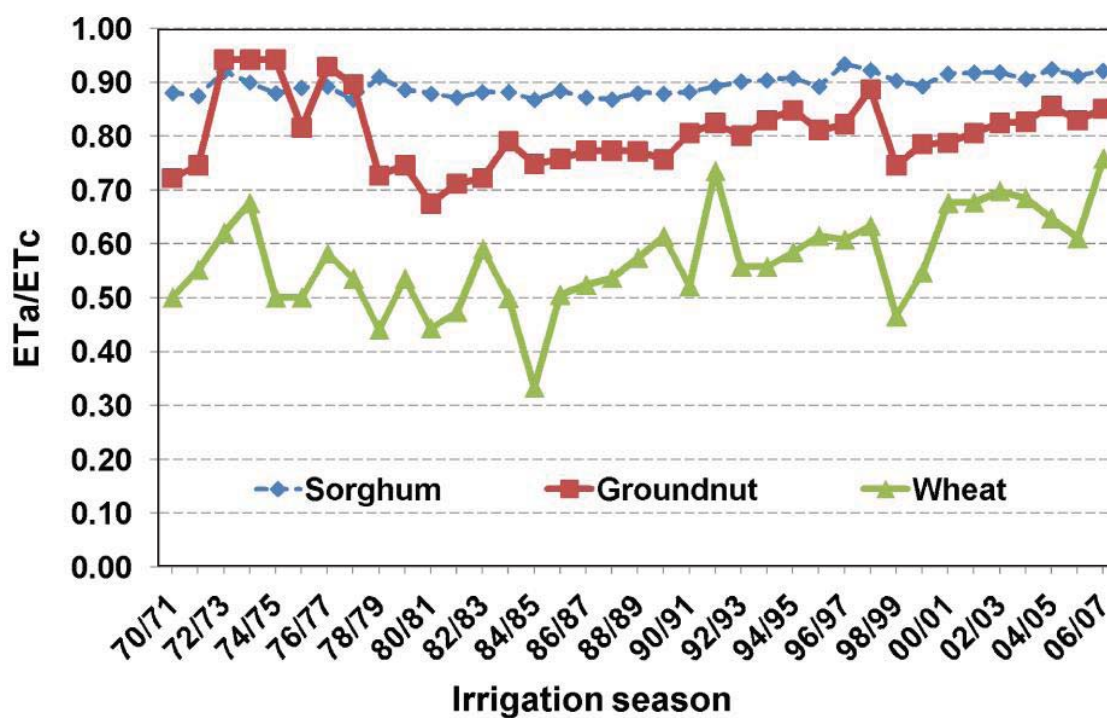


Figure 3-1. Seasonal reference and crop evapotranspiration for the Gezira Scheme

The long-term behavior of crop stress can be seen in Figure 3-2, taking ranges of 0.86–0.93, 0.67–0.94 and 0.33–0.76 for sorghum, groundnut and wheat, respectively. It is clear that the crop stress values for sorghum have not changed significantly over time. Although the sorghum yield (Figure 3-9) is shown to be affected by drought conditions, factors other than climate, such as water, fertilizers, pesticides and anti-diseases, can also play a role in its final levels.

Figure 3-2. Crop water stress (ET_a/ET_c)

3.3.2 Irrigation supply indices

3.3.2.1 Annual assessment

The annual RWS and RIS irrigation performance indicators for the Gezira Scheme are shown in Figure 3-3. Regime Shift Detector (RSD) software (Rodionov, 2004) is used to detect statistically significant shifts in the mean level of the RWS and RIS time series. Accordingly, irrigation management can be classified into two categories, adequate and inefficient irrigation, in terms of meeting evapotranspiration demand. Irrigation management for 1970/71–1993/94 is considered adequate, with an average RIS value of 1.40. A similar result is reported by Plusquellec (1990) for the scheme for roughly the same period. Since then, seasonal irrigation efficiency has been decreasing, with year-to-year variability since 1993/94, from an average of 1.40 and 1.70, to 2.23 and 2.60 for RIS and RWS, respectively. However, visual inspection reveals that irrigation management starts to be inefficient from 1990/91, due to an excess supply of water. The data show that water amounting to twice the crop requirement has been issued from the Sennar reservoir. It is doubtful that the additional water is supplied to overcome the water conveyance and/or for land preparation.

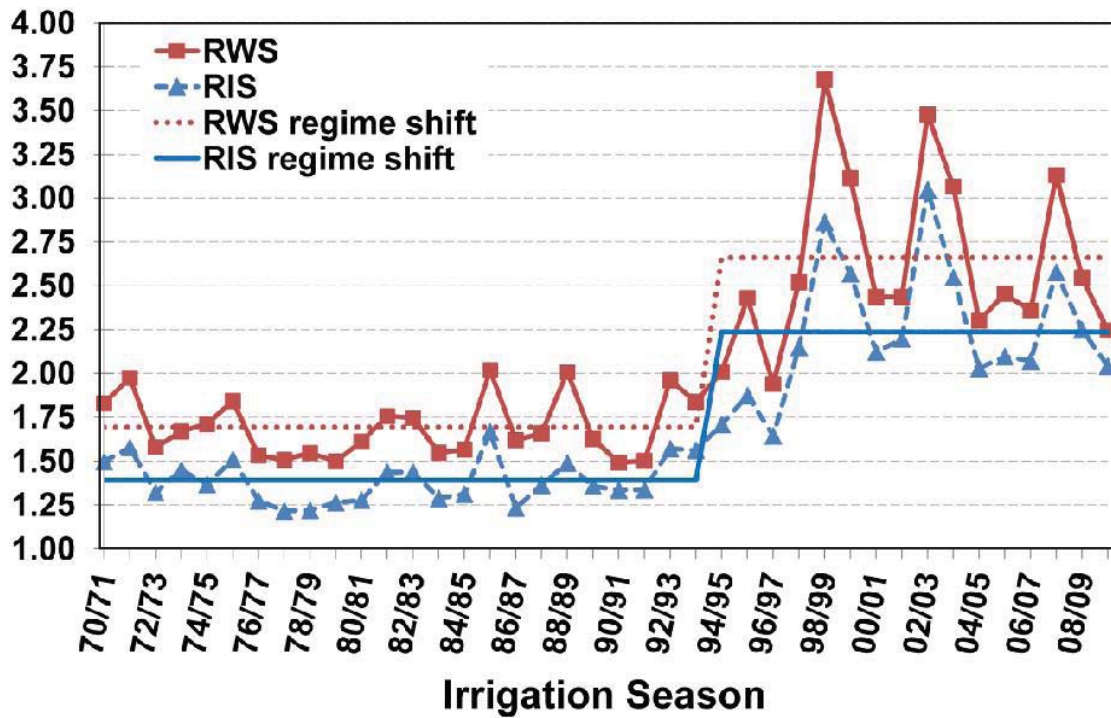


Figure 3-3. Annual Relative Water Supply (RWS) and Relative Irrigation Supply (RIS) for the Gezira Scheme (1970–2010)

Figure 3-4 illustrates the preponderant impact of crop patterns on irrigation efficiency. Since 1989, the cotton area has declined, while sorghum has grown steadily. Guvele (2001) and Elamin et al. (2011) mentioned that the government crop acreage liberalization policy since 1989 has proved inefficient for land use, causing instability in the area of main crops. In addition, irrigation water supply has not improved as a result of the policy, which is likely due to inaccurate estimation of net irrigation need up to 2000. Thereafter, more irrigation water has been released. Moreover, Ahmed (2009) reports that the channels of the Gezira Scheme were over-excavated during the substantial channel de-silting program of 1999.

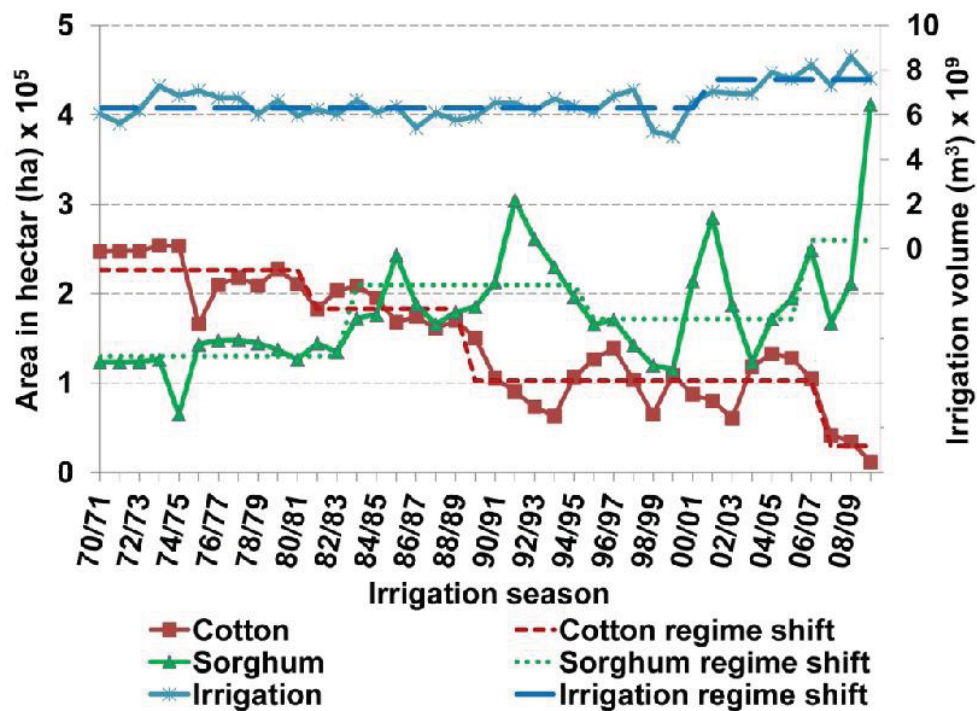


Figure 3-4. Crop area and total irrigation water supply for the Gezira Scheme

3.3.2.2 Seasonal assessment

The evolution of the RWS and RIS indicators for the two crop irrigation seasons (summer and winter) are shown in Figure 3-5. Irrigation management is found to be less efficient through the winter crop season than the summer crop season, especially during the last two decades. This inefficiency results from the fact that most of the cultivated lands are allocated for wheat and the final growing stage of cotton. These winter crops present the lowest demand when the cool climate lowers ET_c , especially for wheat (average = 670 mm/year). On the other hand, the higher efficiency during the summer crop season persisted until two decades ago. In spite of delivering twice the volume of water in the summer season, crop demand was not met, as reported by many researchers (Ahmed, 2009). This could be attributed to the rate of water release (discharge) through the main channels. According to Brouwer et al. (1992), the surface irrigation method in areas located in hot and arid zones requires a greater continuous discharge of 1.5 l/s/ha. Plusquellec (1990) reported that the channels are designed for 12-hour irrigation scheduling to irrigate half the area of the scheme (\cong 0.5 million ha). Therefore, the irrigation system of the scheme uses around 1.4 l/s/ha, which is considered an optimum discharge to satisfy crop demand. However, farmers started to leave field outlet gates open for 24 hours (Plusquellec, 1990), and almost the whole scheme area has been cultivated since the initiation of the government crop acreage liberalization policy of 1989 (Guvele, 2001; Elamin

et al., 2011). This means the irrigation system delivers 0.35 l/s/ha, indicating that the scheme is not fairly supplied with water. More water is withdrawn by the farmers upstream of the main channels, thus causing drought in the downstream zones.

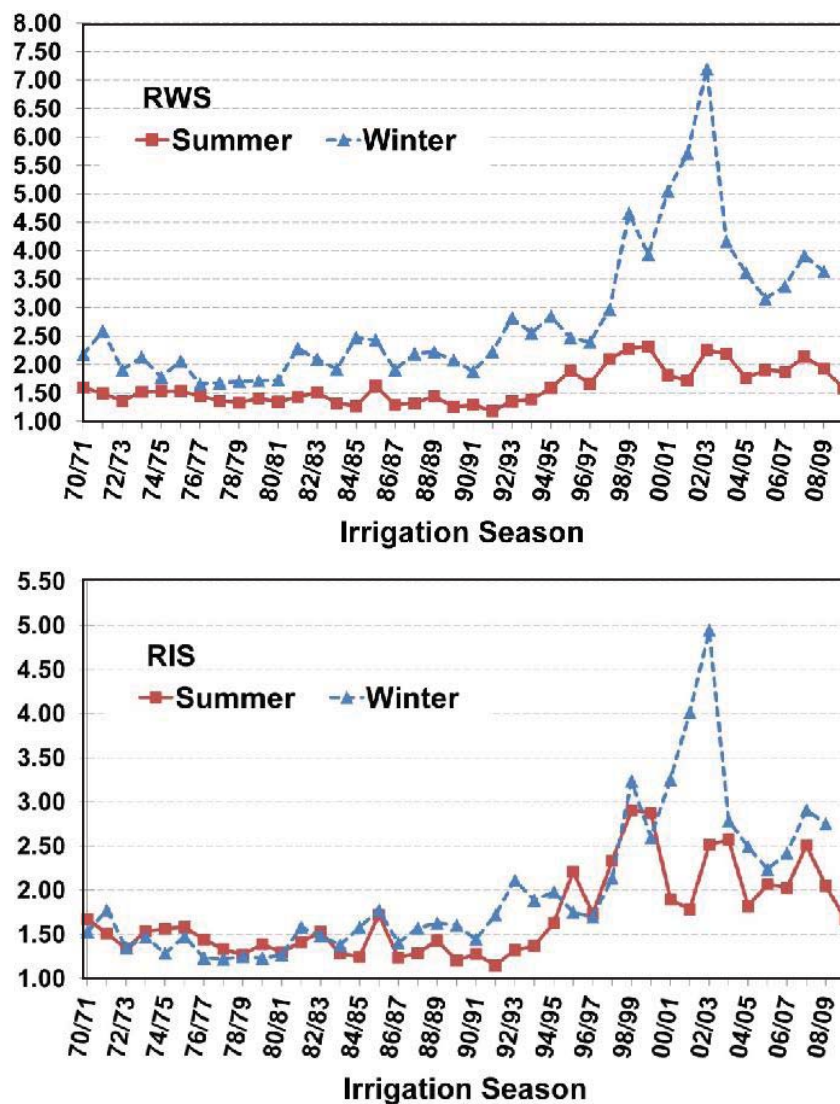


Figure 3-5. Summer and winter Relative Water Supply (RWS) and Relative Irrigation Supply (RIS) for the Gezira Scheme (1970–2010)

3.3.2.3 Monthly assessment

To study irrigation performance in more depth, monthly analysis is also conducted. During June–August, the RWS assessment demonstrates that water supply has been almost twice crop demand since 1994, especially in July, as shown in Figure 3-6.

For the same period, RIS implies that the irrigation water supply is three times crop demand. The exceptionally high RIS values (more than 40) for July in 1970, 1978 and 2007 are attributable to high rainfall (≈ 160 mm) received during these months. This reduced total

demand by 98%, and the total released irrigation water supply covered 20% more than demand. Two reasons can be reported here: firstly, this period includes land preparation and initial growing stages for the main summer crops; and secondly, the rainfall is not taken into account in scheduling irrigation during this part of the year. Both RWS and RIS increase in November and December, a phenomenon that could be explained by the harvest time of the summer crops (sorghum and groundnuts) and the start of land preparation for winter crops (wheat).

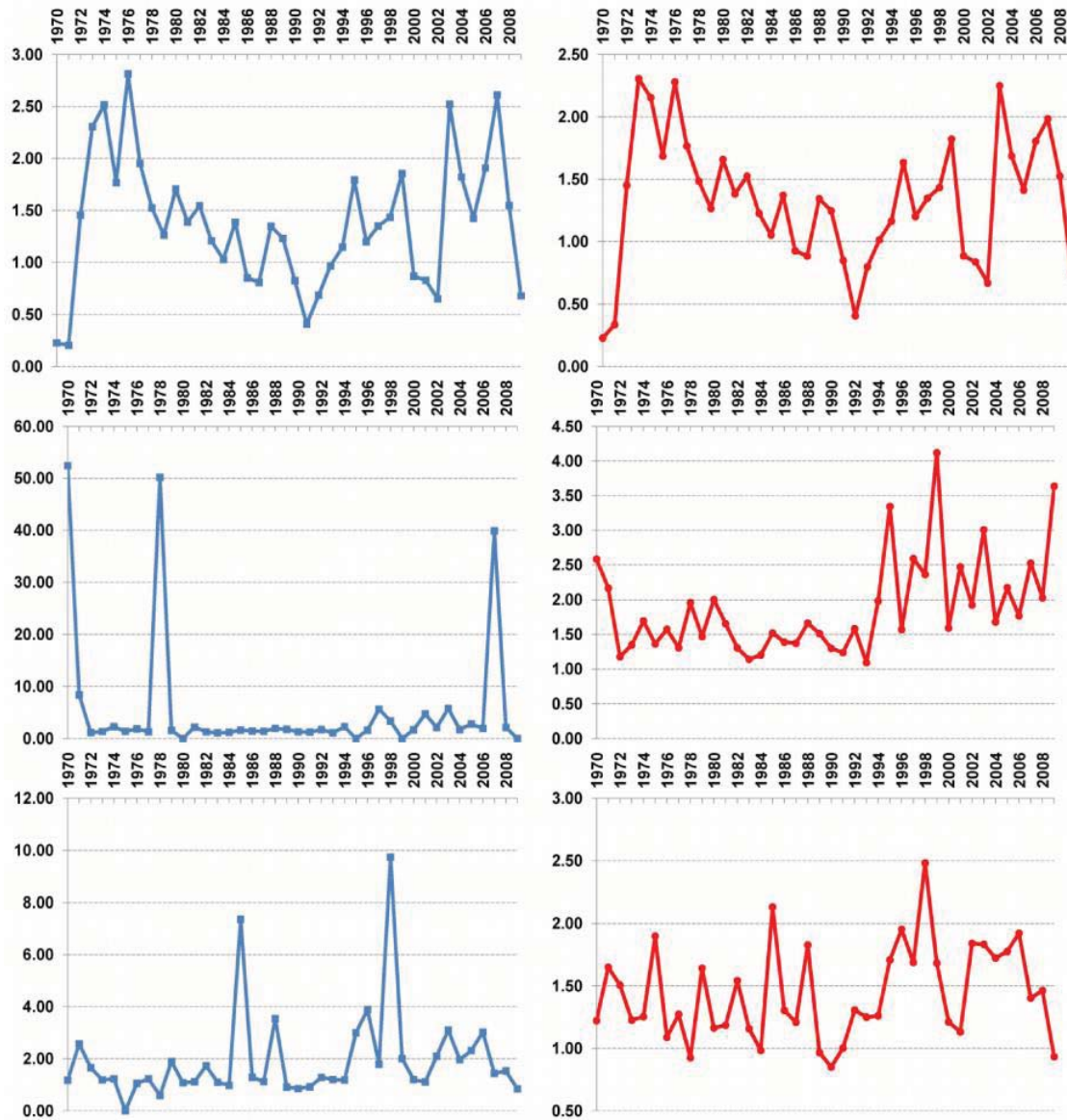


Figure 3-6. Monthly Relative Water Supply (RWS) and Relative Irrigation Supply (RIS) for the Gezira Scheme for June (top), July (middle) and August (bottom)

A closer look at the above results reveals that rainfall variability plays an important role in changing RWS and RIS. In spite of the interannual variability, RWS and RIS values dropped between the late 1970s and the early 1990s, when a dry period was reported in Sudan (Elagib and Mansell 2000; Elagib, 2009). RIS in August 1985 reached a value of 7 when a heavy rainfall (151.24 mm) occurred, which may have decreased the need for irrigation. In conclusion, the Gezira Scheme receives fairly adequate rainfall, which should be directly utilized or harvested for irrigation, despite the intra-seasonal variability.

3.3.3 Rainwater supply

The monthly DP values are presented in Table 3-2 (further analysis is shown in Appendix Two). It can be seen that the rainy season is June–September, and the highest-return period is July–August. The calculated monthly MAI for all crops is less than 1.00, as shown in Figure 3-7, indicating insufficient supply of moisture from precipitation. However, the first half of the initial growing stage for groundnut and sorghum (July and August) presents moderately deficient conditions (0.34–0.45), while the MAI for cotton shows moderately deficient conditions (0.4–0.8) during the same period. The seasonal MD took the ranges 501–863 mm, 616–989 mm and 1014–1336 mm for sorghum, groundnut and cotton, respectively, indicating that around 150 mm per year for sorghum and groundnut, and up to 300 mm for cotton could be saved when the rainfall accounted for irrigation scheduling.

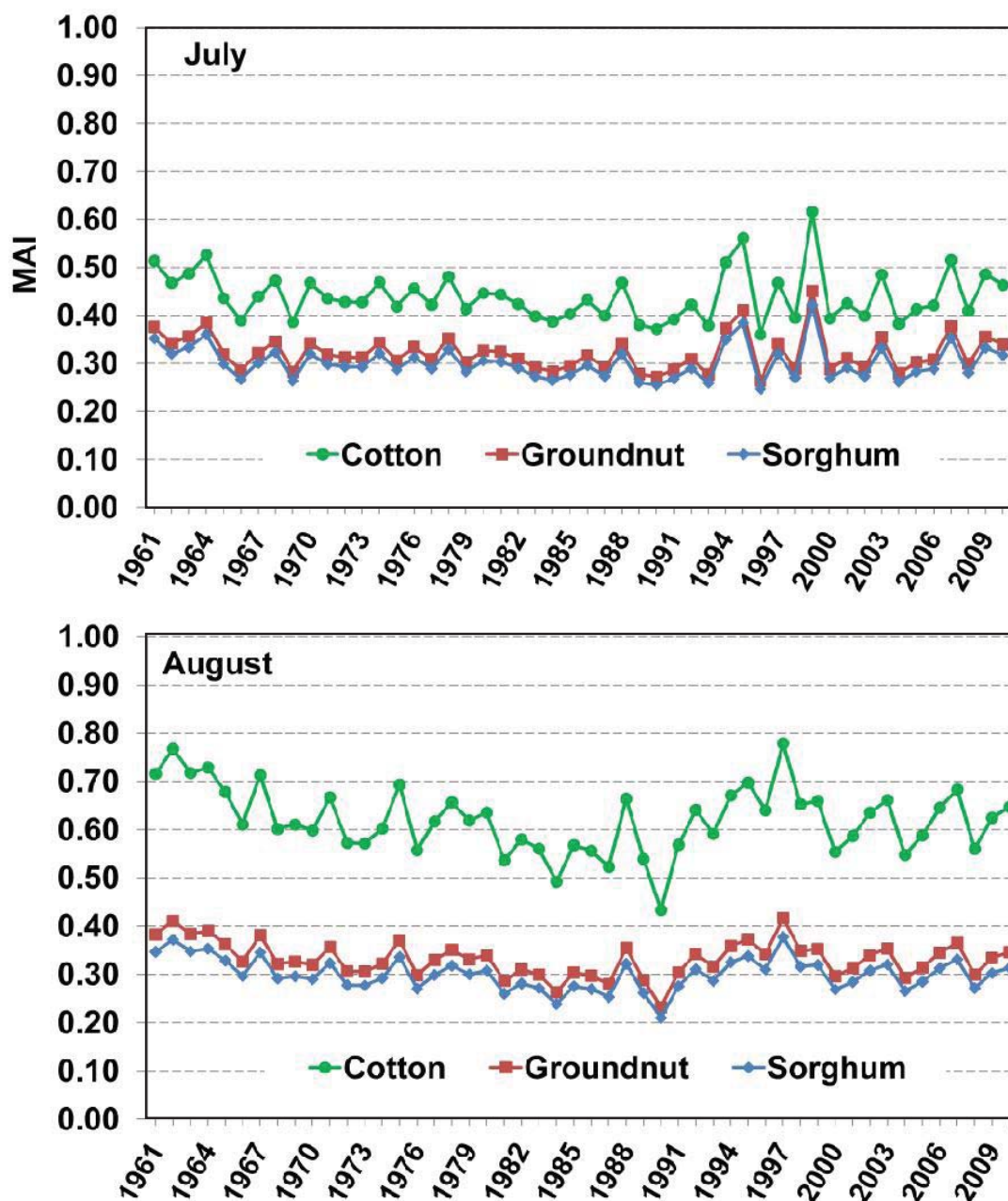


Figure 3-7. Moisture Availability Index (MAI) for July and August

Using the historical RMA assessment of the actual rainwater supply, it can be deduced from Figure 3-8 that the most promising months to utilize the rainfall are July and August. On average, the ratio of rainwater supply to crop demand in July is equal to 0.67, 0.49 and 0.46 for the RMA of cotton, groundnut and sorghum, respectively. It is found that 12 out of 50 years had an RMA of greater than one for cotton, implying that cotton does not need irrigation water during the initial growing stage. Also, for groundnut and sorghum, 4 years out of 50 had RMA values greater than one. In August, the RMA for cotton recorded values of greater than 1 in 15

years, with a 50-year average of 0.79, but did not record greater than one for the other crops. Besides, the 50-year RMA average for groundnut and sorghum indicates that rainwater supply is almost 40% of demand. During the rest of the rainy months, the effective rainfall contributes up to 25% of the demand for the other crops. Based on these results, it is fair to conclude that rainfall could be considered in irrigation scheduling, or be harvested to reduce the crop demand for irrigation water during the rainy season, especially in July and August.

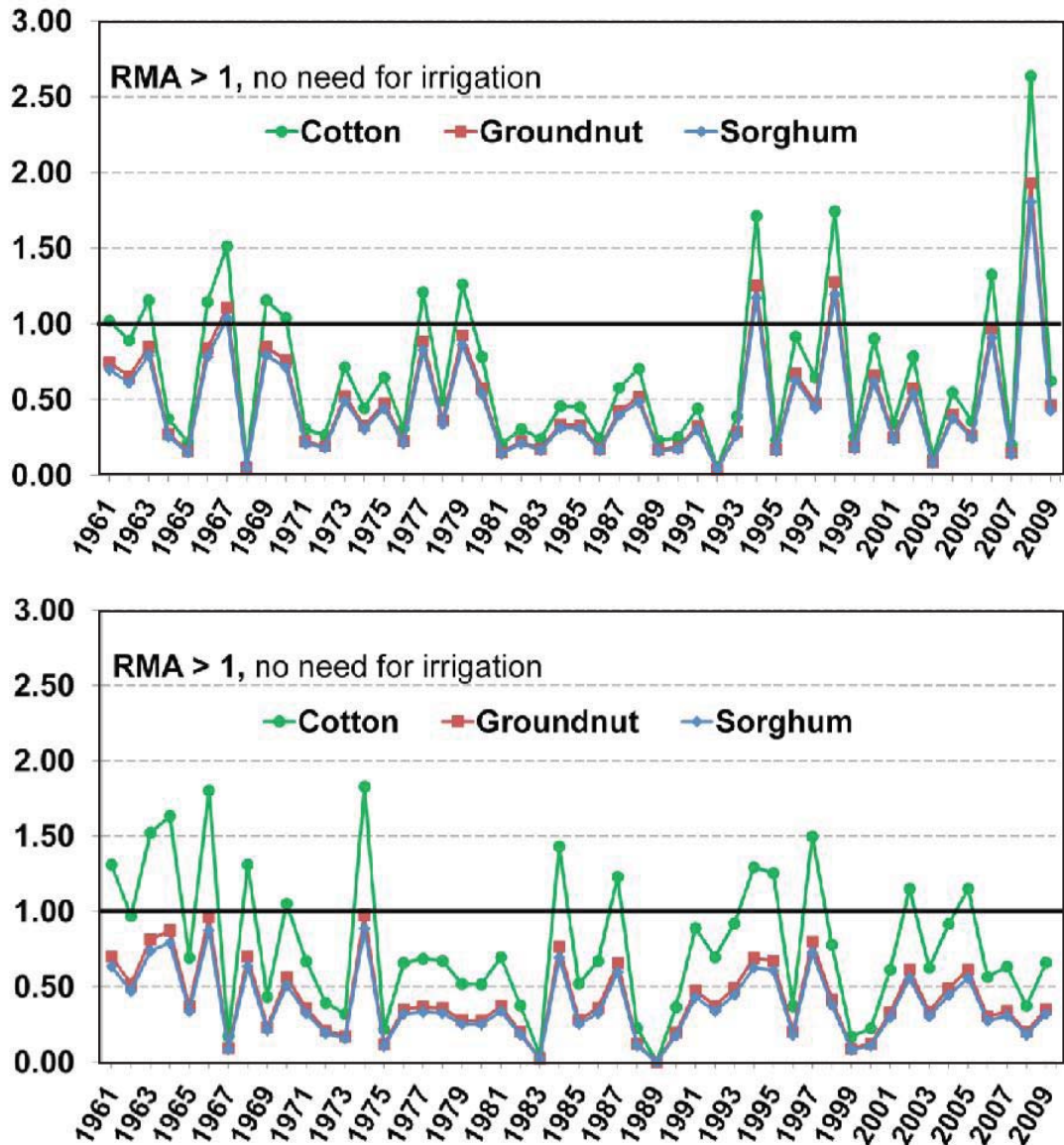


Figure 3-8. Ratio of Moisture Availability (RMA) for July (top) and August (bottom)

3.3.4 Water productivity

3.3.4.1 Crop yield

The yield time series for the four crops are plotted in Figure 3-9 for the Gezira Scheme for 1970–2006. Despite the interannual variability, it can be observed that the yield trend of groundnut decreased until the mid-1980s following the climate drought period (Elagib and Mansell 2000b; Elagib, 2009) and has been increasing thereafter. The regime shift analysis declares that the yields of sorghum and cotton were not significantly affected (except 1975/76–1982 for cotton) by the drought period, because both crops are considered drought-tolerant crops (Rosenow et al., 1983). The improved wheat and sorghum yields witnessed since 2000 might be linked to excess irrigation. However, the cotton yield has remained almost constant, presumably because cotton has not received the official attention it had before the mid-1970s, especially as cotton has considerably reduced in favor of food crops (Mahgoub, 2014).

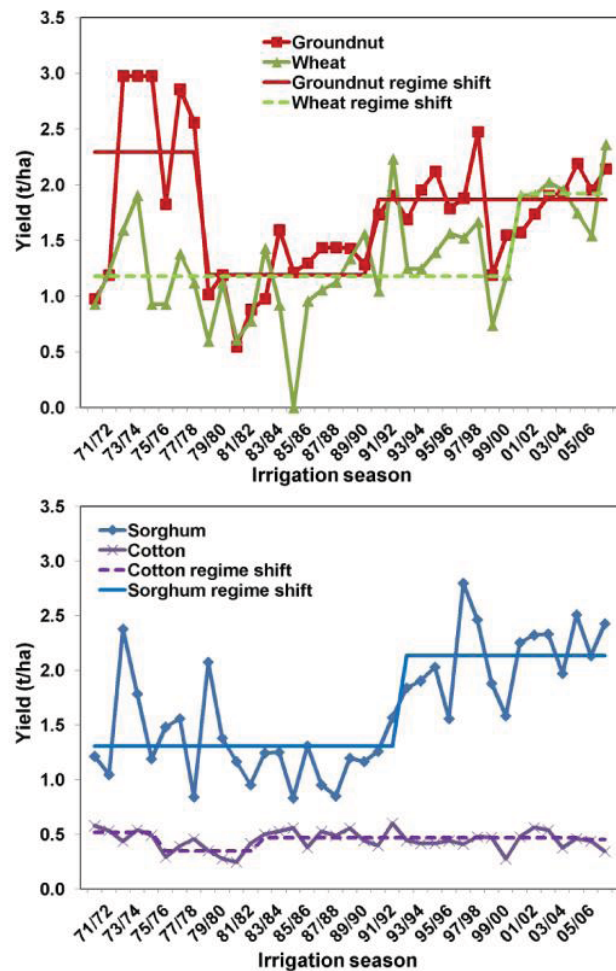


Figure 3-9. Crops yield for the Gezira Scheme

The highest yield in the Gezira Scheme is found to be for groundnut (2.97 t/ha), while the lowest yield was recorded for cotton (0.4 t/ha). The mean yields for groundnut, sorghum and wheat are 1.8, 1.6 and 1.3 t/ha, respectively. As for the latter two crops, both yields are below the attainable yields estimated by FAO (2011) and FAO (2009), respectively, as 3.8–5.7 t/ha and 3.3–4.1 t/ha. Furthermore, the productivity of cotton at country level is no exception: it is only 35%, 47%, 53% and 61% of that reported for Australia, China, Egypt and Pakistan, respectively (Bushara and Barakat, 2010). FAO (2011) mentioned that the factors responsible for seasonal fluctuations and low yields in the Gezira Scheme include water shortages due to poor and inadequate maintenance of the irrigation distribution system. According to the FAO Nile country report for Sudan (2008), as cited in FAO (2011), another reason affecting the crop yield is the “head to tail” (start-to-end of a channel) effect, which represents the inequity of water distribution in an irrigation system. The report mentioned that this effect might reduce the yield by 25%–50%. At the on-farm level, mismanagement of the applied water and lack of fertilizers are significant causes for the drop in yields, especially for sorghum and groundnut (Ibrahim et al., 2002). To improve WUE and crop productivity, rainwater harvesting is proposed as a suitable technique for supplemental irrigation, especially in the arid regions of the African Sahel, thus improving the crop yield by up to 50% (Stroosnijder et al., 2012).

To examine the crop yield response to water, the correlation between the crop yield and the volume of irrigation water is explored. It is worth mentioning here that data for irrigation water delivered to each crop was not obtainable. The derived relationship is attempted using the total irrigation water supply from the Sennar Dam. It is noticed that the crop yield improves with increased irrigation water release. R^2 is 0.45, 0.50 and 0.44 for sorghum, groundnut and wheat, respectively. The significance level (p) for a two-tailed test of a Pearson correlation coefficient is 0.00064, 0.00023 and 0.00023, respectively, for the same crop sequence. On the other hand, the correlation for cotton is very low ($R^2 = 0.003$ at $p = 0.9401$). This is possibly due to cotton having a longer growing period that extends over the summer and winter crop seasons, which is not reflected by the volume of irrigation water released from the Sennar Dam for the whole year. Moreover, the planting date is another decisive factor for low yield, especially for wheat (FAO, 2009).

3.3.4.2 Water Use Efficiency

Figure 3-10 depicts the time series of WUE for the three main crops under consideration. WUE for groundnut, wheat and sorghum took the ranges 0.02–0.04, 0.09–0.36, 0.06–0.33 and 0.1–0.38 kg/m³, respectively. Lower values were obtained for 1978/79–1991/92, a dry period in Sudan, thus initiating higher values of ET_c . Adeeb (2006) estimated the WUE for 16 years

(1988–2004) to have similar values of 0.1–0.22, 0.07–0.27 and 0.15–0.41 kg/m³, respectively. Similar to other crops, cotton WUE decreased until it reached its lowest level (0.018 kg/m³) in 1980/81. Since then it has remained almost constant in view of the steady yield states, as stated earlier. It is worthwhile mentioning that values of ET_c rather than ET_a were utilized in both calculations, thus giving lower WUE values. However, even with half the ET_c values (according to the calculated crop stress factor in Section 3.3.2), it can be deduced that the Gezira Scheme still has lower water productivity compared to values reported elsewhere across the world.

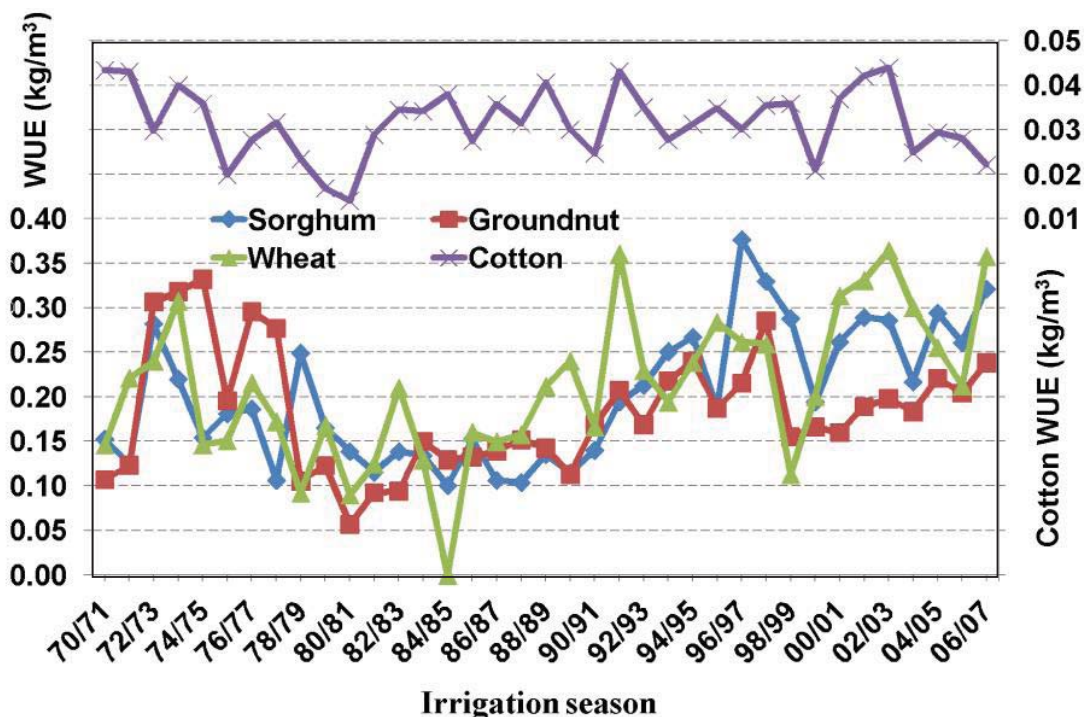


Figure 3-10. Water use efficiency (WUE) for the main crops in the Gezira Scheme

For instance, the worldwide ranges of WUE are 0.6–1.7 kg/m³ for wheat and 0.3–2.2 kg/m³ for sorghum (Zwart and Bastiaanssen, 2004; Zwart and Bastiaanssen, 2007; Sadras et al., 2010), which are much higher than the calculated 40-year average (0.26 and 0.4 kg/m³, respectively) for the Gezira scheme. Taking wheat as an example and using the same methodology for calculating ET_a over the same crop season 2000/01 (2001/02 for Gezira), Figure 3-11 demonstrates that the Gezira achieves the lowest WUE value among nine irrigated farming systems. The highest value is obtained for the Nile Delta in Egypt, where there is a high usage of other inputs, such as fertilizers and pesticides (FAO, 2011). However, the low water productivity of the Gezira Scheme is largely due to mismanagement of irrigation water at the field level (Ibrahim et al., 2002; Adeeb, 2006).

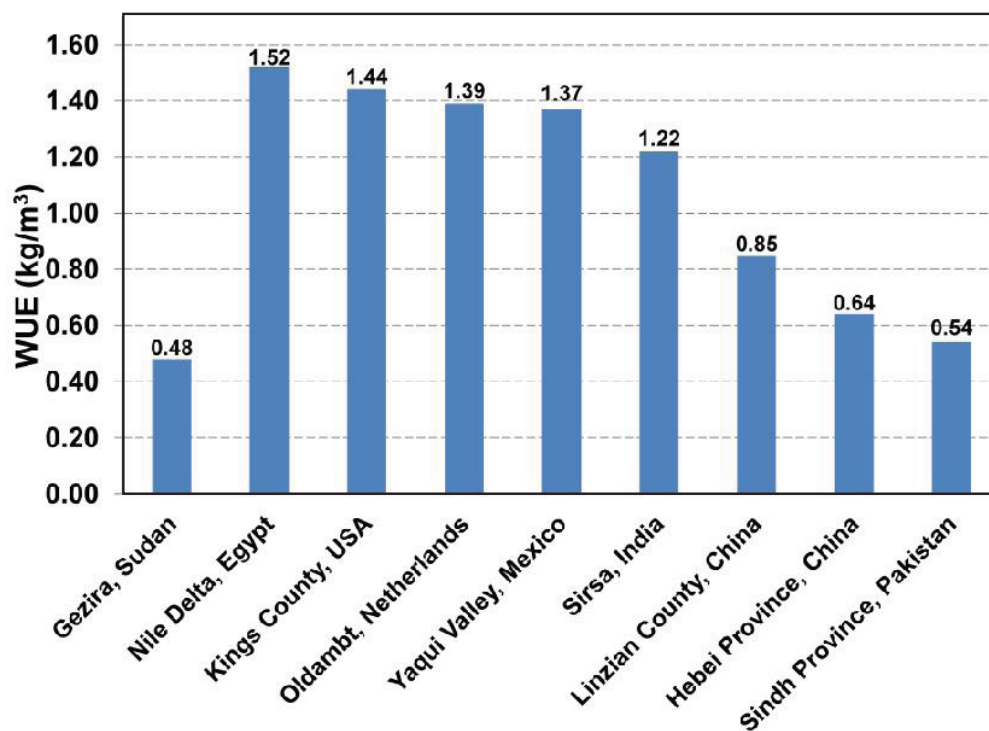


Figure 3-11. Water use efficiency (WUE) for nine irrigated wheat systems

Data source: Gezira: Ahmed et al. (2010); others: Zwart and Bastiaanssen (2007).

3.3.5 Monitoring of spatial efficiency

A visual spatial assessment of drought is provided in Figure 3-12 using the summer crop season MVCI for 2000/01–2013/14. The results indicate that the northern zone of the scheme is always dry, while the southern, central and western parts are generally well-irrigated. Although the Sennar Dam delivers irrigation water amounting to twice the demand during the summer crop season, the system seems to fail in conveying it to the northern part. This may be attributed to the enormous amount of sediment entering the scheme during this season. Ahmed (2009) mentioned that the sediment impounds water in the channels, causing flooding in some areas of the scheme and drought in others.

Another factor is related to the low rate of discharge, as explained in Section 3.3.2.2. On the other hand, the winter crop season tells a different story. Figure 3-13 shows a good spatial distribution of winter MVCI throughout the scheme. It indicates that the scheme receives sufficient irrigation water during this season, because only wheat and end-stage cotton are cultivated over almost all the land. The demand for irrigation water is low, and the supply is then satisfactory, as discussed in Section 3.3.2.2. In addition, the irrigation flows without sediment loads during the winter crop season (Ahmed, 2009).

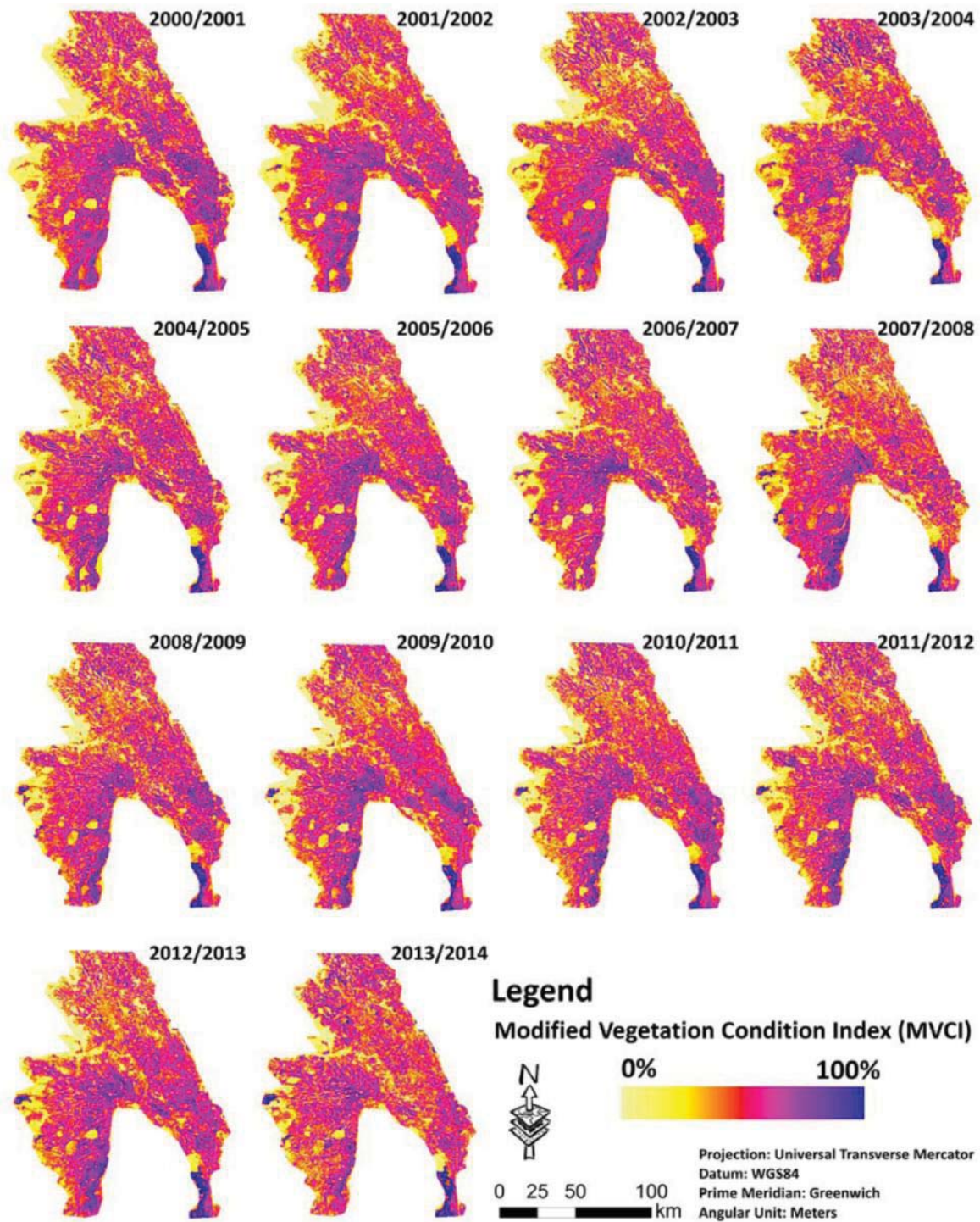


Figure 3-12. Spatial irrigation supply assessment for the summer crop season

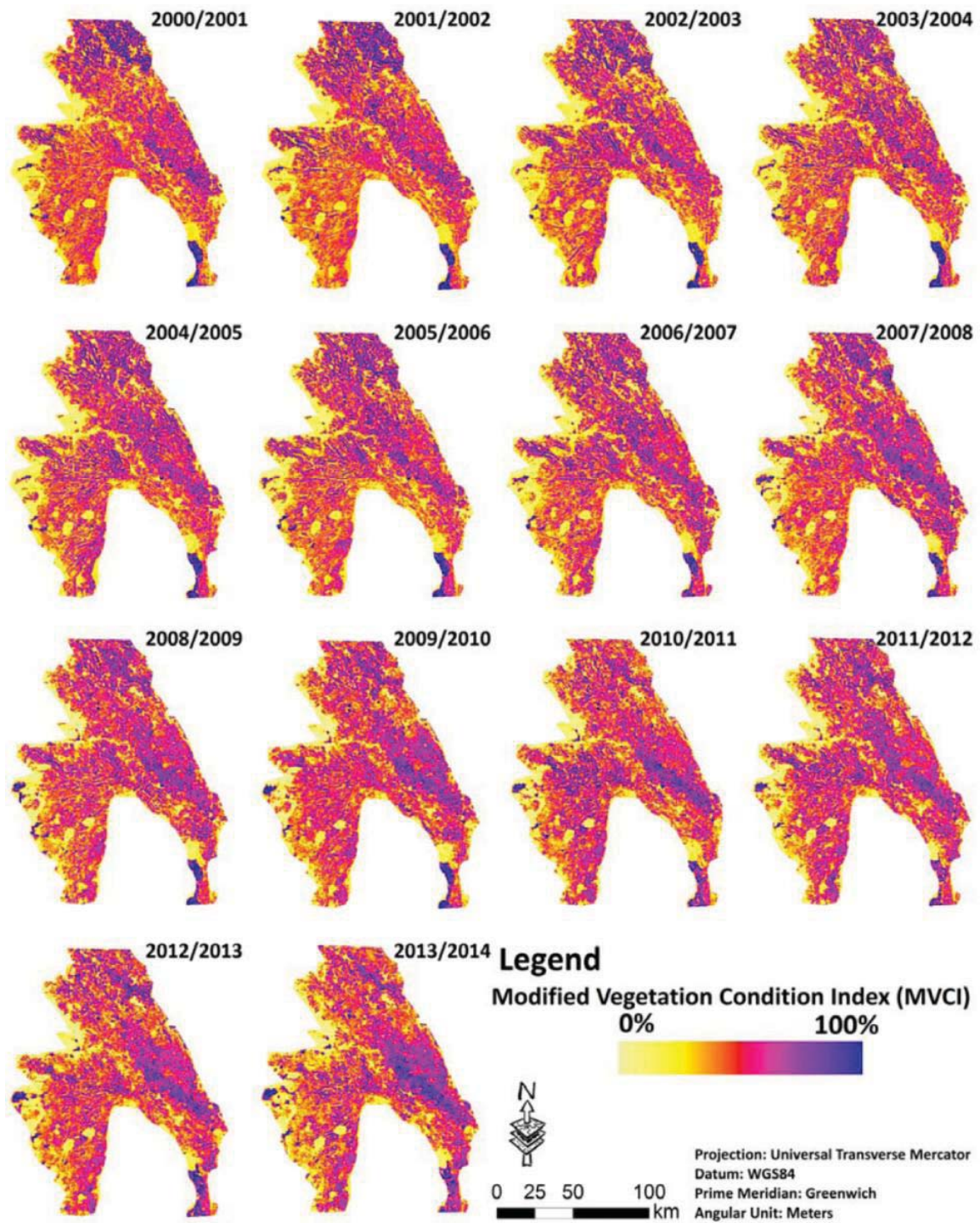


Figure 3-13. Spatial irrigation supply assessment for the winter crop season

To justify the achieved MVCI results, the time series of mean MVCI values (plotted in Figure 3-14) for the whole Gezira Scheme is compared with the RIS and RWS values (Figure 3-5) for both irrigation seasons. As can be seen, the MVCI values respond well to water availability, which is represented by RIS and RWS. A significant positive linear relationship ($p \cong 0.001$) between MVCI and the irrigation indicators for the summer is observed, with R^2 values of 0.66 for RIS, and 0.59 for RWS. On the other hand, higher R^2 values are found ($p < 0.001$) for the winter, with values of 0.76 and 0.78 for RIS and RWS, respectively. According to Figure 3-14, MVCI is in an increasing trend from the summer crop season of 2000/01 until a sudden drop in 2004/05; then an upward trend is noticed. The best situation is encountered during the summer crop season of 2003/04, when the highest RIS (2.34) is estimated. However, the highest MVCI is calculated in 2010/11, with average value of 49% for the whole scheme. In that year, the responsibility for irrigation was changed, as mentioned earlier in Section 2.3.1, with uncontrolled release of more water indicated by a higher MVCI value. During the winter crop season, a consistently low value of MVCI is found in the time series, ranging from 37% to 38% during 2003/04–2008/09, after reaching a peak value of $\cong 40\%$ in 2002/03. In this crop season, the estimated RIS and RWS had the highest values (4.95 and 7.20, respectively). After 2010, the vegetation of the scheme experienced more greening when compared to the other irrigation seasons, as the average MVCI value reaches $\cong 40\%$.

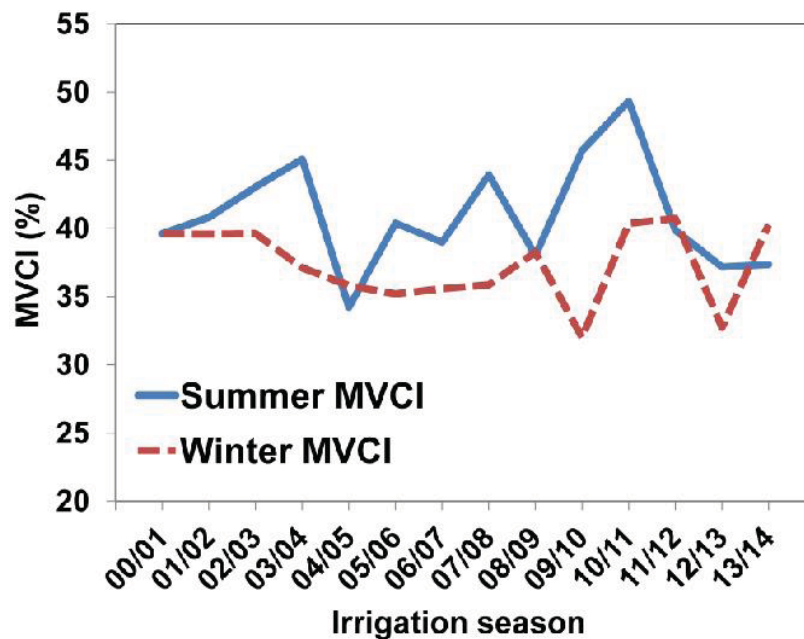


Figure 3-14. Temporal average values of the Modified Vegetation Condition Index (MVCI) for the Gezira Scheme

Another source of data (MOD16) is also used to assess the spatial efficiency. Unfortunately, both ET_a and ET_p values from the MOD16 ET product are very low for the Gezira Scheme compared with other experimental ET studies (i.e. Farbrother (1996), Abdelhadi et al. (2000), Ibrahim et al. (2002), Adeen (2006), Ahmed et al. (2007), Bashir et al. (2008) and Ahmed et al. (2010)). For instance, the mean ET_o in August is around 5.90 mm/day (average 50 years) and the highest calculated ET_c in August is for sorghum, at around 7.1 mm/day. The maximum value of MODIS ET_p for the same month is around 3.0 mm/day. In addition, the crop stress ratio (ks) from the mentioned local studies is around 50%, while the obtained ks value from MODIS ET product does not exceed 10%. This can be explained by the fact that estimation of ET values from irrigation areas cannot be well represented by the MOD16 algorithm alone in arid and semi-arid areas (Mu et al., 2007, 2011). Therefore, the predicted ET_a , ET_p and ks absolute values are not used in this research. However, the spatial pattern of ks is still considered useful information for monitoring drought areas, and can be used for spatial efficiency assessment. Figure 3-15 and Figure 3-16 give a visual spatial assessment of the crop stress factor (ks) for the summer and winter crop seasons for January 2000–August 2008. As can be seen, MSCI shows similar results to ks for the summer crop season, but differs from ks during the winter season, when the northern zone of the scheme is dryer than the other zones. However, the northern zone still receives less water than the rest of the scheme.

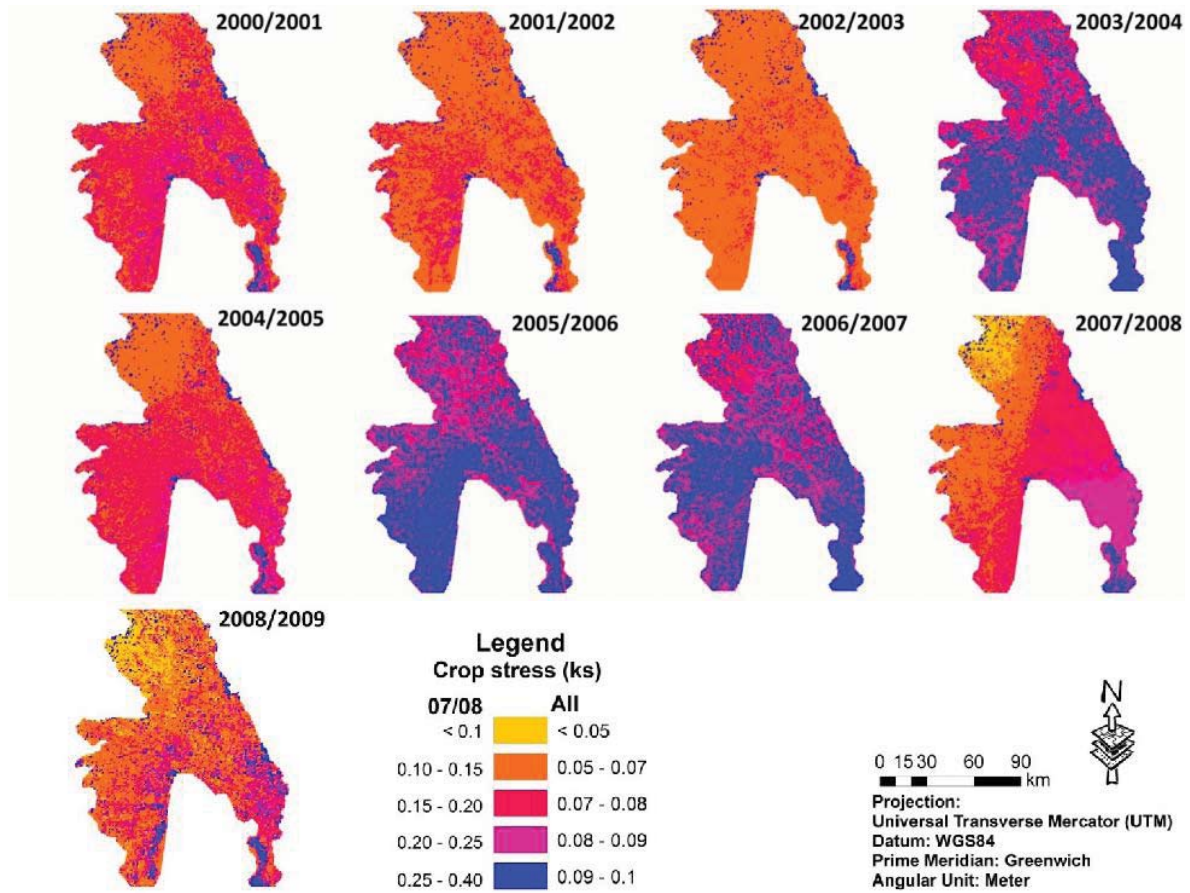


Figure 3-15. Spatial crop stress factor (ks) for the summer crop season

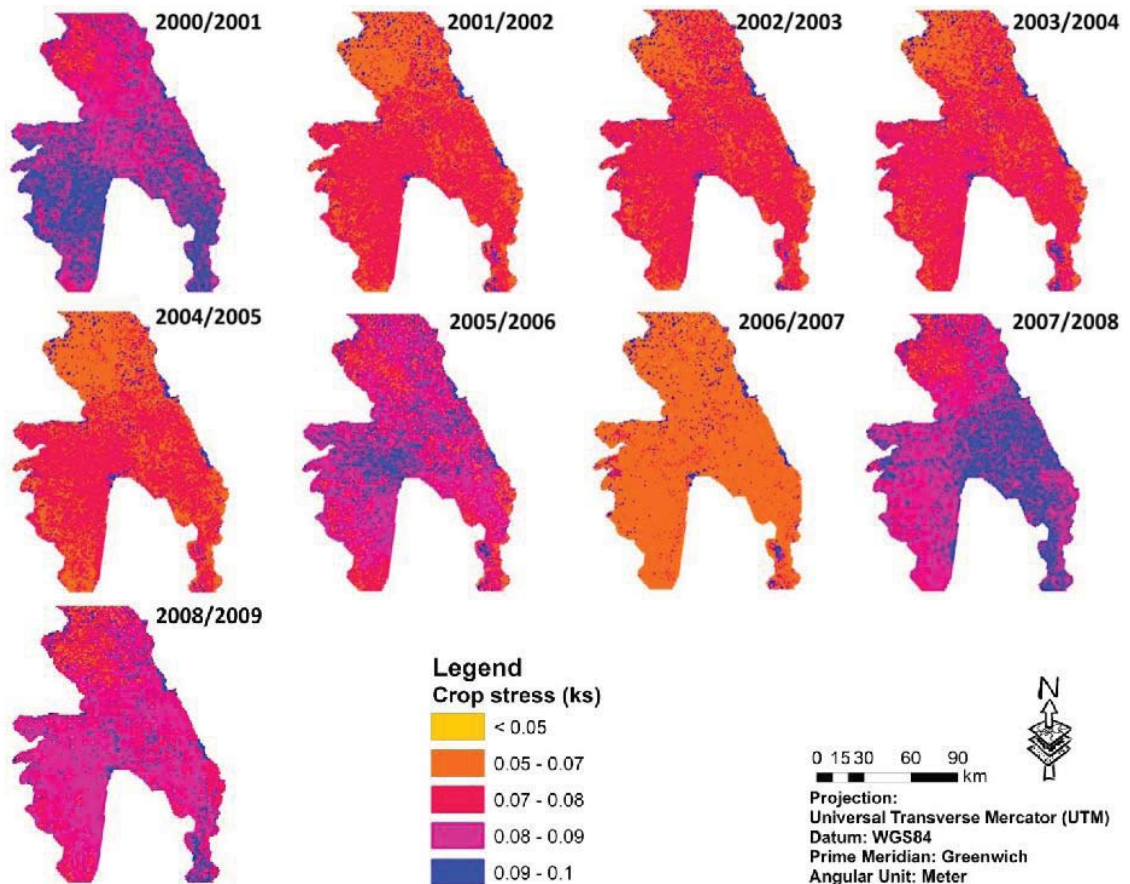


Figure 3-16. Spatial crop stress factor (ks) for the winter crop season

The water distribution assessment shows, in general, that the Gezira Scheme faces water deficit in many areas, especially in the northern part during the summer crop season, whereas water is sufficiently available and well-distributed during the winter season. MSCI is much more powerful for identifying drought areas than the estimated ks from the MOD16 product. Still, further studies for accurate ET_a and ET_p are recommended.

3.4 Conclusions

Irrigation water management study has been conducted by assessing irrigation water supply, rainwater supply, crop productivity and water distribution in the Gezira Scheme. The spatial and temporal characteristics of irrigation performance in the Gezira Scheme are examined for the crop seasons 1961/62–2009/10. Inefficient irrigation water supply of the Gezira Scheme has been witnessed since 1993/94, with RWS of 1.7–2.6 and RIS of 1.4–2.23. RWS and RIS for the winter crop season present higher values than those for the summer crop season, which is arguably linked to the change in crop policy in 1990. Moreover, the monthly MAI for all crops is less than 1.00, indicating inadequate supply of moisture from rainfall. Yet

the rainfall could be utilized in July and August to satisfy part of the crop demand. The average RMA values of 0.67, 0.49 and 0.46 for cotton, groundnut and sorghum, respectively, for July show the proportion of the evapotranspiration that can be partially supplemented by rainfall. However, the rainfall is not accounted for in irrigation scheduling in the scheme. Despite the water availability, the crop productivity analysis indicates that the Gezira Scheme has comparatively lower WUE values than those recorded for other irrigation schemes worldwide. The MVCI indicator reveals poor water distribution, especially during the summer crop season. Spatial drought mapping for the last 13 years has exposed a repetitively dry zone in the northern part of the Gezira Scheme, but well-irrigated zones in the southern, central and western parts. On the other hand, irrigation water is abundantly available during the winter crop season across the whole scheme. The MVCI values respond well to the water availability, which is represented by RIS and RWS.

The results can be used to improve irrigation water management in the scheme. The indicators show that water availability is higher than demand. Moreover, the contribution of rainfall to irrigation is completely overlooked. Rainfall should be harvested and utilized to reduce the need for supplemental irrigation. Also, the inequity of the conveyance system could be an additional factor leading to the low crop productivity of the scheme. Further research is required for accurate estimation of crop water demand using RS techniques. Also, a water policy analysis is required for the lower performance that is observed since the 1990s.

CHAPTER FOUR

DETERMINING THE OPTIMAL REMOTELY SENSED APPROACH TO OBTAINING ACTUAL EVAPOTRANSPIRATION FOR THE GEZIRA SCHEME

4.1 Introduction

Monitoring and quantifying the consumptive use over irrigated agricultural areas, rather than quantifying the delivered irrigation water (Folhes et al., 2009), can help to conserve water by improving efficiency and water productivity (Allen et al., 2011; Martin et al., 2013). Generally, the ET_a of a crop represents the actual water consumption (Allen et al., 1998). ET_a is an important indicator for evaluating irrigation water management practices (Feres and Soriano, 2007), as well as improving the crop productivity through enhancing soil moisture management (Fraiture and Wichelns, 2010). Hence, spatio-temporal information on ET_a assists decision-makers to better quantify water depletion and establishes links between land use and water allocation (Bastiaanssen et al., 2005).

Scholars have developed many methods to estimate evapotranspiration (ET), such as the pan evaporation method, lysimeters, flux profile measurements, the FAO Penman–Monteith method, the Bowen ratio and eddy-correlation measurements (Prueger et al., 1997; Allen et al., 1998; Immerzeel et al., 2006). These methods are point methods based on meteorological information for a specific station, and do not provide spatial patterns of ET_a (Immerzeel et al., 2006; Folhes et al., 2009). If the recommended point method of FAO Penman–Monteith is to be used spatially for estimating crop ET, its stages and crop factors must be known. However, it is often difficult to estimate these factors over large populations of crops and fields (Allen et al., 2011). RS data with high spatial and temporal resolutions are, therefore, a useful tool for providing information on evapotranspiration in this case, but are still limited when cloud cover exists (Immerzeel et al., 2006).

In the Gezira Scheme, estimating ET_a using RS methods has been carried out to determine crop coefficients for specific farms for wheat in 2001/02 (Ahmed et al., 2010) and for sorghum in 2004/05 (Bashir et al., 2007a, 2007b, 2008). Since the Gezira Scheme covers a vast area that lacks an actual water consumption monitoring system, it becomes imperative to develop a suitable tool for monitoring agricultural water use. Therefore, the overall objective

of this chapter is to determine the agricultural water consumption for the Gezira Scheme of Sudan, using RS techniques.

4.2 Materials and methods

4.2.1 Model selection

The most applicable RS method for estimating ET_a in irrigated areas is the surface energy balance method (Bastiaanssen et al., 2005; Immerzeel et al., 2006; Senay et al., 2007; Allen et al., 2008), which has been successfully applied worldwide. Immerzeel et al. (2006) stated that this method is the most complete and highly accurate for this purpose. In addition, it has significant advantages over other RS methods, as it does not need information on crop development stages or specific crop type location (Allen et al., 2008) and captures the actual crop status (Allen et al., 2011). However, there are several different energy balance models of ET_a based on RS data, such as SEBAL (Bastiaanssen et al., 1998a, 1998b), S-SEBI (Roerink et al., 2000), METRIC (Allen et al., 2007a), ETLook (Pelgrum et al., 2010) and SSEBop (Senay et al., 2013).

The SEBAL algorithm has been widely used and validated for irrigated agricultural areas all over the world for the past two decades (Pelgrum and Bastiaanssen, 1996; Bastiaanssen et al., 1998b; Bastiaanssen, 2000; Allen et al., 2005; Immerzeel et al., 2006; Bashir et al., 2007a, 2007b, 2008; Ahmed et al., 2010). The ETLook model is a newer version of the SEBAL algorithm based on an Advanced Microwave Scanning Radiometer-EOS (AMSR-E) passive microwave sensor (Pelgrum et al., 2010). However, the AMSR-E antenna stopped spinning on October 4, 2011 (NASA, 2013). In addition, the METRIC has the same foundation, principles and techniques as used by the SEBAL model (Trezza, 2006; Allen et al., 2007a; Allen et al., 2007b; Allen et al., 2011; Martin et al., 2013), and SEBAL and METRIC need minimal ground data (Folhes et al., 2009), which is hard to obtain for Sudan. Consequently, SEBAL and METRIC are chosen in this research, as they are considered long-term planning tools (Immerzeel et al., 2007) and operationally more applicable. In spite of SEBAL and METRIC being the most complete and accurate models for estimating ET, they are considered complex (Immerzeel et al., 2006; Senay et al., 2009). Therefore, the Simplified Surface Energy Balance (SSEB) (Senay et al., 2007), a simplified version of SEBAL and METRIC, is also addressed in the current research.

4.2.2 Source of data

4.2.2.1 Remote sensing

Landsat sensors have provided the data most used in RS studies on crop ET monitoring via SEBAL and METRIC (Bastiaanssen, 2000; Allen et al., 2003, 2005; Tasumi et al., 2003, 2005; Trezza, 2006). The spectral coverage and spatial resolution (30 m) of Landsat data allow ET estimation at individual agricultural field scale. Fortunately, the Landsat tile (path 173, row 50) covers almost 94% of the total Gezira area, as illustrated in Figure 4-1. All Landsat Enhanced Thematic Mapper Plus (ETM+) L1T images over the Gezira Scheme with cloud cover $\leq 1\%$ are obtained for a period extending from the end of May 2004 to the beginning of December 2004, as listed in Table 4-1.

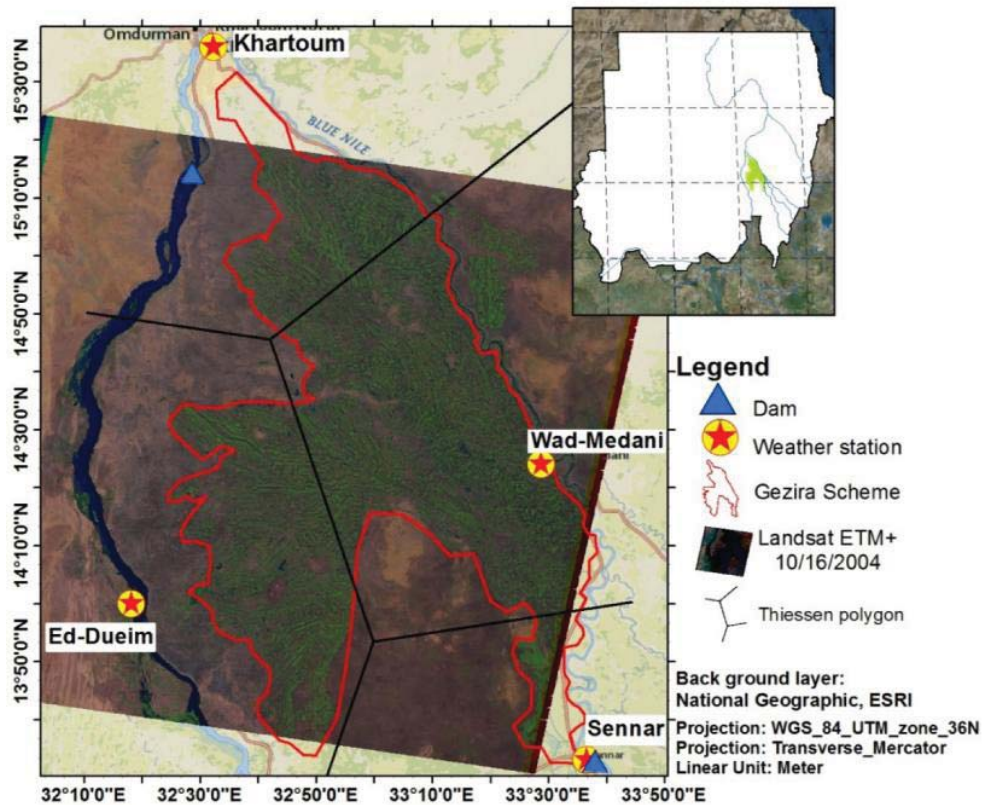


Figure 4-1. Location of the study area and the aerial coverage of Landsat tile

Table 4-1. Landsat ETM+ images used for season 2004/05 in the Gezira Scheme

ID	Date	Landsat scene identifier	Cloud cover (%)
1	May 25, 2004	LE71730502004146ASN03	0
2	Jul. 28, 2004	LE71730502004210ASN01	0
3	Aug. 13, 2004	LE71730502004226ASN01	1
4	Aug. 29, 2004	LE71730502004242ASN01	1
5	Oct. 16, 2004	LE71730502004290ASN01	0
6	Nov. 1, 2004	LE71730502004306ASN00	0
7	Nov. 17, 2004	LE71730502004322ASN00	0
8	Dec. 3, 2004	LE71730502004338ASN00	0

The ETM+ images of scan line corrector (SLC) failure have 22% missing pixels occurring in a repetitive along-scan stripe pattern (Chen et al., 2011). To obtain complete coverage, a pre-process gap-filling is done using the nearest-neighbor statistical method as a similar approach used by Evapotranspiration (2011a, 2011b) (Appendix Three). The Landsat ETM+ wavelength bands 1–61, and 7 (USGS, 2014) are used in this study. The Digital Numbers (DN) of Landsat images are converted to reflectivity by applying Landsat Handbook (2007) equations.

The NDVI product (MOD13Q1), 16-day and 250 m resolution, from MODIS is downloaded for June 2004–November 2004. The MOD13Q1 data set is available for free and is obtained from the Oak Ridge National Laboratory Distributed Active Archive Center (ORNL DAAC, 2011) in GeoTIFF format. Subsequently, the Gezira area is extracted by using the Extract-by-Mask tool in ArcGIS 10 software (ESRI, 2013).

A digital elevation model (DEM) is used within the selected energy balance models to calculate the atmospheric transmissivity (τ_{sw}) and correct the land surface temperature (T_s). The Shuttle Radar Topography Mission (SRTM) DEM data (90 m) is downloaded from the United States Geological Survey (USGS) (USGS, 2013a). The DEM is processed using the Mosaic-To-New-Raster, Con-function, Is-Null, Focal-Statistics and Project-Raster tools in ArcGIS 10 software (ESRI, 2013) for data void filling, mosaicking, and re-projection of the tiles to form a single, seamless DEM for the Gezira area.

4.2.2.2 Ground-observed data

Daily and monthly meteorological data (maximum and minimum air temperature, sunshine hours, wind speed and humidity) are obtained for four meteorological stations, as presented in Table 4-2 and shown in Figure 4-1, from the Sudan Meteorological Authority. The

available daily data are for the satellite image dates mentioned in Table 4-1. In addition, the rainfall data are obtained for the week prior to the satellite overpasses. Also, instantaneous climatic elements, temperature, wind speed and relative humidity are derived at 09:00 GMT due to the lack of observation during the satellite overpass time (\cong 08:00 GMT). The Thiessen polygon method (Chow et al., 1988) is used to define the area covered by each meteorological station.

Table 4-2. Location of the meteorological stations

ID	Station	Latitude	Longitude	Altitude (AMSL)
1	Ed-Dueim	14°00'0.00"N	32°19'48.00"E	378 m
2	Khartoum	15°36'0.00"N	32°32'24.00"E	382 m
3	Sennar	13°33'0.00"N	33°36'36.00"E	418 m
4	Wad Medani	14°24'0.00"N	33°28'48.00"E	408 m

4.2.3 Energy balance method

4.2.3.1 SEBAL

The theoretical and computational basis of SEBAL is described in Bastiaanssen et al. (1998a, 1998b, 2005) and Bastiaanssen (2000). The SEBAL model calculates the instantaneous latent heat flux (λE) for each satellite image pixel from the following energy balance equation:

$$\lambda E = R_n - G - H \quad (\text{W/m}^2), \quad (\text{Equation 4-1})$$

where λ is the latent heat of the vaporization; R_n , the net radiation (W/m^2); G , the soil heat flux (W/m^2); and H , the sensible heat flux (W/m^2). The instantaneous net radiation (R_n) is calculated as a function of incoming and outgoing short- and long-wave radiation. Several derived parameters are used to obtain R_n , such as (1) NDVI, Leaf Area Index (LAI) and Soil Adjusted Vegetation index (SAVI) vegetation indices, (2) surface albedo and (3) T_s . The latter is calculated based on the Landsat Handbook (2007) and Allen et al. (2007a) with elevation adjustment based on DEM, as recommended by Senay et al. (2011). Afterward, G is empirically calculated as a G/R_n fraction. Finally, H is computed using wind-speed observations, surface-to-air temperature differences and empirical surface roughness (Z_{om}). The latter is obtained from an empirical relation (Bastiaanssen, 2000) using SAVI. The process of H is obtained through self-calibration steps between dry ($\lambda E \cong 0$) and wet ($H \cong 0$) pixels. They are manually identified by the user on the image (Bastiaanssen et al., 2005). In this study, the hot anchor pixel is selected where bare agricultural soil is assumed to be dry enough after verifying that there have been no

rainfall events in the week prior to the Landsat overpass dates. The cold pixel is selected from a local water body, as recommended by Bastiaanssen et al. (1998a), which for the present study is located at the Jabal El-Aulia reservoir. Once λE is intended, the daily ET_a from SEBAL (ET_{a-SEBAL}) is calculated as a function of the evaporative fraction (EF), the ratio of latent heat flux over available energy, which is assumed to be constant during daylight hours. EF is defined as

$$EF = \lambda E / (R_n - G), \quad (\text{Equation 4-2})$$

Later, ET_{a-SEBAL} is transformed from W/m² to mm/day using the following equation:

$$ET_{a-SEBAL} = \frac{86400 \times EF \times R_{n-day}}{\lambda} \quad (\text{mm/day}), \quad (\text{Equation 4-3})$$

where 86400 is a constant for daily time scale conversion; R_{n-day} is the daily net radiation, which is aggregated based on Bastiaanssen et al. (1998a) with daily atmospheric transmissivity updates by the modified Ångström coefficients developed by Elagib (2009); and λ is calculated as a function of mean daily air temperature (T_{mean}) as follows:

$$\lambda = 2.501 - 0.00236 \times T_{mean} \times 10^6, \quad (\text{Equation 4-4})$$

4.2.3.2 METRIC

METRIC (Mapping EvapoTranspiration at High Resolution with Internalized Calibration) is a satellite-based image-processing tool for calculating ET_a as a SEBAL foundation (Martin et al., 2013). METRIC is developed by Allen et al. (2007a) and departs from the SEBAL model in terms of cold pixel selection in that it should be located within a well-irrigated homogeneous agricultural field. Methods for selecting proper hot and cold pixels can be found in Allen et al. (2002). In this study, the hot pixel is the same pixel as used in SEBAL, while the cold pixel is always found in the well-irrigated area in the southern part of the Gezira Scheme. At the cold pixel, METRIC utilizes the alfalfa reference ET (ET_r) to establish the energy balance condition (Allen et al., 2011). ET_r and the grass reference ET (ET_o) are calculated using the REF-ET version 3.1 software developed by Allen (2000). METRIC also differs from SEBAL in that it extrapolates daily ET_a by using ET_r rather than daily net radiation (Allen et al., 2008; Allen et al., 2011). Hence, the reference ET fraction (ET_rF) is calculated as follows:

$$ET_r F = 3600 \times \frac{\lambda E}{\lambda \times ET_{r-inst}}, \quad (\text{Equation 4-5})$$

where 3600 is a constant for hourly time scale conversion, λ and λE are as defined in Equations 4-1 and 4-4, respectively, and ET_{r-inst} is instantaneous ET_r (mm/hour). Consequently, METRIC daily ET_a (ET_{a-METRIC}) is calculated from the following equation:

$$ET_{a-METRIC} = ET_{rF} \times ET_{r-24}, \quad (\text{Equation 4-6})$$

where ET_{rF} is as defined above and ET_{r-24} is the daily ET_r (mm/day). Both SEBAL and METRIC are simulated using ERDAS Imagine 2011 (ERDAS, 2013) integrated with ArcGIS 10 (ESRI, 2013) for hot and cold pixel extraction. A user manual for applying SEBAL and METRIC is presented in Appendix Three.

4.2.4 SSEB

Senay et al. (2007) developed and implemented the SSEB model to monitor and assess irrigation performance in Afghanistan. The model was evaluated, and gave comparable results to lysimetric data (Senay et al., 2013) and the METRIC model (Senay et al., 2011). SSEB approaches SEBAL and METRIC with further simplification by stating that ET_a varies linearly with hot and cold pixels. This simplification is manifest in using T_s rather than λE and H to derive the ET fraction (ET_f) (Equation 4-7) based on hot and cold pixels. Senay et al. (2007) argue that the hot pixel of a bare agricultural area experiences little or no ET, while the cold pixel of a well-watered irrigated field experiences maximum ET:

$$ET_f = \frac{TH - T_x}{TH - TC}, \quad (\text{Equation 4-7})$$

where TH and TC are the average of three hot and cold pixels selected for a given scene, respectively, and T_x is the T_s pixel value for the given scene. Hence, the actual daily ET from SSEB is defined as:

$$ET_{a-SSEB} = ET_f \times ET_{r-24}, \quad (\text{Equation 4-8})$$

Senay et al. (2011) improved SSEB ($SSEB_{elvi-ndvi}$) by applying correction factors to T_s and NDVI. Later, another modification was made to SSEB ($SSEB_{op}$) by upgrading the uncomplicated method to the energy balance method (Senay et al., 2013). In the present paper, the T_s enhancement only is considered, and not that for NDVI. The NDVI adjustment formula underestimated the ET_a values for the Gezira Scheme by 80%. In addition, the model performance is conducted using NDVI values; therefore, $SSEB_{elvi}$ is applied in this research in comparison with SEBAL and METRIC.

4.2.5 MOD16 evapotranspiration

The actual and potential (ET_a and ET_p) global evapotranspiration MOD16 ET products (Mu et al., 2011) are used in this comparative study, as the product is now operationally available. The MOD16 ET datasets are estimated using the improved ET algorithm (Mu et al., 2011) instead of the previous version (Mu et al., 2007). The ET algorithm is based on the

Penman–Monteith equation (Monteith, 1964), which is driven by NASA MODIS images (1 km resolution). The product has been available since 2000 as 8-day, monthly and annual interval time series data. Additionally, it has been validated with ET measurements all over the world (Mu et al., 2011; Kim et al., 2012; Velpuri et al., 2013; Ruhoff et al., 2013; Chen et al., 2014). However, it has not been validated yet at the Gezira Irrigation Scheme. The latest improved MODIS 16 ET product locally over the Nile River Basin countries is used in this study (NTSG, 2015).

4.2.6 Seasonal ET_a extrapolation

The calculated evaporative fraction (i.e. EF, ET_{rF} or ET_f) is considered the FAO crop factor (kc) to extrapolate the reference crop ET (i.e. ET_o or ET_r) to daily, monthly or seasonal levels of ET_a (Allen et al., 2002; Allen et al., 2007a). Allen et al. (2007a) mentioned that one satellite image per month is sufficient to represent an accurate kc curve for seasonal ET_a estimation. Hence, the cumulative ET for any period is calculated as

$$ET_{\text{period}} = \sum_{i=m}^n [(\text{evaporative fraction}_i) \times (\text{reference ET}_{\text{per}})] \quad (\text{Equation 4-9})$$

where ET_{period} is cumulative ET for a period beginning on day **m** and ending on day **n**, the evaporative fraction_i, (EF, ET_{rF} or ET_f) is the representative EF for period **i**, and the reference ET_{period} (i.e. ET_o or ET_r) is the total reference ET for the defined period **m** to **n**. For MOD16, the seasonal ET is stacked together using the Cell-Statistics tool in ArcGIS 10 (ESRI, 2013), representing the crop season June–November.

4.2.7 Validation of ET estimates from the models

To evaluate the models for the local conditions, Landsat images are obtained for crop season 2004/05 to allow comparison with earlier studies by Bashir et al. (2007a, 2007b, 2008). The authors used water balance (WB) and SEBAL to estimate ET_a for sorghum at field scale. A similar validation approach has been reported by Folhes et al. (2009) and Senay et al. (2011) by validating their models (METRIC) using previously published studies.

The validation experimental field lies between (14°22'33.10" N, 33°29'50.68" E) and (14°22'30.98" N, 33°29'49.91" E) in the Gezira Scheme (Bashir, M.A., personal communication). However, it is worth mentioning herein that the ET study by Bashir et al. (2007a, 2007b, 2008) used only four Landsat satellite images (July 28, August 29, October 16 and November 17), all from 2004. In this study, additional Landsat images are used (May 25 and December 3) to evaluate the models' performance at the start and end of the crop stages. Also, images on August 13 and November 1 are added to enhance temporal monitoring

resolution. For images captured in August, the cloud cover masking method (Landsat Handbook, 2007) is utilized to mask the clouds by using the thermal band. In addition, the image from August 13 is not used for seasonal ET computation, as the cloud cover is distributed over large areas of the Gezira Scheme. Fortunately, the clouds do not cover the pilot sorghum experimental field on the mentioned day.

4.3 Results and discussion

4.3.1 Evapotranspiration models validation

4.3.1.1 Daily bases

The comparison of daily ET_a measured by the WB method from Bashir et al. (2007a, 2007b, 2008) with daily ET_a estimates using SEBAL, METRIC, SSEB and MOD16 for the sorghum validation site is shown in Table 4-3. The performance of the models differs substantially. Overall, the SEBAL and SSEB models provided ET_a estimates close to the WB measurements. However, the estimated ET_a using both models exceeded the WB figures (see also Bashir et al. (2007a, 2007b, 2008)) at the beginning of the sorghum crop season (July 28) by 59% and 20%, respectively. Yet on May 25, the SSEB model has a low and reasonable ET_a value. The deviation of results from SEBAL could be explained by the overestimation of the actual ET during the dry season as a result of absence of vegetation cover (El Tahir et al., 2012). Generally, the two models give estimates that are 42%–59% of the ET from the WB method. Except for the METRIC and MOD16 models, they overestimated (94%–370%) and underestimated (26%–79%) the measurements, respectively, not only with respect to the experimental WB, but also with respect to ET quoted in previously conducted studies (i.e. Farbrother (1996), Abdelhadi et al. (2000), Ibrahim et al. (2002), Adeeb (2006), Ahmed et al. (2007), Bashir et al. (2008), and Ahmed et al. (2010)).

Table 4-3. ET_a (mm/day) obtained from the four Remote Sensing (RS) models compared with the Water Balance (WB) measurement

Date	WB* (mm)	SEBAL	Error%	METRIC	Error%	SSEB	Error%	MOD16	Error%
May 25, 2004	—	5.16	—	13.32	—	0.43	—	1.15	—
Jul. 28, 2004	2.60	4.14	59.23	11.75	351.92	3.13	20.46	1.70	-34.62
Aug. 13, 2004	—	4.27	—	13.05	—	5.49	—	1.73	—
Aug. 29, 2004	5.90	4.64	-21.29	14.69	149.01	6.22	5.50	1.83	-69.07
Jan. 1, 2004	7.10	6.93	-2.34	20.30	185.98	6.97	-1.90	1.55	-78.17
Jan. 11, 2004	—	5.01	—	12.06	—	4.55	—	1.54	—
Nov. 11, 2004	3.00	2.60	-13.33	5.44	81.22	1.72	-42.69	1.48	-50.83
Dec. 3, 2004	—	2.55	—	10.72	—	0.71	—	1.35	—
Season	489.00	546.00	11.66	1310.00	167.89	510.00	4.29	298	-39.06

Source: *Bashir et al. (2007a, 2007b, 2008)

The root mean square errors (RMSE) between the ET estimated from SEBAL, SSEB and the measured values (Table 4-4) are found respectively to be 0.71 mm/day and 1.02 mm/day, compared to 9.24 mm/day and 3.55 mm/day for METRIC and MOD16, respectively (Table 4-4). The best-fit linear equations with WB are conducted and their parameters are presented in Table 4-4. SSEB results show the highest coefficient of determination ($R^2 = 0.90$ and $p < 0.05$) with the equation, followed by SEBAL with an R^2 value of 0.71 (insignificant).

Table 4-4. The parameters of best-fit linear equations for the four models at the field and scheme levels

Level	WB* Field				NDVI [†] Field			iNDVI [†] Scheme		
	a	b	R ²	RMSE	a	b	R ²	a	b	R ²
SEBAL	1.04	-0.10	0.71	1.02	16.14	-0.03	0.86	95.62	188.89	0.77
METRIC	0.31	0.67	0.74	9.24	28.86	2.47	0.38	281.36	391.92	0.80
SSEB	0.84	0.88	0.90	0.71	23.22	-2.85	0.93	234.38	-477.21	0.75
MOD16	2.19	1.07	0.02	3.55	0.371	1.52	0.06	108.58	-83.83	0.81

*WB = a × Model + b; [†]ET_{model} = a × (NDVI or iNDVI) + b

Bastiaanssen et al. (2005) reported that the typical accuracy of SEBAL at field scale is 85% for one day. Although SEBAL and METRIC have the same energy balance method foundation, METRIC gives higher values than SEBAL. The reason is related to the lower values

of the calculated ET_{r-inst} compared to the instantaneous $ET_{a-METRIC}$, which makes the ET_{rF} factor (Equation 4-5) always greater than one. This may be attributed to the 09:00 GMT climate data utilized to calculate ET_{r-inst} . It is worth mentioning herein that Bashir et al. (2007a, 2007b, 2008) computed the daily ET_a by the ET_{rF} method. The authors used meteorological data taken at around 14:00 local time (11:00 GMT), as it is hard to find the actual meteorological data during satellite overpasses (Bashir, M.A. personal communication). However, Allen et al. (2005) mentioned that error over- or underestimation from METRIC is mainly based on both instantaneous and daily ET_r estimates. Therefore, METRIC has many constraints to be used in such areas (e.g. developing countries) do not have hourly climate data. Another reason could be the vast area covered by the Gezira Scheme. Martin et al. (2013) mentioned that METRIC can function as an operational model for producing maps of ET for regions smaller than a few hundred kilometers in scale. In areas where meteorological data are not available, SEBAL has the advantage of being somewhat independent from such information (SEBAL only needs an estimation of wind speed at satellite time), and estimation of energy balance components is pulled from the satellite image (Trezza, 2006). Furthermore, in the northern central United States, SSEB gave a good ET_a estimation result with measured ET from several crop fields (Senay et al., 2007). Besides, the model estimated ET_a within 4% of the measured ET_a in another study in the US (Singh et al., 2014).

On the other hand, the ET_a rate from MOD16 is low for the Gezira Scheme (see Table 4-3), thus confirming earlier results by Mu et al. (2007, 2011) who found that the estimation of ET_a from irrigation areas cannot be well represented by algorithm. In addition, this result compares well with findings at a basin scale by Yilmaz et al. (2014) on Gezira Scheme. Our results also show that MOD16 cannot accurately estimate ET_a from agricultural field due to the pixel resolution.

4.3.1.2 Seasonal

Estimation of seasonal ET_a from SEBAL, METRIC and SSEB is carried out by aggregating daily ET_a derived from the models proportionally to daily mean reference evapotranspiration from the Wad Medani station (Equation 4-9). The results show that the METRIC model simulated the highest seasonal ET_a (1310 mm) which is around five times the lowest seasonal ET_a obtained from MOD16 (289 mm). The results obtained from both models are far from the ET_a WB-method estimates (489 mm/season) for a period of 92 days (August 28–November 27). On the other hand, the SEBAL and SSEB models fairly estimate the seasonal sorghum ET_a as 546 mm/season and 510 mm/season, respectively, with +11.6% and +4.3% deviation, respectively, from the WB measurements for the same period. It appears

that much of the SEBAL error occurs on individual image acquisition dates. Bastiaanssen et al. (2005) reported that SEBAL error is generally randomly distributed and tends to cancel itself out, and that it also increases to 95% on a seasonal basis.

For the Gezira Scheme, Bashir et al. (2007a, 2007b, 2008) mentioned that the total ET values over the growing season of irrigated sorghum estimated by RS, FAO kc and experimental kc, take a range of 642–704 mm. In the present research, SEBAL and SSEB respectively predict the ET_a over the full period of the growing season of irrigated sorghum to be 708 and 676 mm. The values for SEBAL kc derived during the initial mid-season and late-season crop development stages are 0.61, 0.97, 1.16, and 0.60, respectively. On the other hand, the values for the SSEB model during the previously mentioned stages are 0.44, 0.96, 1.17 and 0.40, respectively. In this case, the values for kc derived from SSEB are close to those estimated by the WB reported by Bashir et al. (2007a, 2007b, 2008).

4.3.2 Spatial variability of actual evapotranspiration

4.3.2.1 Daily ET_a

The daily actual evapotranspiration (ET_{a24}) is computed for 8 days using the four ET models. The four models showed similar spatial daily patterns but with different magnitudes. However, SEBAL and SSEB give reasonable values with only minor differences. The simulated ET_{a24} maps from the four models are presented in Figure 4-2. The values for SEBAL and SSEB range from zero to almost 10 mm, with higher values strongly linked to irrigated areas, wetlands and water. Nevertheless, very low values of ET_{a24} (< 1 mm for SSEB) correspond to barren areas. It is observed from daily ET during the rainy season that the semi-arid vegetation (areas far from the irrigation network) transpires as the soil moisture is available due to the available rainfall. METRIC and MOD16 have a similar ET_a distribution but with different magnitudes, as shown in Figure 4-2. On July 28, SEBAL and SSEB showed relatively high ET over the agricultural fields, although most of the crops are at the initial stage. This could be attributed to high soil moisture (a substantial amount of rainfall fell one day prior to image acquisition) at the root zone at the time of the satellite overpass. The presence of cloud cover on the August 18 image smears the daily ET assessment.

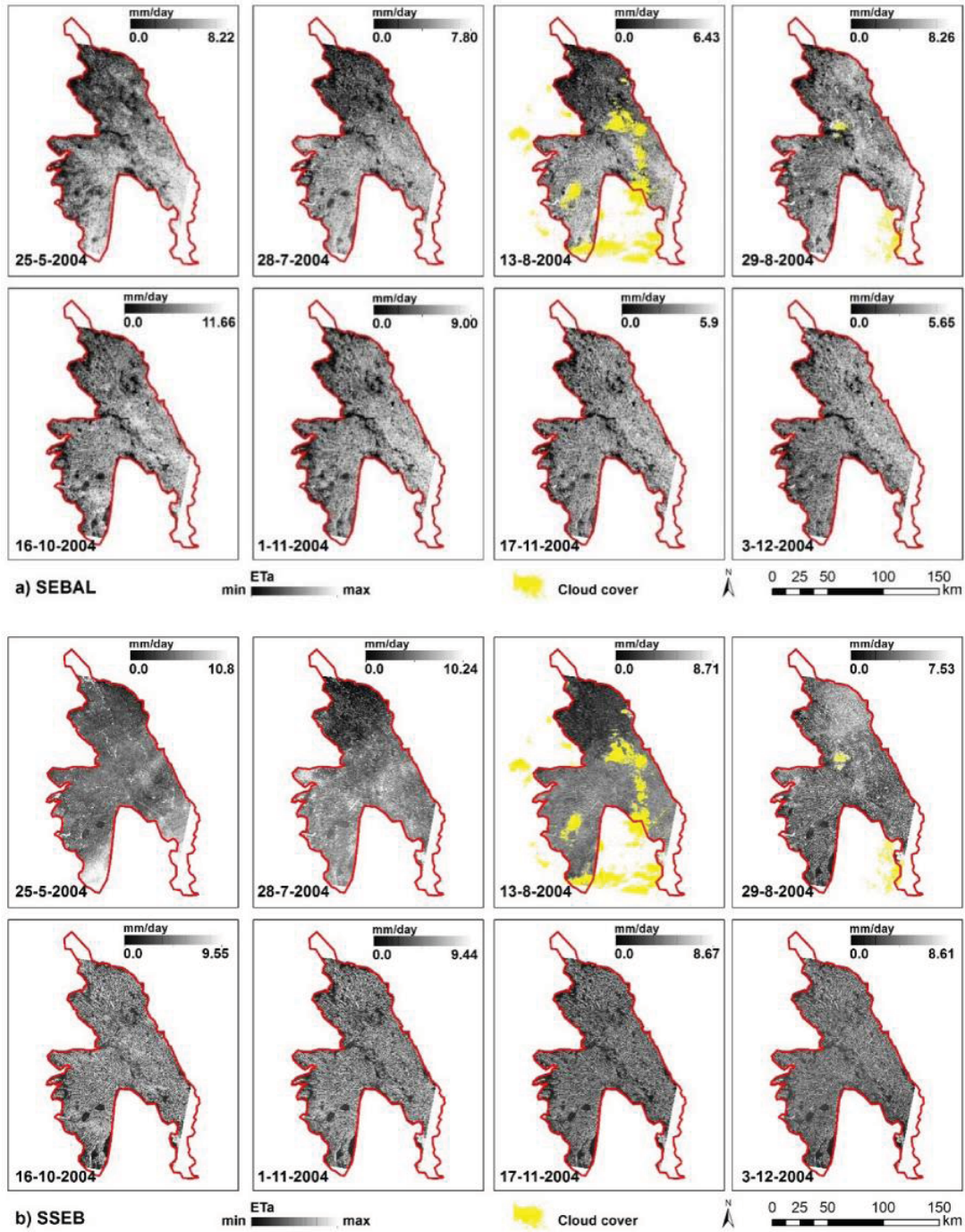


Figure 4-2. Spatial distribution of ET_{a24} from (a) SEBAL, (b) SSEB (c) METRIC and (d) MOD16 models across the Gezira Scheme

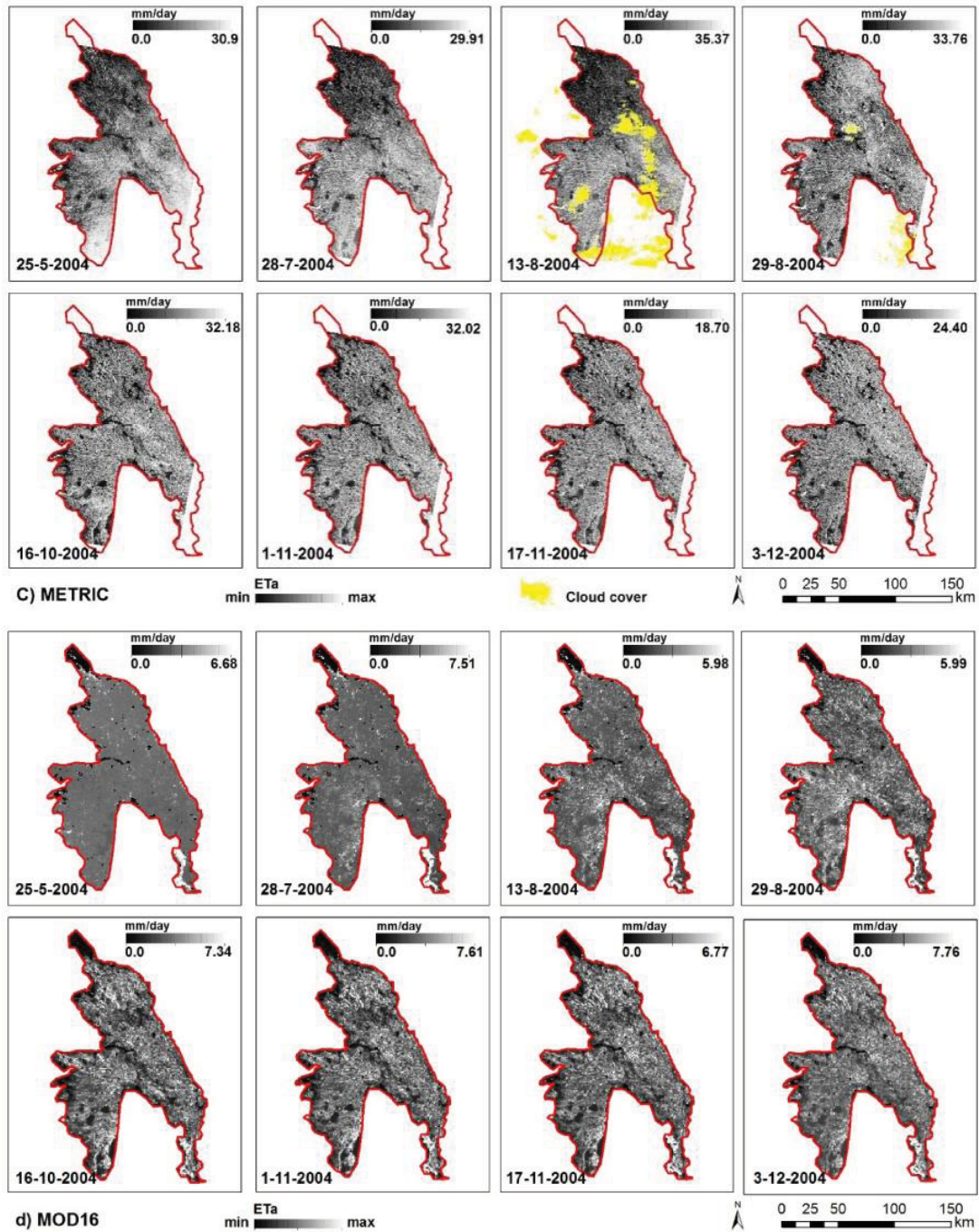


Figure 4-2. (continued)

4.3.2.2 Seasonal ET_a

All four models showed similar spatial patterns of seasonal ET, with decreasing ET from southeast to northeast of the scheme, as displayed in Figure 4-3. The highest ET rates are always observed on the southern part, which is linked to the fact that the area is close to the water supply source (Sennar Dam). Also, higher values are noticed in the well-irrigated areas, especially in the southern and central parts of the scheme, and the water ponds located at the western edge. Comparing the models' magnitudes, however, revealed a large difference in ET estimates. The mean ET of the scheme for the four models takes a range of 222–1372 mm/season. SEBAL and SSEB ET rates are 522 and 342 mm/season, respectively. Since METRIC and MOD16 over- and underestimate the ET values spatially and at field level, both models' results are used only to give a relative ET distribution in the study area.

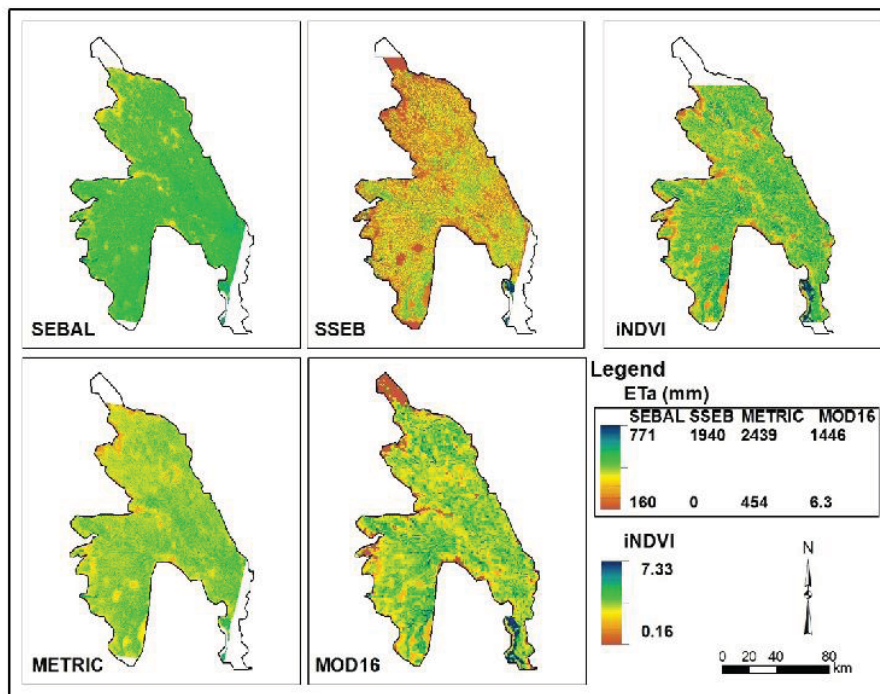


Figure 4-3. Spatial distribution of ET_a season from the four models in comparison with the integrated NDVI (iNDVI)

For further analysis, the seasonal ET magnitude is extracted from SEBAL and SSEB outcomes at the administrative level; boundaries are shown in Figure 4-3. Figure 4-4 provides details of actual seasonal ET in the 2004/05 summer season for each group in the scheme. As can be seen, the northern groups (Abu Gouta, North West, Huda, North and Wad Habouba) have the lowest seasonal ET obtained from the two models. Seasonal ET estimated from the South, Massallamia, Mansi, Wadi Sha’eer, Gamusi, Hosh and Shawal groups (southern and central) is considered the highest, with more than 550 mm from SEBAL and 375 mm from SSEB. From the analysis, variation of ET between the different groups has the potential to identify areas of water stress and waterlogging to improve the WUE of the scheme.

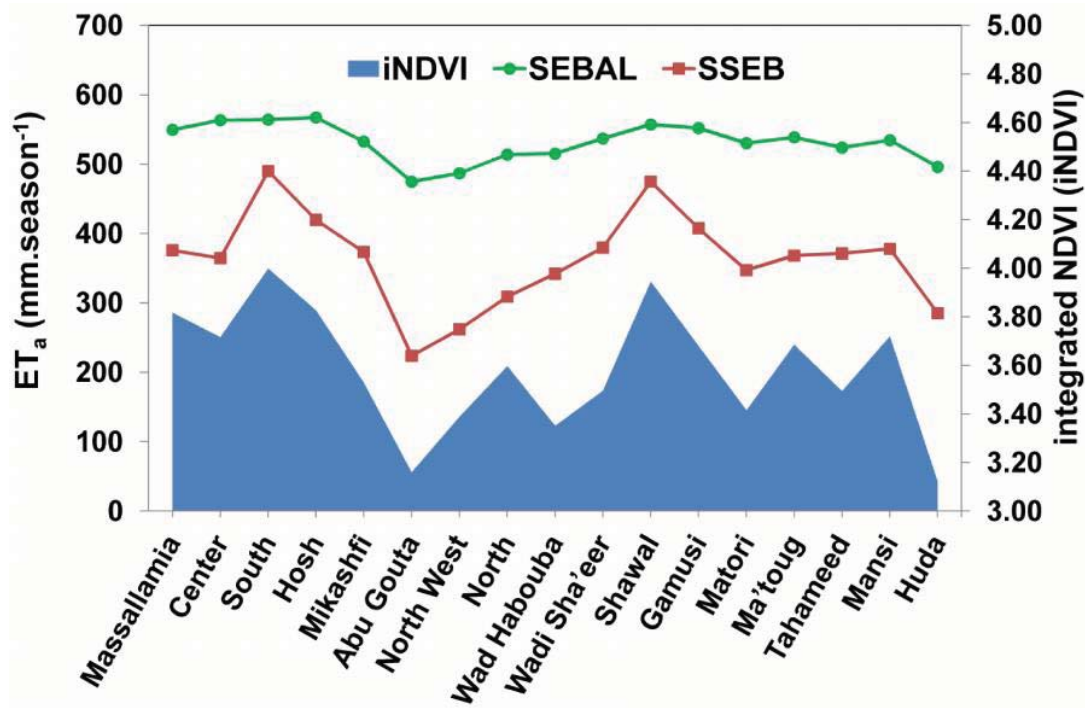


Figure 4-4. Seasonal ET_a and the integrated NDVI for various administrative units of the Gezira Scheme in the 2004/05 summer season

4.3.3 Models performance evaluation

4.3.3.1 Field level

Studies show (Szilagyi et al., 1998; Duchemin et al., 2006; Mutiga et al., 2010) that the actual ET is directly proportional to the canopy density, measured as the NDVI, which often better fits a linear expression.

Figure 4-5 shows the observed relationship between the actual ET from WB and the four models, and the derived NDVI from Landsat images over the validation experimental field. The figure illustrates the influence of the presence of crop development on the actual ET. Results are very similar, especially for the WB method. This results in a high R² value of 0.98

($p = 0.005$), which is related to the good response of crop growth measured by the NDVI and the actual ET. Among the other RS models, SSEB is good for estimating ET at the field scale. The resultant ET is directly proportional to NDVI, with an R^2 value of 0.92. For the SEBAL and METRIC methods, a positive correlation is noticed, which designates the ability of the energy balance models to capture top soil moisture in the study area. The variation could be explained by the energy balance method overestimating the actual ET during the absence of vegetation cover at the beginning of the season, as mentioned in Section 4.3.1.1.

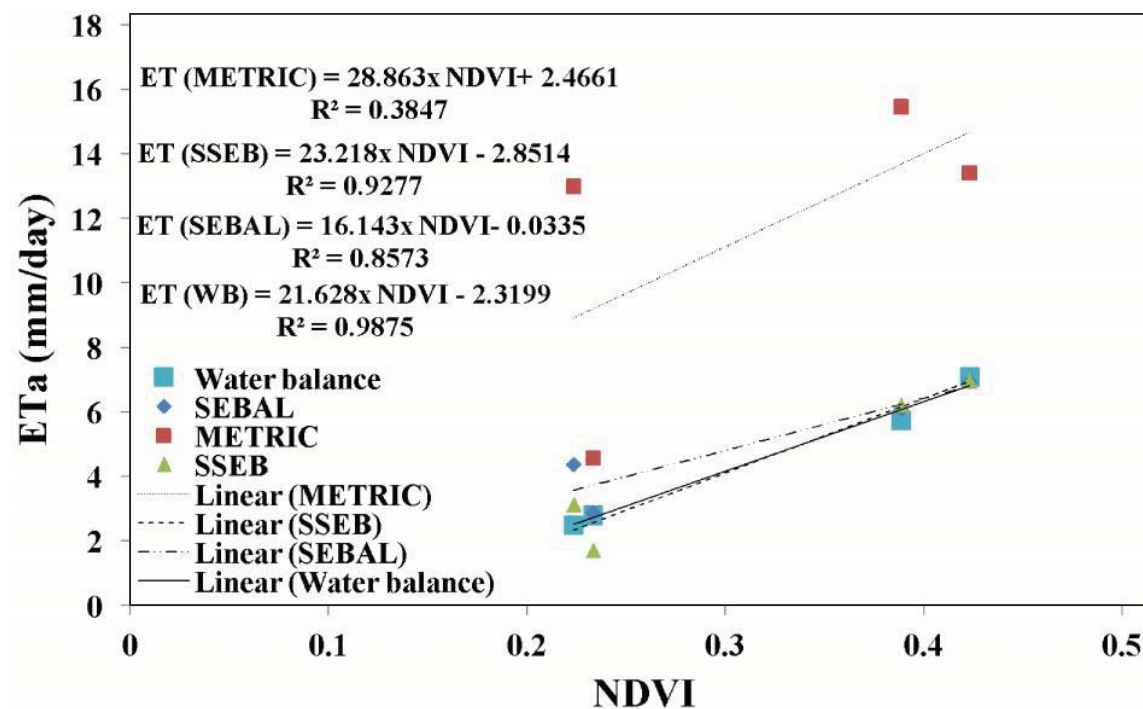


Figure 4-5. Relationship between ET_a from different estimation methods and NDVI for the sorghum field

4.3.3.2 Scheme level

The mean seasonal ET_a values for the most accurate estimation models (SEBAL and SSEB) for each group in the scheme are also compared with their respective $iNDVI$ values obtained from the MODIS NDVI product. A good correlation of about $\cong 75\%$ is obtained (Figure 4-6) for both models. It is observed that ET_a values increase with increasing $iNDVI$ values within the central and southern areas of the scheme (Figure 4-4). However, in the northern part, ET_a values tend to decrease with decreasing $iNDVI$ values. The reason for this could be that crops are more stable in the southern and central parts because irrigation water is regularly received in these areas. This is due to its proximity to the Sennar Dam. In the northern areas, irrigation water decreases and, as a result, reduces the $iNDVI$ values. Bashir et al. (2008)

calculated the seasonal ET by applying the SEBAL algorithm. The authors mentioned that the northern part has the highest seasonal ET in the whole scheme. They compared the ET_a pattern with a false color composite of MODIS bands 4, 2, and 1 (RGB) for visual validation. They emphasized that the simple band combination can give a visual impression of the ET_a distribution in the study area. The comparison of one day's image (instantaneous) with seasonal ET_a (cumulative) might be an ineffective evaluation. Therefore, a closer look for the $iNDVI$ for the northern part for 2004 (Figure 4-3) is conducted. Compared to the $iNDVI$ and the results achieved in the current research, Bashir et al. (2008) succeeded in implementing SEBAL at the field level, but not at scheme level.

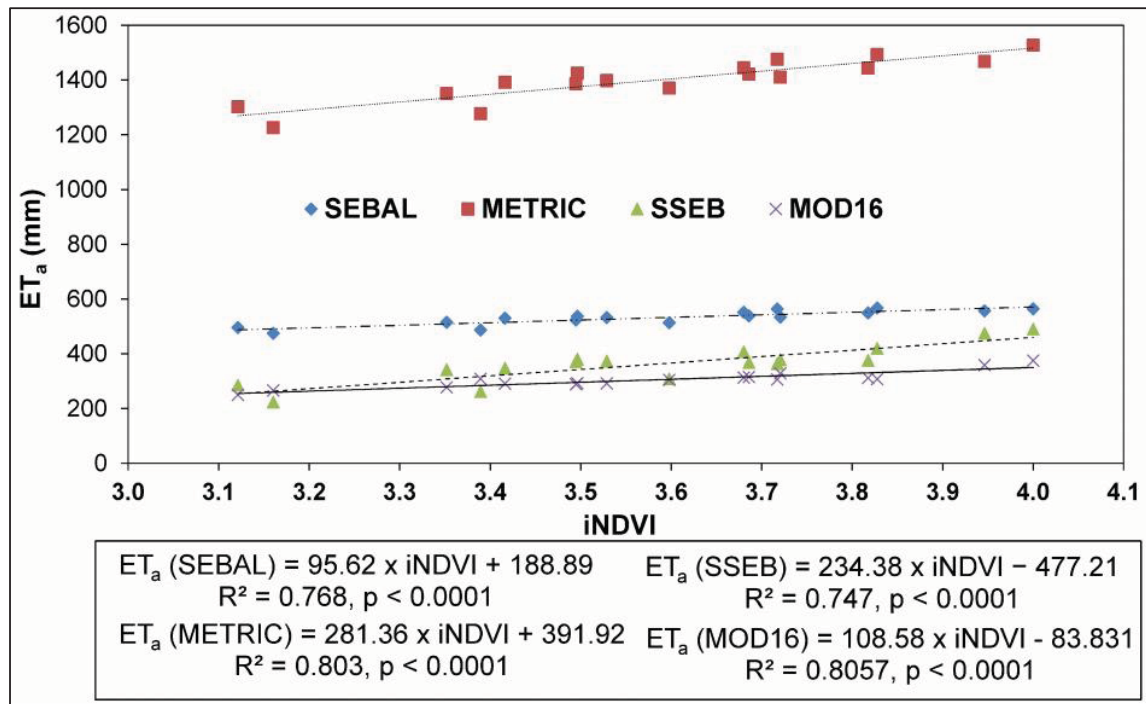


Figure 4-6. The seasonal ET_a from the four models against $iNDVI$ for the summer crop season of 2004/05

A simple WB for the whole region (RWB) is computed for the scheme for the same period, assuming that the scheme is closed. Monthly water supply discharge data are obtained for the main channels (Gezira and Managel) from the former MOIWR office in Wad Medani. The results obtained are used to validate the ET_a derived from RS products. From the RWB concept, the ET_a from RWB (ET_{a-RWB}) is partitioned as follows:

$$ET_{a-RWB} = P + R_{in} - R_{out} - Gr \pm DW, \quad (\text{Equation 4-10})$$

where P is total precipitation, which is the monthly rainfall data from Wad Medani station; R_{in} is irrigation discharge; R_{out} is outflow; Gr is Groundwater recharge; and DW is the change in water storage. The drainage network does not work properly (Plusquellec, 1990). Hence, no return flow from excess irrigation water is reused. Additionally, the Gezira aquifer annual recharge is estimated to be 0.6 BCM (Abdo and Salih, 2012). Hence, R_{out} is assumed to be zero, and the Gr is 0.6 BCM (i.e. no actual measurements). Total irrigation volume is measured as 5.26 BCM, and the total rainfall is 0.6 BCM. Therefore, the seasonal mean ET_a (from Equation 4-10) equals approximately 5.26 BCM for the summer crop season of 2004/05. The value is compared with the four models, as shown in Figure 4-7. The results reveal that the two models SSEB (4.65 BCM) and MOD16 (3.77 BCM) produced results less than the estimated value. SEBAL and METRIC yielded total ET_a 's of, respectively, 7.1 BCM and 18.1 BCM, more than the total supply from irrigation and rainfall. The results obtained show a close estimation on a large scale between ET_a values obtained from SSEB (RS) and those from the RWB approach.

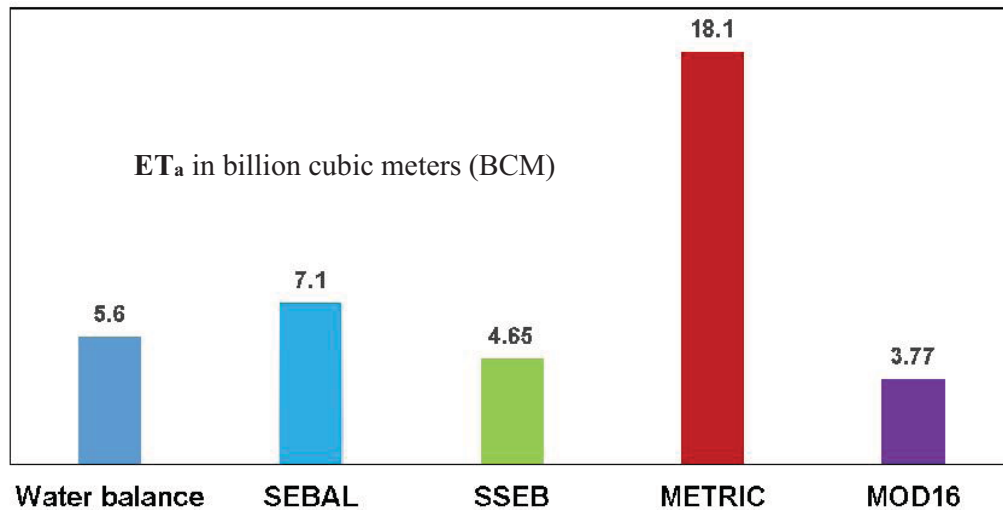


Figure 4-7. Comparison of estimated actual evapotranspiration (ET_a) results from the four remotely sensed (RS) models and the calculated ET_a from the regional water balance (RWB)

4.3.4 Best-performing model

The selection of the best-performing model as followed by Allen (1996) and Elagib and Mansel (2000b) is based on the correlation coefficient (R^2), the linear equation parameters (a and b) and the Root Mean Square Error (RMSE). These measures are evaluated at the field level from the WB measurements and NDVI, and at the scheme level from the iNDVI. The measures of the four models are compared to establish a ranking (of sorts) assigned to each criterion (i.e. the one achieving the highest performance takes number 4, and the lowest, number 1). Later, the sum of the rankings, (i.e. the score) is adopted; hence, the best model is the one having the

highest score. Table 4-5 shows the given scores for each performance criterion, and the ranking of the total scores for the four models.

Table 4-5. Sum of scores for the four models according to each performance criterion

Level	WB Field			NDVI Field		iNDVI Scheme			Score	
	Criterion	a	b	R ²	RMSE	*ET ≈ 0	R ²	*ET ≈ 0		R ²
SEBAL	4	4	2	3	2	2	3	2	2	22
METRIC	2	2	3	1	1	1	2	1	3	15
SSEB	3	3	4	4	4	4	4	4	1	27
MOD16	1	1	1	2	2	3	1	3	4	16

Note: 1) ^cET ≈ 0 for bare soil when NDVI ≈ 0.1; iNDVI ≈ 1.5 as observed from the current research.

2) For best method performance, the constant **a** and slope **b** of a linear regression should tend to 1 and 0, respectively.

The total scores illustrate that SSEB is considered the best model among those compared for estimating ET_a, followed by SEBAL. At the field level, SSEB and SEBAL scored equally for the WB measurements. Nevertheless, SSEB is attained to practically estimate ET_a in the absence of vegetation cover at field level (NDVI ≈ 0.1). Still, the model responds well at the scheme level. Despite the fact that MOD16 has higher performance at large-scale level, the model cannot be used at the field scale, which might be related to the pixel resolution as mentioned earlier. In addition to the good performance score, SSEB has a potential for operational application and requires less application time compared to the complex models.

4.4 Conclusions

The main aim of this study is to test different satellite-based methodologies to obtain reliable evapotranspiration rates for the Gezira Scheme. The first two models, SEBAL and METRIC, are based on the resolution of the surface energy balance. This approach requires T_s for estimating the sensible heat flux (H), and obtaining the ET_a as a residual of the energy balance. SSEB, the third model, uses only T_s to obtain the crop coefficients, then upgrades the FAO reference ET adjust to compute ET_a. Lastly, the ET global MODIS data (MOD16A2) is also used here as a comparison model with the soil WB approach. The results are validated using a published study at field scale during the summer crop season of 2004/05. The three models' outputs have spatial resolution of 30 m, the resolution of Landsat ETM+ satellite images, while the spatial resolution of the MOD16 ET product is 1000 m. The models' performance differed substantially. In order to select the best-performing model, four measures are evaluated: the correlation coefficient (R²), the regression coefficients of the linear equation

and the Root Mean Square Error (RMSE), and the WB magnitudes. Based on ranking criteria, SSEB gives the best performance in terms of ET rate estimation, followed by SEBAL. Among the two applied surface energy balance models, the METRIC model has a lower degree of physical realism than the SEBAL model, while requiring similar input information. This is due to the lower calculated values of instantaneous ET_o, which might be linked to the observed data. In addition, the MOD16 ET has the lowest score of the ranking list.

The SEBAL and SSEB models provided ET_a estimates close to the actual WB measurements with the highest coefficient of determination for SSEB ($R^2 = 0.90$), followed by SEBAL with an R^2 value of 0.71. Except for the METRIC and MOD16 models, they overestimated (94%–370%) and underestimated (26%–79%) the measurements, respectively, not only with the experimental measurements, but also compared to previously conducted studies. In addition, the estimated daily ET_a values for the sorghum experimental field compared relatively well with the corresponding NDVI.

All four models showed similar spatial daily patterns of ET at the scheme with different values. The mean seasonal ET_a values for the most accurate models (SEBAL and SSEB) for each group in the scheme are also compared with their respective iNDVI values. A good correlation of about $\cong 75\%$ is obtained for both models. The variation of ET among the different groups has the potential to identify areas of water stress and waterlogging to improve the WUE of the scheme. SSEB is fairly seen as a suitable operational ET_a model for the scheme, as it also has the potential for more operational applications compared to the others.

CHAPTER FIVE

MONITORING WATER ABSTRACTION FROM LARGE-SCALE IRRIGATION SCHEMES

5.1 Introduction

Traditional irrigation agriculture in Sudan is now facing a big challenge; hence irrigation managers ought to develop water-saving irrigation for sustainable water use. The Gezira Irrigation Scheme is located in a typical arid region (Elagib et al., 2010) with a 50-year average annual precipitation of 300 mm and a 50-year mean annual reference evapotranspiration (ET_0) of about 2221 mm. Accordingly, irrigation is essential for agriculture, as precipitation is far less than CWR. The annual average water diversion to the scheme from the Blue Nile is 6–7 BCM (1970–2012). As stated earlier in Chapter Three, irrigation water efficiency within the scheme has declined significantly since 1993/94. In addition, the irrigation and drainage networks are not working properly, which further exacerbates the water distribution problem in the scheme (Plusquellec, 1990; Ahmed, 2009).

Crop production is less than expected from the scheme, due to frequent drought, inefficient irrigation infrastructure and inconsistent agricultural policies (FAO, 2011; Mahgoub, 2014). The Sudanese government has conducted several reforms and actions in the scheme by changing the agricultural crops and increasing water diversion from the Blue Nile. It is believed that these water policies have an impact on the reported water wastage in the Gezira Scheme. Actual evapotranspiration (ET_a) is a major component of WB in agricultural systems (Bastiaanssen et al., 2005). Understanding the spatial and temporal variability of ET_a is important to tackling water wastage. In the Gezira Scheme, ET_a estimates using RS have been carried out for the winter crop season of 2001 (Bashir et al., 2007a, 2007b, 2009a, 2009b, 2009c; Ahmed et al., 2010), for the summer crop season of 2002 (Bashir et al., 2007a, 2007b), for the summer crop season of 2004 (Bashir et al., 2007c, 2008), for whole of 2006 (El Tahir et al., 2012) and for the summer and winter crop seasons of 2007 (Thiruvarudchelvan, 2010; Mohamed et al., 2011). The studies focused on specific farms or administrative units to determine the crop coefficient, where used to validate the estimates at the regional scale (Bashir et al., 2007c, 2008). El Tahir et al. (2012) compared the estimated ET_a using an RS technique with a modified Thornthwaite WB method for the whole of the

Blue Nile Basin (including the Gezira Scheme). Despite this extensive work, the regional long-term analysis of ET_a assessment has not yet been conducted for the scheme.

As the Gezira Scheme covers a vast area lacking an actual water consumption monitoring system, it becomes imperative to develop a suitable tool for monitoring agricultural water use. In addition, there is a particular need of ET_a time series evaluation under changing water use strategies for better water resource management. This requires evaluation of water policy reforms during past years, as well as further decision support. In this research, the Simplified Surface Energy Balance (SSEB) (Senay et al., 2007) model is applied to the Gezira Irrigation Scheme for mapping its evapotranspiration for the crop summer and winter seasons of 2000–2014. The main objective of this chapter is summarized as monitoring water abstraction from the large-scale Gezira Irrigation Scheme using RS techniques.

5.2 Material and methods

5.2.1 Agricultural water policies for the Gezira Scheme

The Gezira Scheme has evolved through six water policies of distinct and changing phases, as summarized in Figure 5-1. In the first phase, cotton was the only crop that was grown when the project was established (1925–1960). During this period, it was fully controlled and fully financed by the cotton company and the government, and farmers were just tenants obeying orders (Adam et al., 2002). Irrigation was efficient, as irrigation managers proposed a night-storage irrigation system which was strictly applied (Plusquellec, 1990). Later, in the second phase (1961–1980), the original area was extended to the southwest to include the Managel extension (Eldaw, 2004). Other proposed crops, such as wheat, groundnuts and sorghum, became important crops in addition to cotton. The night irrigation system collapsed (Farbrother, 1996), but funds were still provided by the government (Adam et al., 2002).

In the third phase (1981–1990), a water charge policy was introduced for the first time, and tenants were required to pay for irrigation services. However, cost recovery was low, and the government failed to carry out maintenance (Adam et al., 2002). Funds became insufficient to finance the operation and maintenance costs; therefore, the removal of silt from the irrigation channels became an insurmountable challenge (Plusquellec, 2002). Due to lack of financial resources, the Ministry of Irrigation (MOI) was not able to cope with the removal of silt and clearance of weed. As a result, there was a decrease in the instability of crop production (e.g. groundnut (Elamin et al., 2011)), and the average cotton yields decreased and

underwent heavy fluctuations (Eldaw, 2004). In addition, the water policy of the 1980s was aggravated by drought (Elagib et al., 2010). Many reasons, including the government liberalization policy (Guvele, 2001; Elamin et al., 2011), led to inefficient land use, which caused instability in the main crop areas during that era.

In 1991, the economic liberalization policy was introduced, and the government slipped away from financing the scheme (Adam et al., 2002). The policy included price liberalization, privatization and removal of government subsidies. Eldaw (2004) mentioned that the adopted policy was meant to enhance the productive capacity of the agricultural sector. However, the response from the agricultural sector in terms of productivity was insufficient (Elamin et al., 2011). Economic liberalization had lasted eight years before the fifth phase started in 1999 with a major change in the institutional arrangement for water management (Abdelhadi et al., 2004). The responsibility for the irrigation channel system was distributed among three different stakeholders (Adam et al., 2002). Tenants were involved in operating and maintaining ditches irrigating their fields. For minor channels, Sudan Gezira Board (SGB) agricultural engineers took responsibility for operating and maintaining irrigation channels. Ahmed (2009) mentioned that, in this period, the irrigation system in the scheme experienced serious deterioration throughout its long history, due to lack of experience on the part of both Tenants and the SGB in operating and maintaining irrigation channels.

In 2003, Water Users' Associations (WUAs) were established throughout the scheme (Abdelhadi et al., 2004; World Bank, 2010). The aim was to achieve optimum utilization of available water through a participatory process. It was an initial step toward handing full responsibility to tenants. Therefore, in 2005, the Sudanese government endorsed the Irrigation Management Transfer (IMT) concept, as mentioned in World Bank (2000). The tenants became farmers owning their land, fully responsible for any operation and maintenance of ditches and minor channels. Yet the farmers had a free choice of which crop to grow (Woldegebriel, 2011). In addition, the SGB was excluded from operating and maintaining the irrigation channels, and the responsibility passed to the MOIWR (Abdelhadi et al., 2004; Ahmed, 2009). However, responsibility for irrigation was transferred once again to the Ministry of Agriculture, Livestock and Irrigation (formerly the Ministry of Agriculture) in 2010, after the expansion of the MOIWR as the Ministry of Water Resources and Electricity (MWRE) (MWRE, 2014; KRT, 2014).

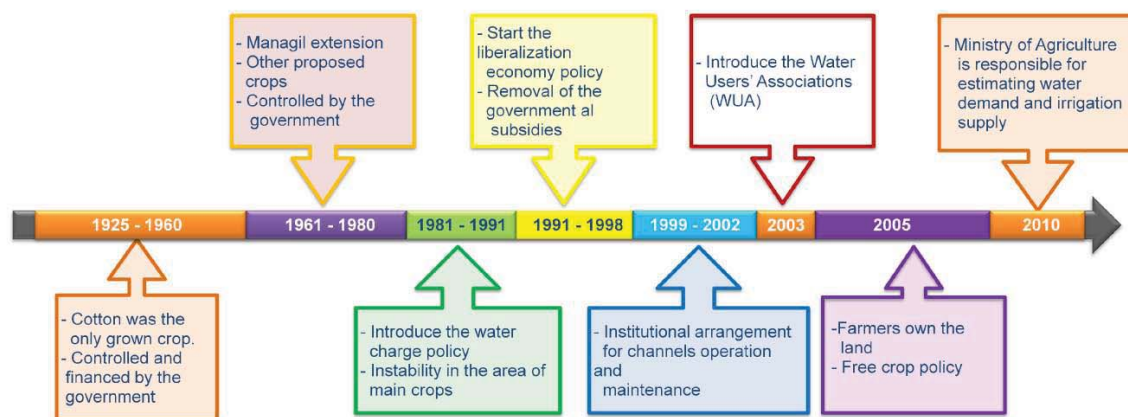


Figure 5-1. Summary of distinct and changing phases of water policy in the Gezira Scheme

5.2.2 Historical RS-based ET estimates at the Gezira Scheme

Bashir et al. (2007a, 2007b) estimated the daily ET_a for the Gezira irrigated scheme using the SEBAL model. Five Landsat 7 ETM+ images were utilized (September and December 2001; and September, October and November 2002). The model has been validated for sorghum at the field scale using a soil moisture depletion method provided by Abdelhadi et al. (2006).

Bashir et al., (2007c) used the same method to examine the seasonal changes in crop coefficients (k_c) and seasonal water requirements for sorghum during the summer crop season of 2004. The validation was undertaken for an experimental sorghum field (30×90 m) by comparing the ET_a from SEBAL with values derived by the WB method. Although the authors used four ETM+ satellite images (July 28, August 29, October 16 and November 17), no gap-filling method has been reported. This implies that the model was limited to a specific part of the scene (field scale) and not valid for the whole scheme. However, the spatial resolution (30 m) of the ETM+ data allows the estimation of ET_a on the scale of individual agricultural fields. Later, Bashir et al. (2008) combined seven MODIS satellite images with the ETM+ images used in 2004, representing the summer crop season, to estimate the daily, monthly and seasonal ET_a not only for the field, but also for the whole scheme. The authors validated the daily ET_a estimated by SEBAL from MODIS data with the daily ET_a calculated by the WB method. They found that MODIS data can predict the ET losses from the agricultural field accurately to within 0.9 mm/d. It is doubtful that the field measurements can be reliably evaluated by MODIS, due to the restriction of the coarse spatial resolutions (≈ 1000 m). However, the study did not refer to any downscaling methods to enhance the spatial resolution of MODIS. At the scheme level, the authors illustrated the spatial distribution for

the seasonal ET_a and found that the northern part has the highest seasonal ET_a values. However, as discussed earlier in Section 4.3.3.2, Bashir et al. (2008) succeeded in implementing SEBAL at field level but not at scheme level.

Bashir et al. (2009a, 2009c) quantified the water demand of different minor channels in one administrative group (Abdelhakam block) at the scheme using four Landsat ETM+ images. Although the study was conducted for the winter wheat crop of 2001/02, the validation was presented for the sorghum summer crop (2001, 2002 and 2004) conducted by Bashir et al. (2007a, 2007b) and Bashir et al. (2008). Afterward, Bashir et al. (2009b) and Ahmed et al. (2010) added eight MODIS images to the earlier season and mentioned that the validation was retrieved from WB to wheat at the Gezira Research Station (GRS). The latter publication introduced three sites in the Gezira Scheme representing the GRS research field, farmers' fields at Abdelhakam block and ordinary farmers' fields (Madina block) to estimate the spatial ET, crop yield and water productivity of wheat. The authors used the downscaling technique to enhance the spatial and temporal resolution at the field scale.

Thiruvarduchelvan (2010) and Mohamed et al. (2011) utilized RS techniques to calculate the irrigation performance indicators at four pilot administrative sites, and the whole Gezira Scheme for the annual crop season of 2007/08 (September 2007–March 2008). The ET maps were adapted from the Waterwatch (Waterwatch, 2014) study of the Nile Basin (IWMI et al., 2009). The mentioned study used the ETLook model to calculate the ET_a every eight days using MODIS satellite images from 2007. One of the limitations of the study was the lack of ET_a for January–March 2008 (the authors used the corresponding months from 2007). Although they verified the assumption by comparing the climatic conditions at the Wad Medani station and found negligible differences between the two years, climatic conditions are not the only factors affecting ET_a . The assumption means that during the mentioned months, the Gezira Scheme has the same crop pattern with the corresponding areas and distribution. Another observed limitation is that the studies did not analyze June–August 2007, due to cloud cover in the satellite images.

5.2.3 SSEB model

SSEB (the Simplified Surface Energy Balance model) (Senay et al., 2007) is addressed in the current research. SSEB is based on RS data in integration with meteorological data for deriving ET_a maps. The model is not as sophisticated one, which makes it operationally more applicable. Senay et al. (2007) developed and implemented the SSEB model to monitor and assess irrigation performance of a large irrigation district in

Afghanistan. Besides, the model was evaluated and gave comparable results among other remotely sensed ET models, as presented in Chapter Four.

SSEB approaches stating that ET_a varies linearly between hot and cold pixels are identified by T_s . The simplification is manifest in using T_s to drive the ET fraction (ET_f) based on hot and cold pixels. Senay et al. (2007) argue that the hot pixel of a bare agricultural area experiences little or no ET, while the cold pixel of a well-watered irrigated field experiences the maximum ET_a . Hence, ET_f is calculated from the following equation:

$$ET_f = \frac{TH - T_x}{TH - TC}, \quad (\text{Equation 5-1})$$

where TH and TC are the average of three hot and cold pixels selected for a given scene, respectively, and T_x is the T_s pixel value for the same scene. ET_f alone is considered a drought risk index, which was implemented by Son et al. (2012) for evaluating the surface moisture content. ET_f is also similar to the Crop Water Stress Index (CWSI) presented by Moran (2004), which is utilized to evaluate and monitor plant ecosystem health. Tang and Li (2014) mentioned that the ET_f index is a very close approximation to soil moisture availability. The lower ET_f value indicates water deficit, which would reduce transpiration and lead to the rise of surface temperature, while relative low temperature stands for the normal healthy vegetation or water ponds (Wu et al., 2013). The combination of this index and the meteorological conditions by the daily reference evapotranspiration gives us useful spatial monitoring information for the scheme (Allen et al., 2007a, 2007b; Senay et al., 2011). Hence, the actual daily ET based on SSEB is defined as

$$ET_{a-SSEB} = ET_f \times k \times ET_o, \quad (\text{Equation 5-2})$$

where ET_f is as defined above, ET_o is the grass reference evapotranspiration and k is a scaling coefficient based on calibration suggested by Senay et al. (2013). In this research, the value of k is taken as 1.2; it is recommended in many studies (e.g. Allen et al., 2007a, 2007b; Senay et al., 2013) to use alfalfa reference ET evapotranspiration ($1.20 \times ET_o$). ET_o is calculated as mentioned in Chapter Three.

As mentioned in Chapter Four, Senay et al. (2011) improved SSEB ($SSEB_{elvi-ndvi}$) by applying correction factors to T_s and NDVI. Later, another modification was implemented to SSEB ($SSEB_{op}$) by upgrading the uncomplicated method to the energy balance method (Senay et al., 2013). In this Chapter, the original SSEB model concept is implemented. Neither enhancements from T_s nor NDVI are considered. The Gezira Scheme is located in a flat area; hence, the difference in elevations can be neglected for T_s calculations. Also, the

NDVI adjustment formula underestimates the $E T_a$ values for the Gezira Scheme. Furthermore, the model performance is conducted using NDVI values. Finally, the seasonal ET from SSEB is calculated according to Section 4.2.6.

5.2.4 Source of data

5.2.4.1 Remote sensing

To run the SSEB model, the T_s product is needed. Landsat satellite images are used in this study because of their high spatial resolution (30 m). The Thematic Mapper (TM) (Landsat 5), ETM+ (Landsat 7) and Landsat 8 (since May 2013) images are downloaded from the USGS Global Visualization (GloVis) website (USGS, 2014). The Landsat tile (path: 173 and row: 50) is used, which fortunately covers around 94% of the total Gezira area. Although Landsat data would be adequate for this study, the temporal frequency (16-day) and cloud cover are limiting factors to obtaining images for the summer crop season. Therefore, MODIS T_s products of 8-day composite (MOD11A2) are downloaded and used, as recommended by Senay et al. (2007). Still, the cloud cover during the rainy months (June–August) limits selection of appropriate images from the MOD11A2 product. Consequently, the daily MODIS T_s (MOD11A1) product is used in the absence of MOD11A2 data during the three rainy months. Both MOD11A1 and MOD11A2 have a spatial resolution of 1000 m and are downloaded from the NASA data center (Mitchell, 2014). Images of the Gezira Scheme with cloud cover $\leq 1\%$ for Landsat products and $\leq 5\%$ for MODIS are obtained for 2000–2014, from the end of May to the beginning of April the year after, as listed in Table 5-1 for the summer crop season, and in Table 5-2 for the winter crop season.

Table 5-1. The day of year of the used Landsat and Moderate Resolution Imaging Spectroradiometer (MODIS) satellite images for the summer crop season

Sensor/Year	Landsat	MOD11A2	MOD11A1
2000	183, 311	169, 265, 289	155, 162, 174, 217, 328, 244
2001	249	161, 193, 241	—
2002	268	161, 177, 257, 289, 313	158, 175, 211, 218, 213
2003	271, 319	193, 289	—
2004	146, 210, 242, 290, 306	—	—
2005	148, 292, 308	209, 225, 265	—
2006	151, 231, 279, 311	201, 265	174, 187, 208
2007	266, 282	225, 313	168, 201
2008	165, 269, 301, 317	—	206
2009	287, 311	161, 225, 265	153, 177, 191, 211, 223, 230, 239
2010	314	161, 185, 225, 265, 289	187, 203, 210, 219, 226, 242
2011	189, 253, 293, 309	265	154, 160, 176, 179, 220, 229, 234
2012	280	257, 265, 273, 289, 297, 313, 321	154, 161, 170, 186, 195, 209, 218, 230, 243
2013	258, 298	265, 273, 281, 289, 297, 313, 321	154, 167, 177, 183, 193, 207, 234

Table 5-2. The day of year of the used Landsat and Moderate Resolution Imaging Spectroradiometer (MODIS) satellite images for the winter crop season

Sensor/Season	Landsat	MOD11A2	MOD11A1
2000/01	41	353, 25, 81	—
2001/02	345, 12, 76	49	—
2002/03	—	353, 17, 49, 73	—
2003/04	50, 62, 88	361, 25	—
2004/05	361, 4, 36, 52, 68, 84, 89	—	—
2005/06	340, 356, 7, 23, 55, 71, 89	—	—
2006/07	343, 359, 10, 26, 49, 81	—	—
2007/08	346, 13, 45, 77	—	—
2008/09	15, 47, 79	353	—
2009/10	343, 10, 26, 34, 50, 66	—	—
2010/11	362	337, 17, 49, 73	—
2011/12	341, 357, 24, 40, 72, 88	—	—
2012/13	344, 360, 10, 26, 42, 58, 90	73	—
2013/14	338, 354, 5, 37, 53, 77, 85	25	—

Bimonthly NDVI data of 250 m resolution (MOD13Q1 data product) are obtained for January 2000 –April 2014 from the Oak Ridge National Laboratory Distributed Active Archive Center (ORNL DAAC, 2011) in GeoTIFF format.

5.2.4.2 Ground-observed data

Daily and monthly meteorological data (maximum and minimum air temperature, sunshine hours, wind speed and air humidity) are procured for the Wad Medani meteorological station (14°24'0.00"N, 33°28 '48.00"E) from the Sudan Meteorological Authority for 2000–2012. Post-2012 data are acquired from the National Climatic Data Center (2014), and daily data are obtained for the used satellite image dates listed in Table 5-1 and Table 5-2. In addition, data for monthly rainfall and irrigation water supply through the main channels (Gezira and Managel) are available for the same period.

5.2.4.3 Data preparation

The ETM+ data has an error caused by SLC failure after May 2003. Every scene has 22% missing pixels occurring in a repeating along-scan stripe pattern (Chen et al., 2011). To obtain complete coverage, a pre-process gap-filling process is applied using the nearest-neighbor statistical method, a similar approach as that used for Evapotranspiration (2011a, 2011b). Landsat bands 1–7 and 61 (low-gain, ETM+) are used in this study. The DN of each band is converted to reflectivity by applying the Landsat Handbook (2007) equations. T_s from Landsat images is calculated based on the Landsat Handbook (2007) from the thermal bands (Band 6 for TM, and Band 61 for ETM+). For Landsat 8, T_s is calculated from the thermal band (Band 10) after radiance conversion following the methodology of USGS (2013). Afterward, the NDVI is derived from the reflectivity-corrected red and near-infrared bands.

The Gezira area is extracted later from Landsat and MODIS tiles using the Extract-by-Mask tool in the ArcGIS 10 software (ESRI, 2013). Finally, the extracted images are projected into Projected Coordinate System with Universal Transverse Mercator (UTM) WGS84 datum so that all pixels in the study area have equal size, thereby making pixel-level analysis easier.

5.2.5 SSEB model performance evaluation

In many studies, the RS estimation of ET_a is tested against *in situ* measurements or catchment WB models (Bastiaanssen et al., 1998b; Allen et al., 2007b; Bashir et al., 2007c, 2008; Yang et al., 2012). In the present study, two scales (field and regional) are adopted to examine the performance of the SSEB model. At the field scale, ET values from the SSEB model match the measured ET from WB for the sorghum experimental field in 2004, as presented in Chapter Four. At the regional scale, the total ET estimated by SSEB for summer (June–November) and winter (December–March) for 2000–2012 is tested with a Regional Water Balance (RWB) model, as described by the following equation:

$$ET_{RWB} = P + R_{in} - R_{out} - Gr \pm DW, \quad (\text{Equation 5-3})$$

where ET_{RWB} is the total ET calculated by an RWB model; P and R_{in} are the total rainfall and total water diversion from the Blue Nile, respectively; and R_{out} is the total outflow. Gr is the rate of groundwater recharge, and DW is the annual variation of soil moisture storage. The drainage network does not work properly (Plusquellec, 1990). Hence, no return flow from excess irrigation water is reused. Besides, the Gezira aquifer annual recharge is estimated to

be 0.6 BCM (Abdo and Salih, 2012). Therefore, R_{out} is assumed to be zero, and Gr, 0.6 BCM (i.e. no actual measurements).

5.3 Results and discussion

5.3.1 Model performance evaluation

The comparison between seasonal ET by the SSEB and RWB models for the summer and winter crop seasons are shown in Figure 5-2 and Figure 5-3. As can be seen, the growing season ET estimated by SSEB for both summer and winter crop seasons generally has the same trend, but does not agree with the output of the RWB model. This could be attributed to inaccurate ET_{RWB} calculation, which is based on assumptions, not records, especially for the water losses ($-Gr$ and $\pm DW$). Theoretically, the calculation of ET_{RWB} in this study represents the total water supply (P and R_{in}) reduced by a constant value ($Gr = 0.6$ BCM).

For the summer crop season, ET_{SSEB} has a positive trend with ET_{RWB} through a linear equation ($R^2 = 0.25$; $p = 0.048$) and is not in good agreement, which is mainly due to the large discrepancy in 2009. It is remarkable that in July 2009 the total seasonal rainfall was recorded as 342 mm, which must be regarded as of doubtful significance, as the recorded average for that month is 87 mm (51 years). If the value for this year is removed, then R^2 significantly improves to 0.55 ($p = 0.0028$). On the other hand, ET_{SSEB} for winter has a better agreement with ET_{RWB} than the summer season. R^2 between the two variables has a value of 0.83, with p less than 0.0001. However, in many years (2000/01–2002/03, 2005/06, 2010/11 and 2011/12), ET_{SSEB} over estimates ET_{RWB} , which could be related to a wrongly assumed DW (the annual variation), as water could be available from the summer season (rain or irrigation). However, one of the limitations faced in this research is a lack of validation data at the regional scale for a long period. Therefore, the assessment focuses on the spatial distribution and trends rather than the absolute values.

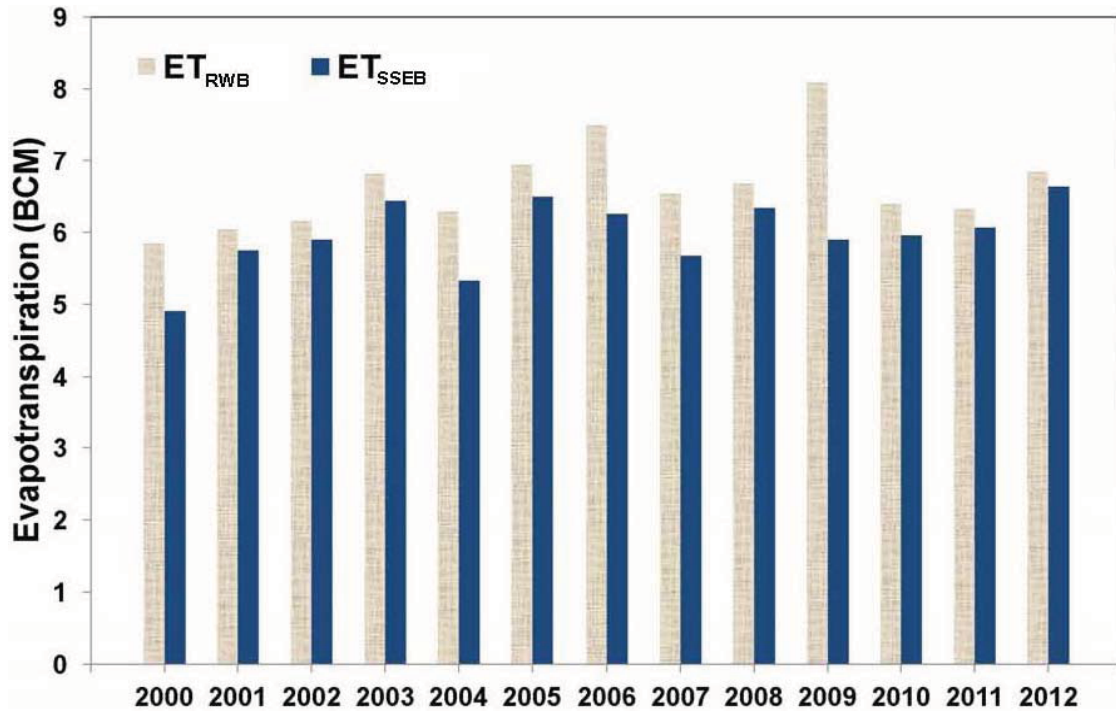


Figure 5-2. Comparison of seasonal ET by SSEB to ET from the Regional Water Balance (RWB) model for the summer crop season

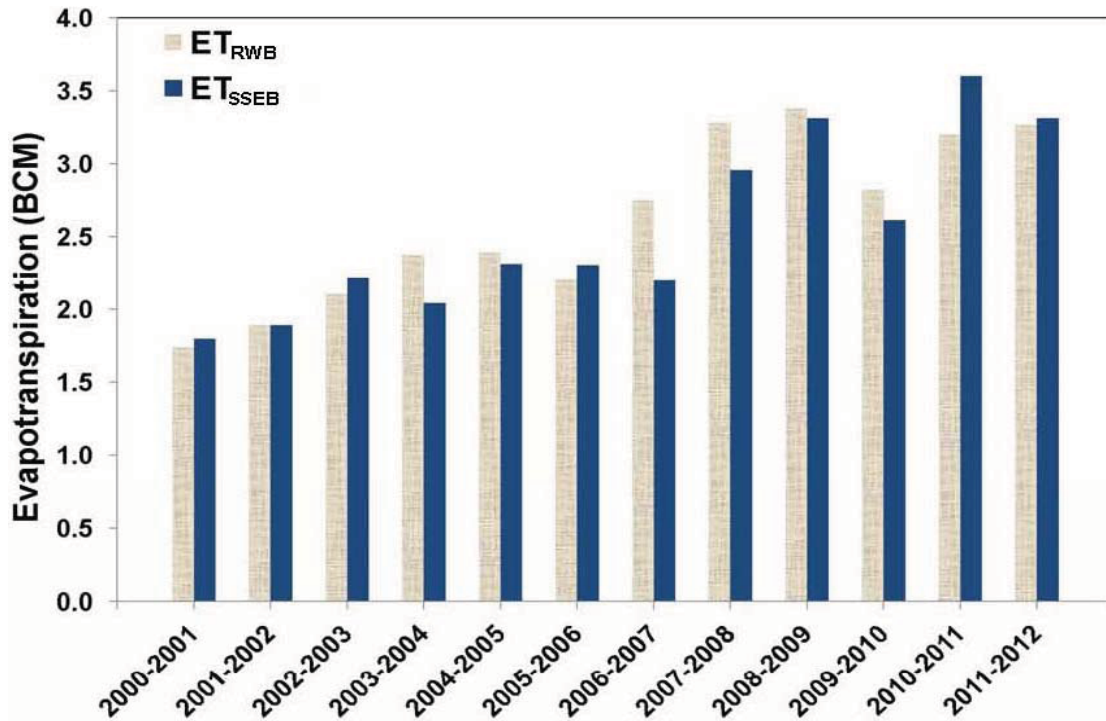


Figure 5-3. Comparison of seasonal ET by SSEB to ET from the Regional Water Balance (RWB) model for the winter crop season

5.3.2 The scheme level

5.3.2.1 Spatio-temporal assessment

RS is a powerful management tool which provides system-wide and spatially distributed information. The collected information supports the identification of drought areas, which can help to conserve water, and later has a role in improving efficiencies and water productivity. The estimated ET from RS scenes has the ability to describe the spatial variation of consumed water over vast areas. The spatial pattern of the summer and winter crop season ET_a 's for the simulated years (2000–2014) for the study area are illustrated in Figure 5-4 and Figure 5-5, respectively. Generally, the seasonal ET_a for the Gezira Scheme is higher in the southern and central parts, and lower in the northern part during the summer crop season. The reason could be that the southern and central areas are closer to the main water supply source (Sennar Dam), which also indicates that the irrigation network failed to convey sufficient water to the northern part in this particular season. This may be attributed to the enormous amount of sediment entering the scheme during this season. Ahmed (2009) mentioned that the sediment impounds water in the channels, causing flooding in some areas of the scheme and drought in others. However, the seasonal summer ET values range from less than 150 mm to over 1350 mm, with the lowest mean seasonal ET occurring in 2000, and highest, in 2012. The lower ET values (< 150 mm) occur over the villages and bare soil areas, while the highest rate of ET (> 750 mm) is observed over well-irrigated agriculture and water bodies (water ponds and irrigation channels). For the winter crop season, it is clear that ET_a is equally distributed throughout the scheme. This indicates that the scheme receives sufficient irrigation water during this season, which could be contributed to by the fact that wheat and end-stage cotton (low water demand) are cultivated over almost the whole land.

The power of applying S-SEB, even without calibration, is that the satellite data, through ET_f , are ideally suited for spatially deriving water-stressed areas, where evaluating the surface moisture content. Then, the use of a reference ET for the assessments establishes a ground reference and reality of climatic conditions representing atmospheric water demand. Therefore, the current assessment does not take into account absolute values rather than spatial distribution and trends.

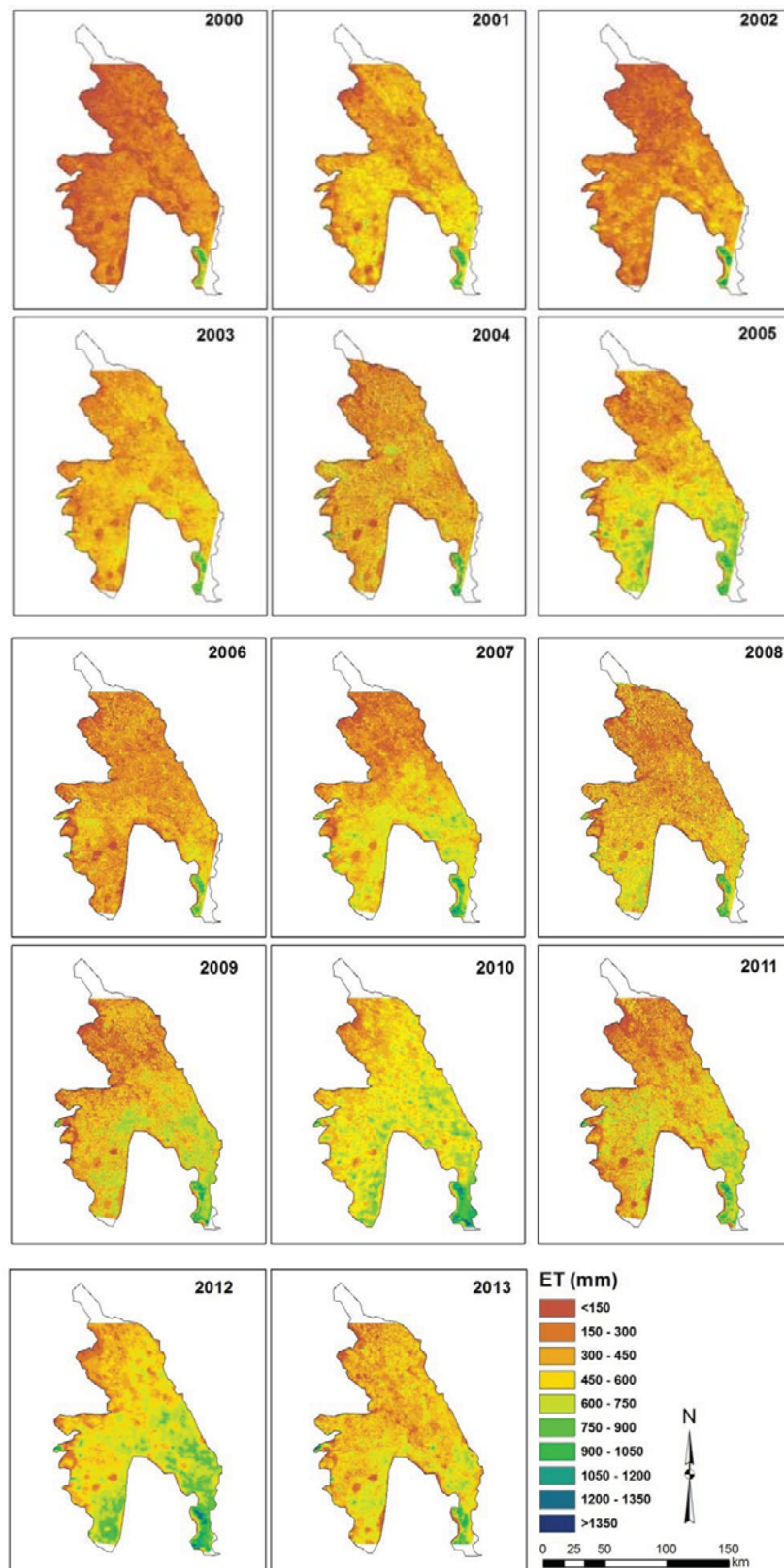


Figure 5-4. Spatio-temporal distribution of seasonal ET estimated by SSEB with a 30 m downscaled pixel resolution for the summer crop season (June–November)

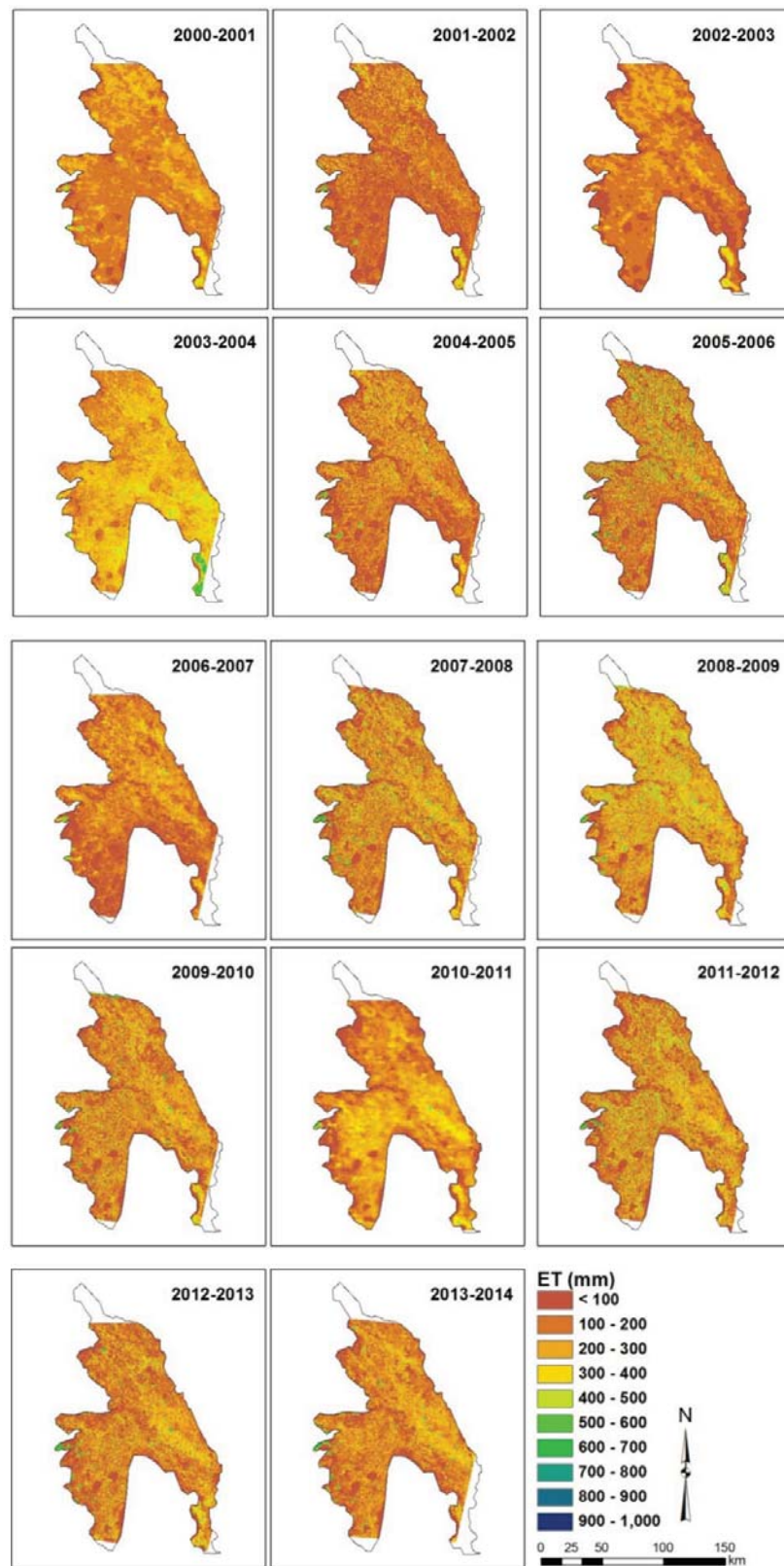


Figure 5-5. Spatio-temporal distribution of seasonal ET estimated by SSEB with a 30 m downscaled pixel resolution for the winter crop season (December–March)

NDVI is widely used to identify vegetation cover and crop production. A linear relationship between NDVI and agricultural yield is always found (Pettorelli et al., 2005; Panda et al., 2010). Hill and Donald (2003) found a good spatio-temporal relationship between total agricultural production and the integrated NDVI (iNDVI) for eight years in Western Australia. Besides, NDVI data is possibly utilized for the land surface response to water variability and identification of drought areas (Kogan, 1995; Anyamba and Tucker, 2005). Hence, NDVI is considered another good indicator for evaluating water policies in terms of crop productivity: the greater is iNDVI, the higher is production. Figure 5-6 and Figure 5-7 respectively show the spatio-temporal distribution of iNDVI for the Gezira Scheme for the summer and winter crop seasons. The well-irrigated areas with higher iNDVI are usually close to the main irrigation channels and southern areas (during the summer crop season), similarly to the ET distribution. For instance, the irrigated areas close to the Sennar Dam reach a seasonal ET of up to 900 mm, with iNDVI \cong 8.0, while the ET value is less than 450 mm in most of the agricultural areas at the northern part. Ahmed and Ismail (2008) reported that sediment removal from the channels, especially in 1999, impacted negatively on the equity of water distribution throughout the Scheme, which is considered one of the major problems of the system. This caused lower production, mainly for fields at the tails of the channels (FAO, 2011).

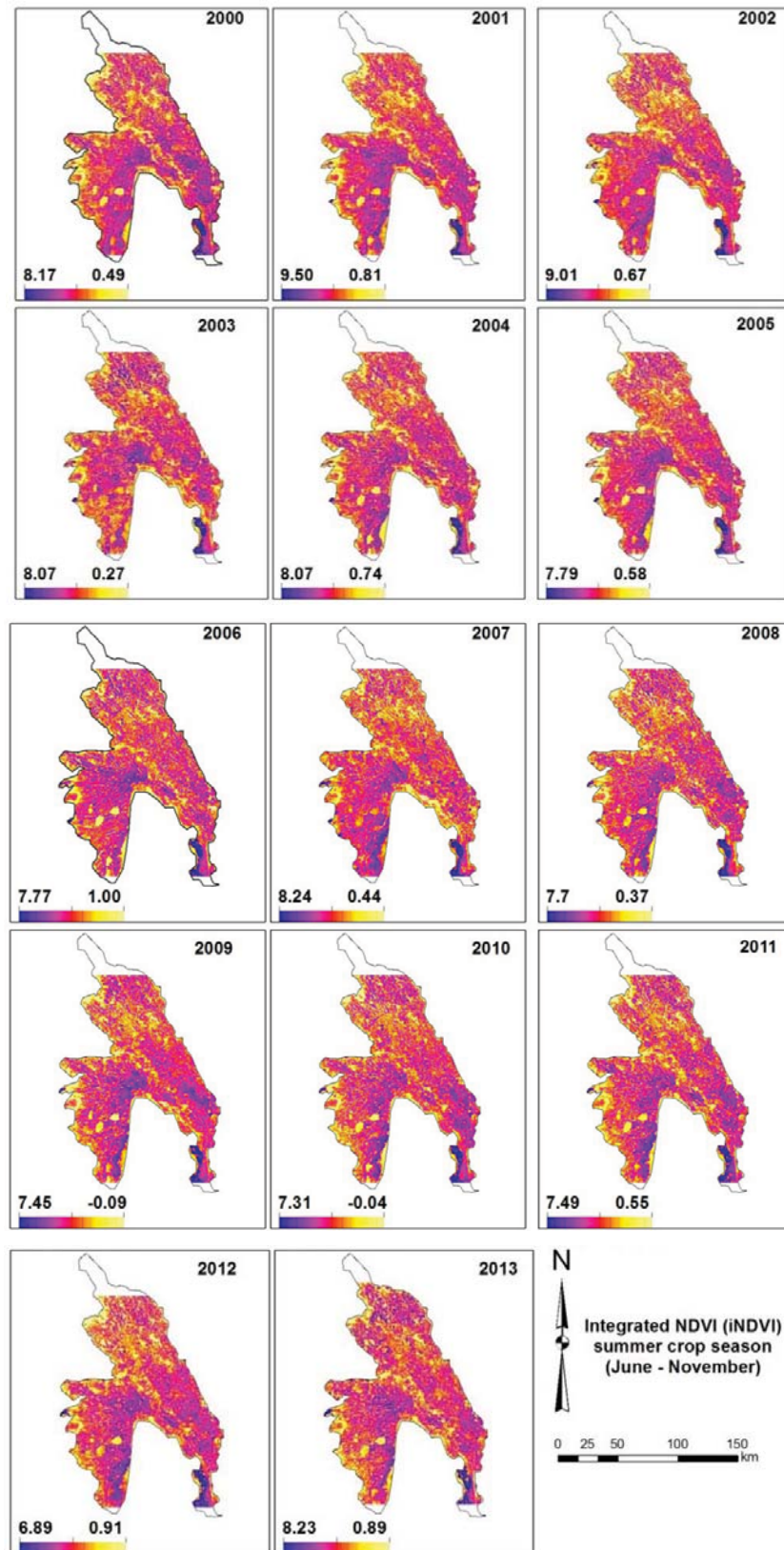


Figure 5-6. Spatio-temporal distribution of integrated NDVI (iNDVI) for the summer crop season

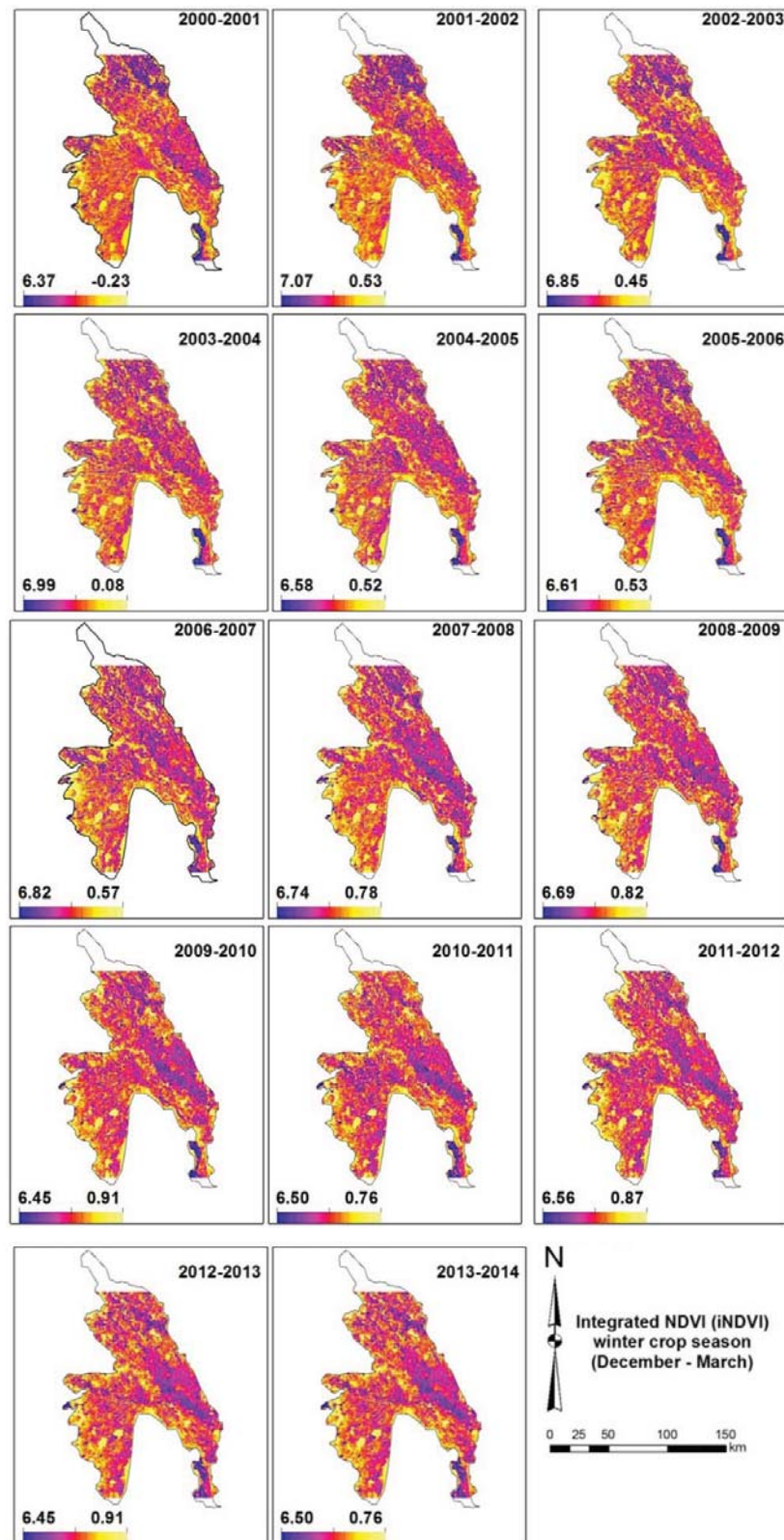


Figure 5-7. Spatio-temporal distribution of integrated NDVI (iNDVI) for the winter crop season

The combination of ET_a and $iNDVI$ maps provides a good monitoring tool for identifying water depressions. Many water ponds are observed, which implies water wastage at the scheme. Such depressions can be easily identified, where a high ET is noticed from the irregular shape of large areas, and validated by a lower $iNDVI$ value. It is well known that negative values of $NDVI$ correspond to water (Pettorelli et al., 2005). Therefore, the MODIS $NDVI$ data is used to classify water areas at the scheme. A closer look at the depressions classified for 2007 is shown in Figure 5-8. The reason for presenting this particular year is that there are many more observed water ponds than in other years. Most of these water depressions are found close to the main irrigation channels, and are of irregular shape. A cross-check using estimated ET confirmed that these areas have high ET values.

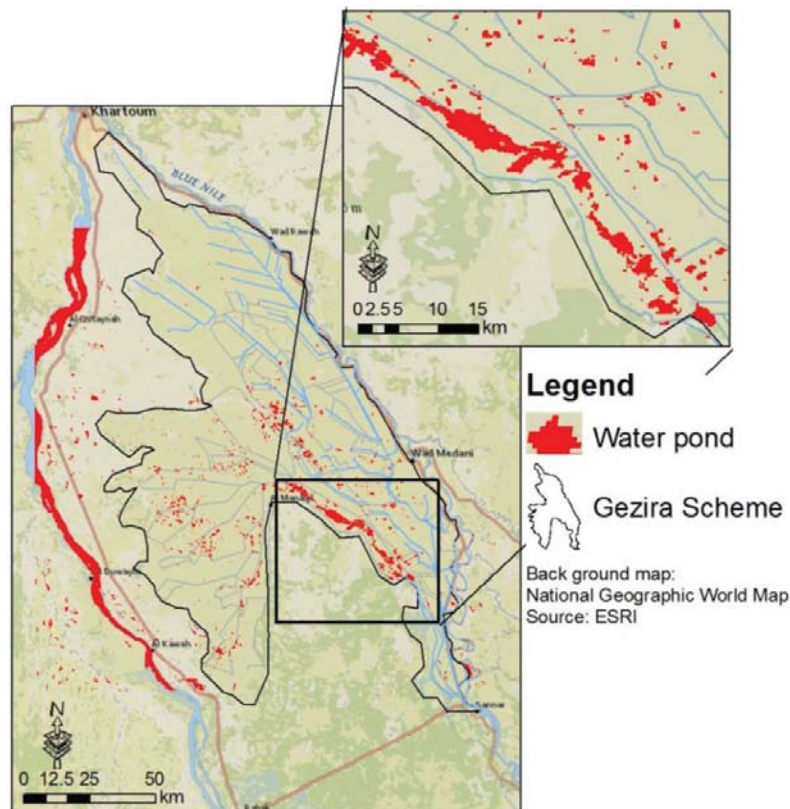


Figure 5-8. Identifying water depressions through main channels of the Managel channel in the 2007 summer crop season

5.3.2.2 Model performance by ET_a - $NDVI$ relationship

Studies show (Szilagyi et al., 1998; Duchemin et al., 2006; Mutiga et al., 2010) that actual ET is directly proportional to canopy density, measured as $NDVI$, which often has a better fit with a linear expression. To further investigate the model performance in the region, ET_a over each pixel is plotted against the integrated $NDVI$ ($iNDVI$) for the summer and

winter crop seasons, respectively, in Figure 5-9 and Figure 5-10. iNDVI is deduced from the MODIS bimonthly NDVI data (MOD13Q1) to compare it with the seasonal ET_a from SSEB. The total area of the Gezira Scheme is masked to include every type of land use within the scheme from the irrigated farms, bare soil and water bonds. For the comparison, all ET_a and iNDVI data cells in this focus area are sampled to 1000 m resolution using the Zonal-Statistics-As-Table tool in the ArcGIS software (ESRI, 2013).

The ET_a results from SSEB are compared to the iNDVI by applying a linear regression to examine the correlation between the two datasets. As can be seen from Figure 5-9 and Figure 5-10, ET_a and iNDVI are positively correlated, and R^2 values take the range 0.35–0.76 for summer, and 0.51–0.80 for winter, with a very high significance level ($p = 0.0$). In general, the result indicates a satisfactory spatial and temporal relationship between the two datasets. The particularly low correlation of the 2007 summer crop season can be explained by the observation of many water depressions across the scheme (Figure 5-8). Lower iNDVI values have a higher seasonal ET, which biases the linear equation. This indicates that the SSEB model is sensitive to the soil moisture for ET_a estimation.

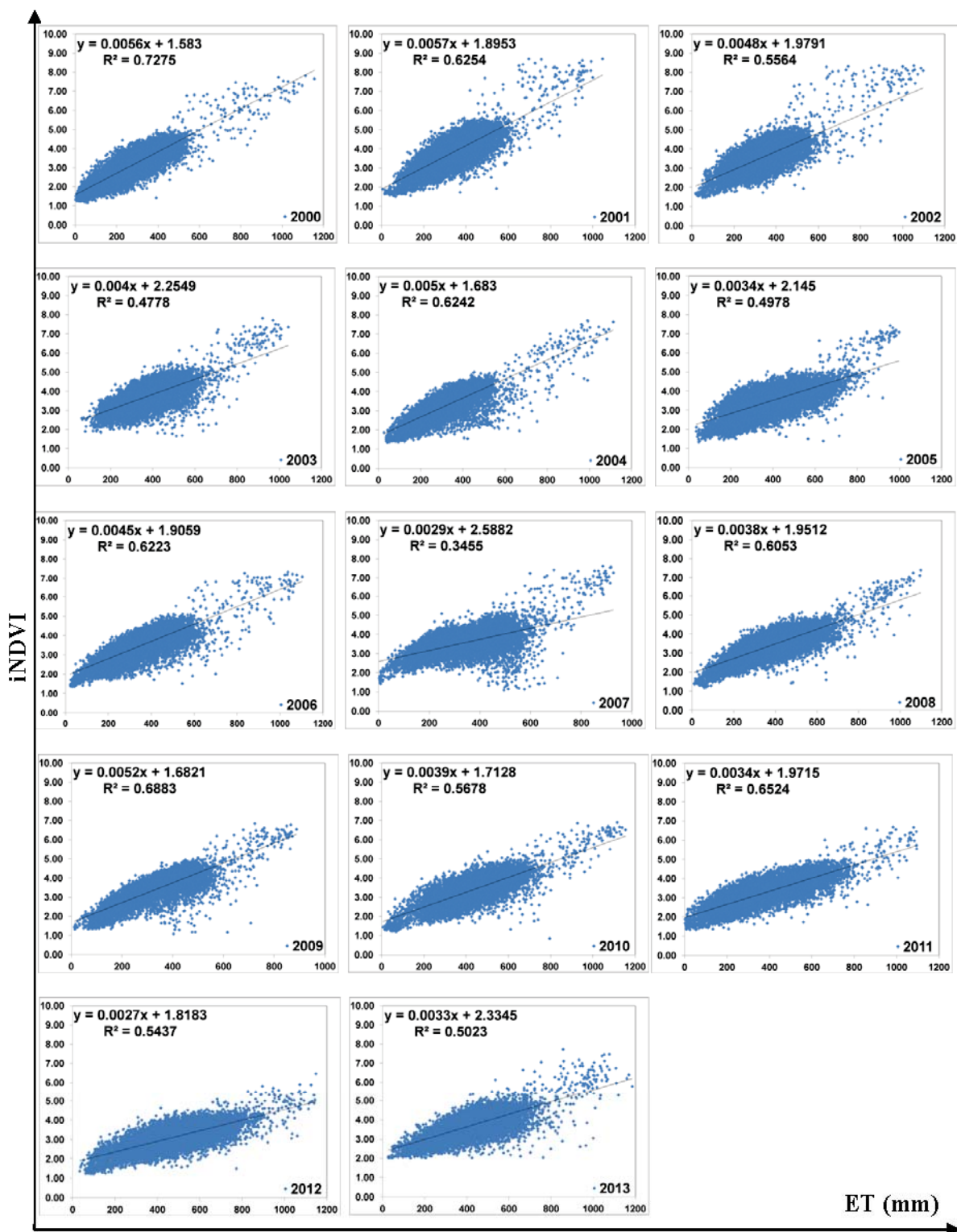


Figure 5-9. Relationship between total summer crop season ET_a estimated by the SSEB model, and integrated NDVI (iNDVI) based on pixel-by-pixel

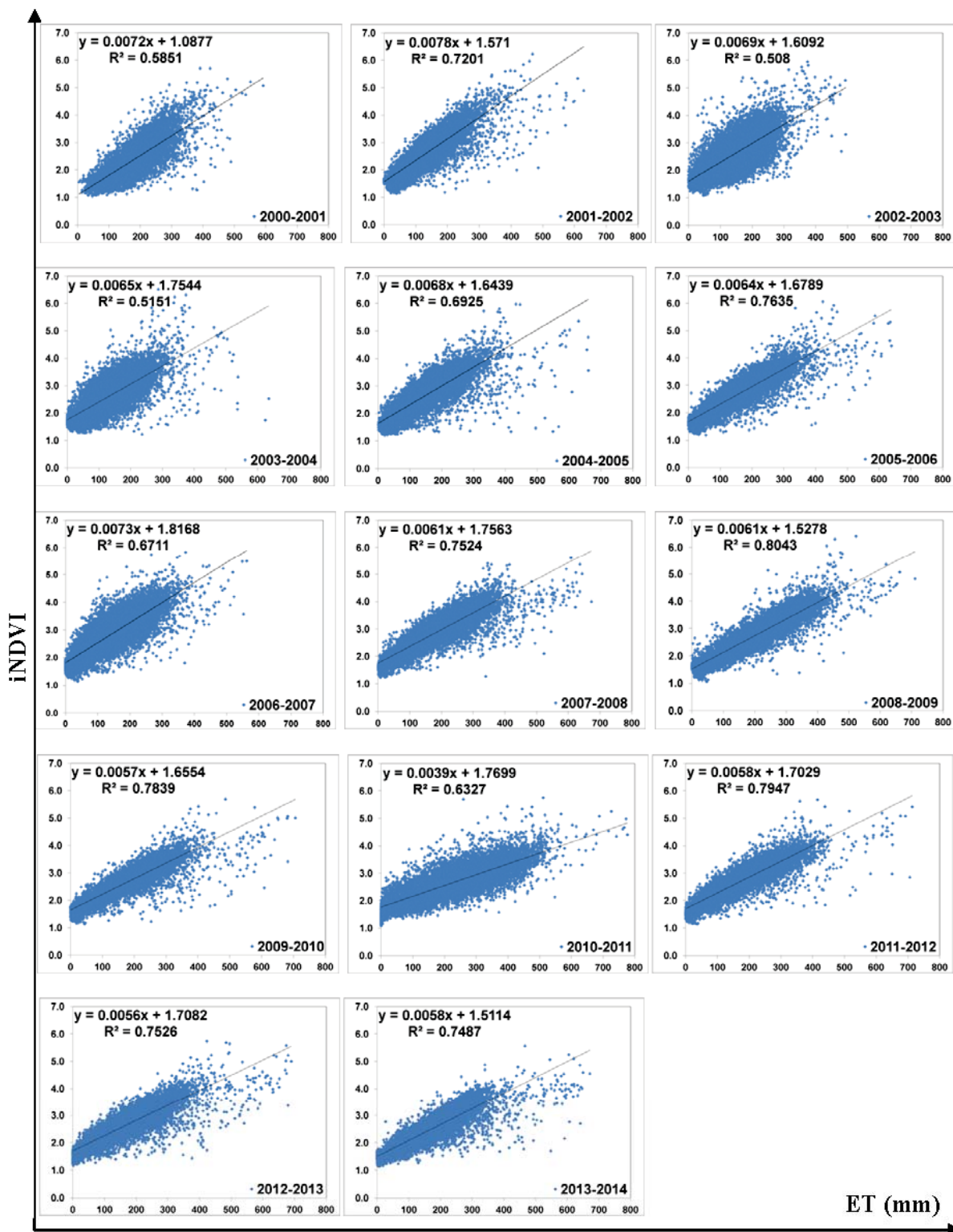


Figure 5-10. Relationship between total winter crop season ET_a estimated by the SSEB model, and integrated NDVI (iNDVI) based on pixel-by-pixel

5.3.2.3 Monitoring water diversion

NDVI is commonly used in assessing the impacts of drought in agricultural areas and understanding the crop response to water availability (Kogan, 1995; Kogan, 1997; Wan et al., 2004). Therefore, the regression analysis is carried out in this study to relate the cumulative monthly irrigation water supply from the Sennar Dam with the integrated NDVI (iNDVI). For 2000–2012, the spatial average values of the integrated monthly MODIS NDVI (iNDVI) for cropped areas in the Gezira Scheme are computed and plotted against the cumulative monthly amounts of irrigation for summer, winter and annual irrigation seasons (Figure 5-11). It is remarkable that the iNDVI values respond well to the applied irrigation water. A significant positive correlation between iNDVI and irrigation water supply is observed, with R^2 values of 0.92, 0.87 and 0.97 for summer, winter and annual irrigation seasons, respectively, ($p < 0.001$). Such a correlation could be used for estimating the diverted quantities of water from the dam to the scheme, assuming that the scheme has the same conditions.

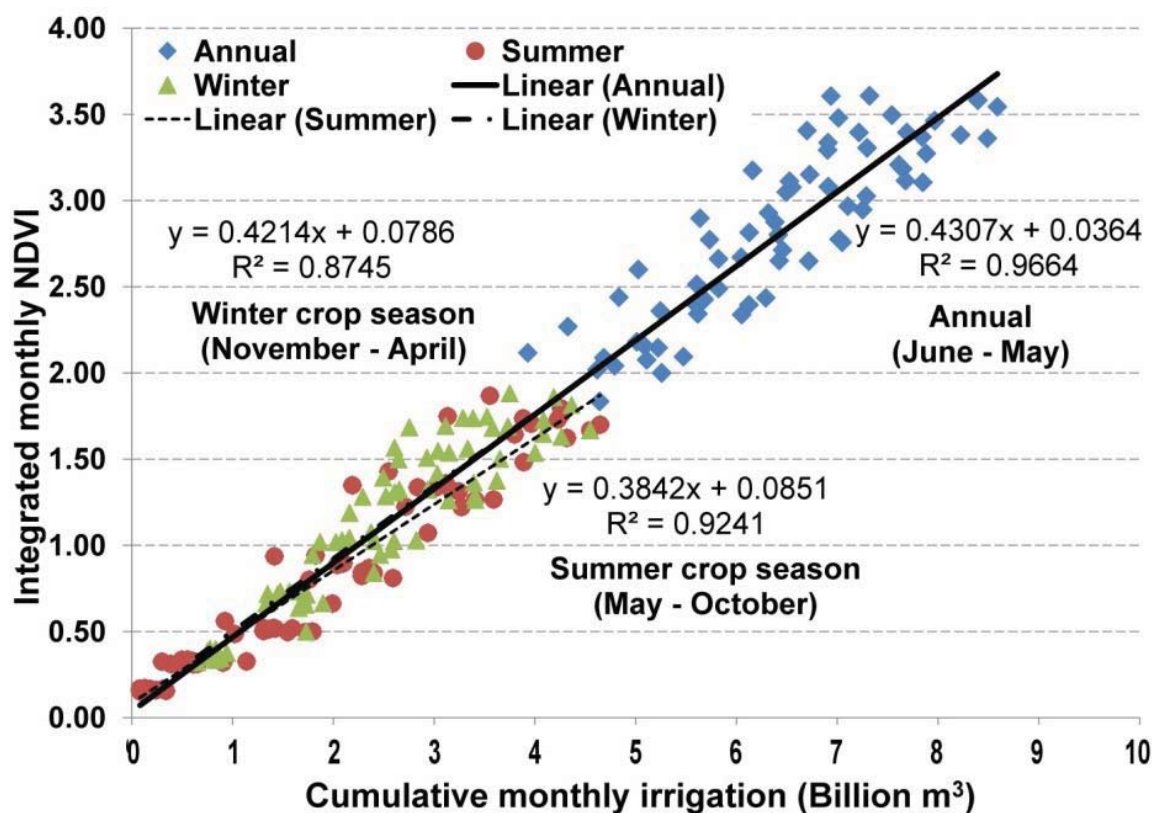


Figure 5-11. Scatter plots with regression lines of cumulative monthly irrigation water supply and iNDVI

5.3.3 The administrative levels

5.3.3.1 Longitudinal spatio-temporal assessment

The Gezira Scheme is subdivided into 17 administrative levels (groups), which receive their supplies from the Gezira and Managel channels (Adam et al., 2002). It is worthwhile assessing each group individually. Therefore, the seasonal ET and iNDVI values are extracted for each group. The uniformity in ET is a good measure of water availability, while iNDVI represents productivity. The groups are categorized according to their geographical locations (Figure 5-12) from the supply point (Sennar Dam) and to the supplied main irrigation channel. Table 5-3 shows the names of the blocks with their corresponding areas in order from south to north for the Gezira channel, and from south to west for the Managel channel.

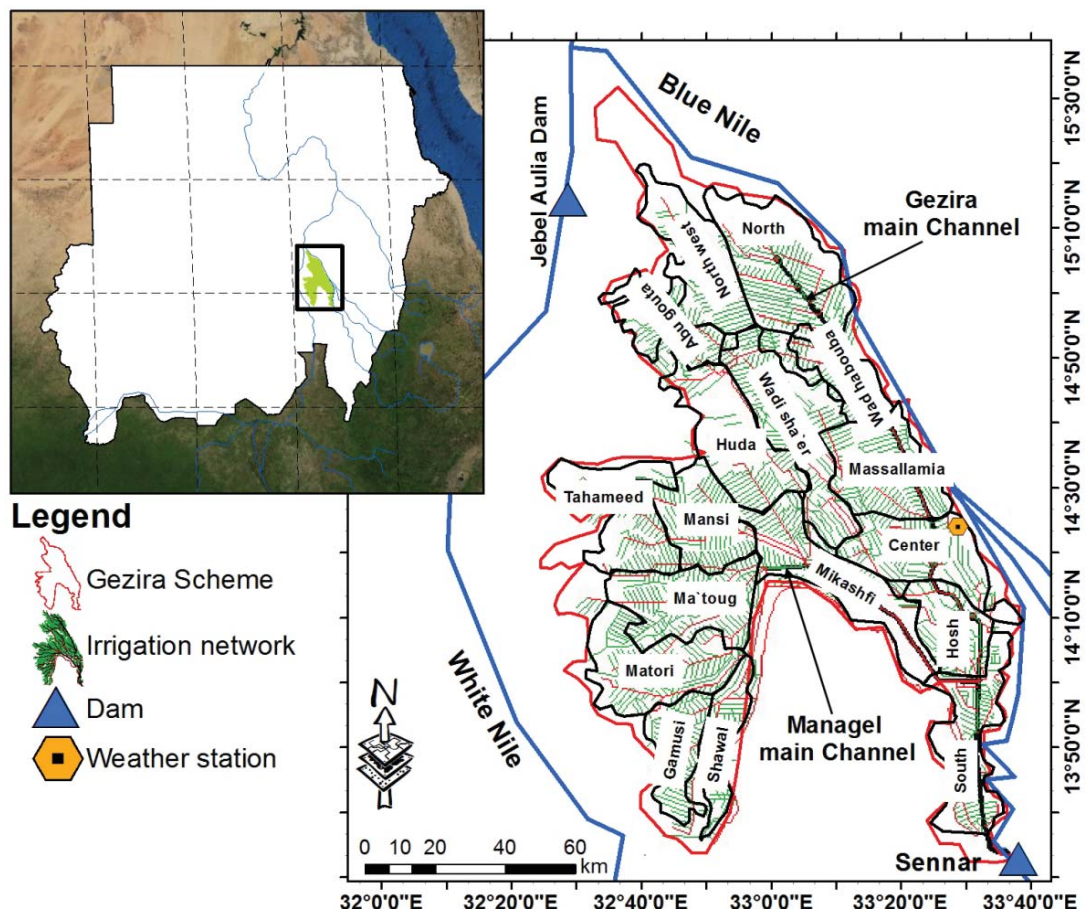


Figure 5-12. Map of the Gezira Irrigated Scheme showing administrative boundaries and main irrigation channels

Table 5-3. The group names with the area in order from upstream to downstream with their corresponding channels

ID	Name (Gezira channel)	Area (km ²)	ID	Name (Managel Channel)	Area (km ²)
1	South	698.2	1	South	698.2
2	Hosh	449.6	10	Mikashfi	811.6
3	Center	712.6	11	Huda	812.3
4	Massallamia	758.7	12	Mansi	571.4
5	Wadi Sha'eer	877.2	13	Tahameed	677.2
6	Wad Habouba	315.2	14	Ma'toug	750.3
7	North	1011.7	15	Matori	809.0
8	North West	683.7	16	Gamusi	409.7
9	Abu Gouta	412.8	17	Shawal	345.9

Head–tail analysis is considered for the main channels (Gezira and Managel). The head is determined by locating the inlet for the channel, starting from the South group, and the tail, at the end (Abu Gouta for Gezira and Shawal for Managel). Then the average of each group for each channel represents the longitudinal profile and provides an overall head–tail analysis. The results are plotted for 15 years for the Gezira channel in the summer (Figure 5-13) and the winter (Figure 5-14), and for the Managel channel during the summer (Figure 5-15) and the winter (Figure 5-16).

For the Gezira channel, the differences in water supply at the head and tail of the channel are visible for the summer season in the distribution of ET and iNDVI, as shown in Figure 5-13. It is clear that the water supply at the tail end (Abu Gouta group) is not sufficient, where lower ET and iNDVI values are observed for the 15 years. The highest ET and iNDVI values are recorded for the South and Hosh groups, which indicates that the water is available during the study period. For the three groups in the central part (Massallamia, Wadi Sha'eer and Wad Habouba), ET for the summer season ranges from 205 to over 500 mm. The highest ET_a value occurs in 2012, but without the same trend of iNDVI, which might be related to overestimation of ET_a for this year. Furthermore, the winter season for the Gezira channel does show significant variation (on average). However, in 2010, the behavior of the channel matches that of the summer season, which could be linked to the changing of the irrigation authority in 2010.

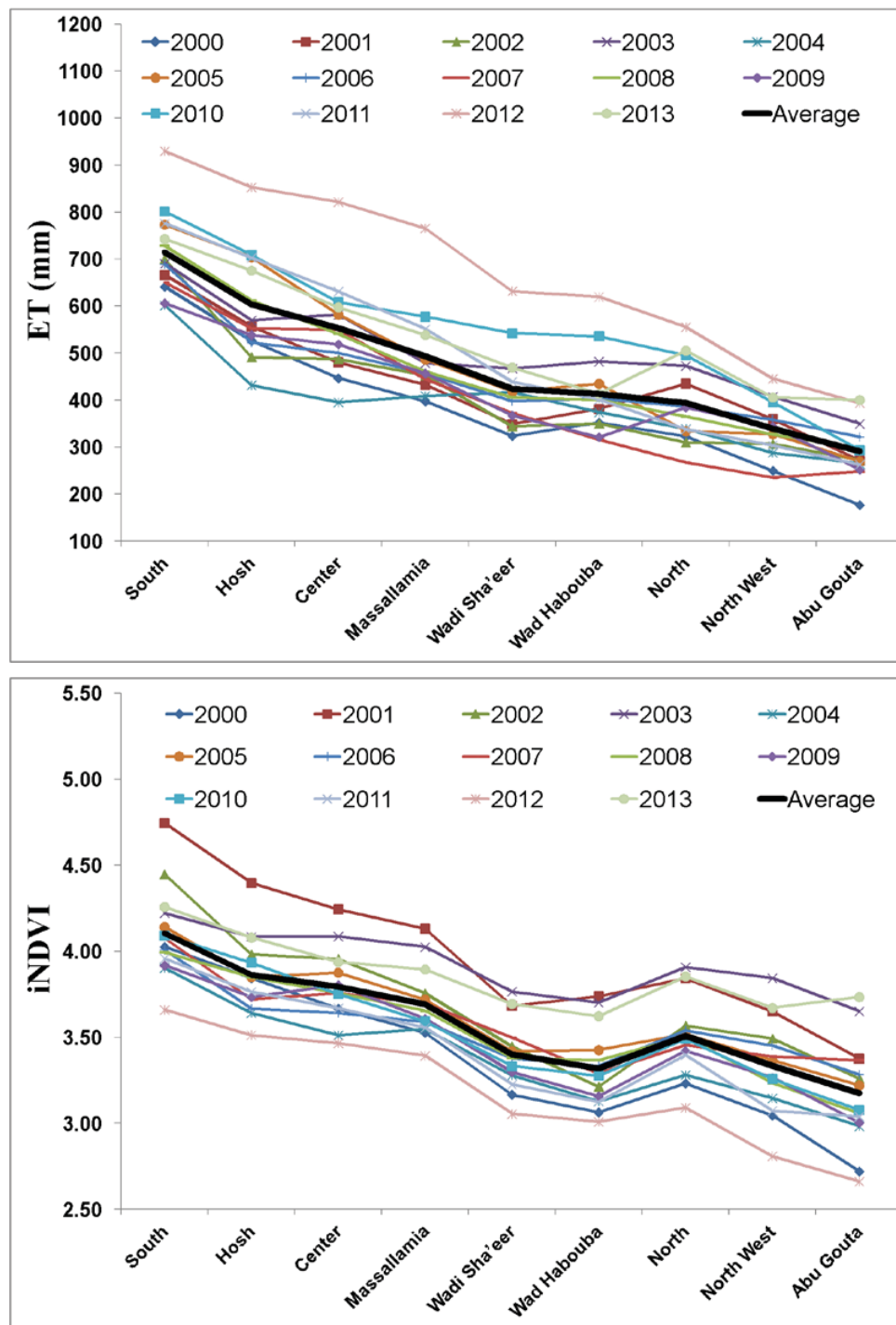


Figure 5-13. Spatial evolution of the average seasonal ET (upper) and integrated NDVI (lower) for each group of the Gezira channel for the summer crop season

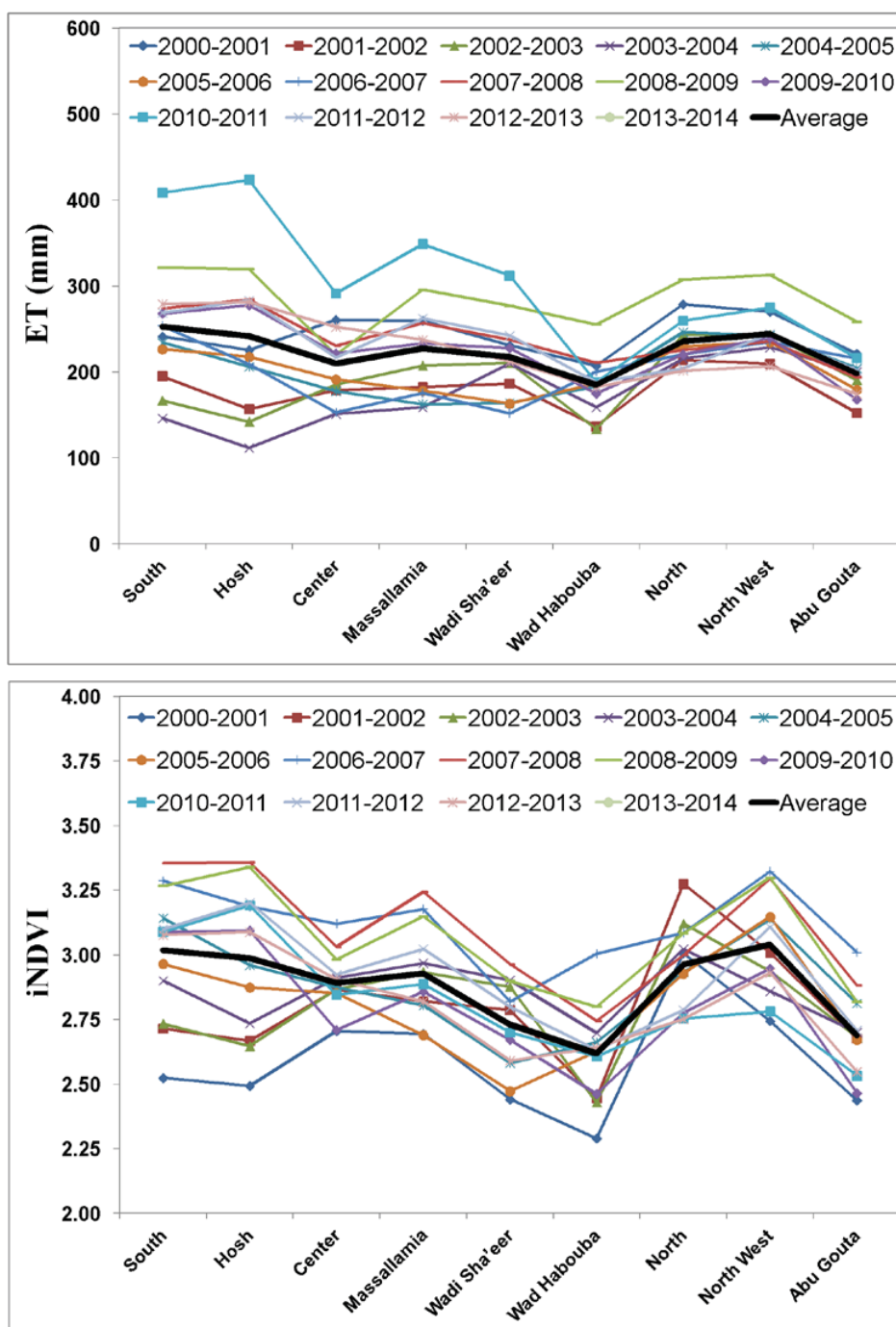


Figure 5-14. Spatial evolution of the average seasonal ET (upper) and integrated NDVI (lower) for each group of the Gezira channel for the winter crop season

On the other hand, the Managel extension tells a different story. As can be seen from Figure 5-15, both ET and iNDVI during the summer crop seasons show an upward spatial trend. The tail end of the channel has water availability and high productive use, due to the fact that the Managel channel is new and has several major branches. This promotes good water distribution, and is confirmed by the irregular shape of water depressions at the end of

the Managel channel. Still, this indicates that water supply is abundantly higher than demand, and wasted. Since 2008, however, new agricultural areas have been detected at the end of the Managel channel, which is considered a good step toward utilizing the excess water from channels.

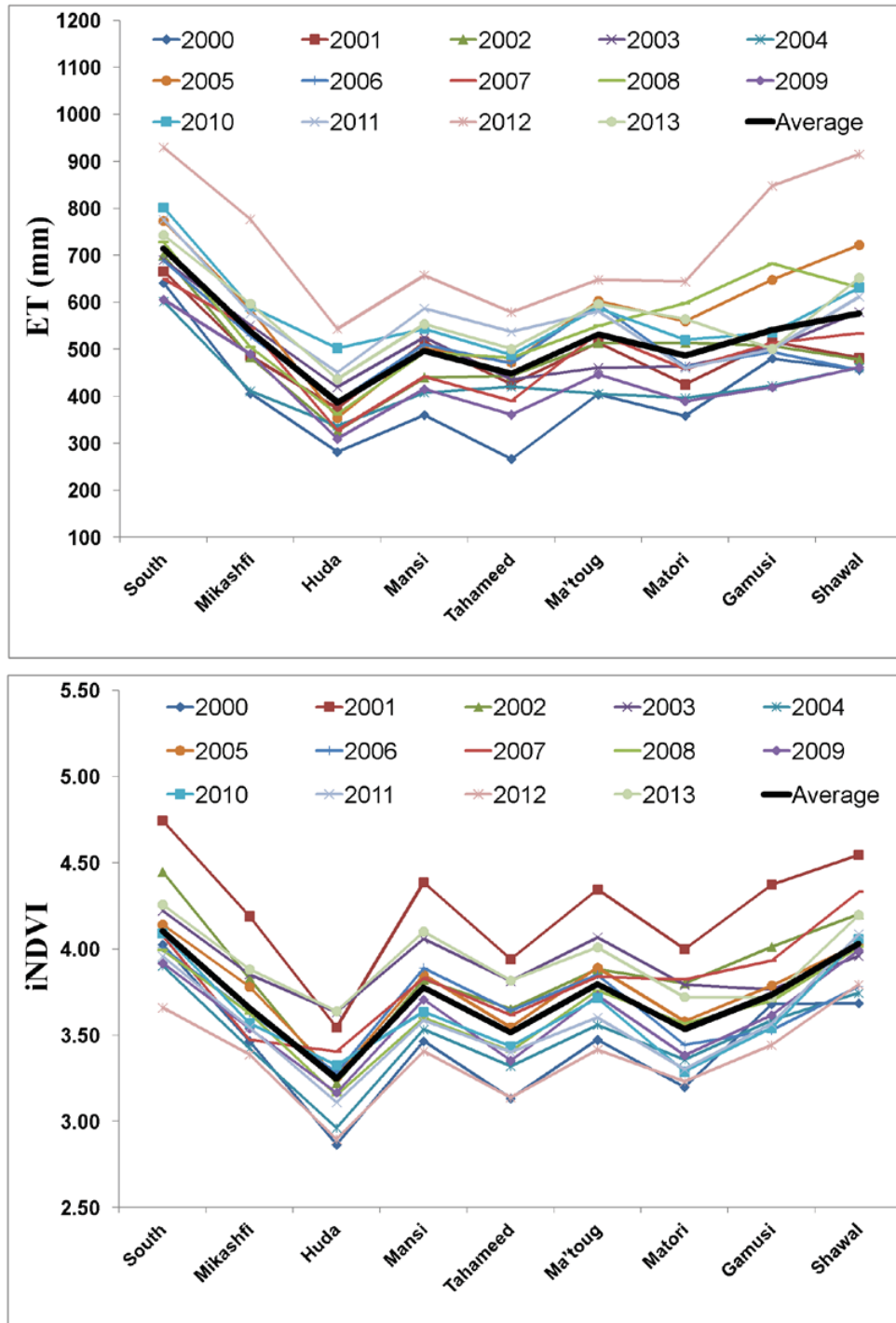


Figure 5-15. Spatial evolution of the average summer crop season ET (upper) and integrated NDVI (lower) for each group of the Managel channel

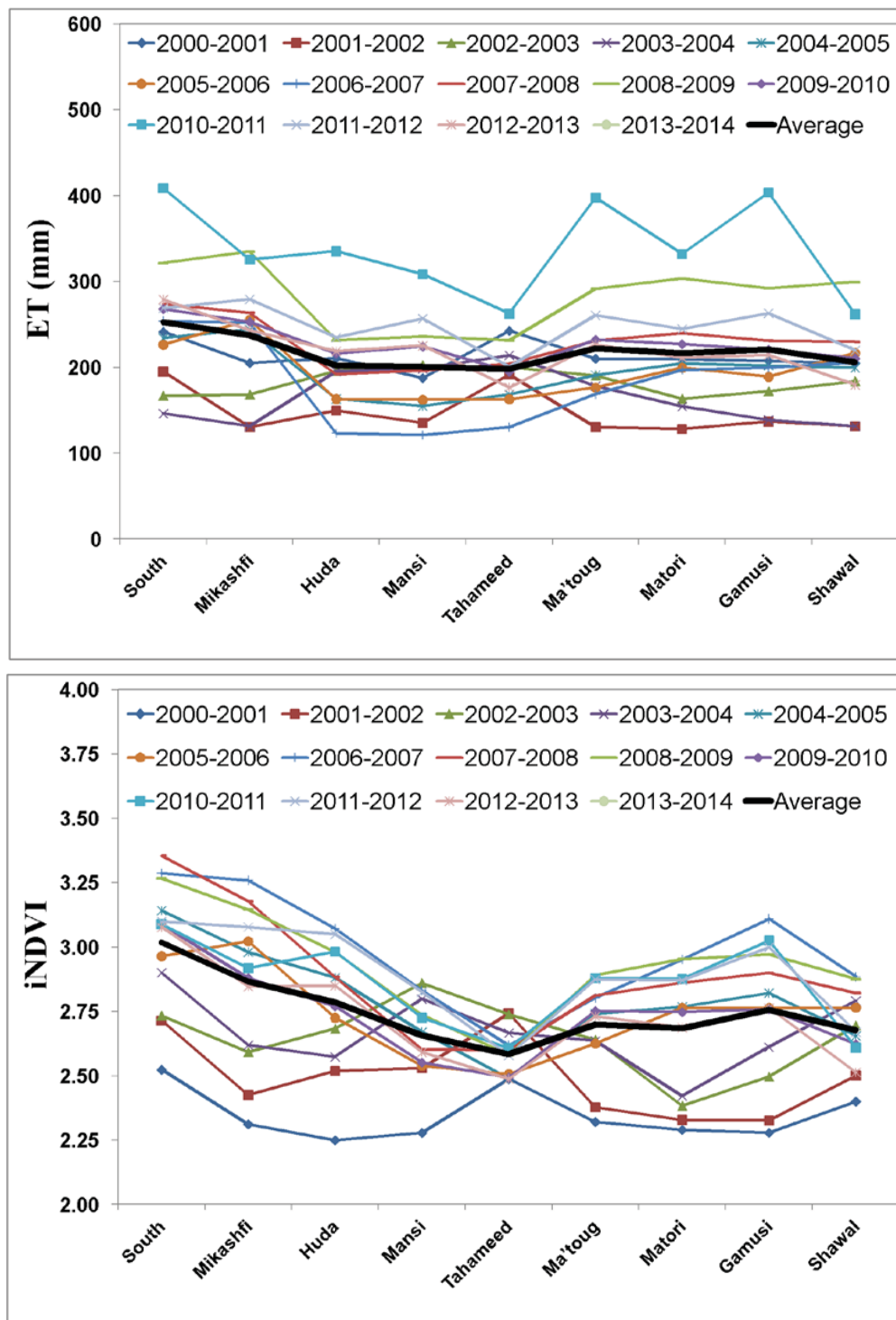


Figure 5-16. Spatial evolution of the average winter crop season ET (upper) and integrated NDVI (lower) of each group for the Managel channel

5.3.3.2 Model performance by ET_a -iNDVI for all groups

To study the model performance in more depth, Figure 5-17 and Figure 5-18 exhibit the scatter plot of the relationships between seasonal ET_{SSEB} and iNDVI at agricultural administrative levels for summer and winter crop seasons, respectively. For summer, the figure shows the similarity in trend between ET_a and iNDVI. The highest correlation coefficient ($R^2 = 0.90$) is found in 2001, the lowest ($R^2 = 0.56$), in 2003. Similarly higher and lower correlations for the winter crop season are observed for the same years. Occasionally, discrepancies occur between the grid results and the group values, with better R^2 for the groups. This is explained by the fact that the point for the groups does not correspond to one pixel, because most pixels in the group are averaged, whereas the grid analysis has a much higher resolution (1000 m) and numbers. The relationship, however, is highly significant ($p < 0.001$).

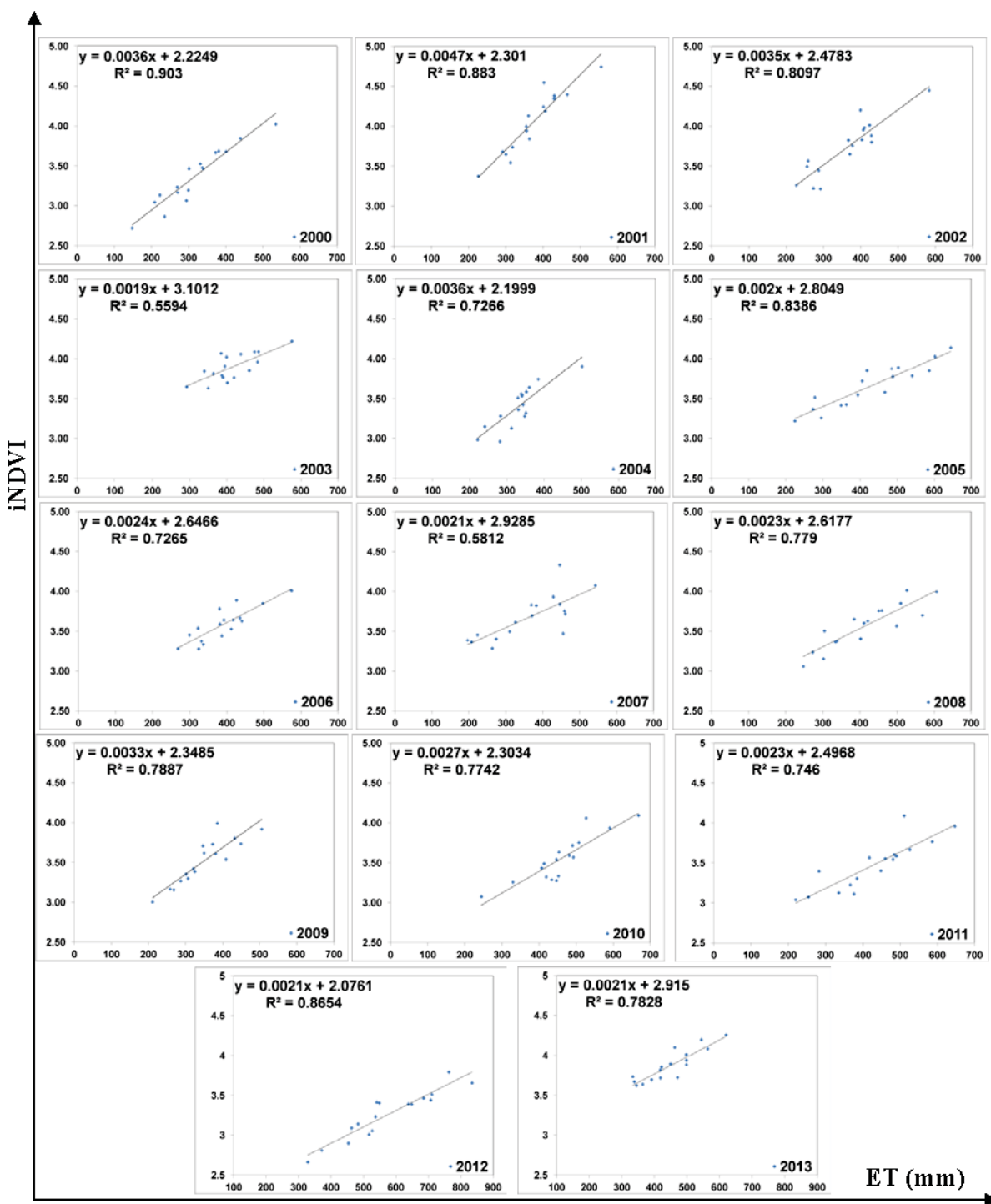


Figure 5-17. Relationship between seasonal actual evapotranspiration (ET_a) estimated by the SSEB model, and integrated NDVI (iNDVI) at blocks for the summer crop season

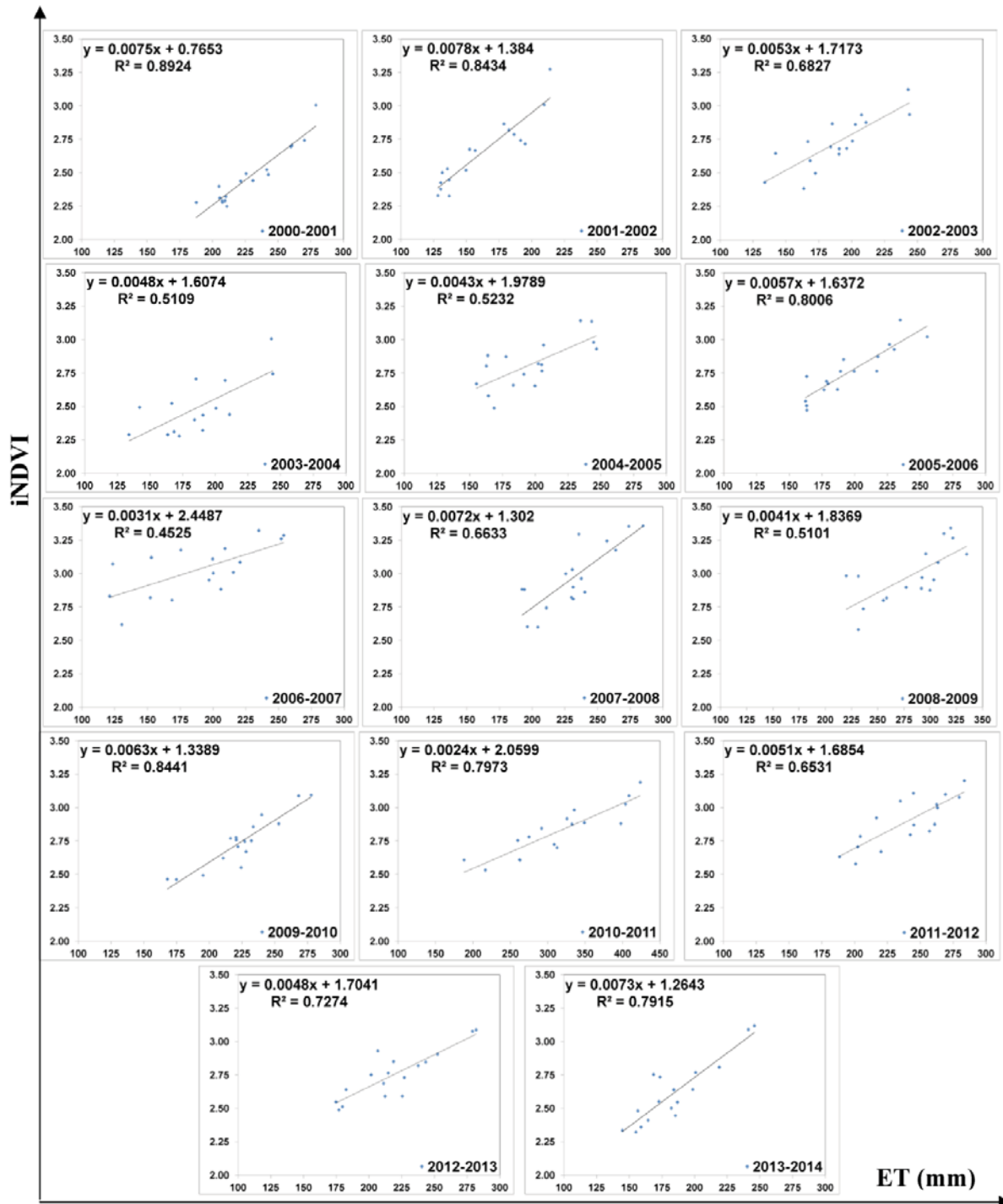


Figure 5-18. Relationship between seasonal actual evapotranspiration (ET_a) estimated by the SSEB model, and integrated NDVI (iNDVI) at blocks for the winter crop season

5.3.4 Evaluation of the applied water policies

The ET_a and NDVI maps for the last 15 years provide an effective tool for evaluating historical water policies. Because 85% of the total supply is released during the summer crop season, the winter season is not taken into consideration for evaluating water policies. In addition, the winter crop season has not been changed during the previous years. Thus, only the June–November crop growing periods are considered. Figure 5-19 shows the variation of both seasonal ET and iNDVI over the Gezira Scheme during the summer crop season. The values of total ET (BCM) and the mean of iNDVI are calculated for each grid pixel in the study area, where the values are calculated over the agricultural lands, bare soil and water ponds. Because of the observed water ponds, the other land-use types, rather than the agricultural lands, are included in this analysis. As can be seen, mean ET_a has an ascending trend, though insignificant ($p = 0.06$), over the past 13 years, while a descending trend ($p = 0.035$) is observed for iNDVI, which indicates that the water is available but not put to productive use.

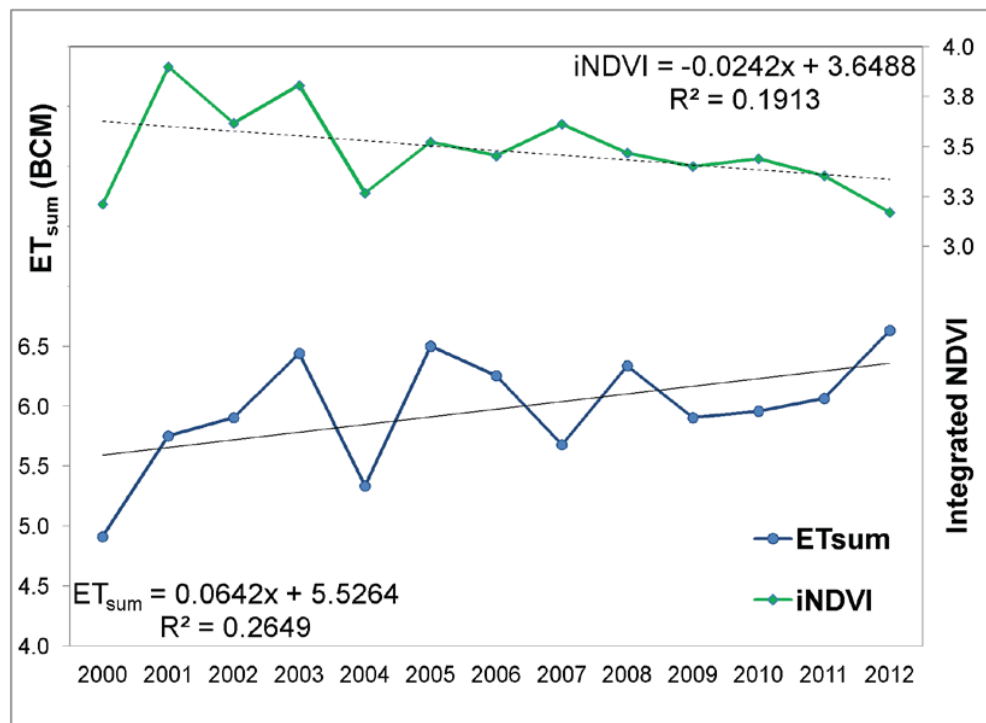


Figure 5-19. Variations of mean seasonal actual evapotranspiration (ET_a) and integrated NDVI (iNDVI) of the Gezira Scheme during the summer crop season

Increasing ET values did not result in increasing iNDVI. This could be linked to either the inequitable distribution of the summer crop season ET or the collected water in different depressions. Another reason could be over- or underestimation of seasonal ET values, as no

validation data is obtainable. In order to correct this anomalous uncertainty in ET_a estimation, the relationship between ET_a over agricultural areas (ET_{agr}) to the total ET_a from S SEB (ET_{sum}) is calculated. The ET_{agr}/ET_{sum} ratio represents the seasonal assessment, which precisely reflects the percentage of water for agricultural areas allocated to the whole scheme throughout the season. ET_{agr} is obtained from agricultural pixels only, which is identified by calculating $NDVI_{max}$ over each pixel. It is known that the agricultural pixel has a value higher than 0.25 (Hill and Donald, 2003; Anyamba and Tucker, 2005; Panda et al., 2010). In the current research, a pixel of $NDVI_{max}$ having a value higher than 0.3 is considered as an agricultural field in the Gezira Scheme. ET_{sum} is the summation of ET over bare soil, rural areas, water ponds and agricultural land. Figure 5-20 shows that the variation in the ratio of ET_{agr} to ET_{sum} on an annual basis has a descending trend ($p = 0.05$) in recent years. This suggests that the water policies in the Gezira Scheme have not had much effect on either its agricultural production or water saving. The downward trend continues until 2005, when WUA was introduced. Then, it rose again until the collapse in 2010, which could be linked to the change in irrigation responsibility mentioned earlier.

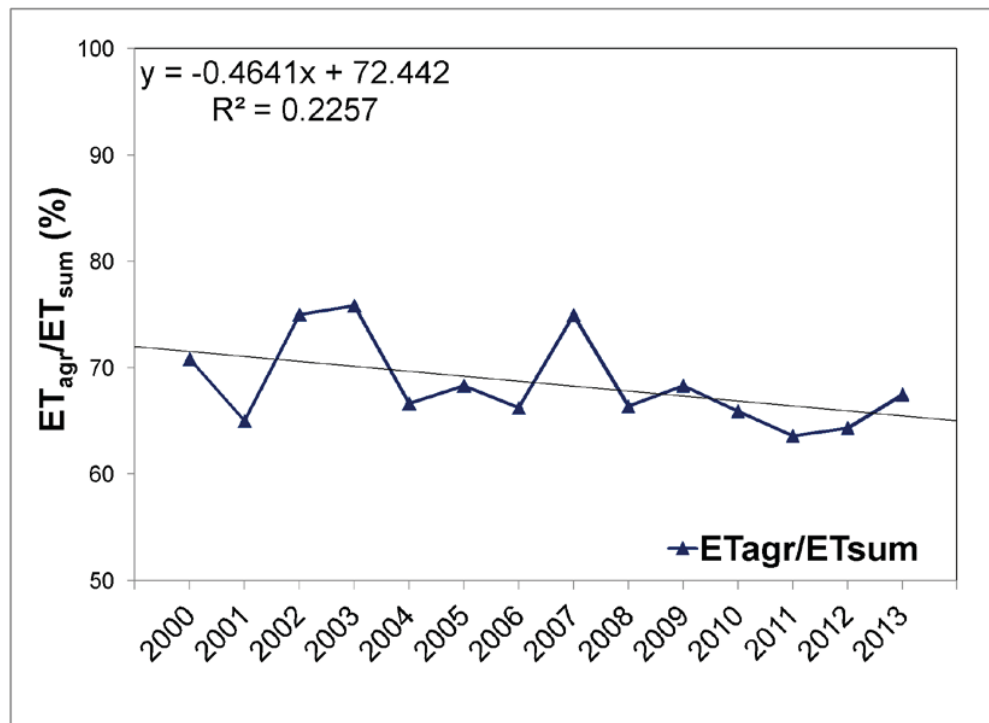


Figure 5-20. Variations of the ratio of actual evapotranspiration over agricultural areas (ET_{agr}) to the total actual evaporated water (ET_{sum}) of the Gezira Scheme

5.4 Conclusions

Summer and winter crop growing season evapotranspiration for 2000–2014 in the Gezira Irrigation Scheme is mapped using the SSEB model, and Landsat and MODIS satellites images. In addition, iNDVI is used as an indicator for crop production assessment. The evaluation is conducted for the whole scheme based on pixel resolution (1000 m) for the 17 administrative groups. The main channels (Gezira and Managel) are also considered in the assessment. The results are summarized as follows:

1. Due to lack of validation data, the current assessment focuses on the spatial distribution and trends rather than absolute values.
2. Spatially, seasonal ET_a and iNDVI for the Gezira Scheme are higher in the southern and central parts, and lower in the northern part. The well-irrigated areas with higher iNDVI are usually close to the main irrigation channels and southern areas, as with ET distribution.
3. Water ponds are identified, which implies there is water wastage at the Scheme.
4. ET_a and iNDVI are positively correlated, R^2 values taking a range of 0.35–0.80 with high significance level ($p = 0.0$), which, in general, indicates a satisfactory spatial and temporal relationship between the two datasets.
5. A significant positive correlation between iNDVI and irrigation water supply is observed, with R^2 values of 0.92, 0.87 and 0.97 for summer, winter and annual irrigation seasons, respectively ($p < 0.001$).
6. For the Gezira channel, the water supply at the tail end (Abo Gouta group) is not sufficient during the summer crop season, where lower ET and iNDVI values are repetitively observed over last 15 years. For the South and Hosh groups, the head of the channel, the highest ET and iNDVI values are recorded, which indicates that the water is available during the study period.
7. For the assessment, the mean ET has an ascending trend over the past 10 years, while a descending trend is observed for iNDVI. Also, the ET_{agr}/ET_{sum} ratio shows a descending trend over recent years. This suggests that the water policies in the Gezira Scheme have not had much effect on either its agricultural production or water saving. This indicates the water is available but not utilized for agricultural production.

CHAPTER SIX

POSSIBLE IRRIGATION MANAGEMENT SCENARIOS AND THEIR IMPLICATIONS FOR DOWNSTREAM FLOW

6.1 Introduction

Life cannot be sustained without water. Irrigated agriculture accounts for approximately 70% of total water consumption across the Nile River Basin. Historically, there has been sufficient water for irrigation and conflict over its usage has not arisen. Currently and in the future, other demands for water such as urban expansion and population growth will place additional pressures on the limited water resources. This will lead to a reduction in the volume of water allocated to agriculture and a desire for water conservation in the irrigation sector. There are approximately 5 million hectares of irrigated land in the Nile Basin (Bastiaanssen and Perry, 2009). Although the Nile Basin has excellent irrigation network systems, there are areas with very weak irrigation performance (Karimi et al., 2013). As stated in previous chapters, the Sudanese Gezira large-scale irrigation scheme has poor performance, which has adversely affected crop production and wastage of water. The Gezira Scheme has experienced severe irrigation water wastage problems in the last two decades (Ibrahim et al., 2002; A deeb, 2006; Elamin et al., 2011). Poor distribution and management of irrigation water are major factors contributing to this situation (Karimi et al., 2013). The irrigation and drainage networks do not work properly, which further exacerbates the water distribution problems of the scheme (Plusquellec, 1990; Ahmed, 2009). Besides, low crop production is a critical issue, on which Sudan should focus crop production enhancement (Bastiaanssen and Perry, 2009).

Chapters Three, Four and Five reveal that seasonal irrigation efficiency has been decreasing since 1993/94. The analysis shows that water amounting to twice CWR has been released from the Sennar reservoir. In spite of the abundant water resources, crop production is less than the expected return from the scheme. This is explained by the remotely sensed spatio-temporal water distribution assessment, which shows that the Gezira Scheme has faced imbalance in water distribution for the last 15 years. Water depressions, particularly in the southern and central parts, are observed during the summer crop season, which lead to the downstream area of the Gezira main channel not being supplied by enough water. The observed water depressions also imply that there is water wastage at the scheme and problems

with the conveyance system. In addition, the rainfall analysis concluded that the Gezira Scheme receives fairly adequate rainfall during the rainy season (June–October), which is not taken into account for irrigation. Generally, there is a potential for saving water of about 2, 4, 4 and 8 m³ for every kilogram produced of sorghum, groundnut, wheat and cotton, respectively, without impairing the yield (Ahmed and Ribbe, 2011). In conclusion, the imbalance of water distribution, inefficient irrigation network and neglect of rainfall are considered reasons, among others, for the low crop productivity and low observed efficiency of the Gezira Scheme.

The Sudanese government has seen the scheme as financially and economically unattractive, and has not acted in the interests of rehabilitation and maintenance, but instead conducted several conservation water policies, handing responsibility for management to the farmers, as mentioned in Chapter Five. Most policies have focused on increasing the supply through the irrigation systems, some on adapting crop management systems to reduce the need for irrigation water (particularly during the summer crop season). For instance, decreasing cotton cultivation has been seen recently in the Gezira Scheme (as discussed in Chapter Three, Section 3.3.2.1). However, the problems of water wastage and low crop productivity still exist.

Improvement of network functionality by means of rehabilitation or upgrading of channels is needed and has been recommended by many researchers (e.g. Plusquellec, 1990; World Bank, 2000; Ahmed and Ismail, 2008; Ahmed, 2009; FAO, 2011). With such a vast area and complex system, an RS monitoring tool and GIS is demanded to identify priorities for the rehabilitation or upgrading of channels.

New irrigation- and yield-enhancement technologies could be seen as a solution for tackling water conservation and achieving higher crop yield. But such technology is always costly and will not be part of a possible scenario (Oweis et al., 1999). Therefore, traditional innovative techniques such as water harvesting need to be developed to ensure the best use of natural precipitation (Ben Mechlia et al., 2009). In addition, Prinz (1996) stated that applying such a water harvesting technique can significantly increase plant production, which is needed for the Gezira Scheme. Ahmed and Ribbe (2011) confirmed that the *in situ* rainwater harvesting techniques furrow and chisel were tested at the Agricultural Research Corporation (ARC) at Wad Medani. They emphasize that the adoption of water harvesting techniques is a feasible option for saving water. Water harvesting for water conservation and increasing yield production is seen as one of the solutions to solve the system inefficiency problem of the scheme. Traditional options based on full irrigation with intensive cropping systems are

probably not the best future scenario, because of chronic water allocation conflict in the region (Karimi et al., 2013).

Quantitative estimates of the impact of enhancing irrigation efficiency are useful for convincing decision-makers about water-saving policies. To obtain numbers in terms of water quantity, a scenario of enhancement in the overall irrigation efficiency of the scheme is assumed, which can draw substantial conclusions about potential water savings. The information will be useful to the decision-makers in their water resources planning activities.

In this chapter, an RS-GIS tool and traditional water conservation management scenario are proposed to tackle the problems of the Gezira Scheme. Firstly, the RS SSEB model is seen as a useful monitoring tool to deal with the inefficiency of the existing irrigation network, especially during the summer crop season. The SSEB model is utilized to identify the well-irrigated, dry and water depression locations over time and space. Secondly, water harvesting is considered as a traditional water conservation strategy at the scheme. Lastly, the implications for downstream flow of the Blue Nile due to a possible increase in scheme efficiency are investigated.

6.2 Material and methods

6.2.1 A drought monitoring tool for the Gezira Scheme

Agricultural drought is an important hazard and complex phenomenon which harms agricultural economies and societies (Wilhite, 2002). It refers to a decline in the soil moisture content and, as a consequence, might cause crop failure (Mishra and Singh, 2010; Son et al., 2012). Traditional drought monitoring indices based on meteorological data (e.g. the Palmer Drought Severity Index (PDSI) and the Standardized Precipitation Index (SPI)) are not valid for large-scale irrigated agricultural areas such as the Gezira Scheme. RS technology makes it possible to retrieve soil moisture and vegetation conditions across large areas (Wu et al., 2013).

The previous chapters, as well as the literature (Ahmed and Ismail, 2008; Ahmed, 2009; FAO, 2011; Karimi et al., 2013), reveal inequity of water distribution in the Gezira Scheme, which is considered one of the major problems of the system. This has caused a lowering of production, mainly for the fields at the tails of the channels (FAO, 2011). Spatial monitoring of the dry and wet areas is needed, which provides essential information on the status of water resources and forms an important basis for decision-making. The SSEB model (Senay et al., 2007) was utilized in previous chapters of this thesis to monitor the seasonal distribution of actual evapotranspiration (ET_a). Herein, it is proposed as an instantaneous

drought monitoring method for the Gezira Scheme. The aim is to provide decision-makers with an immediate monitoring tool to identify water shortage, water depressions and well-irrigated areas. The reported problem could be handled by the decision-makers and the stakeholders to save water, which would lead to increased system irrigation efficiency. The lack of availability of instantaneous climatic data, especially hourly or daily records, is the basic obstacle for a broader use of SSEB. Therefore, the ET fraction (ET_f) of SSEB is utilized as an instantaneous monitoring drought risk index for the scheme. As mentioned in Chapter Five, ET_f is an indicator for representing the soil moisture availability. The index is seen as a good monitoring tool for identifying dry and wet areas. The SSEB model is described in Section 5.2.3 in the previous chapter. Once the climatic data and reference evapotranspiration (ET_o) are determined, the daily, monthly or seasonal ET_a can be calculated by multiplying ET_f by ET_o . However, calibration and validation of the model is still recommended for optimum results.

For the monitoring tool, Agam et al. (2008) recommended using T_s with high-spatial-resolution images over irrigated regions. The reason is related to the reliable estimation of ET_a and crop stress because of the significant moisture variations from one field to another. Therefore, it is proposed herein that Landsat images be used for monitoring. The ETM+ (Landsat 7) and Landsat 8 (LC8) (since May 2013) have 30 m spatial resolution. Monitoring for the 2013/14 crop season using Landsat 8 images with 0% cloud cover, as listed in Table 6-1, is described in this chapter. T_s from Landsat images is calculated based on the thermal band (Band 10) after radiance conversion following USGS (2013) methodology.

Table 6-1. The date of the used Landsat 8 satellite images for the monitoring tool

ID	Name	Julian day	Year	Date	Cloud cover
1	LC81730502013178LGN00	178	2013	Jun. 27	0*
2	LC81730502013258LGN00	258	2013	Sep. 15	0*
3	LC81730502013306LGN00	306	2013	Nov. 02	0
4	LC81730502013322LGN00	322	2013	Nov. 18	0
5	LC81730502013338LGN00	338	2013	Dec. 04	0
6	LC81730502013354LGN00	354	2013	Dec. 20	0
7	LC81730502014005LGN00	005	2014	Jan. 05	0
8	LC81730502014037LGN00	037	2014	Feb. 06	0
9	LC81730502014053LGN00	053	2014	Feb. 22	0
10	LC81730502014085LGN00	085	2014	Mar. 26	0

*Cloud effect is identified while calculating T_s

6.2.2 Water harvesting for the Gezira Scheme

6.2.2.1 Definition and categories of water harvesting

Water harvesting is defined as the collection of concentrated rainfall for its beneficial use (Critchley et al., 1991; Oweis et al., 1999; Narain et al., 2005). It is applied in arid and semi-arid regions where the annual rainfall (250–400 mm) is not sufficient to sustain rain-fed agriculture (Oweis et al., 1999; Ben Mechlia et al., 2009). In terms of volume, this precipitation represents an adequate amount of water (Critchley et al., 1991). However, because it is distributed over a large area, as is the case in the Gezira Scheme, most of the water is lost by evaporation and not productively used. Additionally, utilizing rainfall for the Gezira Scheme during the summer crop season will have a good impact on the siltation problem of the irrigation network. Ahmed and Ribbe (2011) mentioned that the lower the volume of Blue Nile water entering the Scheme, the less silt accumulates in the channels and fields. This is because of the high amount of silt entering the scheme during the rainy season (Ahmed, 2009; Ahmed and Ribbe, 2011).

There are two basic categories of rainwater harvesting systems for plant production: micro- and macro-catchment systems (Critchley et al., 1991). The micro-catchment system refers to *in situ* rainwater harvesting techniques, which are more common than the macro-catchment systems (Biazin et al., 2012). The macro-catchment water harvesting system refers to the case where runoff from hill-slope catchments is conveyed to a cropping area located at the foot of a hill on flat terrain. It is also called the Long Slope Catchment Technique, as the

catchment area is usually 30–200 m in length (Critchley et al., 1991; Prinz and Singh, 2000). The Gezira area is generally flat with a gentle slope to the north and west (Plusquellec, 1990), which does not permit the macro-catchment method to be applied. Therefore, the *in situ* water harvesting technique is seen as a more appropriate application for the Gezira Scheme.

The selection of the best sites for water harvesting schemes must be based on certain criteria that take into consideration the physical and the socioeconomic characteristics of the targeted area (Al-Adamat et al., 2010) . Water harvesting cannot be easily implemented without considering climate characteristics (rainfall, evapotranspiration, etc.), the topography, the soil type and, most significantly, the socioeconomic conditions of the community of the region (Oweis et al., 2012). In this chapter, investigation of physical parameters is undertaken to identify the potential of applying water harvesting at the Gezira Scheme. This will help to maximize utilization of the available rainwater resource. The development of the methodology is built on five steps for the technical assessment only, which are the knowledge of water demanded by different types of crops, the designed amount of rainfall and recommended water harvesting technique.

6.2.2.2 crops water requirements

It is necessary to assess crop water demand when designing water harvesting systems for a agricultural areas (Critchley et al., 1991) . Long-term (1961–2010) monthly average meteorological data for the Wad Medani meteorological station (Lat.14.4 N: Long. 33.5 E) is used to determine crop evapotranspiration (ET_c), which is illustrated in Section 3.2.2.

6.2.2.3 Designed rainfall amount

Rainfall characteristics (intensity and distribution) are important factors in applying water harvesting techniques for an area (Critchley et al., 1991; Prinz and Singh, 2000; Oweis et al., 2012). For agriculture, the design rainfall (DR) is defined as the total amount of rain which provides the plant water requirement over the growing season (Critchley et al., 1991). The quantity of rainfall that produces runoff is a good indicator of the suitability of the area for water harvesting (Prinz and Singh, 2000). DR is determined by means of a statistical probability analysis of annual rainfall time series data with a 67% probability of occurrence from the Wad Medani meteorological station. It is determined using the DISTRIB application in SMADA software (Eaglin et al., 1996) to analyze the monthly and annual rainfall data for 1961–2012, except 2009. A three-parameter, log normal statistical model is found to give the best fit for the distribution.

6.2.2.4 Design model for the catchment

The *in situ* water harvesting system consists of a catchment area (CA) and a cultivated area (CU), where runoff is generated in the CA and collected in the CU (Critchley and Scheierling, 2013). The ratio between the parameters, defined as the cultivated area ratio (CA:CU ratio), should be experimentally determined (Critchley et al., 1991). However, this experimental work seems not to be applicable to the current study. Therefore, the CA:CU ratio can be calculated, as recommended by Critchley et al. (1991), from the following equation:

$$\frac{ET_c - DR}{DR \times Kr \times RC} = \frac{CA}{CU}, \quad (\text{Equation 6-1})$$

where ET_c , DR, CA and CU are as mentioned above, and Kr and RC are the efficiency factor and the runoff coefficient, respectively. Hence, Plusquellec (1990) mentioned that the soil of the Gezira Scheme is uniform and consists mainly of sediments from the Blue Nile, which have a clay content of 50%–60%. The clay soil makes the infiltration of water very slow, and is considered a high runoff coefficient for the CA for generating runoff. Therefore, Kr and RC are assumed to be 0.50 (reflecting the high proportion of runoff from very short catchments) and 0.75 (reflecting the greater efficiency of short-slope catchments), respectively, according to Critchley et al. (1991). In the case of the Gezira Scheme, the estimation of the ratio may affect the efficiency and effectiveness of the proposed system, as no experimental determination exists. Nevertheless, the designed model is based on high-variability features (Rainfall and ET_c). It is therefore necessary to modify the original design yearly in terms of safety measurements to avoid damage in years when rainfall does not equal DR (Critchley et al., 1991). Usually, the CA:CU ratio is in the range 1:1–5:1 for the *in situ* (Micro-catchment) technique (Critchley and Scheierling, 2013).

6.2.2.5 Water harvesting recommended techniques

As mentioned earlier, the *in situ* (Micro-catchment) technique is seen as a suitable water harvesting system for the Gezira Scheme. It is a method of collecting surface runoff from a small CA and storing it in the root zone of an adjacent infiltration basin. This has the potential to improve the soil water content of the rooting zone by up to 30%, depending on rainfall pattern and soil type (Biazin et al., 2012). Examples of micro-catchment system are Negarim and contour bunds (for trees), contour ridges and the inter-row areas (for crops) (Critchley et al., 1991; Prinz and Singh, 2000; Oweis et al., 2012).

Oweis et al. (2012) recommended the inter-row water harvesting technique (Figure 6-1) for either flat land or gentle slopes of up to 4%, which is the same topographic characteristic as the Gezira Scheme. The authors added that it is the only water harvesting technique suitable for absolutely flat land and for areas with annual average rainfall of more than 200 mm. The technique is similar to the Farrow water harvesting technique tested at Wad Medani ARC (Ahmed and Ribbe, 2011). Therefore, it is seen as a suitable technique for the Gezira Scheme.

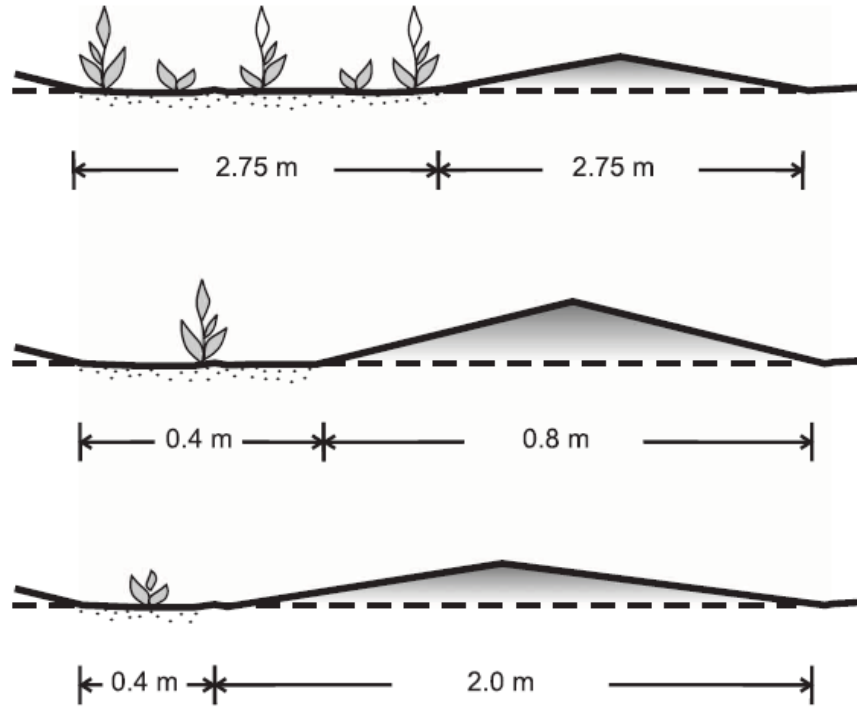


Figure 6-1. The inter-row water harvesting technique (catchment to cropping area ratio changes based on rainfall amount)

Source: Prinz (1996)

6.2.3 Implications of improving irrigation performance on downstream Blue Nile flow

A number of Decision Support System (DSS) models have been developed to assess the impact of future development plans (hydropower and irrigation potential) and climate change within the entire Nile Basin (Guariso and Whittington, 1987; Block et al., 2007; Block and Strzepek, 2010; McCartney and Girma, 2012). Most of these studies have focused on the Blue Nile at the Eastern Nile Basin, as it is the most significant tributary, providing over 70% of the Nile's flow through downstream countries (NBI, 2012).

McCartney and Girma (2012) concluded that the flow of the Blue Nile will be reduced by 22% at the Ethiopia–Sudan border as a consequence of climate change in combination

with upstream water resource development. An earlier study by McCartney et al. (2009) estimated that irrigation demand would increase in the Blue Nile in Sudan and Ethiopia; consequently, the flow of the Blue Nile is reduced by 18% at Khartoum. However, these models have simulated the current large-scale irrigation schemes with their existing irrigation efficiency. Increasing the existing efficiency is seen as a water conservation and management need to face increasing future water demand (Bastiaanssen and Perry, 2009). Furthermore, one of the major constraints faced within the basin is water scarcity, and the irrigated agricultural sector competes for water with the domestic and industrial sectors (Karimi et al., 2013). Relatively little consideration has been given to the implications of enhancing the overall efficiency of downstream flow. Previous observations in the Gezira Scheme indicate that around 6–7 BCM per year of water is applied for irrigation, of which only around 3–4 BCM per year is needed for growing the crops. The overall irrigation efficiency has been very low since 1994 ($\cong 44\%$ on average) and the proposed management scenarios (monitoring tool and water harvesting) could save water and increase the irrigation efficiency. Herein, this section quantifies the amount of water which could be saved by improving irrigation efficiency. The data utilized for this analysis are actual observed irrigation water supply, rainfall and crop water demand, as mentioned in Chapter Three, particularly in Section 3.2.1. The volume of saved water can meet demand from other water users downstream in the Gezira Scheme, as presented in the schematic figure, Figure 6-2.

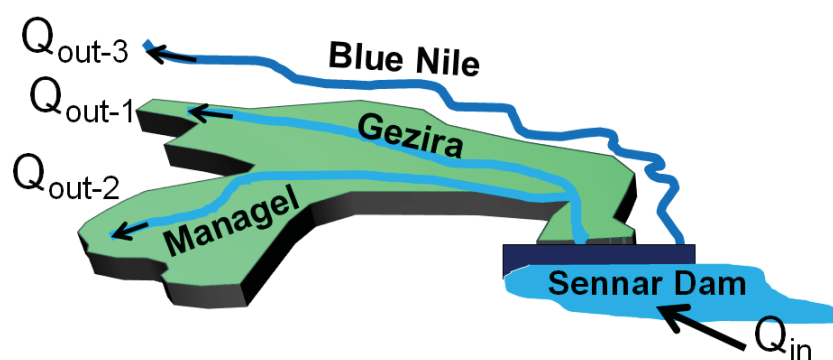


Figure 6-2. Schematic map showing the concept of managing irrigation efficiency through the Gezira and Managel channels ($Q_{out-1} + Q_{out-2}$); the impact will be on Q_{out-3}

6.3 Results and discussion

6.3.1 The Monitoring assessment

6.3.1.1 Spatio-temporal monitoring

The ET_f values from Landsat 8 satellite data using T_s are derived using an automated program written in ArcGIS Model Maker. Figure 6-3 shows the spatial distribution of the ET_f index on ten different dates in 2013 and 2014. As can be seen, the start and end of the irrigation season can be respectively visualized as June 27, 2013 and March 26, 2014. Also, December 20, 2014, is the end of the summer and start of the winter crop seasons. ET_f values are in the range 0.0–1.0. The higher values indicate the wet conditions, presented by water ponds and well-irrigated areas, while the lower values indicate lack of soil moisture (i.e. bare soil). The only part experiencing a dry spell is located in the northern part of the scheme. Approximately, the southern, central and southwestern areas are subjected to wet conditions, where water ponds are always found ($ET_f \cong 0.8-1.0$). This confirms that the irrigation channels in these areas cannot meet demand.

For the whole season, Figure 6-4 demonstrates the water leakage from the irrigation channels in the northern, central and southwestern parts of the scheme. For the Gezira irrigation channel, the dry areas in the northern part could be a result of flooding channels in the central part. The problem is very acute on the flat terrain where excess water is just left to flow and spread across the plain. The overall result is enormous loss of available water. Therefore, water shortage in wide areas is observed. However, the Managel channel supplies more water than is demanded, which is explained by the irregular cold areas ($ET_f = 1.0$) observed at the tail of the channel, as shown by ET_f in Figure 6-3 and the highest ET values in Figure 6-4. These maps also reveal that the scheme has a poorly maintained or no drainage system at all to return excess water into the river.

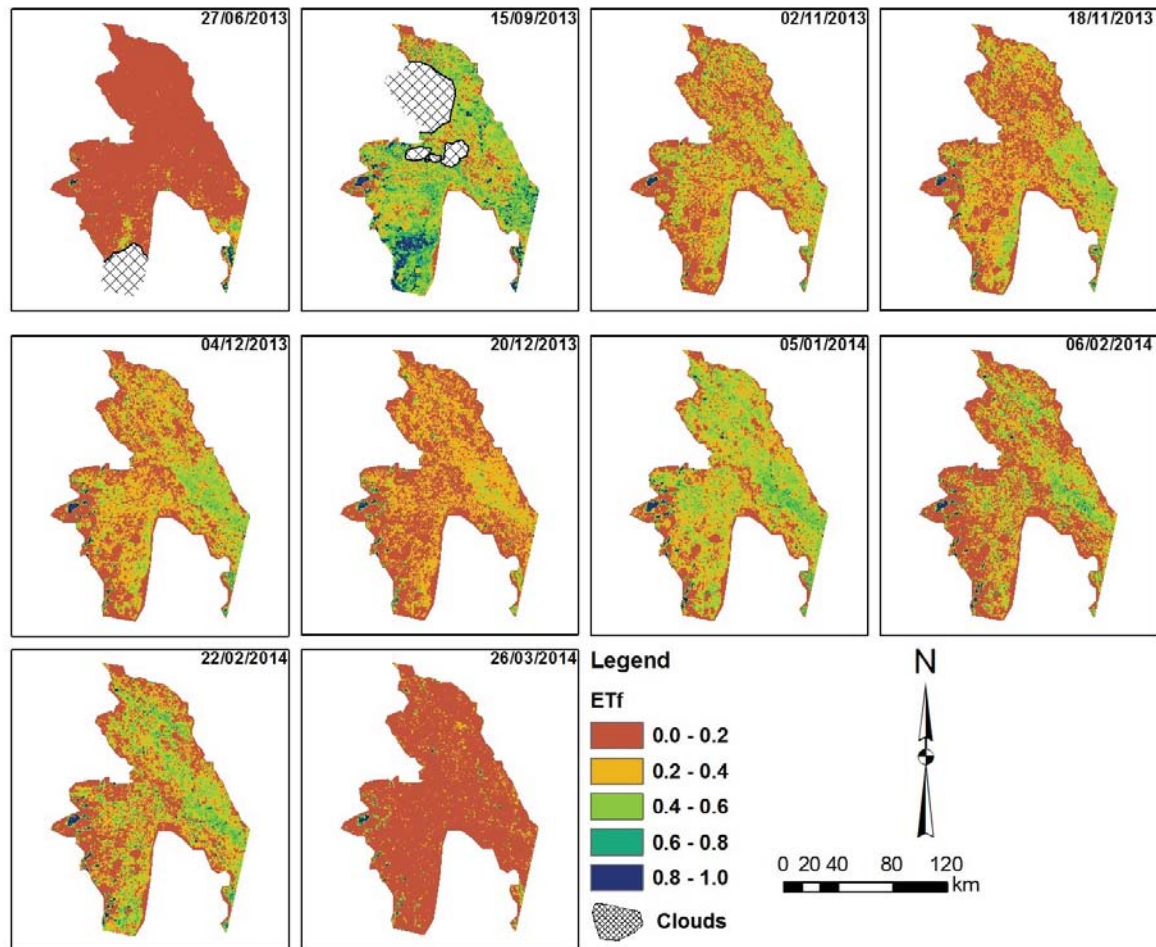


Figure 6-3. Spatial distribution of evaporative fraction (ET_f) over the Gezira Scheme for the 2013/14 irrigation season (images are in order of day of the year)

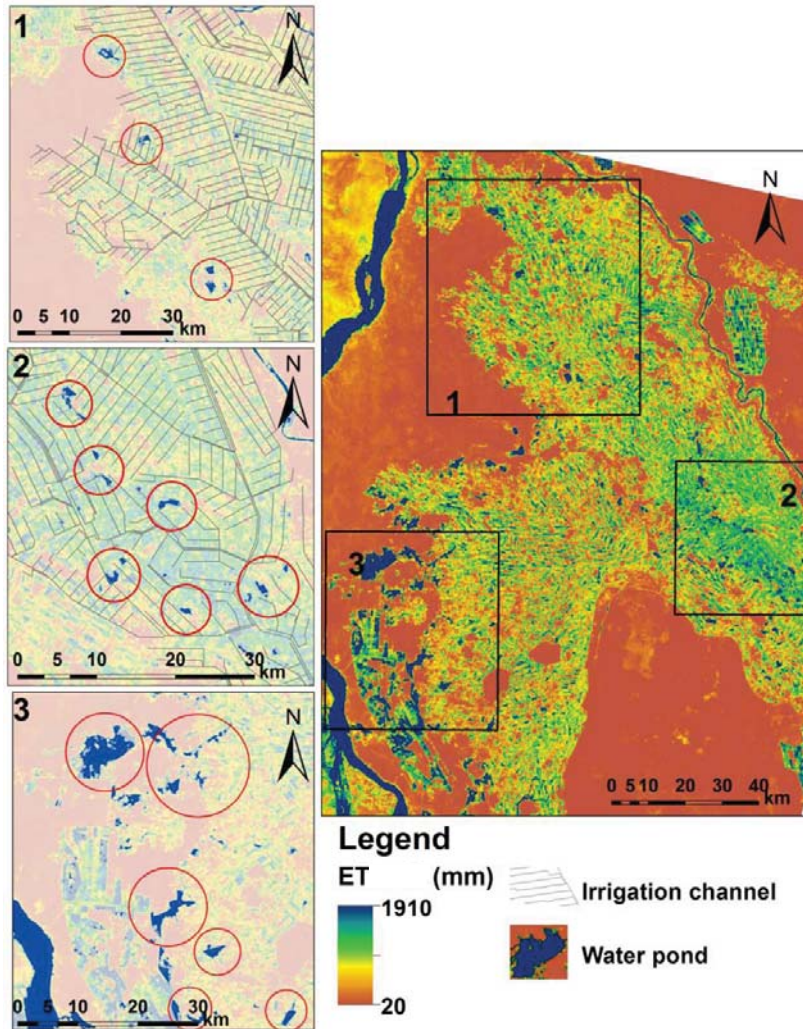


Figure 6-4. Identifying water leakage from the irrigation channels at the northern, central and southwestern parts of the scheme for the 2013/14 irrigation season

The GIS presented by ArcGIS software is a powerful tool to simultaneously assess the information spatially (Nehme and Simões, 1999). In the case of the Gezira Scheme, GIS is used to identify the location and names of irrigation channels with leakage problems. After converting the water ponds from raster format to polygon feature class, the Select-by-location tool is utilized to identify the irrigation channels that intersect with the water ponds. Table 6-2 presents the names of 77 irrigation channels with suspected leakage problems. In current practice, this information helps and supports the decision-making procedure for irrigation network operation and maintenance. The maintenance of these channels will reduce unnecessary water loss through leakage, which might allow more water to flow downstream.

Table 6-2. Reported leakage channels for the irrigation season 2013/14

ID	Channel	Type	ID	Channel	Type	ID	Channel	Type	ID	Channel	Type
1	Gezira	Main	21	Mahali	Minor	41	Wad-el mahi	Minor	61	Abu-hawwa	Minor
2	Tabat	Branch	22	Qarrash el gadid	Minor	42	Toman	Minor	62	Faramaina	Minor
3	Awamra	Major	23	Mansur	Minor	43	Gummuuya	Minor	63	El sihaimab	Minor
4	Abu-gadoun	Minor	24	Samina	Minor	44	Gummuuya branch	Minor	64	Goz kabaro	Minor
5	Umm-mud	Minor	25	El saer	Minor	45	Wad-numan	Minor	65	Saiyala	Minor
6	Wad-el kamil	Minor	26	Wad-el kereil	Minor	46	Nefediya	Minor	66	Al amel huda	Minor
7	Umm futir	Minor	27	Akar	Minor	47	Foqama	Minor	67	Huleiwa	Minor
8	Aburus	Minor	28	Sayir	Minor	48	Shamun	Minor	68	Hag mohammad	Minor
9	Awoda	Minor	29	Ureika	Minor	49	Rizig alla	Minor	69	Abbas shaugi	Minor
10	El uqeida	Minor	30	Ayer	Minor	50	Imam	Minor	70	Bortobeil	Minor
11	Umm-hamid	Minor	31	Abu-udna	Minor	51	Abu-el hasan	Minor	71	Wad-guleid	Minor
12	Abbd-el salam	Minor	32	Edderab	Minor	52	Arbigi	Minor	72	Shaiqab	Minor
13	Elghaia	Minor	33	Gadarin	Minor	53	Escape	Minor	73	Ahmar	Minor
14	Harsh	Minor	34	Khawalda	Minor	54	Wad-adam	Minor	74	Tannub	Minor
15	Ennur	Minor	35	Ramadan	Minor	55	Saad el shafia	Minor	75	Mahas	Minor
16	Qatta	Minor	36	Radma	Minor	56	Wad-elmaak	Minor	76	Wad-matar	Minor
17	Madratta	Minor	37	Shezeikha	Minor	57	Wad-el hindi	Minor	77	Gawada-2	Minor
18	Mieigina	Minor	38	Gabli	Minor	58	Wad-el nur	Major			
19	Futeis	Minor	39	Hag etom	Minor	59	Takala	Minor			
20	El mahala	Minor	40	Gemeiliya	Minor	60	Incina	Minor			

6.3.2 Water harvesting potential

6.3.2.1 Crop water requirements

Monthly averages of maximum and minimum temperatures, percentage of relative humidity, wind speed, actual sunshine hours and crop factor are utilized to calculate ET_c values for the four main crops of the Gezira Scheme, as mentioned in Chapter Three. The monthly ET_c values are converted to seasonal values, which correspond to the growing season only for the summer season crops (sorghum, groundnut and cotton), as listed in Table 6-4. In the case of sorghum and groundnut, ET_c values take averages of 820 and 940 mm/season, respectively. These values represent the total water requirement for the whole growing season, while ET_c for cotton has a value of 1350 mm/season for the whole growing season until February. The water demand of cotton until November is estimated at 825 mm. However, these results have greater values than those obtained by previous scholars, as mentioned in Section 2.5.2, with 4% for cotton and 16% for groundnut and sorghum. This is contributed to by the updating of the solar radiation parameter in the FAO Penman–Monteith formula, which results in increasing ET_o values.

6.3.2.2 Designed rainfall amount

The annual rainfall data are analyzed in order to define the probability of occurrence to determine the designed rainfall amount. The three-parameter, log normal distribution method is applied to determine the designed rainfall value, which gives the best fit for the distribution. The probability of occurrence curve for the observed and predicted data is derived, as shown in Figure 6-5. The correlation between the two datasets is highly significant ($p < 0.001$), with an R^2 value of 0.9424. Subsequently, the return period, the reciprocal of the probability, for the seasonal rainfall is computed and given in Table 6-3. The table shows that rainfall events with a probability of 67%–100%, equivalent to annual rainfall of 186–253 mm, can occur every 1–3 years. Rainfall probability with the range of 33%–67%, amounts to 289–362 mm and could happen every 2–5 years. The designed rainfall value is found to be 253 mm, which will be met or exceeded (on average) in two years out of three, and the harvested rain will satisfy CWR for the same mentioned time period. In addition, the statistical analysis resulted in mean and standard values of 292.69 mm and 14.77 mm, respectively.

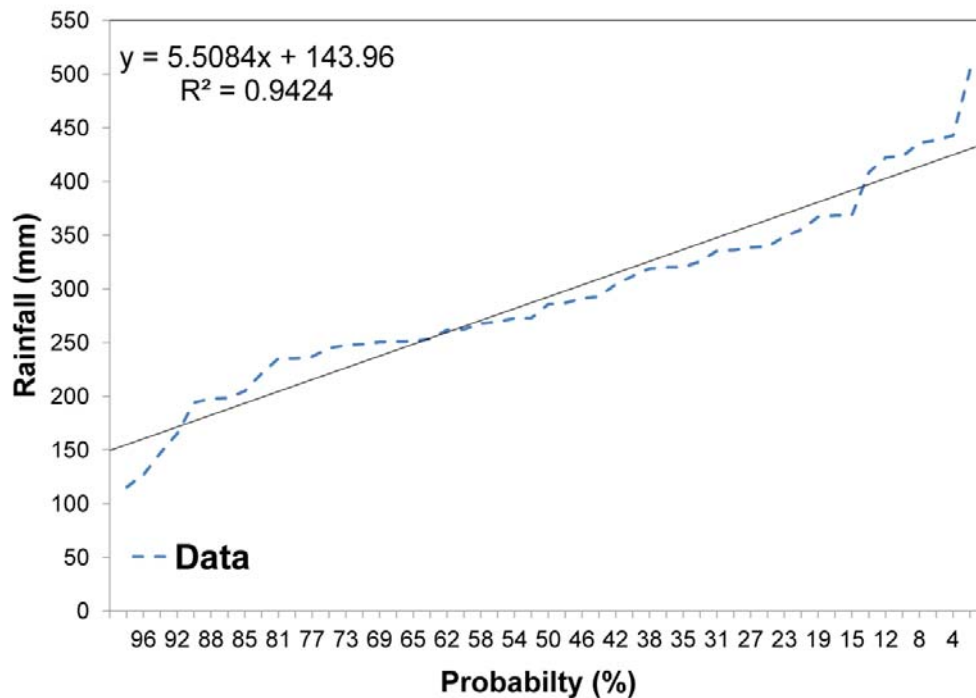


Figure 6-5. Probability diagram of the seasonal rainfall curve for the Wad Medani station

Table 6-3. Probability and return period for the different rainfall values

Probability	Return period (years)	Rainfall (mm)	Standard deviation (mm)
0.01	200.0	528.2	44.0
0.01	100.0	503.0	36.9
0.02	50.0	476.0	30.2
0.04	25.0	446.7	24.3
0.10	10.0	402.5	17.8
0.20	5.0	362.5	14.6
0.33	3.0	326.3	13.3
0.50	2.0	289.5	12.7
0.67	1.5	253.2	12.5
0.75	1.3	234.3	12.6
0.85	1.2	205.7	13.5
0.90	1.1	186.8	14.6

6.3.2.3 Design model for catchment

The system is designed to provide enough runoff to meet CWR. The ratios of the catchment to the cultivated areas (CA:CU) for each crop are determined by applying Equation 6-2. The results are presented in Table 6-4 for the summer crops (sorghum, groundnut and cotton until November).

Table 6-4. Adopted parameter and calculated catchment to cultivated areas ratio (CA:CU)

Crop	ET_c (mm)	DR (mm)	Kr	RC	CA:CU
Sorghum	820.78	253	0.50	0.75	6
Groundnut	947.36	253	0.50	0.75	7
Cotton (Nov)	824.20	253	0.50	0.75	6

From the results, the CA must be six times larger than the cultivated area to fully supply sorghum and cotton (until November) and up to seven times larger for groundnut. The ratio is high, but the system is designed for a dry area, which makes crop demand very high. In addition, the water harvesting option is not seen as a replacement for irrigation; it is meant to utilize the amount of received rainfall at the Scheme. Therefore, the CA:CU ratio can be changed based on the volume of water intended to be conserved. In conclusion, the possibility of accounting for rainfall in irrigation is possible. However, further studies should be conducted to ensure the sustainability of the water harvesting concept at the scheme.

6.3.3 Implications of improving irrigation performance on downstream Blue Nile flow

The annual irrigation efficiency of the Gezira Scheme has been decreasing since 1993/94. As a consequence of enhancing the irrigation distribution efficiency and/or accounting for the rainfall in the irrigation schedule, a predicted management scenario, the overall irrigation efficiency of the scheme is expected to be higher. Herein, a quantitative assessment is conducted of the volume of irrigation water that could be saved when the overall irrigation efficiency is enhanced. Analysis of 1990–2010 reveals that if the irrigation efficiency can be improved by only 1%, an average of around 68 million cubic meters per year of water could be saved and allocated for other purposes. Figure 6-6 summarizes changes in the volume of saved irrigation water when overall irrigation efficiency reaches 75%, for 1990–2010. This level of efficiency is predicted as a possible result from the proposed management scenarios. This could save around 2.6 BCM per year, which can be utilized by other users on the Nile downstream.

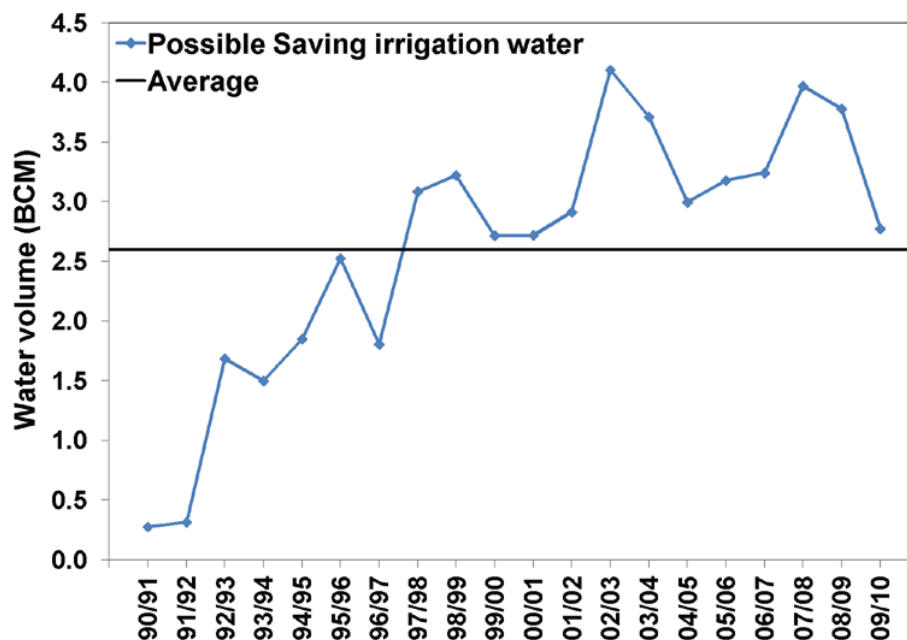


Figure 6-6. Volume of irrigation water that could be saved at an overall irrigation efficiency of 75%

6.4 Conclusions

The conclusions of this chapter are summarized in the following points:

1. Management tools and scenarios such as RS drought monitoring and water harvesting are proposed to tackle the problems (inequity of irrigation distribution and low crop yield) of the Gezira Scheme.
2. The SSEB model is proposed as a water distribution monitoring tool to deal with the inefficiency of the existing irrigation network, especially in the summer crop season, and the wasteful water consumption of the conventional system.
3. Water harvesting is considered as an alternative to traditional conservation strategy solution for water at the Scheme.
4. The implication for downstream flow of the Blue Nile due to increasing irrigation efficiency is also investigated.
5. Monthly monitoring illustrates that the southern, central and southwestern areas are subjected to wet conditions, where water ponds are always found. This confirms that the irrigation channels of these areas have operational problems.
6. For the Gezira channel, the problem is very acute on the flat terrain in the central part, where excess water is just left to flow and spread across the plain. Therefore, water shortage in wide areas is observed at the downstream end of the channel.

7. The Managel channel supplies more water than is demanded, which is explained by the irregular cold areas observed at the tail of the channel. This reveals that the scheme has a poorly maintained or no drainage system at all to return excess water into the river.
8. Around 80 irrigation channels are suspected to have leakage problems for the crop season 2013/14.
9. Water harvesting is potentially applicable in terms of physical analysis. The designed rainfall value is found to be 253 mm, which will be met or exceeded (on average) in two years out of three, and the harvested rain will satisfy CWR for the same time period.
10. The designed CA of the crops must be seven times the size of the cultivated area. The ratio is high; therefore water harvesting could be applied just in accounting for the rainfall for irrigation, not for the full crop supply.
11. If the irrigation efficiency can be improved by only 1%, an average of around 68 million cubic meters of water per year could be saved by the scheme.
12. This level of efficiency (75%) is predicted as a possible result from the proposed management scenarios, which could save around 2.6 BCM per year.
13. All the improvements help optimize water application and opportunities for irrigation, and enable upgraded irrigation scheduling techniques to be applied efficiently.

CHAPTER SEVEN

CONCLUSIONS AND RECOMMENDATIONS

7.1 *Conclusions*

- Many large-scale irrigation schemes worldwide have been facing severe water wastage and have not yielded the expected outcomes. This situation is generally related to a lack of effective evaluation and monitoring tools.
- After reviewing extensive literature, the current research suggests a new methodology for evaluating and monitoring large-scale irrigated areas based on ground-observed and remotely sensed data.
- This study takes the large-scale irrigation of the Gezira Scheme as a case study, as it is the largest scheme in the world under one management.
- Irrigation water management study has been conducted by assessing the irrigation water supply, rainwater supply, crop productivity and water distribution in the Gezira Scheme.
- Inefficient irrigation water supply of the Gezira Scheme has been witnessed since 1993/94. Generally, the winter crop season presents much lower efficiency values than those for the summer crop season.
- The received rainfall is inadequate to fully supply crop water demand, but it could be utilized in July and August to supply part of it. However, the rainfall is not accounted for in irrigation scheduling in the scheme.
- Despite the water availability, the Gezira Scheme has comparatively lower productivity values than those recorded for other irrigation schemes worldwide.
- The well-known VCI, an index derived from NDVI, is modified (MVCI) and applied to the irrigated areas. MVCI reveals poor water distribution, especially during the summer crop season.
- The index has the ability to map the spatial drought by identifying dry and well-irrigated areas, but does not deduct the soil moisture content. Therefore, MVCI cannot be considered alone as a monitoring tool, as water could be wasted and located in other shapes (i.e. water depressions).

- RS ET_a is found to be the best monitoring model. The spatio-temporal information of ET_a is required to better quantify water depletion and establishes links between land use and water allocation.
- Several RS models have been developed for estimating ET_a . Four different models based on the energy balance method – SEBAL, METRIC, SSEB and MOD16ET – are applied to assess the optimal approach of obtaining ET_a and running as a monitoring tool for the scheme.
- Most of the equations used in the SEBAL, METRIC and SSEB models are updated to the current state of the art to give more accurate results.
- Different open-source satellite images such as Landsat and MODIS can be analyzed to obtain spatial ET_a .
- A new methodology is introduced in the current research to comprehensively evaluate the models' performance based on a set of statistical indicators at field and scheme levels.
- Based on ranking criteria, the SSEB and SEBAL models provide ET_a estimates close to the actual measurements.
- METRIC and MOD16 results overestimate and underestimate the measurements, respectively.
- All four models show similar spatial daily patterns of ET over the scheme but differ in terms of absolute values.
- The SSEB model gives the best performance and is selected as the operational monitoring ET_a tool because of its simplicity of processing over large areas.
- Similarly to MSCI distribution, the seasonal ET_a from SSEB is higher in the southern and central parts, and lower in the northern part of the scheme.
- The study proposes a new spatio-temporal evaluation method to investigate the model performance by plotting the ET_a over each pixel respectively against the integrated NDVI (iNDVI).
- When validation data is absent, the ratio of remotely sensed ET_a from agricultural areas (ET_{ag}) to the total ET_a from the scheme (ET_{sum}) (ET_{ag}/ET_{sum}) can be used to conduct long-term assessment. The ratio indicates that water policies in the Gezira Scheme have not had much effect on either agricultural production or water savings. This indicates the water is available but not utilized for agricultural production.

- The study has identified water ponds, indicating that there is water wastage over the scheme, which is considered another reason for the inefficiency.
- iNDVI can be used as an indicator to evaluate water policies in terms of crop productivity: the greater is iNDVI, the higher is production.
- RS drought monitoring and water harvesting can be used as management tools and scenarios for large-scale irrigation systems.
- The SSEB model can be proposed as a water distribution monitoring tool to deal with the inefficiency of the existing irrigation network. The model identifies the channels which have leakage problems. This confirms that the irrigation channels of these areas have operational problems. Such information might be very useful for reducing losses at the scheme.
- Rainwater harvesting is addressed and found to be applicable as an alternative solution for accounting for rainfall in irrigation.
- The study proposes a new methodology to assess, evaluate and monitor large-scale irrigation systems. It shows innovation in identifying the problems of the scheme, as well as proposing management scenarios to enhance irrigation water management practice. Improved agricultural water management in terms of crop, water and land management can increase food production, thereby alleviating poverty and hunger in an environmentally sustainable manner.

7.2 Recommendations

- Despite the FAO Penman–Monteith reference evapotranspiration (ET_o) remaining the most desirable method for computing ET_o , the method should be calculated based on the adjusted parameters for the regional studies. The calculated ET_o values from the updated solar radiation parameter have greater values and are more accurate than those not updated. An accurate determination of ET_o is essential for an accurate computation of crop water demand.
- More meteorological stations are needed to cover the whole Gezira area to better represent actual conditions.
- One of the limitations faced is a lack of validation data at the regional scale. Therefore, further measurements of groundwater level, the volume of the observed water ponds and the amount of drainage water are needed to validate the results. Also, measuring the amount of ET_a by deploying lysimeter devices or eddy covariance towers is also recommended.
- During the rainy months (June–October), it is recommended that the MODIS daily T_s product (MOD11A1) be used rather than the 8-day MODIS T_s product (MOD11A2). Cloud cover is represented by no-data values averaged within the MOD11A2 product, which thus biases ET_a calculations.
- Rainfalls should be harvested and utilized to reduce the need for supplemental irrigation.
- The inequity of the conveyance system could also be an additional factor leading to the low crop productivity of the scheme.
- Further research is required for accurate RS estimation of crop water demand.
- A water policy analysis is required for the lower performance period since the 1990s.
- Rainfall characteristics (intensity and distribution) are important features in applying water harvesting techniques to an area. Therefore, further analysis of daily rainfall should be conducted.
- It is recommended that a socioeconomic analysis be conducted for water harvesting, as it is not considered in the current research.
- A social study is needed to assess the effect of inefficient irrigation performance on farmers and livestock population.
- It is recommended that the intended methodology be followed to improve irrigation water management in the scheme by increasing overall irrigation efficiency.

- Most of the equations in the SEBAL and METRIC algorithms are developed for different climates. Calibration of these equations is necessary.
- Using more high-spatial-resolution images per crop season will lead to more accurate results when downscaling.
- Higher-spatial-resolution images (i.e. Advanced Spaceborne Thermal Emission and Reflection Radiometer (ASTER) or Landsat images) are needed for studying small agricultural fields.
- Economic analysis using different indicators is still needed to investigate crop productivity.
- There is an urgent need to develop adequate irrigation water monitoring facilities on a regular and long-term basis, and to increase field investigation in order to ensure effective applications of emerging RS and GIS technologies for sustainable development and management.
- Further study is recommended to monitor soil moisture by using active and passive microwave techniques.
- It is always reported that the Gezira Scheme has no salt problem, and that as a result there is no leaching water requirement. It is doubtful that an 80-year-old irrigation has no salinity problem. Therefore, it is recommended that a field test for salinity be conducted in different places over the scheme.

REFERENCES

- Abdelhadi, A.W., Adam, H.S., Hassan, M.A., Hata, T., 2004. Participatory management: Would it be a turning point in the history of the Gezira scheme?. *Irrigation and Drainage*, 53(4), 429-436.
- Abdelhadi, A.W., Bashir, M.A., Farah, S.M., Hata, T., 2006. Implication of Late Sown Irrigated Sorghum on Productivity and Water Management. *Sudan Journal of Agriculture Research* 6, 1-10
- Abdelhadi, A.W., Hata, T., Tanakamaru, H., Tada, A., Tariq, M.A., 2000. Estimation of crop water requirements in arid region using Penman–Monteith equation with derived crop coefficients: a case study on Acala cotton in Sudan Gezira irrigated scheme. *Agricultural Water Management* 45(2), 203-214
- Abdo, G., Salih, A., 2012. Challenges facing groundwater management in Sudan. *Global Advanced Research Journal of Physical and Applied Sciences (GARJPAS)*.1(1), 01-11.
- Achamyeleh, K., 1993. Problems and prospects for intercountry cooperation for integrated water resources development of the Nile River Basin. United Nations, Economic Commission for Africa.
- Adam, H.S., Abdelhadi, A.W., Hata, T., 2002. Promotion of participatory water management in the Gezira Scheme in Sudan. In *Irrigation Advisory Services and Participatory Extension in Irrigation Management*, Workshop Organized by FAO-ICID, 18th Congress on Irrigation and Drainage (pp.21-28).
- Adam, H., 2008. *Agroclimatology: Crop water requirement water management*. Gezira Printing Publishing Co.LTD. Wad Medani, Sudan.
- Adeeb, A.M., 2006. Water productivity of food crops in Gezira Scheme, Sudan. In: *International Conference on Environmentally Sound Technology in Water Resources Management*. Gaborone, Botswana.11-13 September 2006. IASTED- Canada, pp 502-802.
- Agam, N., Kustas, W.P., Anderson, M.C., Li, F., Colaizzi, P.D., 2008. Utility of thermal image sharpening for monitoring field-scale evapotranspiration over rainfed and irrigated agricultural regions, *Geophysical Research Letters*,35, L02402.
- Ahmed, A.A., 2009. Gezira Scheme irrigation system performance after 80 years of operation. In: *International Conference on Water, Environment, Energy and Society*, 12-16 Jan.2009, New Delhi, India.

- Ahmed, A.A., Ismail, U.H.E.A., 2008. Sediment in the Nile River system. Consultancy Study requested by UNESCO. Accessed on 14 3. 2014, From: http://www.irtces.org/isi/isi_document/sediment%20in%20the%20nile%20river%20system.pdf
- Ahmed, B.M., Tanakamaru, H., Tada, A., 2010. Application of Remote Sensing for Estimating Crop Water Requirements, Yield and Water Productivity of Wheat in the Gezira Scheme. *International Journal of Remote Sensing* 31(16), 4281-4294
- Ahmed, M.S., Ribbe, L., 2011. Analysis of water footprints of rainfed and irrigated crops in Sudan. *Journal of Natural Resources and Development*, 03, 20–28
- Ahmed, S.H., Abdelhadi, A.W., Elhadi M.A., Adam, H.S., 2007. Water requirements of the main crops in the Gezira Scheme. *Sudan Journal of Agricultural Research* Vol.9, PP.67-89
- Al-Adamat, R., Diabat, A., Shatnawi, G., 2010. Combining GIS with multicriteria decision making for siting water harvesting ponds in Northern Jordan. *Journal of Arid Environments*, 74(11), 1471–1477.
- Alexandridis, T.K., Cherif, I., Chemin, Y., Silleos, G.N., Stavrinou, E., Zalidis, G.C., 2009. Integrated Methodology for Estimating Water Use in Mediterranean Agricultural Areas. *Remote Sensing*, 1, 445–465
- Allen, R.G., 1996. Assessing integrity of weather data for reference evapotranspiration estimation. *Journal of Irrigation and Drainage Engineering*, 122(2), 97-106.
- Allen R.G., Tasumi, M., Trezza R., 2007a. Satellite-based energy balance for mapping evapotranspiration with internalized calibration (METRIC) – model. *Journal of Irrigation and Drainage Engineering*, ASCE 133: 380–394
- Allen, R.G., Rohison, C.W., Ricardo, T., Magali, G., Jeppe, K., 2008. Comparison of Evapotranspiration Images From MODIS and Landsat Along The Middle Rio Grande Of New Mexico. In Pecora 17-The Future of Land imaging...Going Operational (p.11). Denver, Colorado. November 18 - 20, 2008.
- Allen, R.G., Tasumi, M., Trezza, R., Waters, R., Bastiaanssen, W., 2002. SEBAL (Surface Energy Balance Algorithms for Land). Advance Training and User's Manual–Idaho Implementation, version, 1.
- Allen, R., Irmak, A., Trezza, R., Hendrickx, J.M.H., Bastiaanssen, W., Kjaersgaard, J., 2011. Satellite-based ET estimation in agriculture using SEBAL and METRIC. *HYDROLOGICAL PROCESSES*, 4027, 4011–4027 John Wiley & Sons, Ltd.

- Allen, R.G, Tasumi M, Morse A, Trezza R, Wright JL, Bastiaanssen, W., Kramber, W., Lorite I, Robison C., 2007b. Satellite-based energy balance for mapping evapotranspiration with internalized calibration (METRIC) – applications. *Journal of Irrigation and Drainage Engineering*, ASCE 133: 395–406.
- Allen, R.G., 2000. REF-ET: Reference evapotranspiration Calculation Software, University of Idaho, Moscow, Idaho.
- Allen, R.G., Morse, A., Tasumi, M., 2003. Application of SEBAL for western US water rights regulation and planning. *International Workshop on Remote Sensing of evapotranspiration for Large Regions. IEC Meeting of International Commission on Irrigation and Drainage (ICID) Proceedings*, p.54
- Allen, R.G., Pereira, L.A., Raes, D., Smith, M., 1998 *Crop evapotranspiration*. FAO Irrigation and Drainage Paper 56. FAO, Rome, Italy, 293 pp.
- Allen, R.G., Tasumi, M., Morse, A., Trezza, R., 2005. A Landsat-based energy balance and evapotranspiration model in Western US water rights regulation and planning. *Irrigation and Drainage Systems* 19, 251–268
- Anyamba, A., Tucker, C.J., 2005. Analysis of Sahelian vegetation dynamics using NOAA-AVHRR NDVI data from 1981–2003. *Journal of Arid Environments* 63(3), 596-614
- Bandara, K.M.P., 2003. Monitoring irrigation performance in Sri Lanka with high-frequency satellite measurements during the dry season. *Agricultural Water Management* 58(2), 159–170
- Bashir M.A., T.Hata, A.Tada, H.Tanakamaru, Abdelhadi A.W., 2007a. Estimating actual evapotranspiration using Surface Energy Balance Algorithm for Land (SEBAL) for Gezira scheme. Part I: Determination and calculation of intermediate parameters. *Sudan Journal of Agricultural Research* 8, 65-76.
- Bashir, M.A., Hata, T., Tanakamaru, H., Abdelhadi, A.W., Tada, A., 2007c. Remote Sensing Derived Crop Coefficient for Estimating Crop Water Requirements for Irrigated Sorghum in the Gezira Scheme, Sudan. *Journal of Environmental Informatics*, 10(1), 47–54
- Bashir, M.A., Hata, T., Tanakamaru, H., Abdelhadi, A.W., Tada, A., 2008. Satellite-based energy balance model to estimate seasonal evapotranspiration for irrigated sorghum: a case study from the Gezira scheme, Sudan. *Hydrology & Earth System Sciences* 12(4).
- Bashir, M.A., Tada, A., Tanakamaru, H., 2009b. Remote Sensing For Diagnosing Actual Depletion and Water Use Efficiency. *Thirteenth International Water Technology Conference, IWTC 13, Hurgada, Egypt*, 1145-1157

- Bashir, M.A., Tanakamaru, H., Tada, A.2009a. Remote sensing-based estimates of evapotranspiration for managing scarce water resources in the Gezira scheme, Sudan. From Headwaters to the Ocean: Hydrological Change and Water Management-Hydrochange 2008, 1-3 October 2008, Kyoto, Japan, 38 1. Taylor & Francis Group, London, ISBN 978-0-415-47279- 1.
- Bashir, M.A., Tanakamaru, H., Tada, A.2009c. Spatial and Temporal Analysis of Evapotranspiration Using Satellite Remote Sensing Data: A Case Study in the Gezira Scheme, Sudan. *Journal of Environmental Informatics*, 13(2), 86-92.
- Bashir, M.A., Hata, T., Tada, A., Tanakamaru, H., Abdelhadi, A.W., 2007b. Estimating actual evapotranspiration using Surface Energy Balance Algorithm for Land (SEBAL) for Gezira scheme. Part II: Application and validation. *Sudan journal of agriculture research* 8, 77-87
- Bastiaanssen, W.G.M., 2000. SEBAL-based sensible and latent heat fluxes in the irrigated Gediz Basin, Turkey. *Journal of hydrology*, 229(1), 87-100
- Bastiaanssen, W.G.M., Menenti, M., Feddes, R.A., Holtslag, A.A.M., 1998a. A Remote Sensing Surface Energy Balance Algorithm for land (SEBAL): 1. Formulation. *Journal of Hydrology* 212-213, 198-212.
- Bastiaanssen, W.G.M., Pelgrum, H., Wang, J., Ma, Y., Moreno, J.F., 1998b. A remote sensing surface energy balance algorithm for land (SEBAL) 2. Validation. *Journal of Hydrology*, 212-213, 213–229
- Bastiaanssen, W.G.M., Noordman, E.J.M., Pelgrum, H., Davids, G., Thoreson, B.P., Allen, R.G., 2005. SEBAL model with remotely sensed data to improve water-resources management under actual field conditions. *Journal of Irrigation and Drainage Engineering* 131(1), 85-93.
- Bastiaanssen, W., Perry, C., 2009. Agricultural Water Use and Water Productivity in the Large Scale Irrigation (LSI) Schemes of the Nile Basin. Final Report, Nile Basin Initiative (NBI).
- Bastiaanssen, W.G., Bos, M.G., Souza, R.A., Cavalcanti, E.B., Bakker, M.M., 2001. Low cost satellite data for monthly irrigation performance monitoring: benchmarks from Nilo Coelho, Brazil. *Irrigation and Drainage Systems* 15, 53–79
- Ben Mechlia, N., Oweis, T., Masmoudi, M., Khatteli, H., Ouessar, M., Sghaier, N., Anane, M., Sghaier, M., 2009. Assessment of supplemental irrigation and water harvesting potential: methodologies and case studies from Tunisia. ICARDA, Aleppo, Syria. 36 pp.

- Biazin, B., Sterk, G., Temesgen, M., Abdulkedir, A., Stroosnijder, L., 2012. Rainwater harvesting and management in rainfed agricultural systems in sub-Saharan Africa – A review. *Physics and Chemistry of the Earth*, 47-48, 139–151.
- Biswas, A.K., 1984. Monitoring and evaluation of an irrigation system. *International Journal of Water Resources Development*, Vol 2: No1, pp 3-2
- Block, P., Strzepek, K., 2010. Economic analysis of large-scale upstream river basin development on the Blue Nile in Ethiopia considering transient conditions, climate variability, and climate change. *Journal of Water Resources Planning and Management*, 136 (2), 156–166.
- Block, P., Strzepek, K., Rajagopalan, B., 2007. Integrated management of the Blue Nile basin in Ethiopia: hydropower and irrigation modeling. IFPRI Discussion Paper 00700 Washington DC: International Food Policy Research Institute.
- Borgia, C., Marina, G.-B., Mateos, L., 2012. Patterns of variability in large-scale irrigation schemes in Mauritania. *Agricultural Water Management*, 112, 1–12.
- Bos and Clemmens, 1990. Statistical methods for irrigation system water delivery performance evaluation. *Irrigation and Drainage Systems* 4: 345-365
- Bos, M.G., Nugteren, J., 1990. On irrigation efficiencies. 4th edition. Wageningen, The Netherlands: International Institute for Land Reclamation and Improvement.
- Brouwer, C., Hoevenaars, J.P.M., Van Bosch, B.E., Hatcho, N., Heibloem, M., 1992. Irrigation Water Management Training Manual no.6-Scheme Irrigation Water Needs and Supply. FAO Land and Water Development Division, UN.
- Bushara, M.O., Barakat, H.E., 2010. Decomposing Total Factor Productivity Change of Cotton Cultivars (Barakat-90 and Barac (67) B) in the Gezira Scheme (1991–2007) Sudan. In 2010 AAAE Third Conference/AEASA 48th Conference, September 19-23, 2010, Cape Town, South Africa (No.96648). African Association of Agricultural Economists (AAAE) & Agricultural Economics Association of South Africa (AEASA).
- Carlson, T.N., Ripley, D.A., 1997. On the relation between NDVI, fractional vegetation cover, and leaf area index. *Remote sensing of Environment*, 62(3), 241-252.
- Chen, Z., 2005. Overview of large irrigation systems in Southeast Asia. In: Chen, 2007. The future of large rice-based irrigation systems in Southeast Asia. Proceedings of the Regional Workshop on the Future of Large Rice-Based Irrigation Systems in Southeast Asia. Viet Nam, Oct.26-28 Food and Agriculture Organization (FAO) of the United Nations.

- Chen, J., Zhu, X., Vogelmann, J.E., Gao, F., Jin, S., 2011. A simple and effective method for filling gaps in Landsat ETM+ SLC-off images. *Remote Sensing of Environment*, 115(4), 1053-1064
- Chen, Y., Xia, J., Liang, S., Feng, J., Fisher, J.B., Li, X., ...Yuan, W., 2014. Comparison of satellite-based evapotranspiration models over terrestrial ecosystems in China. *Remote Sensing of Environment*, 140, 279-293.
- Clemmens, A.J., Bos, M.G., 1990. Statistical methods for irrigation system water delivery performance evaluation. *Irrigation and Drainage Systems* 4(4), 345–365
- Critchley, W., Scheierling, S.M, 2013. Chapter 2: Water harvesting for crop production in Sub-Saharan Africa Challenges, concepts and practices. In Critchley, W., Gowing, J. (Eds): *Water Harvesting in Sub-Saharan Africa*. Routledge publisher, 711 Third Avenue, New York, NY 1001, USA. Routledge is an imprint of the Taylor & Francis Group.
- Critchley, W., Siegert K., Chapman, C., 1991. *Water harvesting, A Manual for the Design and Construction of Water Harvesting Schemes for Plant Production*. Food and Agriculture Organization (FAO) of the United Nations, Rome, FAO.
- Doorenbos, J., Kassam, A.H., 1979. *Yield response to water*.FAO Irrigation and Drainage Paper No.33. Food and Agriculture Organization of the United Nations (FAO), Rome.
- Duchemin, B., R., Hadria, S.Erraki, Gilles Boulet, Philippe Maisongrande, Abdelghani Chehbouni, Richard Escadafal et al., 2006. Monitoring wheat phenology and irrigation in Central Morocco: On the use of relationships between evapotranspiration, crops coefficients, leaf area index and remotely-sensed vegetation indices. *Agricultural Water Management* 79, 1-27
- Eaglin, R.Eaglin, L., Wanielista, M., 1996. *SMADA: Stormwater management and design aid user's manual*.Retrieved on October 17, 2013 and available from: <http://ucf-rainfall.pbworks.com/SMADA-Documentation>
- El Tahir, M.E.H., Wenzhong, W., Xu, C.Y., Youjing, Z., Singh, V.P., 2012. Comparison of Methods for Estimation of Regional Actual Evapotranspiration. In *Data Scarce Regions: Blue Nile Region, Eastern Sudan*. ASCE Journal of Hydrologic Engineering, 17(4), 578-589
- Elagib, N.A., 2009. Improved Ångström coefficients for estimating incoming radiation across Sudan. *Sudan Engineering Society Journal* 55(52), 59–70

- Elagib, N.A., 2010. Trends in intra-and inter-annual temperature variabilities across Sudan. *Ambio* 39(5-6), 413-429
- Elagib, N.A., Alvi, S.H., Mansell, M.G., 1999. Day-length and extraterrestrial radiation for Sudan: a comparative study. *International Journal of Solar Energy* 20(2), 93–109
- Elagib, N.A., Mansell, M.G., 2000a. Recent trends and anomalies in mean seasonal and annual temperatures over Sudan. *Journal of Arid Environments*, 45(3), 263-288
- Elagib, N.A., Mansell, M.G., 2000b. Climate impacts of environmental degradation in Sudan. *GeoJournal* 50(4), 311–327
- Elamin, M., Ellatif, A., Abdelaziz, H.H., 2011. Analysis of agricultural production instability in the Gezira scheme. *Journal of the Saudi Society of Agricultural Sciences* 10(2), 53–58
- Eldaw, A.M., 2004. The Gezira Scheme: perspectives for sustainable development. Reports and Working Papers 2/2004, German Development Institute Tulpenfeld 4 · D-53113 Bonn.
- ESRI, 2013. ArcGIS 9 2-10, California, USA. Retrieved on October 24, 2013 and available from: <http://www.esri.com/software/arcgis/index.html>
- Evapotranspiration, P., 2011a. Completion report on the production of evapotranspiration maps for year 2004 for the Upper Klamath and Sprague area of Oregon using Landsat Images and the METRIC model: Twin Falls, Idaho, March 2011, Revised March 28, 2011, 55 p., accessed June 27, 2013, at http://water.usgs.gov/GIS/dsdl/Report_KBRA_OPWP_ET_2004_ETplus.pdf.
- Evapotranspiration, P., 2011b. Completion report on the production of evapotranspiration maps for year 2006, Landsat path 45 covering the Upper Klamath and Sprague area of Oregon using Landsat Images and the METRIC model: Twin Falls, Idaho, May 2011, 64 p., accessed June 27, 2013, at http://water.usgs.gov/GIS/dsdl/Report_KBRA_OPWP_ET_2006_ETplus.pdf
- FAO, 1996. Irrigation Scheduling: From theory to practice – Proceedings. Water reports 8 Proceedings of the ICID/FAO Workshop on Irrigation Scheduling, Rome, Italy, 12-13 September 1995 Food and Agriculture Organization (FAO) of the United Nations, Rome.
- FAO, 1997 Irrigation potential in Africa: A basin approach. Food and Agriculture Organization (FAO) of the United Nations, Rome.

- FAO, 2002. Crops and Drops - making the best use of water for agriculture. Food and Agriculture Organization (FAO) of the United Nations, Rome.
- FAO, 2003. Agriculture, food and water. A contribution to the World Water Development Report. The Food and Agriculture Organization of the United Nations (FAO).Rome, Italy.
- FAO, 2009. Wheat production potential in Sudan. Food and Agriculture Organization (FAO) of the United Nations, Rome. Retrieved on October 19, 2013 and available from: <http://www.fao.org/ag/AGP/AGPC/doc/field/Wheat/africa/sudan/sudanagec.htm>
- FAO, 2011. Farming systems report synthesis of the country reports at the level of the Nile Basin. Food and Agriculture Organization (FAO) of the United Nations, Rome. Retrieved on October 1, 2013 and available from: <http://www.fao.org/nr/water/faonile/>
- Farbrother, H.G., 1996. Water management options in the Sudan Gezira: A review. Chatham, UK: Natural Resources Institute. ISBN: 0-85954-450-8
- Fereres E, Connor DJ., 2004. Sustainable water management in agriculture. In: Cabrera E, Cobacho R, eds. Challenges of the new water policies for the XXI century. Lisse, The Netherlands: A.A. Balkema, 157–170
- Fereres, E., and Soriano, M.A., 2007. Deficit irrigation for reducing agricultural water use. *Journal of Experimental Botany*, Vol.58, No.2, pp.147–159, 2007 Integrated Approaches to Sustain and Improve Plant Production under Drought Stress Special Issue.
- Foerster, S., Kaden, K., Foerster, M., Itzerott, S., 2012. Crop type mapping using spectral–temporal profiles and phenological information. *Computers and Electronics in Agriculture* 89, 30–40
- Folhes, M.T., Renno, C.D., Soares, J.V., 2009. Remote sensing for irrigation water management in the semi-arid Northeast of Brazil. *Agricultural Water Management* 96, 1398–1408
- Fraiture, C.D., Wichelns, D., 2010. Satisfying future water demands for agriculture. *Agricultural Water Management*, 97, 502–511.
- Gleick, P.H., 2000 A look at twenty-first century water resources development. *Water International*, 25(1), 127-138
- Gillies, R.R., Kustas, W.P., Humes, K.S., 1997. A verification of the 'triangle' method for obtaining surface soil water content and energy fluxes from remote measurements of the Normalized Difference Vegetation Index (NDVI) and surface. *International Journal of Remote Sensing*, 18(15), 3145-3166.

- Godfray, H.C.J., Beddington, J.R., Crute, I.R., Haddad, L., Lawrence, D., Muir, J.F., Pretty, J., Robinson, S., Thomas, S.M., Toulmin, C., 2010. Food security: the challenge of feeding 9 billion people. *Science*, 327(5967), 812-818
- Gowda, P.H., Chavez, J.L., Colaizzi, P.D., Evett, S.R., Howell, T.A., Tolk, J.A., 2008. ET mapping for agricultural water management: present status and challenges. *Irrigation science*, 26(3), 223-237
- Guariso, G., and Whittington, D., 1987. Implications of Ethiopian water development for Egypt and Sudan. *International Journal of Water Resources Development*, 3(2), 105-114
- Guvele, C.A., 2001. Gains from crop diversification in the Sudan Gezira scheme. *Agricultural Systems* 70(1), 319–333.
- Hamid, S.H., Mohamed, A.A., Mohamed, Y.A., 2011. Towards a performance-oriented management for large-scale irrigation systems: case study, Rahad scheme, Sudan. *Irrigation and Drainage* 60: 20-34
- Hargreaves, G., 1975 Moisture availability and crop production. The Structures and Environment Division of ASAE, (No.74-4010), 980–984
- Hill, M.J., Donald, G.E., 2003. Estimating spatio-temporal patterns of agricultural productivity in fragmented landscapes using AVHRR NDVI time series. *Remote Sensing of Environment* 84, 367–384
- Ian, R., 2012. Quasi crop and food supply assessment mission to Sudan. Food and Agriculture Organization (FAO) of the United Nations, Rome.
- Ibrahim, A.A., Stigter, C., Adam, H.S., Adeeb, A.M., 2002. Water-use efficiency of sorghum and groundnut under traditional and current irrigation in the Gezira Scheme, Sudan. *Irrigation Science* 21(3), 115–125
- Immerzeel, W.W., Droogers, P., Gaur, A., 2007. Remotely Sensed Based Hydrological Model Calibration for Basin Scale Water Resources Planning (p.192).Wageningen. Retrieved from www.futurewater.nl
- Immerzeel, W.W., Droogers, P., Gieske, A., 2006. Remote Sensing and Evapotranspiration Mapping: State of the Art (p.39).Wageningen, Netherlands.
- IWMI, WorldFish, ILRI, NBI, 2009. The Nile Basin Focal Project, CPWF Project Number 59 Report.
- Karimi, P., Molden, D., Notenbaert, A., Peden, D., 2013. Nile Basin farming systems and productivity. In: Awulachew, S.B., Molden, D., Smakhtin, V., Peden, D., (Eds.), 2013.

- The Nile River Basin: Water, Agriculture, Governance and Livelihoods. Routledge. ISBN-13: 978-1849712835
- Kim, H.W., Hwang, K., Mu, Q., Lee, S.O., Choi, M., 2012. Validation of MODIS 16 global terrestrial evapotranspiration products in various climates and land cover types in Asia. *Korean Society of Civil Engineers (KSCE)*. 16(2), 229-238
- Kiziloglu, F.M., Sahin, U., Kuslu, Y., Tunc, T., 2009. Determining water – yield relationship, water use efficiency, crop and pan coefficients for silage maize in a semiarid region. *Irrigation Science* 27, 129–137
- Kloezen, W.H., Garcés-Restrepo, C., 1998. Assessing irrigation performance with comparative indicators: The case of the Alto Rio Lerma Irrigation District, Mexico. Research Report 22. Colombo, Sri Lanka: International Water Management Institute (IWMI).
- Kogan, F.N., 1995. Droughts of the late 1980s in the United States as derived from NOAA polar-orbiting satellite data. *Bulletin of the American Meteorological Society* 76(5), 655-668
- Kogan, F.N., 1997. Global drought watch from space. *Bulletin of the American Meteorological Society* 78(4), 621-636.
- KRT, 2014. Responsibilities of the Ministry of Agriculture, Livestock and Irrigation. Khartoum State (KRT). Accessed on 23/4/2014 from: <http://www.krt.gov.sd/agri.php>
- Landsat Handbook, 2007. Landsat 7 Science Data Users Handbook, 2007 URL: http://ltpwww.gsfc.nasa.gov/IAS/handbook/handbook_toc.html, National Aeronautics and Space Administration (last date accessed 10 March 2014).
- Leenhardt, D., Trouvat, J., Gonzalès, G., Pérarnaud, V., Prats, S., Bergez, J.-E., 2004. Estimating irrigation demand for water management on a regional scale I.ADEAUMIS, a simulation platform based on bio-decisional modelling and spatial information. *Agricultural Water Management*, 68, 207–232.
- Li, L., Ying, Z., Feng, Y., Guoqiang, S., 1998. Monitoring drought of Guizhou using remote sensing vegetation index. *Journal of Guizhou Meteorology*, 22, 50–54
- Mahgoub, F. 2014. Current Status of Agriculture and Future Challenges in Sudan. The Nordic Africa Institute Production: Byrå4 Print on demand, Lightning Source UK Ltd. ISBN 978-91-7106-748-7
- Malano, H., Burton, M., 2001. Guidelines for benchmarking performance in the irrigation and drainage sector. Food and Agriculture Organization (FAO) of the United Nations, Rome.

- Martin, T.C., Allen, R.G., Brazil, L.E., Burkhalter, J.P., and Polly, J.S., 2013. Evapotranspiration Estimates from Remote Sensing for Irrigation Water Management (Chapter 13) in J.J., Qu et al.(eds.), *Satellite-based Applications on Climate Change*, DOI 10 1007/978-94-007-5872-8_13, Springer Science+Business Media Dordrecht 2013.
- McCartney, M., Ibrahim, Y.A., Sileshi, Y., Awulachew, S.B., 2009 Application of the Water Evaluation And Planning (WEAP) Model to Simulate Current and Future Water Demand in the Blue Nile. Awulachew, S.B., Erkossa, T., Smakhtin, V., Fernando, A.(Eds): *Improved Water and Land Management in the Ethiopian Highlands: Its Impact on Downstream Stakeholders Dependent on the Blue Nile. Intermediate Results Dissemination Workshop February 5-6, 2009, Addis Ababa, Ethiopia. Organized by International Water Management Institute (IWMI) Sub-regional Office for East Africa and Nile Basin, Addis Ababa, Ethiopia*
- McCartney, M., Alemayehu, T., Easton, Z.M., Awulachew, S.B., 2012. Simulating current and future water resources development in the Blue Nile River Basin. In: Awulachew, S.B.; Smakhtin, V.; Molden, D.and Peden, D., (Eds), *The Nile River Basin: Water, Agriculture, Governance and Livelihoods*, 269 Abingdon, Oxford, UK: Earthscan.
- McCartney, M.P., Girma, M.M., 2012. Evaluating the downstream implications of planned water resource development in the Ethiopian portion of the Blue Nile River, *Water International*, 37:4, 362-379
- Ministry of Irrigation and HEE, 1975 *Control and use of the Nile water of the Sudan*. Printed by KHARTOUM UNIVERSITY PRESS PO 321, Khartoum, The Democratic Republic of the Sudan.
- Mishra, A.K., Singh, V.P., 2010. A Review of Drought Concepts. *Journal of Hydrology* 391, 202–216.
- Mitchell, A., 2014. Reverb the next generation metadata and service discovery tool. Accessed on 14/4/2014 from: <http://reverb.echo.nasa.gov>
- Mohamed, Y.A., Thiruvarudchelvan, T., Mamad, N., Mul, M., Van der Zaag, P., 2011. Assessment of irrigation performance of large irrigation systems using satellite data: the case of the Gezira Scheme, Sudan. *The International Commission on Irrigation and Drainage (ICID) Conference, 15-23 October, Tehran, Iran.*
- Mohammed, M.Y., 2008. Effective rainfall under central Gezira (Sudan) conditions. In: *Third international conference on water resources and arid zones, Riyadh, Saudi- Arabia.*
- Molden, D.J., Gates, T.K., 1990. Performance measures for evaluation of irrigation water delivery systems. *Journal of Irrigation and Drainage Engineering* 116 (6), 804–823.

- Monteith, J.L., 1964. Evaporation and environment. The state and movement of water in living organisms. Symposium of the society of experimental biology, Vol.19 (pp.205–234).Cambridge: Cambridge University Press.
- Moran, M., 2004. Thermal infrared measurement as an indicator of plant ecosystem health. In: Quattrochi, D.A., Luvall, J.C., (Eds): Thermal Remote Sensing in Land Surface Processing. CRC Press.
- Mu, Q., Heinsch, F.A., Zhao, M., Running, S.W., 2007. Development of a global evapotranspiration algorithm based on MODIS and global meteorology data. Remote Sensing of Environment, 111 (4), 519–536.
- Mu, Q., Zhao, M., and Running, S.W., 2011. Improvements to a MODIS global terrestrial evapotranspiration algorithm. Remote Sensing of Environment, 115(8), 1781-1800
- Mutiga, J.K., Su, Z., Woldai, T., 2010. Using satellite remote sensing to assess evapotranspiration: Case study of the upper Ewaso Ng'iro North Basin, Kenya. International Journal of Applied Earth Observation and Geoinformation, 12, 100-108
- Mukhtar, G., 1997. The Gezira Scheme: The Greatest on Earth, Khartoum. MSc Gezira University.
- MWRE, 2014. Ministry of Water Resources and Electricity (MWRE) website. Accessed on 23/4/2014 from: <http://www.wre.gov.sd/index.php/pages/pageDetails/22/About-MED.html>
- Narain, P., Khan, M.A., Singh, G., 2005. Potential for Water Conservation and Harvesting against Drought in Rajasthan, India. Working Paper 104 (Drought Series: Paper 7).Colombo, Sri Lanka: International Water Management Institute (IWMI).
- NASA Land Processes Distributed Active Archive Center (LP DAAC), 2013. Moderate Resolution Imaging Spectroradiometer (MODIS) Land Cover (MCD12Q1), publisher (LP DAAC), Available on-line [<http://reverb.echo.nasa.gov/reverb/>] from Reverb, Andrew Mitchell, U.S.A. Accessed on November 19, 2013.
- NASA, 2013. AMSR-E Data from: <http://wwwghcc.msfc.nasa.gov/AMSR/>
- National Climatic Data Center, 2014. NNDC Climate Data Online. Land-based observations. Accessed on April 20, 2014 from: <http://www7.ncdc.noaa.gov/CDO/cdoselect.cmd>
- NBI, 2012. State of the River Nile Basin Report. Nile Basin Initiative (NBI) Publishing.
- Nehme, C.C., Simões, M., 1999. Spatial decision support system for land assessment. ACMGIS Press New York, USA, ACM 1-58113-235-2/99/0011.

- NTSG, 2015. Numerical Terradynamic Simulation Group. CHCB room 428 • The University of Montana 32 Campus Drive, Missoula, MT 59812
Accessed from: <http://www.ntsug.umt.edu/project/mod16> on 24/06/2015.
- ORNL DAAC, 2011. Oak Ridge National Laboratory Distributed Active Archive Center (ORNL DAAC). MODIS subsetted land products, Collection 5 Available on-line [<http://daac.ornl.gov/MODIS/modis.html>] from ORNL DAAC, Oak Ridge, Tennessee, U.S.A. Accessed on November 18, 2013.
- Oweis, T., Hachum, A., Kijne, J., 1999. Water Harvesting and supplementary irrigation for improved water use efficiency in dry areas. SWIM Paper 7 Colombo Sri Lanka: International Water Management Institute (IWMI).
- Oweis, T., Prinz, D., Hachum, A., 2012. Water Harvesting for Agriculture in the Dry Areas. CRC Press/Balkema P.O.Box 447, 2300 AK Leiden, the Netherlands.
- Panda, S.S., Ames, D.P., Panigrahi, S., 2010. Application of vegetation indices for agricultural crop yield prediction using neural network techniques. *Remote Sensing*, 2(3), 673-696.
- Pelgrum, H., Bastiaanssen, W.G.M., 1996. An Intercomparison of Techniques to Determine the Area-Averaged Latent Heat Flux from Individual in Situ Observations: A remote Sensing Approach Using the European Field Experiment in a Desertification-Threatened Area Data. *Water Resources Research* 32, 2775–2786.
- Pelgrum, H., Miltenburg, I., Cheema, M., Klaasse, A., Bastiaanssen, W., 2010. ETLook a Novel Continental Evapotranspiration Algorithm. *Remote Sensing and Hydrology Symposium*, Jackson Hole, Wyoming, USA. (10875 – 10877).
- Penman, H.L., 1948. Natural evaporation from open water, bare soil and grass. *Proceedings of the Royal Society of London. Series A. Mathematical and Physical Sciences* 193(1032), 120-145
- Petes, L.E., Brown, A.J., Knight, C.R., 2012. Impacts of upstream drought and water withdrawals on the health and survival of downstream estuarine oyster populations. *Ecology and evolution* 2(7), 1712-1724
- Pettorelli, N., Vik, J.O., Mysterud, A., Gaillard, J.M., Tucker, C.J., Stenseth, N.C., 2005 Using the satellite-derived NDVI to assess ecological responses to environmental change. *Trends in Ecology and Evolution* 20(9), 503-510
- Plusquellec, H., 1990. The Gezira Irrigation Scheme in Sudan: Objectives, Design, and Performance (World Bank Technical Report, No.120). Washington, DC.

- Plusquellec, H., 2002. How design, management and policy affect the performance of irrigation projects. Bangkok, Thailand: FAO. Accessed on 27/1/2014 from: <http://www.fao.org/docrep/004/ac799e/ac799e00.htm#Contents>
- Prinz, D., 1996. Water Harvesting: Past and Future. In: Pereira, L.S., (ed.), Sustainability of Irrigated Agriculture. Proceedings, NATO Advanced Research Workshop, Vimeiro, 21-26. 03. 1994, Balkema, Rotterdam, 135-144
- Prinz, D., Singh, A., 2000. Technological Potential for Improvements of Water Harvesting, Prepared for Thematic Review IV.2: Assessment of Irrigation Options. Retrieved on April 15, 2014 from: <http://www.dams.org/docs/kbase/contrib/opt158.pdf>
- Prueger, J.H., Hatfield, J.L., Aase, J.K., Pikul, J.L., 1997. Bowen-ratio comparisons with lysimeter evapotranspiration. *Agronomy journal* 89(5), 730-736.
- Rodionov, S.N., 2004. A sequential algorithm for testing climate regime shifts. *Geophysical Research Letters* 31(9).
- Rosenow, D.T., Quisenberry, J.E., Wendt, C.W., Clark, L.E., 1983. Drought tolerant sorghum and cotton germplasm. *Agricultural Water Management* 7(1), 207-222.
- Roerink, G.J., Su, Z., Menenti, M., 2000. S-SEBI: a simple remote sensing algorithm to estimate the surface energy balance. *Physics and Chemistry of the Earth* 25, 147-157
- Rosenberg, D.M., McCully, P., Pringle, C.M., 2000. Global-scale Environmental Effects of Hydrological Alterations: Introduction. *Bioscience* 50 (9) 746-751.
- Rosegrant, M.W., Cai, X., Cline, S.A., 2002. *World Water and Food to 2025: Dealing With Scarcity*. International Food Policy Research Institute. Washington D.C., USA. ISBN 0-89629-646-6
- Ruhoff, A.L., Paz, A.R., Aragao, L.E.O.C., Mu, Q., Malhi, Y., Collischonn, W., Running, S.W., 2013. Assessment of the MODIS global evapotranspiration algorithm using eddy covariance measurements and hydrological modelling in the Rio Grande basin. *Hydrological Sciences Journal*, 58(8), 1658-1676.
- Sadras, V.O., Grassini, P., Steduto, P., 2010 Status of water use efficiency of main crops. SOLAW Background Thematic Report - TR07 Food and Agriculture Organization (FAO) of the United Nations, Rome.
- Salvador, R., Martínez-Cob, A., Cavero, J., Playán, E., 2011. Seasonal on-farm irrigation performance in the Ebro basin (Spain): Crops and irrigation systems. *Agricultural Water Management* 98(4), 577-587

- Savva, A.P., Frenken, K., 2002. Monitoring the Technical and Financial Performance of an Irrigation Scheme. Irrigation Manual Module 14 Food and Agriculture Organization (FAO).
- Senay, G.B., Budde, M.E., Verdin, J.P., 2011. Enhancing the Simplified Surface Energy Balance (SSEB) approach for estimating landscape ET: Validation with the METRIC model. *Agricultural Water Management*, 98(4), 606–618
- Senay, G.B., Budde, M.E., Verdin, J.P., Rowland, J., 2009. Estimating Actual Evapotranspiration from Irrigated Fields Using a Simplified Surface Energy Balance Approach. In: Thenkabail, P., Turrall, H., Biradar, C., & Lyon, J.G.(Eds.). *Remote sensing of global croplands for food security*. CRC press is an imprint of Taylor & Francis Group, LLC. (317-329).
- Senay, G.B., Budde, M., Verdin, P.J., Melesse, A.M., 2007. A Coupled Remote Sensing and Simplified Surface Energy Balance Approach to Estimate Actual Evapotranspiration from Irrigated Fields. *Sensors*, 7, 979–1000
- Senay, G.B., Stefanie, B., Ramesh, K., Singh, P.H., Gowda, N.M., Velpuri, H.A., James P.V., 2013. Operational Evapotranspiration Mapping Using Remote Sensing and Weather Datasets: A New Parameterization for the SSEB Approach. *Journal of the American Water Resources Association (JAWRA)* 49(3), 577-591.
- Shih, S., 1987 Using crop yield and evapotranspiration relations for regional water requirement estimation. *JAWRA Journal of the American Water Resources* 23 (3), 435–442.
- Singh, R.K., Senay, G.B., Velpuri, N.M., Bohms, S., Scott, R.L., Verdin, J.P., 2014 Actual Evapotranspiration (Water Use) Assessment of the Colorado River Basin at the Landsat Resolution Using the Operational Simplified Surface Energy Balance Model. *Remote Sensing*, 6(1), 233-256.
- Smith, M., Steduto, P., 2012. Yield response to water: the original FAO water production function. In: P. Steduto, T.C. Hsiao, E. Fereres, D. Raes (Eds.), *Crop Yield Response to Water*. FAO Irrigation and Drainage Paper, vol.66 FAO, Rome (2012), pp 505
- Son, N.T., Chen, C.F., Chen, C.R., Chang, L.Y., Minh, V.Q., 2012. Monitoring agricultural drought in the Lower Mekong Basin using MODIS NDVI and land surface temperature data. *International Journal of Applied Earth Observation and Geoinformation*, 18, 417-427
- Stanzel, P., Öze, A., Smakhtin, V., Boelee, E., Droogers, P., 2002. Simulating impacts of irrigation on the hydrology of the Karagan Lagoon in Sri Lanka. Working Paper 44 Colombo, Sri Lanka: International Water Management Institute.

- Stroosnijder, L., Moore, D., Alharbi, A., Argaman, E., Biazin, B., van den Elsen, E., 2012. Improving water use efficiency in drylands. *Current Opinion in Environmental Sustainability* 4(5), 497–506.
- Szilagyi, J., Rundquist, D.C., Gosselin, D.C., Parlange, M.B., 1998. NDVI relationship to monthly evaporation. *Geophysical Research Letters* 25(10), 1753-1756.
- Tang, H. and Li, Z.-L., 2014. *Quantitative Remote Sensing in Thermal Infrared: Theory and Applications*, Springer Remote Sensing/Photogrammetry. Springer-Verlag Berlin Heidelberg.
- Tasumi, M., 2003. Progress in Operational Estimation of Regional Evapotranspiration Using Satellite Imagery. Ph.D. Dissertation. Moscow: University of Idaho.
- Tasumi, M., Trezza, R., Allen, R.G., Wright, J.L., 2005 Operational Aspects Of Satellite-Based Energy Balance Models For Irrigated Crops In The Semi-Arid U.S. *Irrigation and Drainage Systems* 19, 355–376.
- Thiruvarudchelvan, T., 2010 Irrigation Performance of Gezira Scheme in Sudan: Assessment of Irrigation Efficiency using Satellite Data. Master thesis, UNESCO-IHE Institute for Water Education, TU-Delft.
- Trezza, R., 2006. Estimation of Evapotranspiration From Satellite-Based Surface Energy Balance Models For Water Management In The Rio Guarico Irrigation System, Venezuela. In AIP Conference Proceedings.852, 162-169
- UNEP, 2007 Sudan - Post-Conflict Environmental Assessment, Chapter 8: Agriculture and the Environment. By the United Nations Environmental Program (UNEP) available at: http://postconflict.unep.ch/publications/sudan/08_agriculture.pdf, accessed: 19/01/2014
- USGS, 2013a. U.S. Geological Survey Global Visualization Viewer (USGS GloVis).Landsat and other satellite products. Available on-line [<http://glovis.usgs.gov>].Accessed on November 18, 2013.
- USGS, 2013b. Using the USGS Landsat 8 Product. Accessed on 29/1/2014 from: http://landsat.usgs.gov/Landsat8_Using_Product.php
- USGS, 2014 USGS Global Visualization Viewer (GloVis).Accessed on 12/12/2013 from: <http://glovis.usgs.gov/>
- Van Dam, J.C., Malik, R.S., 2003. Water productivity of irrigated crops in Sirsa district, India: Integration of remote sensing, crop and soil models and geographical information systems. Food and Agriculture Organization (FAO) of the United Nations, Rome.

- Van Oel, P.R., Krol, M.S., Hoekstra, A.Y., De Araújo, J.C., 2008. The impact of upstream water abstractions on reservoir yield: the case of the Orós Reservoir in Brazil. *Hydrological sciences journal* 53(4), 857-867
- Velpuri, N.M., Senay, G.B., Singh, R.K., Bohms, S., and Verdin, J.P., 2013. A comprehensive evaluation of two MODIS evapotranspiration products over the conterminous United States: Using point and gridded FLUXNET and water balance ET. *Remote Sensing of Environment* 139, 35-49
- Viala, E., 2008 Water for food, water for life a comprehensive assessment of water management in agriculture. *Irrigation and Drainage Systems* 22(1), 127-129
- Wahaj, R., Maraux, F., Munoz, G., 2007. Actual Crop Water Use in Project Countries: A Synthesis at the Regional Level. Policy Research Working Paper 4288 (p.56). Washington, DC. Retrieved on October 30, 2013 and available from: <http://documents.worldbank.org/curated/en/2007/07/7998373/actual-crop-water-use-project-countries-synthesis-regional-level>
- Wan, Z., Wang, P., Li, X., 2004 Using MODIS land surface temperature and normalized difference vegetation index products for monitoring drought in the southern Great Plains, USA. *International Journal of Remote Sensing* 25(1), 61-72.
- Wardlow, B.D., Egbert, S.L., 2008 Large-area crop mapping using time-series MODIS 250 m NDVI data: An assessment for the US Central Great Plains. *Remote Sensing of Environment* 112(3), 1096-1116.
- Waterwatch, 2014 Waterwatch: an eLEAF company. Retrieved 15 February 2010, from <http://www.waterwatch.nl>
- Wilhite, D.A., 2002. Preparing for drought: a methodology. In: Wilhite, D.A. (Eds), *Drought: a Global Assessment*. Routledge, New York, USA, pp.89–104
- Woldegebriel, E., 2011, Irrigation Management Transfer in the Gezira Scheme, Sudan - A Case Study on Farmers' Operation and Maintenance Strategies in Tuweir Minor Canal, Master Thesis Wageningen University. Accessed on 21/3/2014 from: <http://edepot.wur.nl/167523>
- World Bank, 2010 Sudan - The World Bank and the Gezira scheme in the Sudan: political economy of irrigation reforms. Working Paper No.69873. Washington, DC: World Bank. From: <http://documents.worldbank.org/curated/en/2010/06/16371308/sudan-world-bank-gezira-scheme-sudan-political-economy-irrigation-reforms>

- Wu, J., Zhou, L., Liu, M., Zhang, J., Leng, S., Diao, C., 2013. Establishing and assessing the Integrated Surface Drought Index (ISDI) for agricultural drought monitoring in mid-eastern China. *International Journal of Applied Earth Observations and Geoinformation*, 23, 397–410
- Yang, Y., Shang, S., Jiang, L., 2012. Remote sensing temporal and spatial patterns of evapotranspiration and the responses to water management in a large irrigation district of North China. *Agricultural and forest meteorology*, 164, 112-122.
- Yilmaz, M.T., Anderson, M.C., Zaitchik, B., Hain, C.R., Crow, W.T., Ozdogan, M., Chun, J.A., Evans, J., 2014. Comparison of prognostic and diagnostic surface flux modeling approaches over the Nile River basin. *Water Resources Research* 50(1), 386-408.
- Zhang, X., Chen, S., Sun, H., Shao, L., Wang, Y., 2011. Changes in evapotranspiration over irrigated winter wheat and maize in North China Plain over three decades. *Agricultural Water Management* 98(6), 1097–1104
- Zwart, S.J., Bastiaanssen, W.G., 2007. SEBAL for detecting spatial variation of water productivity and scope for improvement in eight irrigated wheat systems. *Agricultural Water Management* 89(3), 287-296.
- Zwart, S.J., Bastiaanssen, W.G.M., 2004. Review of measured crop water productivity values for irrigated wheat, rice, cotton and maize. *Agricultural Water Management* 69(2), 115–133.

APPENDIX ONE

FIELD VISIT

A.1.1 Visiting locations and crop pattern

Two field visits were conducted in 2011/2012 and 2012/2013 seasons. A total of 1343 ground-truth points were obtained from the field survey as shown in Figure A.1-1. It was proposed reaching uniformly distributed points over the entire Gezira region. Due to resources and time limitation, it would not be possible to visit all planned ground-truth locations. Besides, the collected 1343 points were not in good distribution to perform crop classification for all Gezira Scheme. Thus, crop classification for the whole Gezira is not taking in this research. However, the conducted field visits were very useful for better understanding the situation of the scheme.

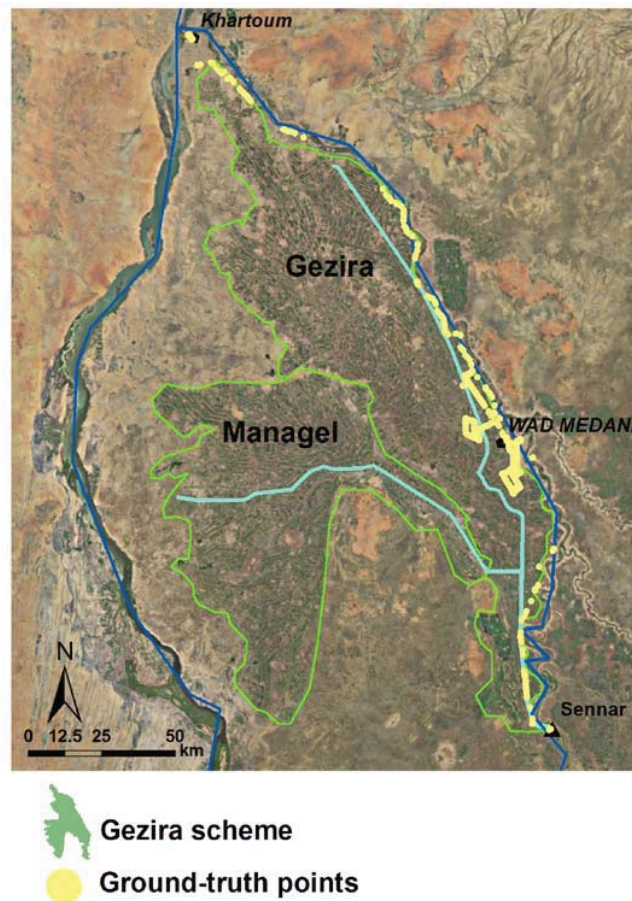


Figure A.1-1. Location of the 1343 points of observed points

The stay was mainly in Wad Medani city, where the management authorities are located, i.e. Sudan Gezira Board. Therefore, further field observations were conducted in two blocks (Muslmya and Wassat). In general 10 to 20 visits were conducting for each block for the two seasons. At each block, several fields, ranging from 10 to 150, were identified on the images as well as other land cover classes. Figure A.1-2 gives an example of the sites visited and the observed crop patterns.

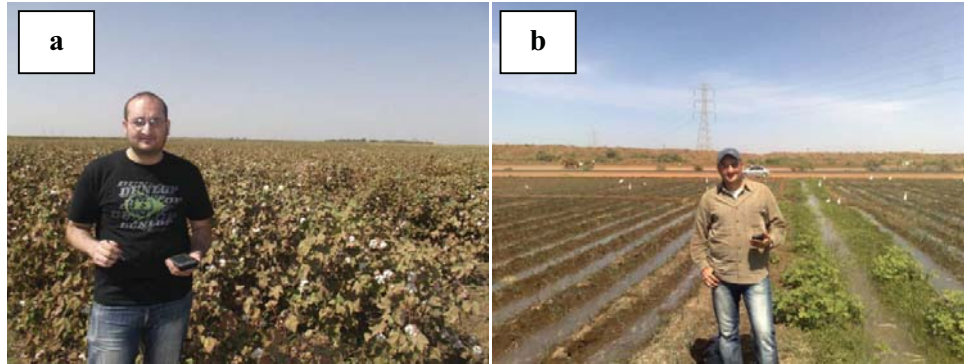


Figure A.1-2. Two different fields observed during the field visits; a) Cotton in 2011/2012 and b) irrigated wheat in 2012/2013

During the field visits, it became clear that there is a typical growing season for each crop. For the summer crop season, cotton, sorghum and groundnuts shared the same season but in different growth stages. Besides, there was difference in crop growing stage due to delay in sowing date. During the winter crop season wheat, cotton and sunflower were found. All information collected in the field was digitized. To navigate through the field a Geotac pocket PC with GPS and ArcMap built in was used. It was very useful as it had the ability to store the satellite images and create shapefile with the observed data. This allowed for real time navigation in the field without the need of accurate topographical maps on sometimes very small field tracks.

A.1.2 Irrigation system

Starting with the inlet point, a visit was conducted to Sennar dam. Interviews with the working engineers have been conducted to understand the method of measuring discharge. In addition, daily data discharge data for recent years were obtained as it was not available at the Ministry of Irrigation in Khartoum.



Figure A.1-3. Sennar dam (a and b) and Gezira irrigation channel (main channel: c and record station: d)

The irrigation system has many hydraulic structures (i.e. barrages, weirs ... etc) to control the flow. However, it is observed that these structures are very old and there is a lack of maintenance. As can be seen from Figure A.1-4, one of the gates of minor channel are controlled by wood sheet, which is inefficient for stopping the water.



Figure A.1-4. Basatna barrage (a) and the outlet is controlled by wood sheet (b)

The weeds problem was also observed during the field visit, Figure A.1-5. The weeds covered one of the irrigation channels which are considered a problem of conveying the water

through the system. As a result, farmers intend to use pumps to irrigate their crops. However, there was an observation of removing the weeds and sediment from one of the minor channel.



Figure A.1-5. Minor channel covered by weeds (a), farmers start using pump for irrigation (c) and the removal process (b)

A.1.3 Collected data

1. Historical daily and mean monthly climatic elements (maximum and minimum temperatures, wind speed, sunshine hours and rainfall) for the period 1961-2012 are collected from Sudan Meteorological Authority in Khartoum.
2. Actual water supply data are obtained as irrigation discharge for the main channels (Gezira and Managel) from the former Ministry of Irrigation and Water Resource office in Wad Medani.
3. Crop yield data and cultivated areas with crop calendar for cotton, groundnut, wheat, sorghum and vegetables for the period 1970 -2010 are acquired from the former Ministry of Agriculture in Khartoum.
4. Other data were collected during the discussion with the irrigation and agricultural engineers and farmers during the field visit as shown in Figure A.1-6.



Figure A.1-6. Discussion and obtaining valuable information from irrigation engineers and farmers

APPENDIX TWO

OBTAINED AND ANALYZED DATA

A.2.1 Seasonal crop evapotranspiration (ET_c)

Table A.2-1. Seasonal crop Evapotranspiration in mm for the main crops

Year	Groundnuts	Sorghum	Cotton	Wheat	Year	Groundnuts	Sorghum	Cotton	Wheat
1961	904	770	1331	654	2005	992	854	1450	727
1962	812	706	1240	641	2006	957	819	1376	661
1963	862	748	1248	612	2007	900	756	1338	659
1964	883	749	1322	672	2008	978	849	1373	648
1965	907	782	1321	654	2009	976	823	1448	711
1966	962	839	1404	695	2010	980	833	-	-
1967	905	783	1325	651					
1968	918	807	1283	608					
1969	942	836	1250	565					
1970	927	805	1318	637					
1971	913	796	1222	550					
1972	968	844	1375	664					
1973	971	844	1324	619					
1974	936	813	1322	635					
1975	896	773	1274	616					
1976	934	820	1310	641					
1977	966	837	1371	652					
1978	924	794	1339	652					
1979	965	834	1385	669					
1980	970	836	1400	683					
1981	968	843	1339	626					
1982	954	826	1387	681					
1983	1040	900	1477	715					
1984	1064	934	1427	657					
1985	940	829	1278	598					
1986	980	858	1424	708					
1987	1034	898	1473	716					
1988	948	821	1341	633					
1989	1003	888	1383	651					
1990	1141	1015	1455	631					
1991	1029	901	1376	620					
1992	921	807	1216	546					
1993	1003	865	1393	643					
1994	896	760	1256	585					
1995	885	760	1220	551					
1996	954	835	1278	583					
1997	874	743	1299	642					
1998	868	747	1271	658					
1999	768	653	1155	593					
2000	933	816	1251	608					
2001	983	861	1312	577					
2002	921	804	1215	556					
2003	963	816	1373	650					
2004	1052	911	1466	684					

A.2.2 Monthly probability analysis for Wad Medani station

Table A.2-2. Monthly dependable rainfall analysis (1961-2010)

Month	Propabilty	Return period (year)	Rain (mm)	Std. (mm)
June	0.01	100.0	83.3	14.4
	0.02	50.0	74.0	11.0
	0.04	25.0	64.5	8.1
	0.10	10.0	51.1	5.2
	0.20	5.0	40.0	4.0
	0.50	2.0	22.2	3.1
	0.75	1.3	10.6	2.6
July	0.01	100.0	297.0	67.6
	0.02	50.0	259.4	48.0
	0.04	25.0	222.3	32.3
	0.10	10.0	173.4	18.7
	0.20	5.0	135.4	14.4
	0.50	2.0	79.7	10.6
	0.75	1.3	47.3	6.8
August	0.01	100.0	260.9	28.8
	0.02	50.0	240.3	23.4
	0.04	25.0	218.2	18.5
	0.10	10.0	185.4	13.3
	0.20	5.0	156.1	10.7
	0.50	2.0	103.9	9.1
	0.75	1.3	65.5	8.8
September	0.01	100.0	109.1	13.3
	0.02	50.0	99.7	10.7
	0.04	25.0	89.8	8.3
	0.10	10.0	75.3	5.9
	0.20	5.0	62.6	4.6
	0.50	2.0	40.4	3.9
	0.75	1.3	24.6	3.6
October	0.01	100.0	78.6	24.8
	0.02	50.0	66.2	16.6
	0.04	25.0	54.3	10.4
	0.10	10.0	39.2	5.8
	0.20	5.0	27.9	4.9
	0.50	2.0	12.2	3.3
	0.75	1.3	3.7	1.8
November	0.01	100.0	4.3	56.2
	0.02	50.0	2.8	34.3
	0.04	25.0	1.7	19.0
	0.10	10.0	0.8	6.1
	0.20	5.0	0.4	0.4
	0.50	2.0	0.1	3.8
	0.75	1.3	0.0	4.7

A.2.3 Monthly probability analysis for Wad Medani station

Month	Probability	Return period	Rain (mm)	Month	Probability	Return period	Rain (mm)
April	0.01	100	19.48	May	0.01	100	74.63
	0.02	50	12.77		0.02	50	62.42
	0.04	25	7.98		0.04	25	50.43
	0.1	10	3.86		0.1	10	34.93
	0.2	5	1.95		0.2	5	23.45
	0.333	3	1.03		0.333	3	15.12
	0.5	2	0.53		0.5	2	8.51
	0.75	1.3	0.19		0.75	1.3	1.85

Month	Probability	Return period	Rain (mm)	Month	Probability	Return period	Rain (mm)
June	0.01	100	83.29	July	0.01	100	296.62
	0.02	50	74		0.02	50	263.28
	0.04	25	64.45		0.04	25	228.14
	0.1	10	51.11		0.1	10	178.57
	0.2	5	40.04		0.2	5	138.12
	0.333	3	30.84		0.333	3	106.07
	0.5	2	22.2		0.5	2	78.22
	0.75	1.3	10.55		0.75	1.3	45.82

Month	Probability	Return period	Rain (mm)	Month	Probability	Return period	Rain (mm)
August	0.01	100	264.16	September	0.01	100	110.88
	0.02	50	242.75		0.02	50	101.08
	0.04	25	219.75		0.04	25	90.67
	0.1	10	185.82		0.1	10	75.53
	0.2	5	155.8		0.2	5	62.38
	0.333	3	129.36		0.333	3	51
	0.5	2	103.1		0.5	2	39.92
	0.75	1.3	65.11		0.75	1.3	24.33

Month	Probability	Return period	Rain (mm)	Month	Probability	Return period	Rain (mm)
October	0.01	100	83.62	November	0.01	100	4.33
	0.02	50	69.76		0.02	50	2.79
	0.04	25	56.25		0.04	25	1.71
	0.1	10	38.97		0.1	10	0.8
	0.2	5	26.37		0.2	5	0.39
	0.333	3	17.39		0.333	3	0.2
	0.5	2	10.44		0.5	2	0.1
	0.75	1.3	3.74		0.75	1.3	0.03

APPENDIX THREE

ENERGY BALANCE MODELS (SEBAL AND METRIC)

A.3.1 SEBAL and METRIC manual

A.3.1.1 Downloading Landsat images

1. Go to <http://glovis.usgs.gov/> website
2. Select the study area for Gezira (**path 173 and row 50**)
3. Select the date or the period (e.g. start from March, 2011)
4. Make the Cloud cover = 0% or max 1%
5. Select the available images by add them to the list

A.3.1.2 Image initial preparation

After extracting the bands from the ZIP file, ERDAS Layer Staking tool is used to convert the separated images to one image (multi bands). For Landsat 5 images, layers from 1 to 7 are added while for Landsat 7 bands 1 to 5, 61¹ and 7 are utilized. For the latter sensor, a pre-process gap-filling is done using the nearest-neighbor statistical method as shown in Figure A.3-1.

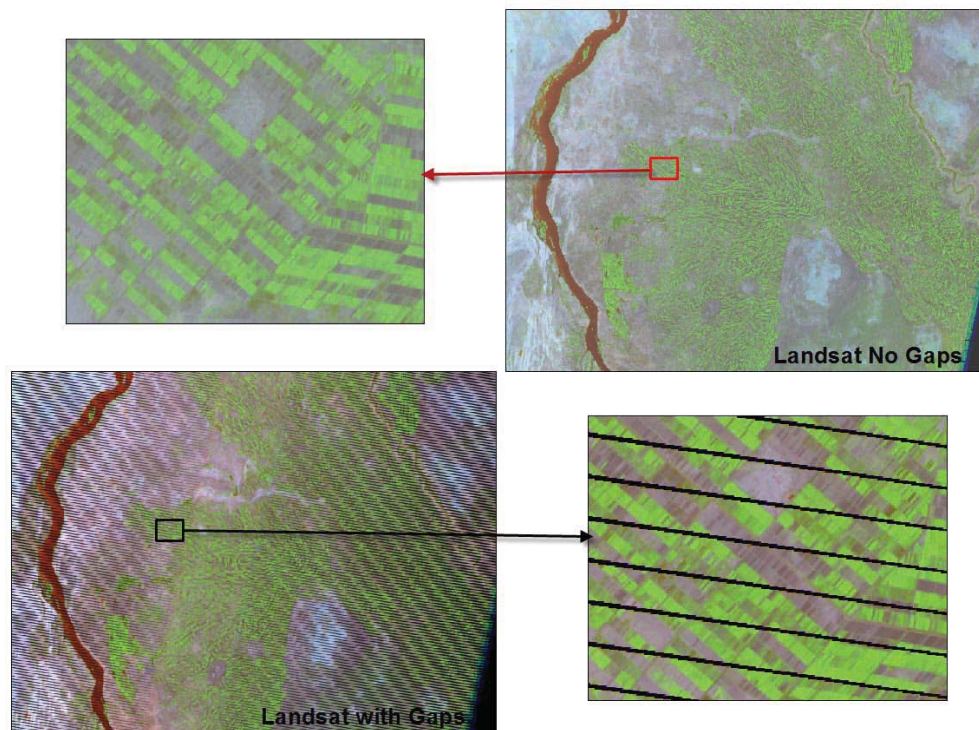


Figure A.3-1: Landsat gap filling using

¹ The recommended band to be used is B61 = band 6L (low gain)

A.3.1.3 Energy balance equation

To solve the energy balance equation ($\lambda ET = R_n - G - H$), the main parameters have to be calculated as following.

A.3.1.3.1 Calculate R_n the net radiation flux at the surface (W/m²)

Figure A.3-2 shows the flow chart of the required parameters to get R_n . There are 4 main components with **9 models** has to be built to compute R_n .

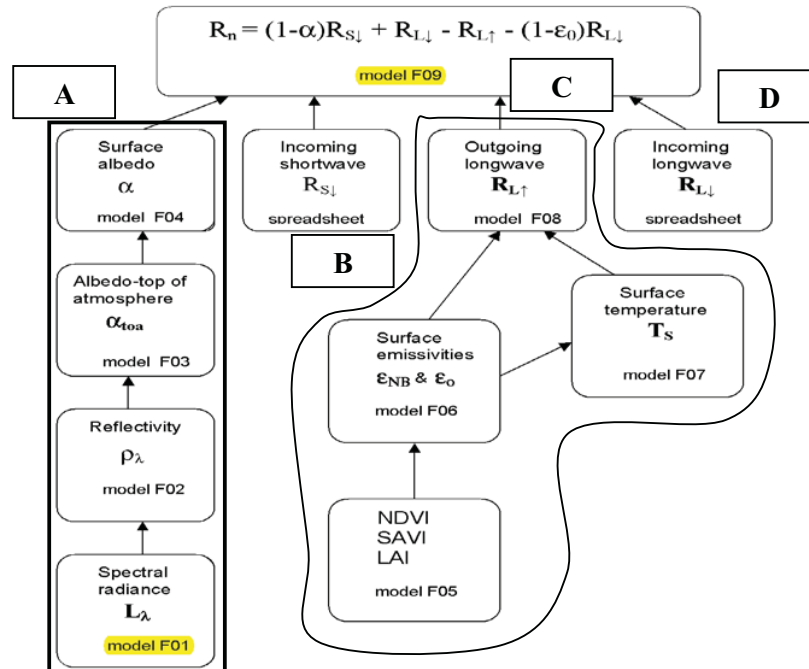


Figure A.3-2: Flow Chart of the Net Surface Radiation Computation.

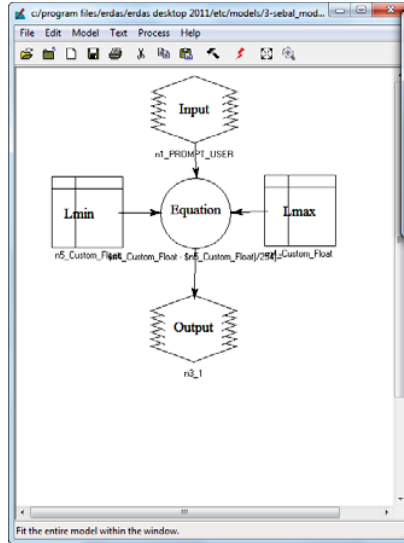
A. Surface Albedo (α) (Models 1 to 4)

1. Model 01 (Spectral Radiance (L_λ))

The following equation is built in Model Maker in Erdas imagine software. The equation is obtained from **Landsat handbook (2007)**

$$L_\lambda = \left(\frac{LMAX - LMIN}{QCALMAX - QCALMIN} \right) \times (DN - QCALMIN) + LMIN$$

Getting Lmax, Lmin, QCALmax and QCALmin from the header file of the Landsat image. The values are FIXED for all Landsat 7 images for the study area. Run **Model_f01** then specify the output location. To ease the procedures, the output file is named as **1-lr.tif**.



Equation: $((\$n4_Custom_Float - \$n5_Custom_Float)/254) * (\$n1_PROMPT_USER - 1) + \$n5_Custom_Float$

2. Model F02 (reflectivity for each band (ρ_λ))

$$\rho_p = \frac{\pi \cdot L_\lambda \cdot d^2}{ESUN_\lambda \cdot \cos\theta_s}$$

- $L_\lambda = 1\text{-lr.tif}$
- $ESUN_\lambda$ is the mean solar exo-atmospheric irradiance for each band ($W/m^2/\mu m$),

Table 6.3. $ESUN_\lambda$ for Landsat 5 TM (Markham and Barker, 1986), and for Landsat 7 ETM+ (Landsat 7 Science User Data Handbook Chap.11, 2002), both are in $W/m^2/\mu m$

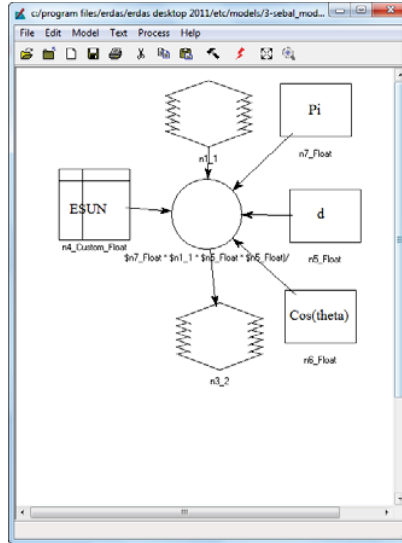
	Band 1	Band 2	Band 3	Band 4	Band 5	Band 6	Band 7
Landsat 5	1957	1829	1557	1047	219.3	-	74.52
Landsat 7	1969	1840	1551	1044	225.7	-	82.07

Note: a dummy value of 1 is entered for band 6.

- $\cos \theta = 0.755$ and d Earth-Sun distance in astronomical units = 1.024 From the Excel sheet
- $Pi = 3.142857$

The output of this is **2-pr.tif**

$$(\$n7_Float * \$n1_1 * \$n5_Float * \$n5_Float)/(\$n4_Custom_Float * \$n6_Float)$$



3. Model F03 (albedo at the top of the atmosphere (α_{toa}))

$$\alpha_{toa} = \sum (\omega_{\lambda} \times \rho_{\lambda})$$

Where: ρ_{λ} reflectivity for each band the output of this is **2-pr.tif**
 w_{λ} is the weighting coefficient from the following table

Table 6.4. *Weighting coefficients, ω_{λ}*

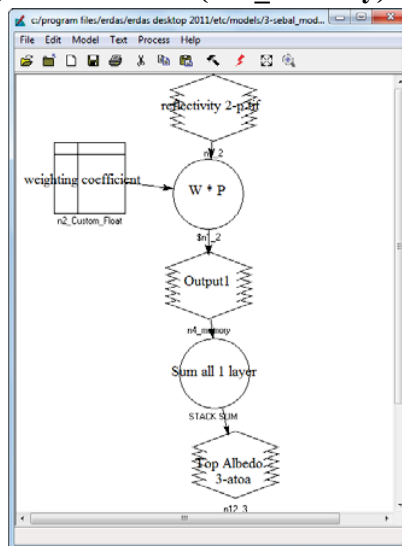
	Band 1	Band 2	Band 3	Band 4	Band 5	Band 6	Band 7
Landsat 5	0.293	0.274	0.233	0.157	0.033	-	0.011
Landsat 7	0.293	0.274	0.231	0.156	0.034	-	0.012

Note: a dummy value of 0 is entered for band 6.

Then make Stack SUM to be a one layer

The output is **3-atoa.tif**

\$n1_2 * \$n2_Custom_Float; STACK SUM (\$n4_memory)



4. Model F04 (Surface albedo (α))

$$\alpha = \frac{\alpha_{toa} - \alpha_{path_radiance}}{\tau_{sw}^2}$$

Where: α_{toa} is the output is **3-atoa.tif**

$\alpha_{path_radiance}$ is a constant = **0.03** based on Bastiaanssen (2000)

τ_{sw} is the atmospheric transmissivity which is calculated from:

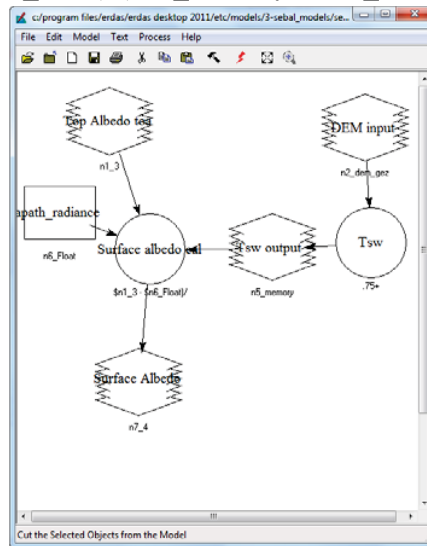
$$\tau_{sw} = 0.75 + 2 \times 10^{-5} \times z$$

Where; z is the elevation above sea level (m).

Here Z is the digital elevation model (DEM) (above sea level). Surface albedo takes the range from **0.1 to 0.8**.

$$\tau_{sw} = 0.75 + (0.00002 * \$n2_dem_gez)$$

$$\text{Surface albedo} = (\$n1_3 - \$n6_Float) / (\$n5_memory * \$n5_memory)$$



B. Incoming Shortwave Radiation ($R_{S\downarrow}$)

$$R_{S\downarrow} = G_{SC} \times \cos \theta \times d_r \times \tau_{sw}$$

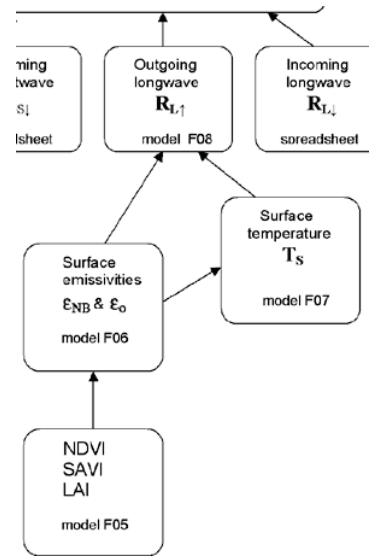
Where:

- G_{sc} is the solar constant (1367 W/m²),
- $\cos \theta$ is the cosine of the solar incidence angle as in step 2 above,
- d_r is the inverse squared relative earth-sun distance, and
- τ_{sw} is the atmospheric transmissivity.

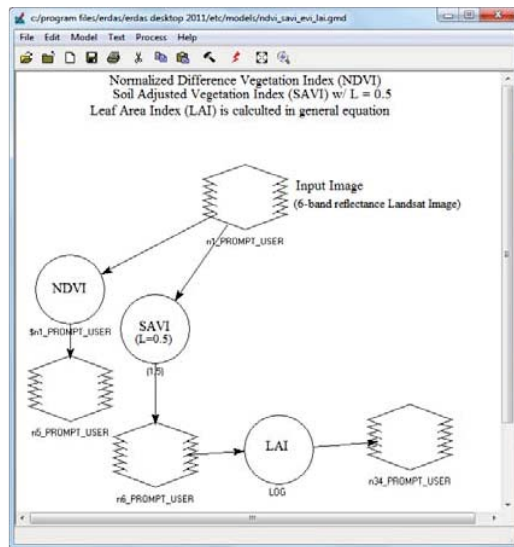
This calculation is done with the SEBAL/METRIC spreadsheet.

C. Outgoing longwave radiation ($R_{L\uparrow}$)

Outgoing longwave radiation ($R_{L\uparrow}$) is computed using the Stefan-Boltzmann equation with a calculated surface emissivity and surface temperature. Surface temperatures are computed from satellite image information on thermal radiance. The surface emissivity is the ratio of the actual radiation emitted by a surface to that emitted by a black body at the same surface temperature. The emissivity is computed as a function of a vegetation index. Starting with the vegetation indices, Model F05 are utilized.



5. Model F05 (NDVI, SAVI and LAI)



1. NDVI

The NDVI is the ratio of the differences in reflectivities for the near-infrared band (ρ_4) and the red band (ρ_3) to their sum:

$$NDVI = (\rho_4 - \rho_3) / (\rho_4 + \rho_3)$$

where; ρ_4 and ρ_3 are reflectivities for bands 4 and 3 and are output image from model F02. model_f05_(ndvi-savi)_1.gmd is used and the output is 5-NDVI.tif

$$(\$n1_PROMPT_USER(4) - \$n1_PROMPT_USER(3)) / (\$n1_PROMPT_USER(4) + \$n1_PROMPT_USER(3))$$

2. SAVI

The SAVI is an index that attempts to “subtract” the effects of background soil from NDVI so that impacts of soil wetness are reduced in the index. It is computed as:

$$SAVI = 1.5 \times \frac{\rho_4 - \rho_3}{0.5 + \rho_4 + \rho_3}$$

where; L is a constant for SAVI.

$$(1.5) * ((\$n1_PROMPT_USER(4) - \$n1_PROMPT_USER(3)) / (\$n1_PROMPT_USER(4) + \$n1_PROMPT_USER(3) + 0.5))$$

3. LAI

LAI is computed for southern Idaho using the following empirical equation:

$$LAI = -\frac{\ln\left(\frac{0.69 - SAVI_{ID}}{0.59}\right)}{0.91}$$

(LOG ((0.69 - \$n6_PROMPT_USER) / 0.59)) / -0.91

6. Model F06 (Surface emissivity (ε))

Surface Emissivity (ε₀)

The surface emissivities are computed in model F06 using the following empirical equations, where NDVI > 0:

$$\epsilon_{NB} = 0.97 + 0.0033 \text{ LAI}; \quad \text{for LAI} < 3 \quad (16a)$$

$$\epsilon_0 = 0.95 + 0.01 \text{ LAI}; \quad \text{for LAI} < 3 \quad (16b)$$

and $\epsilon_{NB} = 0.98$ and $\epsilon_0 = 0.98$ when $\text{LAI} \geq 3$.

For water and snow we use “filters” in the model to set the value of ϵ_{NB} and ϵ_0 :

- For water; $\text{NDVI} < 0$ and $\alpha < 0.47$, $\epsilon_{NB} = 0.99$ and $\epsilon_0 = 0.985$
- For snow; $\text{NDVI} < 0$ and $\alpha \geq 0.47$, $\epsilon_{NB} = 0.99$ and $\epsilon_0 = 0.985$

7. Model F07 (Effective at Satellite Temperature (T_{bb}))

T_{bb} is calculated from the following equation from Landsat Handbook (2007)

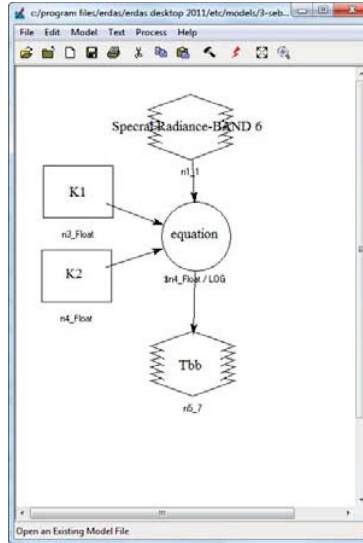
$$T_{bb} = \frac{K_2}{\ln\left(\frac{K_1}{L_6} + 1\right)}$$

where K_1 and K_2 are constants and obtained from the following table:

Table 1. Constants for Equation 19 for Landsat 5 TM in $mW/cm^2/sr/\mu m$ (Markham and Barker, 1986), and for Landsat 7 ETM+ in $W/m^2/sr/\mu m$ (Landsat 7 Science User Data Handbook Chap.11, 2002)

	K1	K2
Landsat5 TM Band6	607.76	1260.56
Landsat7 ETM+ Band6	666.09	1282.71

The L_6 used file is 1-Lr.tif by using Band no 6. The output file is 7-Tbb.tif.



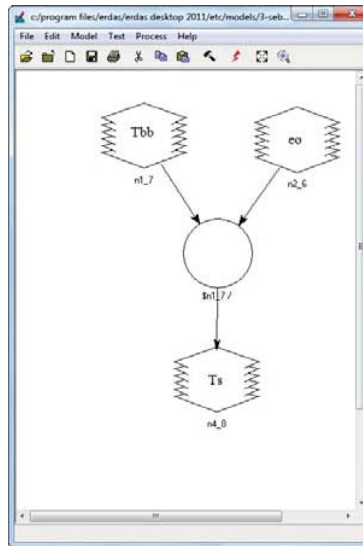
$$n4_Float / \text{LOG} (1 + (n3_Float / n1_1(6)))$$

8. Model F08 (Surface Temperature (T_s))

The surface temperature is calculated from

$$T_s = \frac{T_{bb}}{\epsilon_0^{0.25}}$$

The T_{bb} and eo used files are 7-Tbb.tif and 6-eo.tif, respectively. The output file is 8-Ts.tif.



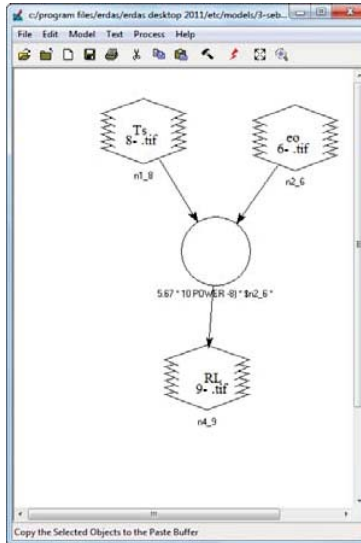
$$n1_7 / (n2_6 \text{ POWER } 0.25)$$

9. Model F09 (Outgoing Longwave Radiation R_{L↑})

Outgoing Longwave Radiation R_{L↑} is calculated from:

$$R_{L\uparrow} = \epsilon_0 \times \sigma \times T_s^4$$

Where: ϵ_0 is 6-co.tif, T is 8-Ts.tif and σ is Stefan-Boltzmann constant ($5.67 \times 10^{-8} \text{ W / (m}^2 - \text{K}^4)$). The output file is 9-RL.tif.



$$(5.67 * 10 \text{ POWER } -8) * \$n2_6 * (\$n1_8 \text{ POWER } 4)$$

D. Choosing the “Hot” and “Cold” Pixels

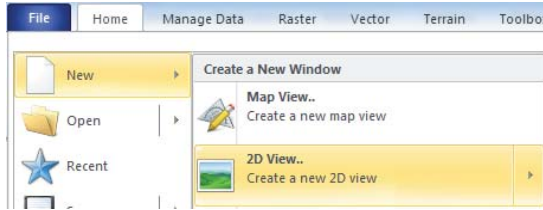
- The SEBAL/METRIC process utilizes two “anchor” pixels to fix boundary conditions for the energy balance.
- “Cold” pixel: a wet, well-irrigated crop surface with full cover $T_s \approx T_{air}$
- “Hot” pixel: a dry, bare agricultural field $ET \approx 0$


Cold pixel:

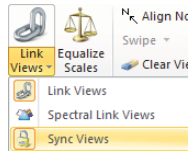
- The selection of the first pixel is for SEBAL as recommended by Bastiaanssen et al. (1998a). The cold pixel is generally selected from a water body. Herein, it is assumed that $ET_a = R_n - G$ where $H=0$.
- The second selection of the cold pixel for METRIC, as followed by Allen et al. (2007a), is well-irrigated field. It presumes that the ET_a at the cold pixel is closely predicted by the ET_a rate from a large expanse of alfalfa vegetation. Therefore assume that $ET_a = 1.05 ET_r$, at the cold pixel, where ET_r is the rate of ET from the alfalfa reference. Then, H for the cold pixel is calculated as $H = R_n - G - 1.05 ET_r$.

Steps to identify cold pixels using ERDAS:

1. Open the image or subset image and view it in true color (layer combination of 3,2,1) and in false color (layer combination of 4,3,2). This is in viewer no 1. Then select new viewer from File>New>2D view “Viewer no 2”.



2. Open the T_s image in Viewer no 2 with the **Pseudo Color** option. Link the two images from  button in any viewer. Then from Link viewer select Sync views



3. On the T_s image use “Raster – Attributes” to observe the range of T_s values.
4. Make a first guess for T_{cold} by looking at some fully covered agricultural fields (dark green in true color and red in false color). Insert a color gradation around the selected temperature.
5. View the colored T_s image and select a point that represents a “cold” (wet) agricultural field. Do not select an extreme cold point but one that is representative of a well-watered full cover crop. For the best results, the cold pixels should have a surface albedo in the range of 0.22 to 0.24 (corresponding to a full covered reference alfalfa field). It should have a Leaf Area Index in the range of 4 to 6 (corresponding to full covered agricultural field).
6. Observe other areas of the image for similar temperatures.
7. Select T_{cold} from a pixel in the center of the chosen field that represents a very cold, but not extremely cold, point in the image.
8. Record the coordinates and temperature of the “cold” pixel.

Hot pixel:

- The hot pixel it is assumed no ET_a is occurred. Therefore, $H_{\text{hot}} = R_n - G$. The pixel is utilized for the both Models SEBAL and METRIC
- The “hot” pixel should be located in a dry and bare agricultural field where one can assume there is no evapotranspiration taking place. It is recommended that one NOT use a hot desert area, an asphalt parking lot, a roof, or other such extremely hot areas.

Steps to identify hot pixel using ERDAS:

1. Repeat the first 3 steps of selecting the cold pixel.
2. The “hot” pixel should have a surface albedo similar to other dry and bare fields in the area of interest. It should have a LAI in the range of 0 to 0.4 and NDVI (0.13 to 0.18) is for bare soil.

E. Incoming Longwave Radiation ($R_{L\downarrow}$)

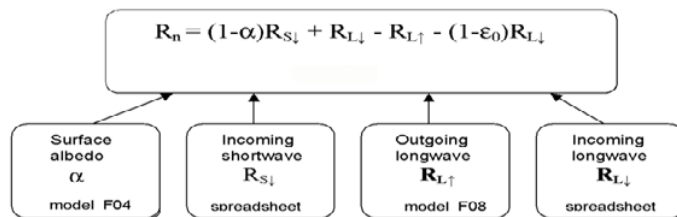
$$R_{L\downarrow} = \epsilon_a \times \sigma \times T_a^4$$

where:

- $\epsilon_a = 1.08 \times (-\ln \tau_{sw})^{.265}$
- where: $\tau_{sw} = 0.75 + 2 \times 10^{-5} \times z$ where: z is the elevation above sea level (m) **401.248** m.a.s.l.
- σ is the Stefan-Boltzmann constant ($5.67 \times 10^{-8} \text{ W/m}^2/\text{K}^4$)
- T_a is daily average temperature in Kelvin

F. Solving the Surface Radiation Balance Equation for Rn

10. Model F10 (Net Surface radiation Rn)



Where:

1. α : Surface Albedo from Model04 (4-a.tif)
2. $R_{S\downarrow}$: Incoming shortwave
3. $R_{L\downarrow}$: Incoming Longwave
4. $R_{L\uparrow}$: Outgoing Longwave from Model09 (9-RL.tif)
5. ϵ_0 : Surface Emissivity from Model06 (6-eo.tif)

Values for R_n can range from 100 – 700 W/m^2 , depending on the surface. This completes the first step of the SEBAL/METRIC procedure. The output file is 10-Rn.tif.

A.3.1.3.2. Soil Heat Flux (G)

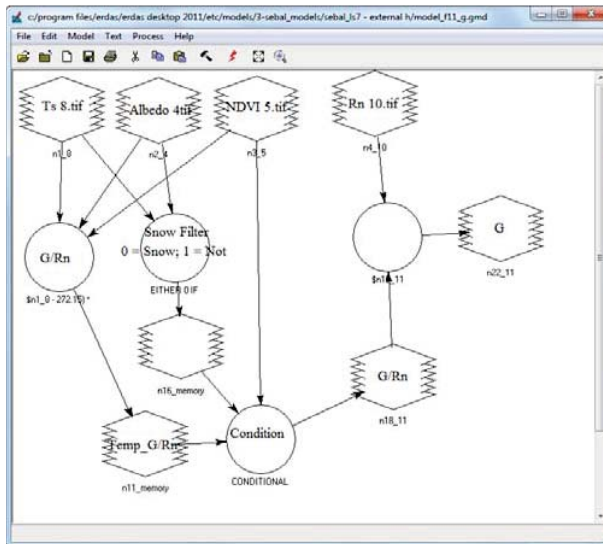
11. Model F11_ (Soil Heat Flux (G))

$$\frac{G}{R_n} = \frac{T_s}{\alpha} (0.0038\alpha + 0.0074\alpha^2) (1 - 0.98NDVI^4)$$

Where:

1. Ts: Surface Temperature from Model08 (8-ts.tif)
2. α: Surface Albedo from Model04 (4-a.tif)
3. NDVI: NDVI from Model05 (5-NDVI.tif)
4. Rn: Net Surface radiation from Model10 (10-Rn.tif)

Here, G/Rn ratio is calculated. Besides, there are some filtration procedures in this equation. If NDVI < 0; assume clear water, **G/Rn = 0.5** and If Ts < 4 °C and α > 0.45; assume snow, G/Rn = 0.5. The output file is 11- G.tif.



$$G/Rn = (\$n1_8 - 272.15) * ((0.0038 * \$n2_4) + (0.0074 * \$n2_4 * \$n2_4)) * (1 - (0.98 * \$n3_5 \text{ POWER } 4)) / (\$n2_4)$$

$$\text{Condition} = \text{CONDITIONAL} \{ (\$n3_5 < 0) 0.5, (\$n3_5 \geq 0) \$n11_memory, (\$n16_memory < 1) 0.5, (\$n16_memory > 0) \$n11_memory \}$$

$$G = \$n18_11 * \$n4_10$$

A.3.1.3.3. Sensible Heat Flux (H)

$$H = (\rho \times c_p \times dT) / r_{ah}$$

ρ = 1.225 kg/m³, c_p is air specific heat (1004 J/kg/K), dT (K) is the temperature difference (T₁ – T₂) between two heights (z₁ and z₂), and r_{ah} is the aerodynamic resistance to heat transport (s/m).

By using SEBAL spread excel sheet and Erdas Modeler, the next steps have to be calculated:

1. The momentum roughness length (z_{om}) is empirically estimated from the average vegetation height around the weather station using the following equation (Brutsaert, 1982): z_{om} = 0.12h

$z_{om} = 0.015$ is chosen for this calculation.

2. The Wind speed (200m)
3. The momentum roughness length (Zom)

12. Model F12_ (momentum roughness length (Zom))

Zom is calculated from each pixel using Model12 from:

$$Zom = \exp(-5.809 + 5.62 \text{ SAVI})$$

The output file is 12-Zom.tif.

4. The friction velocity (u*) and Aerodynamic Resistance to Heat Transport (rah)

13. Model F13_ (The friction velocity (u*) and Aerodynamic Resistance to Heat Transport (rah))

A. The friction velocity (u_*) is calculating from:

$$u^* = \frac{ku_x}{\ln\left(\frac{z_x}{z_{om}}\right)}$$

For each pixel using the ERDAS Model Maker tool.

- a. $K = 0.41$
- b. $Z_x = 200 \text{ m}$
- c. $U_{200} = 4.235 \text{ (m/s)}$
- d. $Zom = 12\text{-Zom .tif}$

The output file is 13-Ustar .tif.

B. **Initial** Aerodynamic Resistance to Heat Transport (r_{ah}) from:

$$r_{ah} = \frac{\ln\left(\frac{z_2}{z_1}\right)}{u^* \times k}$$

For each pixel using the ERDAS Model Maker tool.

- a. $K = 0.41$
- b. $Z_2 = 2 \text{ m}$
- c. $Z_1 = 0.1 \text{ m}$
- d. $U^* = 13\text{-Ustar .tif}$

The output file is 13-rah.tif.

5. Near Surface Temperature Difference (dT)

The dT is calculated from $dT = b + aT_s$ where a and b are constants calculated from SEBAL_PreCalc_Auto_Iteration_H_V3.xls and T_s is the Surface Temperature. dT needs the following parameters to be calculated:

1. datum Elevation	0 S.M.L	b. Elevation	DEM
2. Day of Year	header file	c. Cos(theta)	header file
3. Temperature lapse rate	Const 6.5	d. T ransmit-tance (tsw)	Calculated
4. Windspeed 200m	4.235	e. Albedo	Arc
5. Inst Etr 0.11	Calculated	f. NDVI	Arc
6. Following for Cold & Hot:		g. LAI	Arc
a. Coordinates (X,Y)	Sec D, pg6	h. Ts	Arc

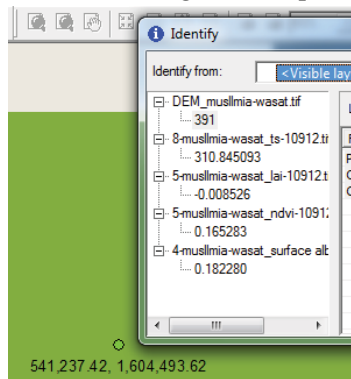
dT as well as a and b constants are within the following steps:

a) Reference Evapotranspiration (ET_r):

Form the header image file, the scene center scan time of the image is 07:58:16.7410690Z in Greenwich Mean Time (GMT). Sudan doe s not ope rate Daylight-Saving Time and Sudan Standard Time is 3 hours ahead of (GMT+3). It means that the scene center scan time of the image is **10:58:16.7410690Z** in East Africa Time Zone (EAT).

Instantaneous ET_r was calculated using the REF-ET software. It is assumed that the ET_r for 10:58 is the same as 9:00.

b) From ArcGIS get the required information for Hot and Cold Pixels



c) From the excel file Param2_17-11-2004.xls

Input the parameters then you get a and b constants **a = -0.10179**, **b = 38.7634**

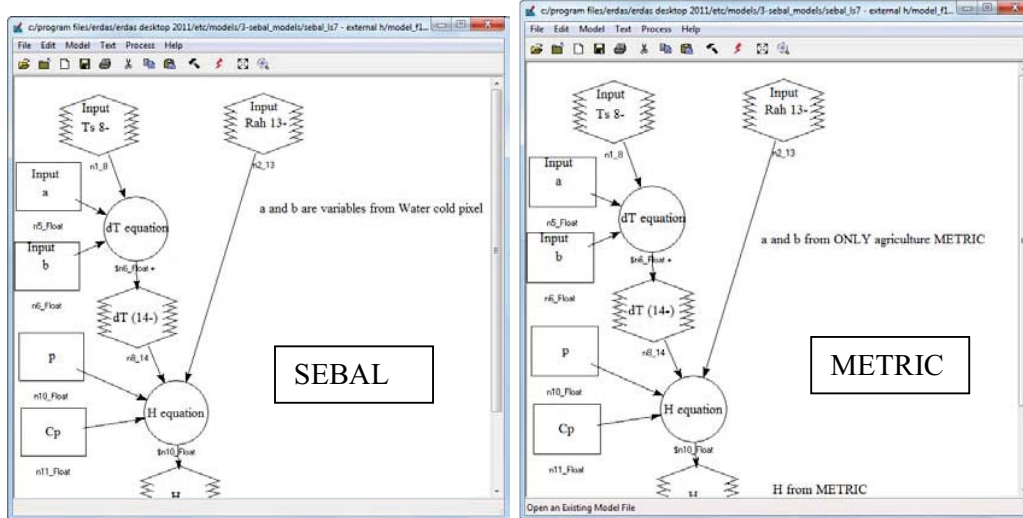
14. Model F14_ (Sensible Heat Flux (H))

The sensible heat flux (H) is calculated from $H = (\rho \times c_p \times dT) / r_{ah}$ where:

$\rho = 1.225 \text{ kg/m}^3$, c_p is air specific heat (1004 J/kg/K), dT (K) = $b + aT_s$ ($T_s = 8\text{-ts-.tif}$), and

$r_{ah} = 13\text{-rah.tif}$

Please note herein that, there are two H values obtained, one for SEBAL and the second for METRIC. This is due to the selection of the cold pixels.



$$H = \$n10_Float * \$n11_Float * \$n8_14 / \$n2_13$$

A.3.1.3.4. **Evapotranspiration (ET)**

C. Instantaneous ET (ET_{inst}) and Reference ET Fraction (ET_rF)

15. METRIC Model F15 (Instantaneous ET (ET_{inst}) and Reference ET Fraction (ET_rF))

1. Instantaneous ET (ET_{inst})

$$ET_{inst} = 3600 \frac{R_n - G - H}{\lambda}$$

Where: ET_{inst} is the instantaneous ET (mm/hr), 3600 is the time conversion from seconds to hours, $R_n = 10 - ***_r_tif$, $G = 11 - ***_g_tif$, $H = 14 - ***_h_tif$ and $\lambda = \{2.501 - 0.00236 (T_s - 273)\} * 10^6$ (J/kg). Where: $T_s = 8 - ***_t_s_tif$. The output file is $15 - ***_ETinst.tif$.

2. Reference ET Fraction (ET_rF)

$$ET_rF = \frac{ET_{inst}}{ET_r}$$

where: $ET_{inst} = 15 - ***_ETinst.tif$. The output file is $15 - ***_ETrF.tif$.

3. 24-Hour Evapotranspiration (ET_{24})

Daily value of ET (ET_{24}) is calculated from $ET_{24} = ET_rF \times ET_{r_24}$

where: $ET_rF = 15 - ***_ETrF.tif$ and ET_{r_24} is the daily reference evapotranspiration from REF-ET program. METRIC computes the ET_{24} by assuming that the instantaneous ET_rF computed in model 15 is the same as the 24-hour average.

C. Instantaneous ET (ET_{inst}) and Evaporative Fraction (EF)

15. SEBAL Model_M15_Evaporative Fraction (EF)

Evaporative fraction Λ , which is the ratio of latent heat flux over available energy

$$\Lambda = \frac{\lambda AE}{\lambda AE + H} = \frac{\lambda AE}{R_n - G_o}$$

Where: $\lambda AE = R_n - G_o - H$

16. Model_M16_Evaporative Fraction (EF)

The daily actual ET is calculated based on the combination of the following equations:

$$AE_{day} = \frac{\Delta R_{n\ day}}{28.588}$$

The net radiation is aggregated as daily net radiation (Rn-day) as following:

$$R_{n-day} = (1 - 1.1\alpha)K_{\downarrow day} - 110\tau_{day}$$

The daily income shortwave radiation ($k_{\downarrow day}$) is calculated from the following equation:

$$K_{\downarrow day} = 11.5741\tau_{day}K_{\downarrow day}^{toa}$$

Table 8: Alternative Coefficients Pertaining to Country-Wide Equations (Linear)

Month	c ₁	c ₂	*R ²
January	0.255	0.483	0.600
February	0.158 ^s	0.611	0.554
March	0.238	0.543	0.667
April	0.204	0.566	0.704
May	0.241	0.514	0.704
June	0.288	0.461	0.670
July	0.294	0.450	0.725
August	0.307	0.413	0.547
September	0.250	0.503	0.661
October	0.161	0.597	0.674
November	0.190	0.557	0.647
December	0.162 ^f	0.607	0.477

T₃₂₂ (17-Nov-2004) = 0.19 + 0.557 (0.91)

T_{day} 0.701532

$$K_{\downarrow day}^{toa} = \frac{24}{\pi} G_{SC} E_o \sin\delta \sin\varphi \left[\frac{\pi}{180} \omega_s - \tan\omega_s \right] \quad (4.26)$$

where G_{sc} is the solar constant= 0.0820 (MJm⁻² min⁻¹), ω_s is the sunset hour angle (rad), Φ is the latitude (rad), and δ is the solar declination (rad). The conversion from decimal degrees to radians is given by:

$$\text{Radians} = \pi/180 \text{ (decimal degrees)}$$

Φ is the latitude (rad)

$$\delta = 0.409 \sin(2\pi/365 J - 1.39) \quad (5.12f)$$

$$\omega_s = \arccos [-\tan(\phi)\tan(\delta)] \quad (5.12g)$$

Where J is the number of the day in the year between 1 (1 January) and 365 or 366 (31 December).

Equation 4.26 is calculated using the excel sheet

$$K_{topday} = H_o \text{ (MJ/m-2)}$$

30.09227

Sample calculation (Gezira)										
Day	Dn	solar declination (°)	Lat (°)		sunset hr angle, ω_s (rad)	So (hrs)				Ho (MJ/m-2)
1	322	-19.82109039	14.5	-0.09322	1.477445	11.28685	38.5112	0.906825	-0.12543	30.09227

4. Seasonal Evapotranspiration (ET_{seasonal})

A seasonal evapotranspiration map can be derived from the 24-hour evapotranspiration data by extrapolating the ET_{24} proportionally to the reference evapotranspiration (ET_r) by assuming that the ET for the entire area of interest changes in proportion to the change in the ET_r at the weather station.

1. The first step is to decide the length of the season for which ET is desired (i.e., March 1 to October 31).
2. The second step is to determine the period represented by each satellite image within the chosen season (i.e., if the first two images for the above season are on March 15 and April 8, then the period represented by the March 15th image would be March 1 to March 27).
3. The third step is to compute the cumulative ET_r for the period represented by the image. This is simply the sum of daily ET_r values over the period. These 24-hour values can be computed using the University of Idaho REF-ET software described in Appendix 3. The same ET_r method must be used through the SEBAL process. ET_r should represent the alfalfa reference ET, which is a larger value than for the clipped grass reference (ET_o).
4. The fourth step is to compute the cumulative ET for each period as follows:

$$ET_{period} = ET_r F_{period} \sum_1^n ET_{r-24}$$

where; $ET_{r_period}F$ is the representative ET_rF for the period, ET_{r-24} is the daily ET_r , and n is the number of days in the period. Units for ET_{period} will be in mm when ET_{r-24} is in mm/day.

5. The fifth step is to compute the seasonal ET by summing all of the ET_{period} values for the length of the season.

The following difficulties encountered in the computation of seasonal ET must be understood:

1. If there is some cloud cover in one of the images used for the seasonal ET computation, then there can be no ET or ET_rF values represented for this area during the period represented by the image. One can assign ET_rF values to the cloud-covered areas by interpolating between the ET_rF values for the images on either side of the cloud-covered image.
2. When the ET_r at the weather station is not representative of the entire area (i.e., where the image spans many mountain valleys or includes both coastal and inland areas having different effects from clouds or wind that are not well correlated across the image), then the image should be broken down into sub-images, each with its own value of ET_r . In this situation, simple SEBAL runs should be made for each sub-image.
3. If an agricultural field is dry on the day of the image and is then irrigated on a following day, the increase in ET for this field during the representative period of the image will not be considered in the computation of seasonal ET. This problem can be minimized if many satellite images are used for the computation of seasonal ET with each image representing a shorter time period. One can also apply a water balance model to each pixel that includes irrigation and precipitation as inputs.